

IRIDIUM-CATALYZED ASYMMETRIC HYDROGENATION FOR SYNTHESIS
OF CHIRAL CYCLIC AMINES

By

YUHUA HUANG

A dissertation submitted to the

Graduated School-New Brunswick

Rutgers, The State University of New Jersey

In Partial Fulfillment of the Requirements

For the degree of

Doctor of Philosophy

Graduate Program in Chemistry and Chemical Biology

Written under the direction of

Professor Xumu Zhang

And approved by

New Brunswick, New Jersey

October, 2016

ABSTRACT OF THE DISSERTATION

**IRIDIUM-CATALYZED ASYMMETRIC HYDROGENATION FOR
SYNTHESIS OF CHIRAL CYCLIC AMINES**

by YUHUA HUANG

Dissertation Director:

Professor Xumu Zhang

Chiral cyclic amines play extremely important roles in pharmaceutical and agrochemical industries. Over the past several decades, synthesis of chiral cyclic amines has been one of the major tasks in organic chemistry. Among various methods for chiral cyclic amine synthesis, transition metal-catalyzed asymmetric hydrogenation is one of the most desired approaches. It is highly efficient, atom economic and environmental friendly. Development of new efficient catalytic systems in asymmetric hydrogenation for various pyridine derivatives and other N-heteroaromatic compounds are the focus of this dissertation.

The asymmetric reduction of pyridine compounds remains a long-standing challenge in modern synthesis due to the high stability of the aromatic rings. The difficulty to hydrogenate the pyridines also ascribed to the inhibitory effect from the amine product and the coordination difficulty of the pyridine substrates to the transition metal center. With the addition of an easy-removal protecting group, benzyl,

on the nitrogen, the pyridine ring was dearomatized. This strategy proved to help achieve direct reduction on pyridines under mild conditions to access cyclic piperidines. Collaborating with Merck Catalysis group, we used the high-through-put approach to screen over 200 ligands and identified an unusual MP2-SegPhos ligand. A neutral iridium–MP2-SegPhos catalytic system was developed to hydrogenate various *N*-benzyl-2-arylpyridines with high enantioselectivities. Successful examples of *N*-alkyl pyridines reduction by this Ir-MP2 catalytic pathway display the potential of broader application in chiral amine synthesis. Reduction of di-substituted pyridines and isoquinoline substrates were also fulfilled with good to excellent enantioselectivity.

Mechanism studies have remained unclear despite the significant progress made in the reduction methodologies. The three double bonds (both C=C and C=N bonds) present in the pyridine ring adds additional complexities. Based on the NMR studies and isotopic experimental evidences an outer-sphere mechanism was proposed involving two tautomerizations and proton-hydride delivery. Crucial tetrahydropyridine complex and other key intermediates were identified and characterized. This mechanism study provide an insight on understanding the hydrogenation of pyridinium salt using iridium catalyst, which might contribute to the future rational design of more efficient catalyst and expand the scope of Ir-catalyzed asymmetric hydrogenation for pyridines and heteroaromatics.

ACKNOWLEDGEMENTS

I would like to offer my sincere gratitude to my graduate advisor, Professor Xumu Zhang. His research program is not only broad and industrial practical in terms of the methodological development but also deep in terms of the mechanistic insights. Xumu has given me the opportunity to conduct research while being a full-time researcher at Merck Research laboratories. I enjoyed the freedom of being able to explore my own scientific realm while his guidance and encouragement enabled me to accomplish my entire Ph.D. studies and eventually lead to this dissertation. Xumu's enthusiasm in science is unquenchable and inspiring. I benefited tremendously from his deep insights in catalysis field.

I would like to thank Dr. Alan Goldman and Dr. Leslie Jimenez for sharing their insights when they taught me in class and served in my committee. Special thanks goes to Dr. Ian Davies of Merck Research Laboratories as my committee member and mentor. He provided strong support for my researches conducted at the Catalyst center and High pressure labs at Merck. I benefit tremendously from the insightful discussions with him. Dr. Davies always challenges me scientifically, at the same time, never loses his faith in me.

I would like to thank my collaborators at Rutgers Dr. Mingxin Chang and Mr. Shaodong Liu. An enormous thanks also goes to all my Merck collaborator Dr. Yonggang Chen, Mr. Mark Weisel, Dr Yizhou Liu and Dr. Yi Ning Ji Chen.

For the past decade, Dr Frank Bennett has been my mentor at Merck/Schering

Plough. He has inspired my interests in science and is still my role model. I have been blessed for his always being by my side to lend his hearty supports.

I would like to express special thanks to my parents. Their love and support has always been a great encouragement for me. My deepest gratitude goes to my husband, Wei Yu, for his unreserved love and support throughout this journey. He has always been there cheering me up through the good times and bad. This dissertation is dedicated to him and our children Clara, Chloe and Charles.

Last but not least, I offer my regards and blessings to all of those who supported me in any respect during my doctoral study.

TABLE OF CONTENTS

ABSTRACT.....	ii
ACKNOWLEDGEMENT.....	iv
LIST OF TABLES.....	viii
LIST OF FIGURES.....	x
LIST OF SCHEMES.....	xii
Chapter 1 Overview.....	1
1.1 Introduction and background.....	1
1.2 Asymmetric hydrogenation of N-heteroarenes and arenes.....	5
1.2.1 Asymmetric hydrogenation of quinolines.....	10
1.2.2 Asymmetric hydrogenation of isoquinolines	14
1.2.3 Asymmetric hydrogenation of quinoxalines	15
1.2.4 Asymmetric hydrogenation of pyridines	18
1.2.5 Asymmetric hydrogenation of other heteroarenes and arenes.....	23
1.3 Strategies for asymmetric hydrogenation of aromatic compounds.....	27
References.....	29
Chapter 2 Iridium-Catalyzed Asymmetric Hydrogenation of Pyridine.....	33
2.1 Introduction.....	33
2.2 Asymmetric hydrogenation of simple N-benzylpyridinium salts.....	40
2.2.1 Initial results and reaction optimization.....	40
2.2.2 Substrate scope.....	53
2.2.3 Conclusion.....	56
2.3 Asymmetric hydrogenation of disubstituted N-Benzylpyridinium salts	57
2.4 Asymmetric hydrogenation of 2-alkyl-N-benzylpyridinium salts.....	64
2.5 Experimental section.....	67
2.5.1 General remarks.....	67
2.5.2 General procedure for synthesis of 2-aryl pyridines.....	67
2.5.3 General procedure for asymmetric hydrogenation 2-Aryl Pyridinium Salts.....	69

References.....	82
Chapter 3 Asymmetric Hydrogenation of Other N-Heteroaromatics.....	84
3.1 Introduction and background.....	84
3.2 Asymmetric hydrogenation of quinoline mechanism.....	88
3.3 Asymmetric hydrogenation of isoquinoline	94
3.4 Asymmetric hydrogenation of quinoline	105
3.5 Experimental section.....	108
3.5.1 General remarks.....	108
3.5.2 General procedure for synthesis of 2-isoquinoline.....	108
3.5.3 General procedure for asymmetric hydrogenation of quinoline and isoquinoline.....	110
References.....	118
Chapter 4 Mechanism studies on Iridium-catalyzed Asymmetric Hydrogenation ...	120
4.1 Introduction and background.....	120
4.2 Results and discussion.....	125
4.2.1 NMR studies on catalyst complex.....	125
4.2.2 Isomerization.....	127
4.2.3 Identification of intermediates.....	134
4.2.4 Kinetic studies	137
4.2.5 Outer-sphere mechanism proposal.....	140
4.3 Conclusion.....	142
4.4 Experimental section.....	144
4.4.1 Typical procedure of deuterium hydrogenation of pyridinium salts.....	144
4.4.2 NMR studies on catalyst complex.....	145
4.4.3 Deuterium content quantification by NMR.....	148
4.4.4 Enamine and ketone identification.....	160
4.4.5 Kinetic data.....	167
References.....	172

LIST OF TABLES

Table 2-1. Screening of metals for asymmetric hydrogenation of 2-phenylpyridinium salts.....	45
Table 2-2. Solvent screening for asymmetric hydrogenation of <i>N</i> -benzyl-2-phenylpyridium bromide	47
Table 2-3. <i>Mixed</i> solvent screening for asymmetric hydrogenation of <i>N</i> -benzyl-2-phenylpyridium bromide.....	48
Table 2-4. Temperature, pressure and catalyst loading screening for asymmetric hydrogenation of <i>N</i> -benzyl-2-phenylpyridium bromide	49
Table 2-5. Screening of additive and mix solvents for asymmetric hydrogenation of 2-phenylpyridinium salts.....	50
Table 2-6. Catalyst loading and concentration for asymmetric hydrogenation of 2-phenylpyridinium salts	51
Table 2-7. Counter ion screening.....	51
Table 2-8. Substrate scope for asymmetric hydrogenation of <i>N</i> -benzylpyridinium salts.....	54
Table 2-9 . Preliminary screening results for hydrogenation of 2-methyl-5-phenyl pyridinium salt.....	60
Table 2-10. Asymmetric hydrogenation of 2,5-di-substituted substrates.....	61
Table 3-1. Asymmetric hydrogenation of 1-phenyl-isoquinoline with chiral	

ligands	98
Table 3-2. Solvent effects on asymmetric hydrogenation of 1-phenyl-isoquinoline..	99
Table 3-3. Additive effects on asymmetric hydrogenation of 1-phenyl-isoquinoline	101
Table 3-4. Asymmetric hydrogenation of isoquinoline by Ir-MP ² -SegPhos	102
Table 3-5. Asymmetric hydrogenation of 2-phenyl-quinoline by MP ² -SegPhos.....	107

LIST OF FIGURES

Figure 1-1. Selected Pharmaceutical Biologically Active Ingredients	2
Figure 1-2. Milestones in chiral ligands design.....	3
Figure 1-3. Chiral ligands developed by our group for hydrogenation	4
Figure 1-4. Chiral compounds yielded from asymmetric hydrogenation.....	5
Figure 1-5. The number of potential substrates for asymmetric hydrogenation.....	6
Figure 1-6. Challenges of hydrogenation of aromatic compounds.....	7
Figure 1-7. P-Phos, difluorPhos, spiroPO and dendritic GnDenBINAP.....	14
Figure 2-1. Selected pharmaceutical targets and structures with chiral piperidine ...	34
Figure 2-2. Selected results of ligand screen for asymmetric hydrogenation of N-alkyl-2-phenylpyridium bromide substrates using iridium catalysts	42
Figure 2-3. Chiral ligands structures	43
Figure 2-4. Order of Electron Donating Ability of Phosphorus Ligands.....	44
Figure 2-5. Di-substituted chiral piperidine in pharmaceutical drug candidates.....	58
Figure 2-6. Interesting di-substituted substrates for hydrogenatoin.....	59
Figure 2-7. Natural products and pharmaceutical agents containing chiral piperidin-3-ol motif.....	62
Figure 3-1. Structures of selected chiral THIQ.....	84
Figure 3-2. Structures of chiral ligands for initial screening.....	97
Figure 3-3. Pharmaceutical products containing THQ.....	105
Figure 4-1. Piperidine derivatives as prescription drugs.....	121

Figure 4-2. Structure of MP ² -SegPhos.....	125
Figure 4-3. Proposed Catalyst Complex structures based on NMR.....	126
Figure 4-4. Isotopic labeling experiment using deuterium gas.....	128
Figure 4-5. Isotopic labeling experiment using deuterium water as additive.....	129
Figure 4-6. Isotopic labeling experiment on di-substituted pyridine.....	133
Figure 4-7. Validation of IR-sensor monitor method against NMR analysis.....	138
Figure 4-8. Half concentration of (1) versus standard concentration time-adjusted profile.....	139
Figure 4-9. Kinetic analysis of the reaction of (1) to (2).....	140
Figure 4-10. Additive effects.....	141
Figure 4-11. Multiplicity-edited HSQC of the enamine intermediate (4).....	164
Figure 4-12. Multiplicity-edited HSQC of the mixture of enamine (4) and ketone (10) intermediates.....	165
Figure 4-13 ¹ H- ¹³ C HMBC spectrum of the mixture of enamine (4) and ketone (10).....	165
Figure 4-14. NMR data collected at 6 time point and the end point.....	166

LIST OF SCHEMES

Scheme 1-1. The first example of enantioselective hydrogenation of aromatic compounds.....	9
Scheme 1-2. Ruthenium-BINAP system for furan hydrogenation.....	9
Scheme 1-3. Rh/Josiphos system for pyrazine hydrogenation.....	9
Scheme 1-4. The first example of enantioselective hydrogenation of aromatic compounds with >90% enantioselectivity	9
Scheme 1-5. Ir-catalyzed asymmetric hydrogenation of 2-substituted quinolines.....	10
Scheme 1-6. Ir-catalyzed asymmetric transfer hydrogenation of quinolines	11
Scheme 1-7. Ir-catalyzed asymmetric hydrogenation of quinolines with silane/water.....	12
Scheme 1-8. Ru-catalyzed asymmetric hydrogenation of quinolines.....	12
Scheme 1-9. (S)-C3*-TunePhos catalyzed asymmetric hydrogenation of quinolines	13
Scheme 1-10. Chloroformates activated asymmetric hydrogenation of isoquinolines	15
Scheme 1-11. Ir-catalyzed asymmetric hydrogenation of quinoxalines	16
Scheme 1-12. Cationic dinuclear triply halogen-bridged iridium complexes for asymmetric hydrogenation of quinoxalines	17
Scheme 1-13. Organocatalyzed asymmetric transfer hydrogenation of quinoxalines	17
Scheme 1-14. Diastereoselective hydrogenation of pyridines with Pd(OH) ₂ /C	19
Scheme 1-15. Rhodium-catalyzed step-wise hydrogenation of pyridines	20
Scheme 1-16. Iridium-Catalyzed asymmetric hydrogenation of N-benzoyliminopyridinium ylides	20

Scheme 1-17. Iridium-catalyzed asymmetric hydrogenation of 7,8-dihydroquinolin-5(6 <i>H</i>)-ones.....	21
Scheme 1-18. Brønsted acid-catalyzed enantioselective reduction of pyridines	22
Scheme 1-19. Iridium-catalyzed asymmetric hydrogenation of 2-substituted pyridinium salts with a directing group.....	22
Scheme 1-20. Pd-catalyzed asymmetric hydrogenation of <i>N</i> -unprotected indoles....	24
Scheme 1-21. Pd-catalyzed asymmetric hydrogenation of simple pyrroles.....	24
Scheme 1-22. Ru-catalyzed asymmetric hydrogenation of imidazoles	25
Scheme 1-23. Ru-catalyzed 4-substituted 2-phenyloxazoles	25
Scheme 1-24. Iridium-catalyzed asymmetric hydrogenation of furan derivatives ...	26
Scheme 1-25. Ru/NHC-catalyzed asymmetric hydrogenation of carbocyclic ring of quinoxalines.....	27
Scheme 2-1. First highly enantioselective asymmetric hydrogenation of quinolines	36
Scheme 2-2. The first example for asymmetric hydrogenation of pyridines.....	38
Scheme 2-3. Direct asymmetric hydrogenation of pyridines	38
Scheme 2-4. Utility of chiral auxiliary on the 2-position of pyridine to induce chirality.....	38
Scheme 2-5. Step-wise hydrogenation of pyridine.....	39
Scheme 2-6. Asymmetric hydrogenation of <i>N</i> -iminopyridinium ylides	39
Scheme 2-7. Asymmetric hydrogenation of pyridinium salts	39
Scheme 2-8. Asymmetric hydrogenation of pyridinium salts with different benzyl substitutes.....	52
Scheme 2-9. Iridium-catalyzed asymmetric hydrogenation of 2-phenylpyridinium	

salts 4.....	56
Scheme 2-10. Product transformation from 5-methoxy-2-aryl piperidines 17.....	64
Scheme 2-11. Asymmetric hydrogenation of 2-alkyl pyridines.....	65
Scheme 3-1. First asymmetric hydrogenation of 2-methyl-quinoline	86
Scheme 3-2. Asymmetric hydrogenation requiring activating reagents.....	87
Scheme 3-3. Ir-Asymmetric transfer hydrogenation	87
Scheme 3-4. Dinuclear iridium complexes catalyzed asymmetric hydrogenation....	87
Scheme 3-5. Strong Brønsted acid promoted asymmetric hydrogenation of isoquinolines and quinolines.....	88
Scheme 3-6. Proposed mechanism for asymmetric hydrogenation of quinolines.....	90
Scheme 3-7. Proposed mechanism for the asymmetric hydrogenation of indoles	91
Scheme 3-8. Enhancing effects of salt formation on catalytic activity and enantioselectivity for asymmetric hydrogenation of isoquinolinium salts.....	92
Scheme 3-9. Iridium-catalyzed isoquinoline reduction mechanism.....	93
Scheme 3-10. Intramolecular reductive amination.....	95
Scheme 3-11. Industrial production of solifenacin.....	96
Scheme 3-12. Product scale-up toward the synthesis of (+)-Solifenacin.....	104
Scheme 4-1. Proposed mechanism for asymmetric hydrogenation of quinolines.....	123
Scheme 4-2. Plausible mechanism for the chemoselective transfer hydrogenation. ..	124
Scheme 4-3 Proposed tautomerization process.....	131
Scheme 4-4. Hydrogenation of di-substituted pyridinium salt.....	132
Scheme 4-5 Hydrogenation of enamine 4 to piperidine.....	135

<i>Scheme 4-6.</i> By-product ketone formed with water present.....	136
<i>Scheme 4-7.</i> Synthesize keytone 10	136
<i>Scheme 4-8.</i> Outer-sphere mechanism in asymmetric hydrogenation of pyridine....	143

Chapter 1

Overview

1.1 Introduction and Background

During the past half century, the increasing demand of pharmaceutical drugs, agrochemicals and other fine chemicals has intrigued a large field of interests to produce enantiopure chemicals (Figure 1-1).¹ Among numerous asymmetric catalytic technologies, homogenous transition metal-catalyzed asymmetric hydrogenation plays a particularly important role in the preparation of diverse pharmaceuticals, natural products, agrochemicals, and so on. It is highly efficient, environmental friendly and cost effective. Asymmetric hydrogenation of prochiral unsaturated compounds is undoubtedly one of the most extensively studied methodologies in modern organic chemistry.²

For the past forty years, the advances made from academia research on asymmetric hydrogenation were frequently recognized with industrial application, which in turn, provide driving force for its academia basic research.³ As a result, a large number of catalytic systems have been developed since the seminal discoveries of CAMP and DIPAMP by Knowles,⁴ and DIOP by Kagan⁵ (Figure 1-2). DIPAMP represented an early successful example of chiral ligand designs. This bidentate diphosphine ligand was found to be very selective to the synthesis of L-DOPA – a

chiral amino acid for the treatment of Parkinson's disease and dopamine-responsive dystonia.

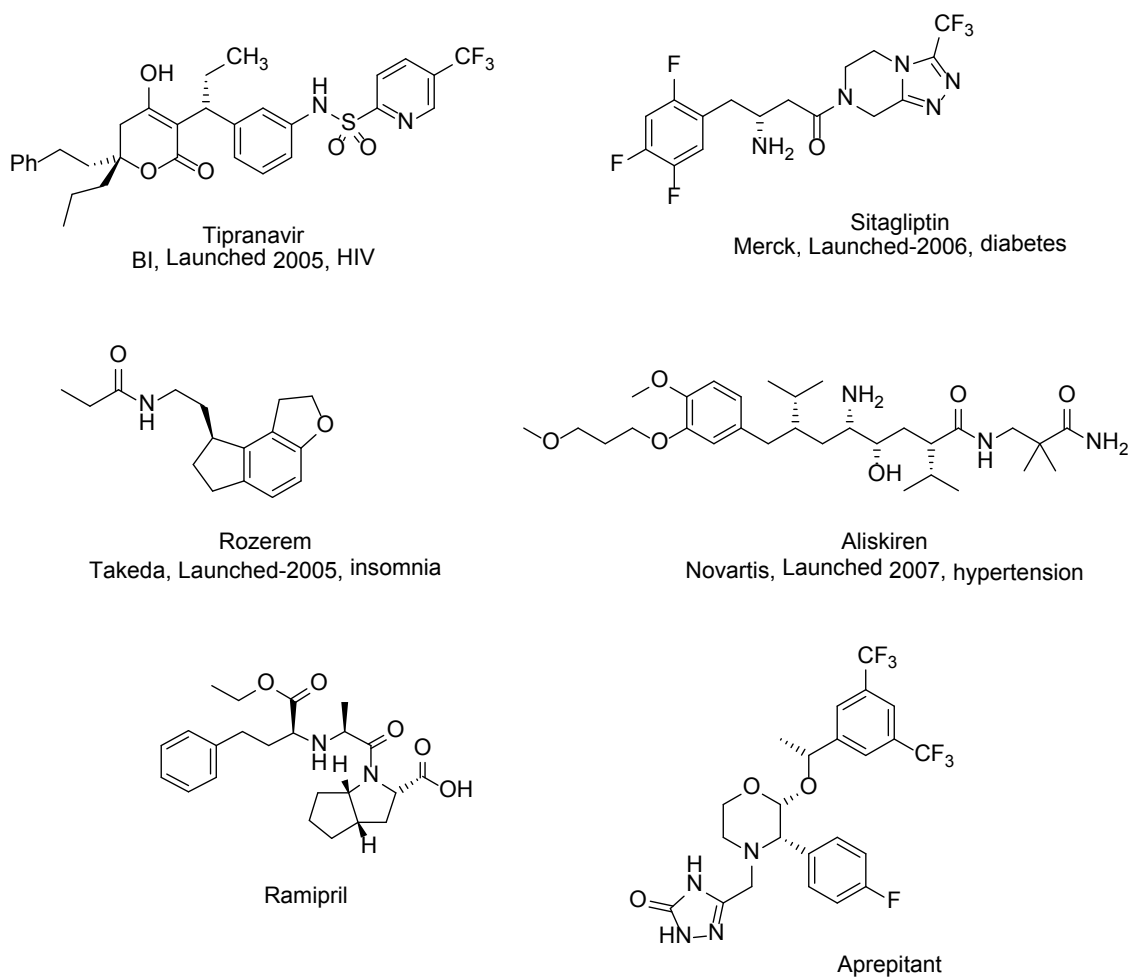


Figure 1-1 Selected Pharmaceutical Biologically Active Ingredients.

In 1980 the discovery of binaphthyl moiety as chiral ligand motifs by Noyori led to the major milestone ligand BINAP (Figure 1-2).⁶ Noyori's BINAP-Ru system not only delivered extraordinary results for hydrogenation of olefins, but also work excellently for ketone reduction, which significantly expand the substrates scope. DuPhos,⁷ JosiPhos,⁸ PHOX⁹ and MonoPhos¹⁰ were also among those successful ligands and added new motifs for chiral ligands design (Figure 1-2).

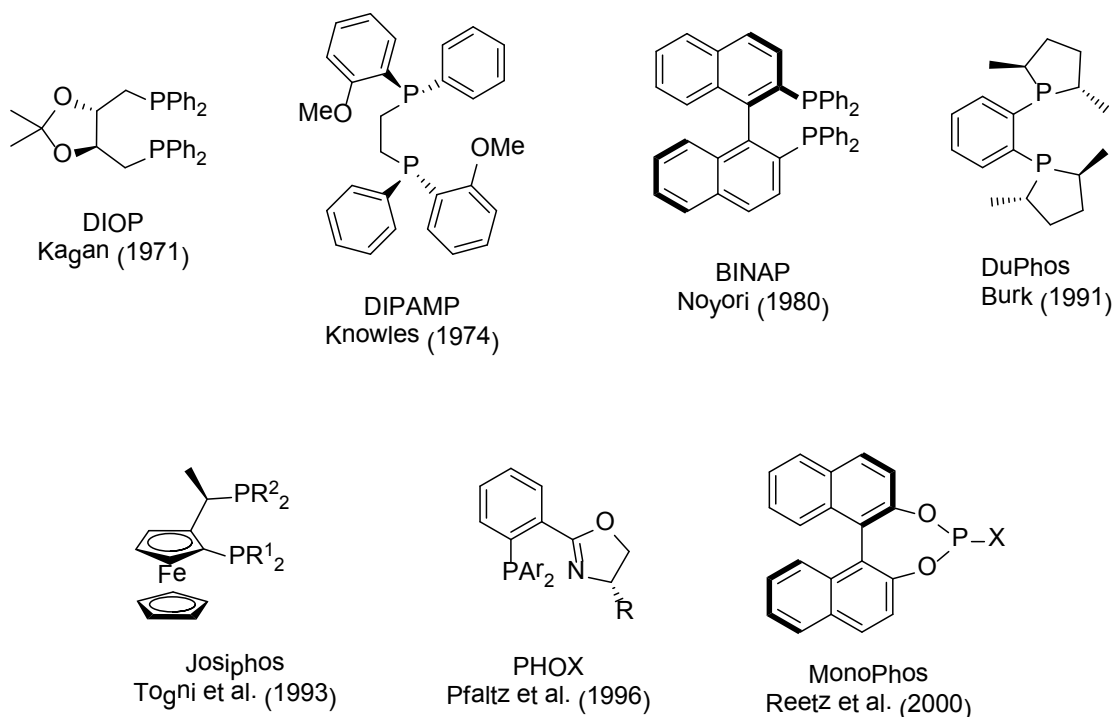


Figure 1-2. Milestones in Chiral Ligands Design.

In the early 1990s, Burk's discovery of DuPhos family proved to be one of the most efficient ligands for a wide variety of substrates such as α -, and β -dehydroamino acid derivatives, enol acetates, N-acylhydrazones, enamides, enol esters and β -keto ester derivatives.¹¹

In the 21st century, tremendous progress in asymmetric asymmetric hydrogenation were made on the development of high performance ligands. For example, Imamoto made significant contributions in developing P-chiral BisP* ligands.¹² Zhang's group¹⁴ developed the more rigid cyclic P-chiral TangPhos¹³ and DuanPhos (Figure 1-3). With the development of vast number of powerful chiral ligands, asymmetric hydrogenation provided both high enantioselectivities and turnover numbers for a wide range of prochiral unsaturated substrates, such as cyclic and acyclic imines,

iminium salts, functionalized and unfunctionalized olefins (including dehydro amino acids and esters, dehydro amino alcohols, enamines and enamides), simple and functionalized ketones (Figure 1-4).¹⁵ Practical applications with low catalyst loading and complex substrate structures have continued to emerge. The transition metals also were expanded from precious rhodium, ruthenium and iridium to cobalt, nickel and even iron.

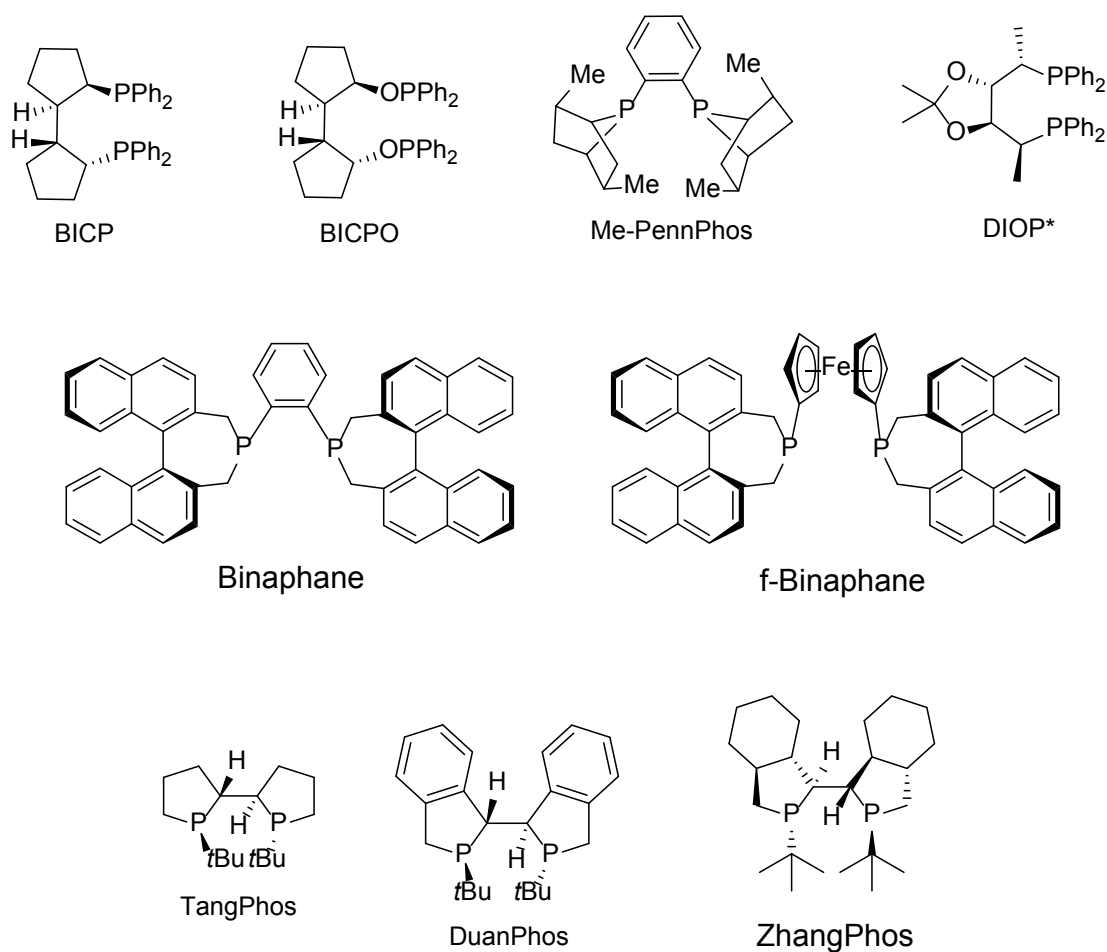


Figure 1-3. Chiral ligands Developed by Zhang's Group for Hydrogenation.

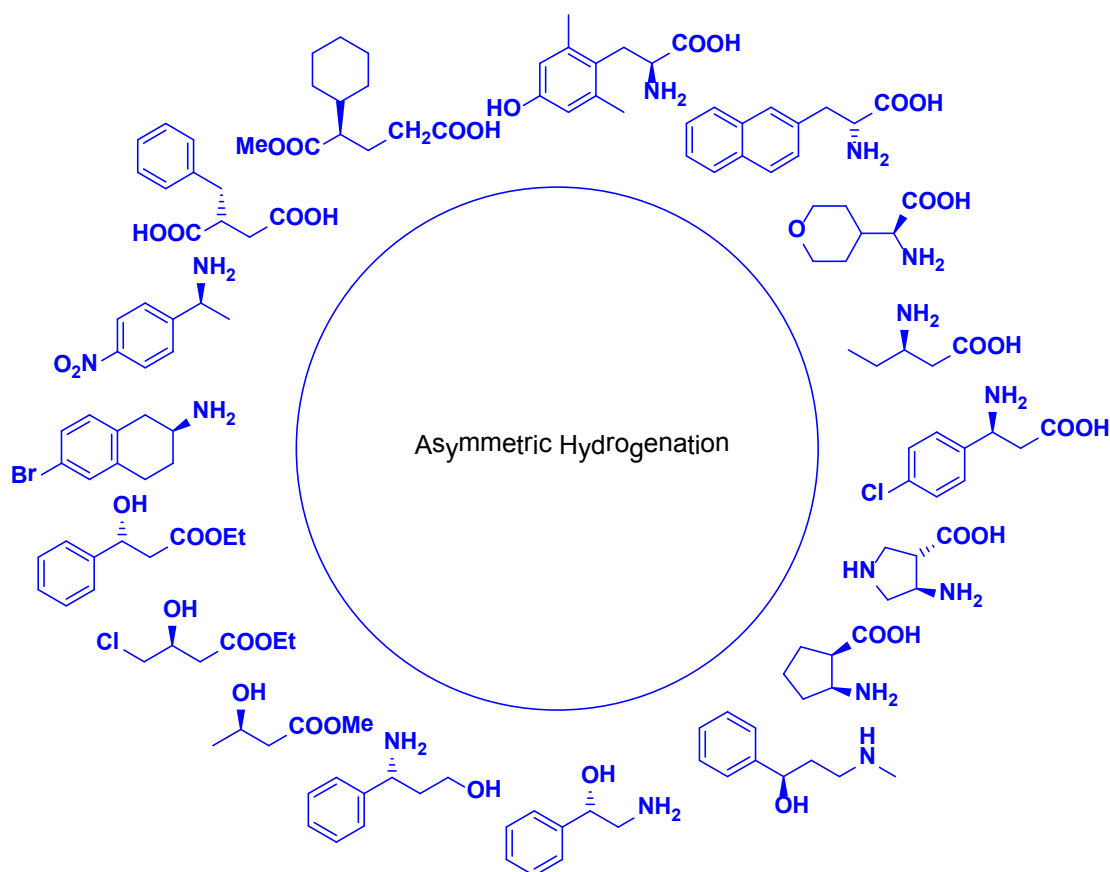


Figure 1-4. Chiral Compounds Yielded from Asymmetric Hydrogenation.

1.2 Asymmetric Hydrogenation of N-heteroarenes and Arenes

Compared to the most common types of unsaturated substrates for asymmetric hydrogenation, such as ketones, imines, and olefins, the asymmetric hydrogenation of heteroaromatic and aromatic compounds will give the greatest number of potential chiral compounds. First, many aromatic compounds are readily available and complicated substitution patterns can be easily achieved. Assuming that there are 10 choices for the substituents at every position of the common arene ring (benzene), up to 10^5 and 10^6 of compounds can be derivated from hydrogenation of pyridines and

arenes (Figure 1-5). Besides, the number will be dramatically increased while the aromatic rings can fuse with other rings on an edge to provide polycyclic compounds such as naphthalenes, quinolines, quinoxalines, indoles, benzofurans, etc. Given the right combination of ligands and catalysts, asymmetric hydrogenation could provide efficient and straightforward access to the corresponding chiral saturated and partially saturated compounds bearing cyclic skeletons. However, the past effort has mainly focused on asymmetric hydrogenation of ketones and alkenes and excellent results have been achieved. In sharp contrast, the asymmetric hydrogenation of arenes/heteroarenes is a much less explored area.

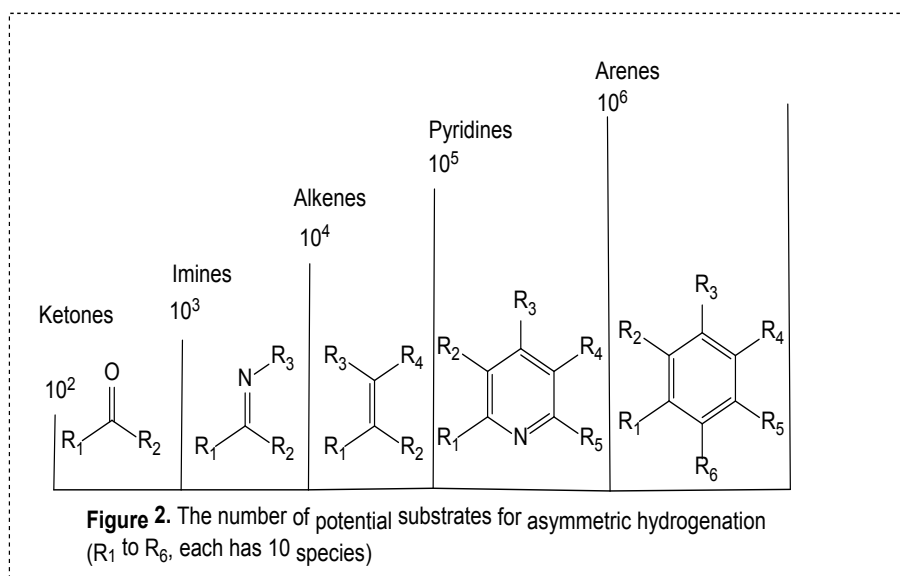


Figure 1-5 The Number of Potential Substrates for Asymmetric Hydrogenation (R₁ and R₆, each has 10 choices).

This may be ascribed to the following reasons. First, the high stability of these aromatic compounds caused low activity; harsh conditions often are needed to destroy the aromaticity, which adversely affects the enantioselectivity.¹⁶ Secondly, some

heteroaromatic compounds containing nitrogen and sulfur atoms may poison and/or deactivate the chiral catalysts. Third, the lack of secondary coordinating group in simple aromatic compounds may be responsible for the difficulty in achieving high activity and/or enantioselectivity.

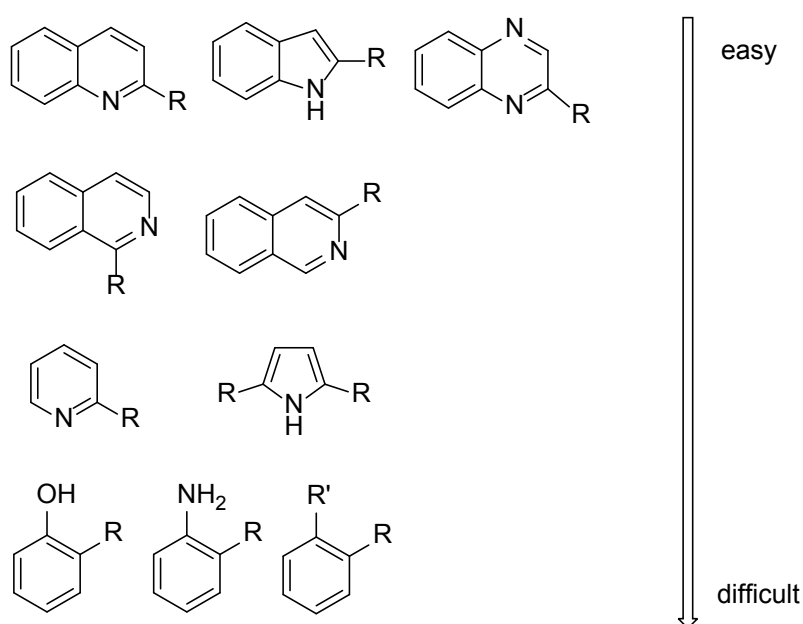
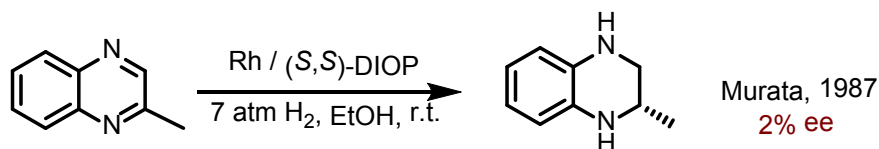


Figure 1-6. Challenges of Hydrogenation of Aromatic Compounds.

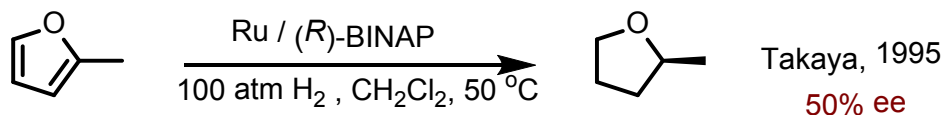
Normally, bicyclic aromatic compounds are relatively easy to hydrogenate due to the lower aromaticity with one aromatic ring reserved in the hydrogenation process. Single-ring aromatic compounds containing nitrogen and oxygen atoms are also relatively easy to hydrogenate, especially those with aromatic amines as products. Yet single-ring aromatic compounds such as simple pyridines and benzene derivatives are the most challenging substrates for hydrogenation (Figure 1-6). Not surprisingly, most current studies on asymmetric hydrogenation of aromatic compounds mainly focus on

bicyclic aromatics and single ring heteroaromatics containing nitrogen or oxygen atoms.

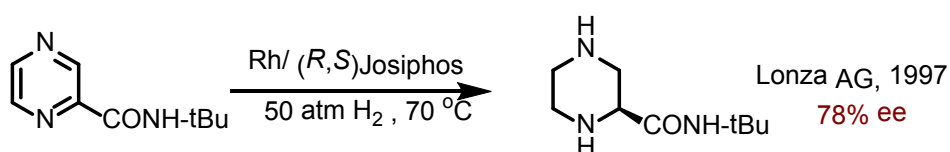
Despite the above challenges, the asymmetric hydrogenation of aromatic compounds has been investigated. In 1987 Murata and co-workers reported the first example of homogeneous asymmetric hydrogenation of aromatic compounds in which they subjected 2-methylquinoxaline in ethanol under hydrogen using $\text{Rh}[(\text{S,S})\text{-DIOP}]\text{H}$ as catalyst. However, only 2% ee was obtained (Scheme 1-1).¹⁷ In 1995 Takaya and co-workers achieved a significant improvement (50% ee) in the hydrogenation of 2-methylfuran using a chiral Ru complex with (*R*)-BINAP ligand as catalyst (Scheme 1-2).¹⁸ In 1997 Lonza AG filed a patent on asymmetric hydrogenation of pyrazinecarboxylic acid derivatives using $[\text{Rh}(\text{COD})\text{Cl}]_2/\text{Josiphos}$ (up to 78% ee) (Scheme 1-3).¹⁹ One year later, Bianchini developed an orthometalated dihydride iridium complex for hydrogenation of 2-methylquinoxaline to 1,2,3,4-tetrahydro-2-methylquinoxaline with up to 90% ee (Scheme 1-4).²⁰ Notably, this is the first example of asymmetric hydrogenation of aromatic compounds with >90% ee, while conversion is not satisfactory. These pioneering works demonstrated the feasibility of highly enantioselective hydrogenation of aromatic compounds and have opened a new avenue to the synthesis of chiral heterocyclic compounds from readily available aromatic compounds. Considering the diversity of aromatic compounds and the great importance of the corresponding hydrogenated products, the discovery of new highly efficient catalytic systems will make a major impact in organic synthesis and industrial application.



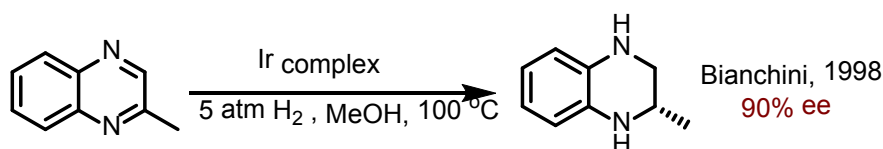
Scheme 1-1. The First Example of Enantioselective Hydrogenation of Aromatic Compounds.



Scheme 1-2. Ruthenium-BINAP System for Furan Hydrogenation.



Scheme 1-3. Rh/Josiphos System for Pyrazine Hydrogenation.



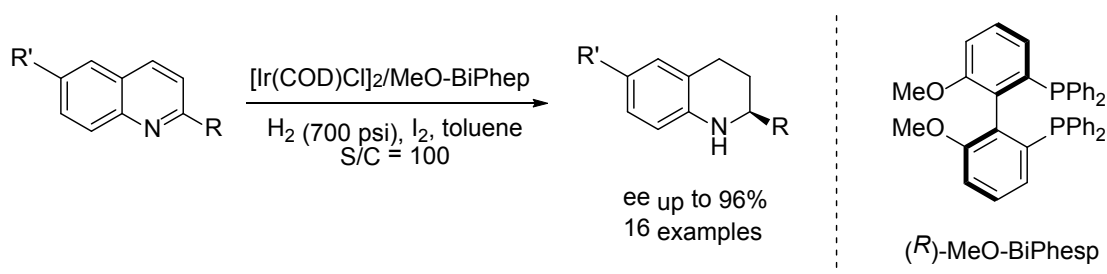
Scheme 1-4. The First Example of Enantioselective Hydrogenation of Aromatic Compounds with >90% Enantioselectivity.

In this chapter, we present an overview of the achievements of asymmetric hydrogenation of important classes of heteromatic/aromatic compounds. The development of effective catalytic systems and their applications in the synthesis of

numbers of chiral compounds are summarized.

1.2.1 Asymmetric Hydrogenation of Quinoline Derivatives

1,2,3,4-Tetrahydroquinolines are ubiquitous in both natural alkaloids and synthetic molecules. The asymmetric hydrogenation of readily available quinolines provided a concise and straightforward access to chiral 1,2,3,4-Tetrahydroquinolines in an atom efficient way. In 2003, Zhou reported the first example of highly enantioselective hydrogenation of quinolines with iridium catalyst generated in situ from $[\text{Ir}(\text{COD})\text{Cl}]_2$ and axially chiral bisphosphine ligand MeO-BiPhep with the addition of iodine as activator (Scheme 1-5).²¹

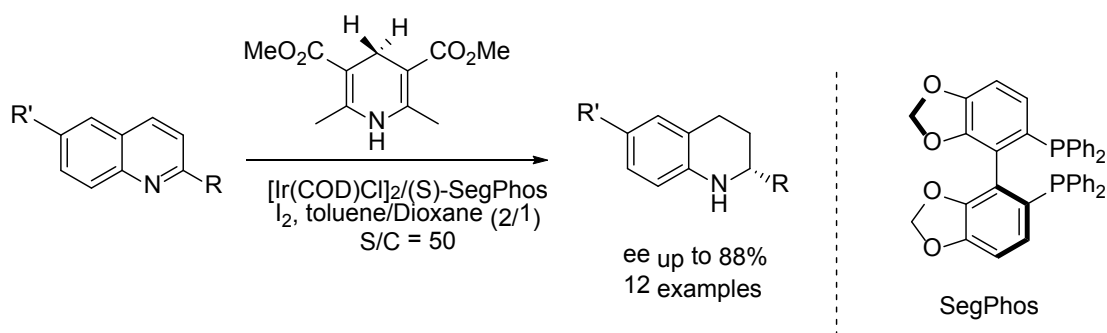


Scheme 1-5. Ir-catalyzed Asymmetric Hydrogenation of 2-substituted Quinolines.

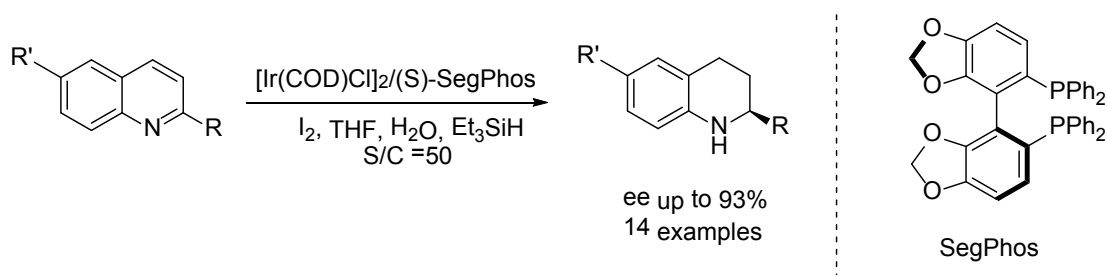
Since then numerous catalysts involved various chiral transition-metal catalysts and organocatalysts have been developed for the asymmetric hydrogenation in quinolines. Most of the studies focused on highly effective bidentate phosphorus ligands, especially atropisomeric biaryl diposphine ligands. Diphosponite ligands,

and phosphine-phosphoramidite ligands as well as other phosphorus-containing ligands such as *N,P*-ligands, *S,P*-ligands, and monodentate phosphine ligands, have been proven effective for iridium-catalyzed asymmetric hydrogenation of quinolines. Phosphine free ligands such as chiral diamine ligands were also successfully applied to asymmetric hydrogenation of quinolines with iridium complex. For these catalytic systems, iodine was the most commonly used additive to activate the catalyst.²¹ Chloroformates as well as Brønsted acids were often employed to activate the substrates.^{22, 23}

Meanwhile the asymmetric transfer hydrogenation catalyzed by iridium complex was also realized. Other types of hydrogen sources, such as Hantzsch ester and water in combination with saline, was introduced with the Ir/P-P*/I₂ catalytic system (Scheme 1-6 and Scheme 1-7).^{24, 25}



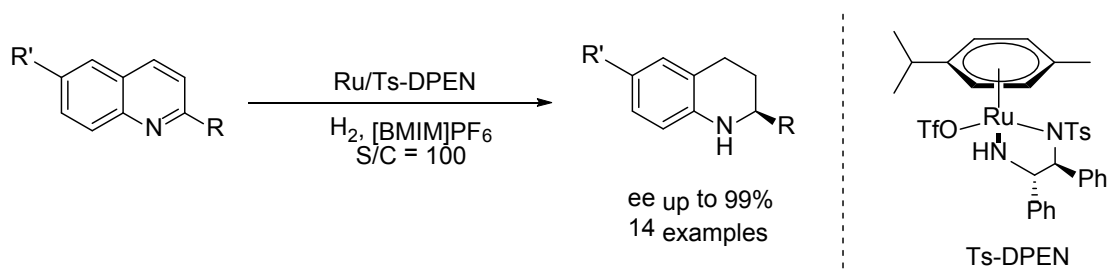
Scheme 1-6. Ir-Catalyzed Asymmetric Transfer Hydrogenation of Quinolines.



Scheme 1-7. Ir-Catalyzed Asymmetric Hydrogenation of Quinolines with Silane/Water.

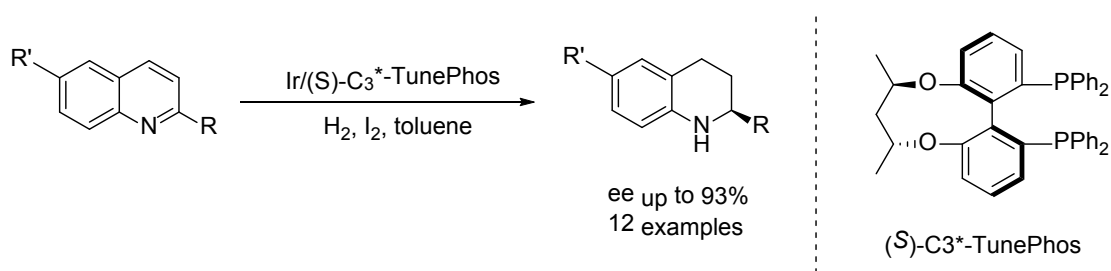
It was notable that most of the catalytic system for quinoline hydrogenation suffered from low catalytic activity (a low substrate-to-catalyst ratio of 100). This may be ascribed to the deactivation of iridium catalyst by formation of catalytically unreactive dimers and trimers through hydride-bridged bonds under hydrogen atmosphere.²⁶

After the great success iridium had achieved in the asymmetric hydrogenation of quinolines, air-stable Ru/Rh/Ts-DPEN catalyst also found its application in this field and up to 99% ee was obtained (Scheme 1-8).²⁷



Scheme 1-8. Ru-Catalyzed Asymmetric Hydrogenation of Quinolines.

Zhang's group also contribute to this field by applying the 3,5-tBu-phenyl-substituted ligand (S)-C3*-TunePhos to achieve enantioselectivity of up to 93% and greater than 90% conversions (Scheme 1-9).



Scheme 1-9. (S)-C3*-TunePhos Catalyzed Asymmetric Hydrogenation of Quinolines.

In Summary, direct catalytic asymmetric hydrogenation of quinolines constitutes the most convenient route to enantiomerically pure tetrahydroquinolines, which are not only useful synthetic intermediates but also structural moieties in biologically active alkaloids. Several efficient catalytic systems have been successfully developed though the asymmetric hydrogenation of quinolines still suffered from low reactivity in most cases (S/C ratio of 100). Nevertheless, electron-deficient ligands such as P-Phos and DifluorPhos were found to be more reactive (S/C ratio up to 43 000). Ligand with rigid backbone such as SpiroPO or with encapsulation of the ligand into a dendrimer framework (**L12**) to inhibit deactivation also increased the productivity (Figure 1-7). The development of more efficient catalytic systems to promote this process is highly desirable.

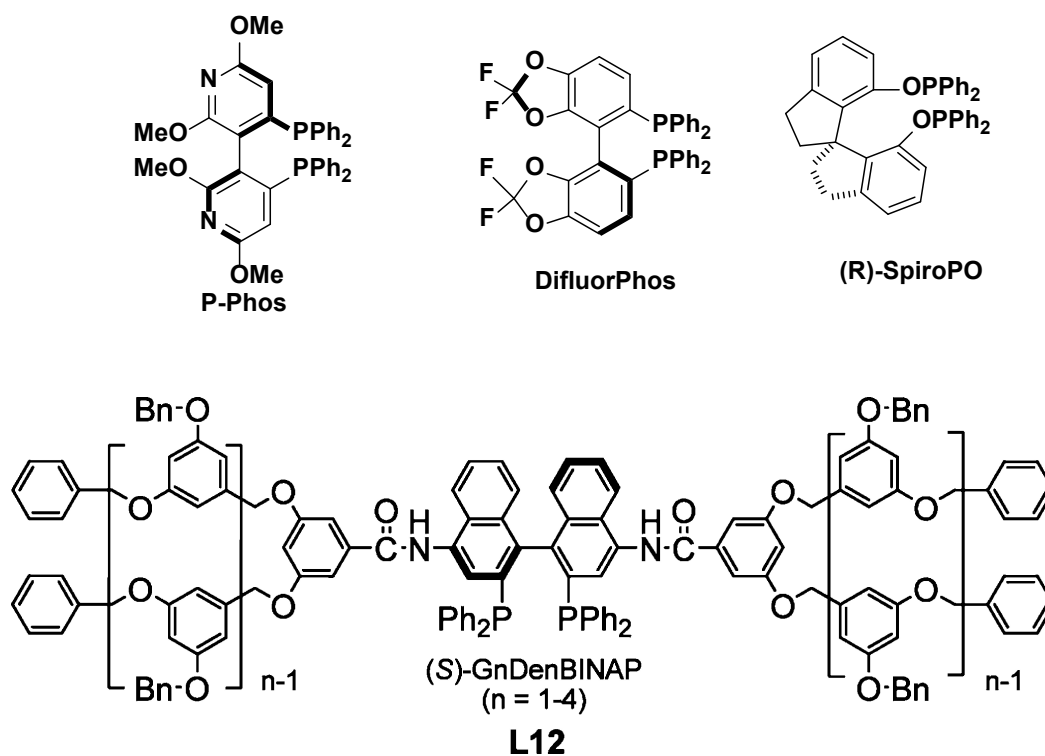
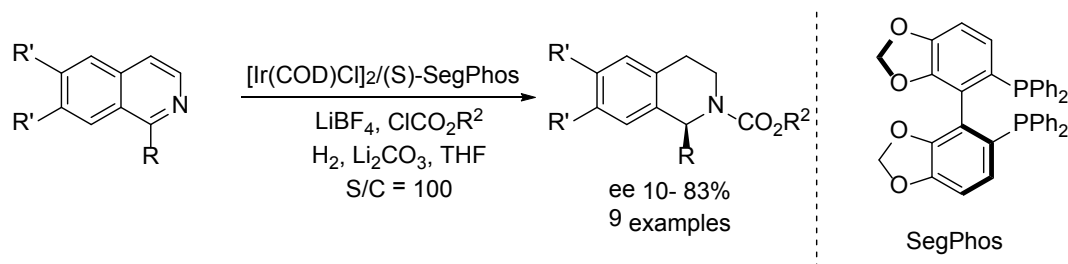


Figure 1-7. P-Phos, DifluorPhos, SpiroPO and Dendritic GnDenBINAP.

1.2.2 Asymmetric Hydrogenation of Isoquinoline Derivatives

Isoquinoline is one of the most challenging substrates for asymmetric hydrogenation. It shows no activity to a number of catalytic systems, which are efficient for asymmetric hydrogenation of ketones, alkenes, and imines. In 2006, Zhou and coworkers reported the first example on asymmetric hydrogenation of isoquinolines by using $[\text{Ir}(\text{COD})\text{Cl}]_2/(\text{S})\text{-SegPhos}$ with chloroformates as activating reagents as in the case of quinolines (Scheme 1-10).²² However, the asymmetric hydrogenation of isoquinolines was more difficult than quinolines – only partially hydrogenated 1,2-dihydroisoquinolines were obtained as products. Under the optimal conditions, only 10-83% ee was achieved. Apparently more efficient catalyst systems

are needed to be developed.



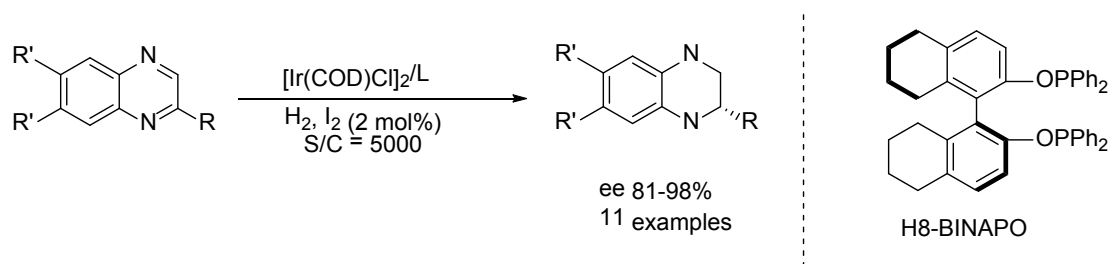
Scheme 1-10. Chloroformates Activated Asymmetric Hydrogenation of Isoquinolines.

1.2.3 Asymmetric Hydrogenation of Quinoxaline Derivatives

The asymmetric hydrogenation of quinoxalines provides the chiral tetrahydroquinoxalines, which are of great biological interest.²⁸ A number of transition metal catalysts involving rhodium, iridium, and ruthenium complexes as well as organocatalysts were developed for the enantioselective hydrogenation of quinoxalines. The combination of transition metal catalyst and organocatalyst in one pot with successive hydrogenation and transfer hydrogenation sequence was also developed for reduction of quinoxalines.

As mentioned above, the first example of asymmetric hydrogenation of quinoxaline was reported in 1987 by Murata and co-workers. $\text{Rh}[(S,S)\text{-DIOP}]\text{H}$ was used as the catalyst for the hydrogenation of 2-methylquinoxaline but only 2% ee was obtained (Scheme 1-1).¹⁷ In 1998, Bianchini developed an orthometalated dihydride iridium complex for hydrogenation of 2-methylquinoxaline to

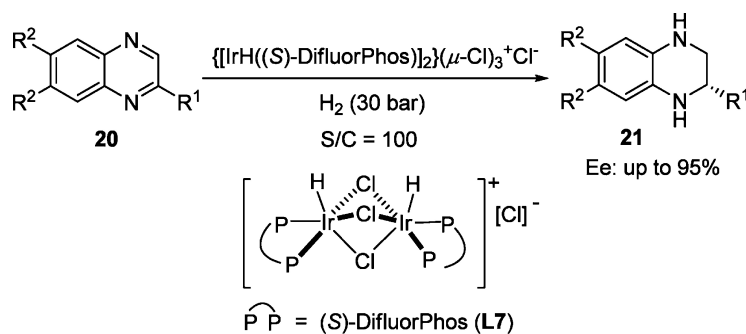
1,2,3,4-tetrahydro-2-methylquinoxaline with up to 90% ee and moderate yield (54%) in MeOH (Scheme 1-4).²⁰ More recently, A highly efficient iridium-catalyzed asymmetric hydrogenation of quinoxalines was developed with (R)-H8-BINAPO as the ligand. This catalytic system provided chiral tetrahydroquinoxalines with good to excellent enantioselectivities (81-98% ee) and full conversion (S/C = 5000) (Scheme 1-11).²⁹ Notably, iodine plays a crucial role for achieving excellent enantioselectivity in reduction of quinoxalines, which is in agreement with Ir-catalyzed asymmetric hydrogenation of quinolines.



Scheme 1-11. Ir-Catalyzed Asymmetric Hydrogenation of Quinoxalines.

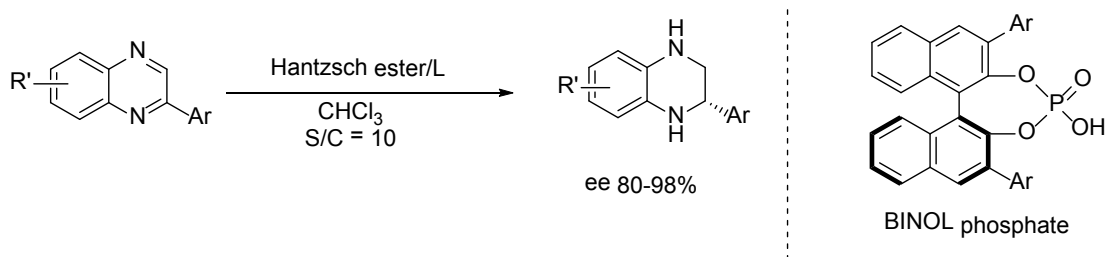
In 2010, Ohshima, Mashima, and Ratovelomanana-Vidal et al. reported that a cationic dinuclear triply halogen-bridged iridium complexes $\{[\text{IrH}((S)\text{-DifluorPhos})]_2(\mu\text{-Cl})_3\}^+\text{Cl}^-$ bearing a chloride catalyzed asymmetric hydrogenation of 2-alkyl- and 2-aryl-substituted quinoxalines resulting in considerably improved ee (86–95%) over the corresponding iodo-iridium catalyst (Scheme 1-12).³⁰ This unprecedented halide dependence was consistent with their previous work on the asymmetric reduction of 2-substituted quinolinium salts, where

chloro- and bromo-iridium catalysts also gave superior catalytic performance over the corresponding iodo-iridium catalyst.³¹



Scheme 1-12. Cationic Dinuclear Triply Halogen-Bridged Iridium Complexes for Asymmetric Hydrogenation of Quinoxalines.

In addition to the success achieved by transition metal catalyzed asymmetric hydrogenation of quinoxalines, asymmetric transfer hydrogenation also was extended to the field of synthesis of 2-Aryl-tetrahydroquinoxalines by Rueping. With the help of BINOL phosphate (R)-L28f and Hantzsch ester, excellent enantioselectivities (80-98% ee) was obtained in good yield (73-98%) (Scheme 1-13),³² yet alkyl-substituted quinoxalines suffered lower enantioselectivities under the same conditions.

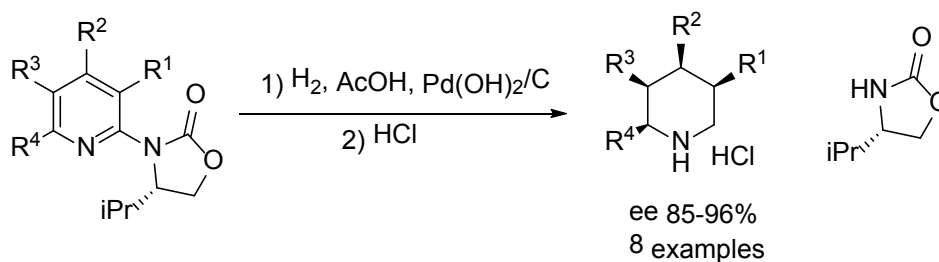


Scheme 1-13. Organocatalyzed Asymmetric Transfer Hydrogenation of Quinoxalines.

1.2.4 Asymmetric Hydrogenation of Pyridine Derivatives

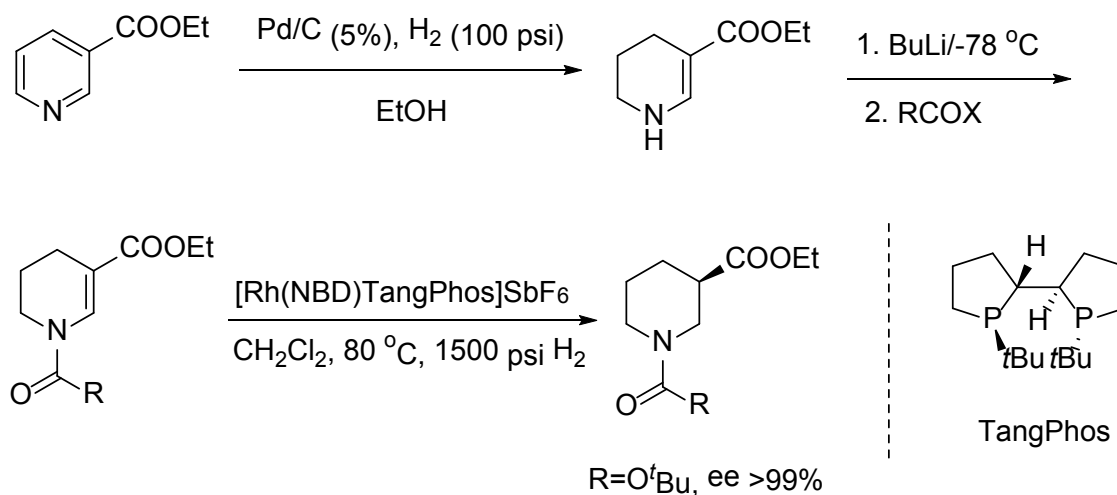
Chiral piperidines are ubiquitous substructures in natural alkaloids and many biologically relevant molecules.^{33,34} Among the numerous methodologies,³⁵ asymmetric hydrogenation of pyridine derivatives is undoubtedly the most direct and effective approach to obtain optically active piperidines. However, until now, there are only limited reports about hydrogenation of pyridine derivatives.

Two major hydrogenation approaches have been investigated to access chiral piperidines: the diastereoselective hydrogenation of a chiral precursor and the enantioselective hydrogenation of a prochiral substrate with a chiral catalyst. For diastereoselective hydrogenation, efforts were made to covalently bond methyl-2-nicotinic acid to several optically pure auxiliaries in the presence of supported metallic catalysts. However, low diastereoselectivity was obtained.^{36,37} Glorius and co-workers reported a breakthrough on highly efficient diastereoselective hydrogenation of *N*-(2-pyridyl)-oxazolidinones by using a chiral oxazolidinone as the auxiliary and Pd(OH)₂/C as the catalyst (Scheme 1-14).³⁸ The addition of acid in this transformation not only activates the pyridine for hydrogenation, but also suppresses the product piperidine to poison the catalyst. The high diastereoselectivity is ascribed to strong hydrogen bonding between the pyridinium and oxazolidinone moiety in acetic acid.



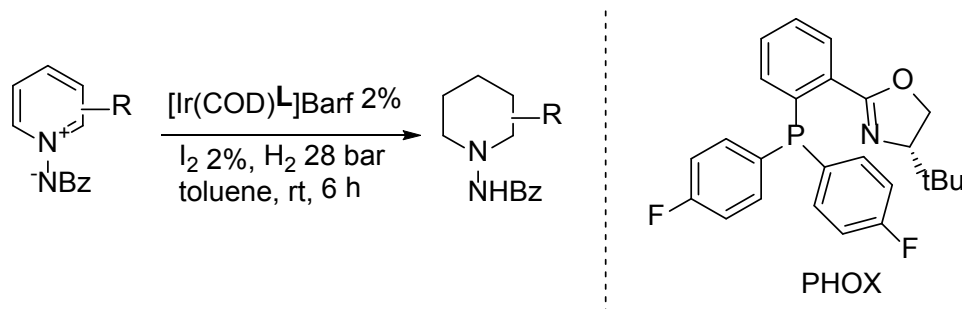
Scheme 1-14. Diastereoselective Hydrogenation of Pyridines with $\text{Pd(OH)}_2/\text{C}$.

Significant efforts have been devoted to the enantioselective hydrogenation of a prochiral substrate with a chiral catalyst. In 2000, Studer and co-workers investigated the asymmetric hydrogenation of 2- or 3-substituted pyridine derivatives by screening various combination of $\text{Rh(NBD)}_2\text{BF}_4$ and chiral ligands.³⁹ However, only low enantioselectivities (up to 25%) were obtained. In 2006, Zhang, Lei, and co-workers reported an indirectly enantioselective hydrogenation of 3-substituted pyridine derivatives (Scheme 1-15).⁴⁰ In this process partial hydrogenation of 3-substituted nicotines with Pd/C gave tetrahydropyridines, followed by *N*-protection with RCOX , and then enantioselective homogeneous hydrogenation using $\text{Rh(NBD)(TangPhos)SbF}_6$ as the catalyst gave complete hydrogenation piperidines. However, high H_2 pressure (102 atm) and temperature (80 °C) were necessary to get practical conversion.



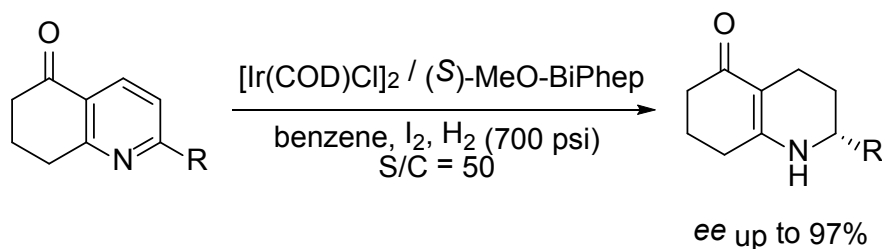
Scheme 1-15. Rhodium-Catalyzed Step-wise Hydrogenation of Pyridines.

In 2005, Charette and co-workers examined the asymmetric hydrogenation of *N*-iminopyridinium ylides and excellent enantioselectivities were achieved.⁴¹ They found that cationic iridium complex of phosphinooxazoline with tetrakis(3,5-bis(trifluoromethyl)phenyl)borate (BARF) as the counterion and a catalytic amount of iodine provided the highest enantioselectivities (54–90% ee) (Scheme 1-16). The obtained hydrogenation adducts can be converted to the corresponding piperidine derivatives with Raney nickel or lithium in ammonia to cleave the N–N bond.



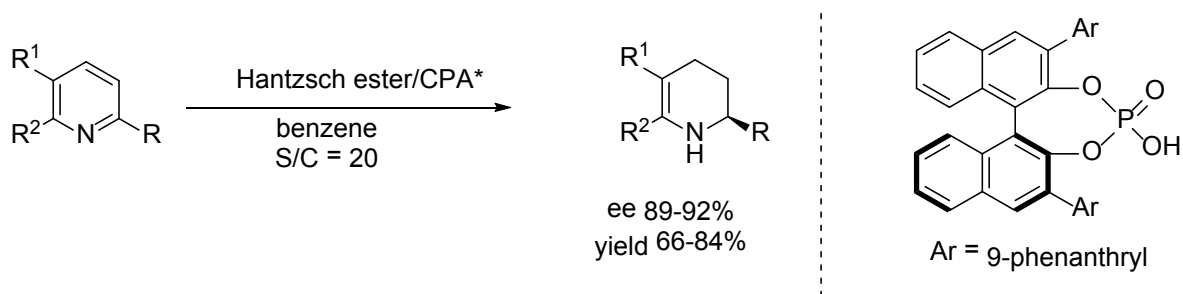
Scheme 1-16. Iridium-Catalyzed Asymmetric Hydrogenation of *N*-Benzoyliminopyridinium Ylides.

In 2008, Zhou and co-workers revealed that the $[\text{Ir}(\text{COD})\text{Cl}]_2/(S)\text{-MeO-BiPhep}/\text{I}_2$ catalyst system could effectively catalyzed asymmetric hydrogenation of pyridine derivatives (Scheme 1-17) as it did for quinolines.^{21,42} Good yields and excellent enantioselectivities (84–97% ee) were obtained for a variety of 2-alkyl and 2-phenyl substituted 7,8-dihydro-quinolin-5(6*H*)-ones (Scheme 1-17). Nevertheless, this catalyst system is not general for other pyridine derivatives. For acyclic trisubstituted substrate bearing ester at the 3-position there is no catalytic activity. For the 2,6-dimethylpyridine-3-carbonitrile, low conversion of 21% and 85% ee were obtained. In contrast, substrates with acyl group at the 2-position can be hydrogenated with full conversion but with low ee.⁴²



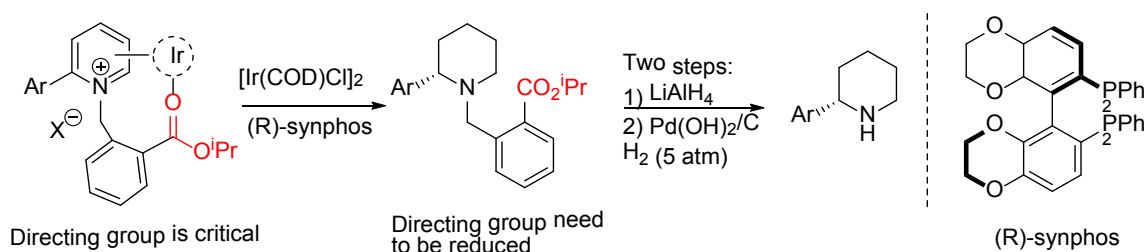
Scheme 1-17. Iridium-Catalyzed Asymmetric Hydrogenation of 7,8-Dihydroquinolin-5(6*H*)-ones.

More recently, Rueping and co-workers successfully achieved asymmetric transfer hydrogenation on the strong electron-withdrawing substitutes at the 3-position of pyridines with excellent enantioselectivities and moderate to good yield.⁴³ They proposed the pyridine was activated by Bronsted acid through protonation (Scheme 1-18)



Scheme 1-18. Brønsted Acid-Catalyzed Enantioselective Reduction of Pyridines.

In 2012, Zhou and coworkers have reported the successful asymmetric hydrogenation of *N*-(2-CO₂*i*Pr)benzylpyridinium where the ester is believed to act as a directing group for the catalyst (Scheme 1-19).⁴⁴ However the drawback of this strategy is, for most cases, extra steps are required for removing the activating groups to get to the desired chiral piperidines.

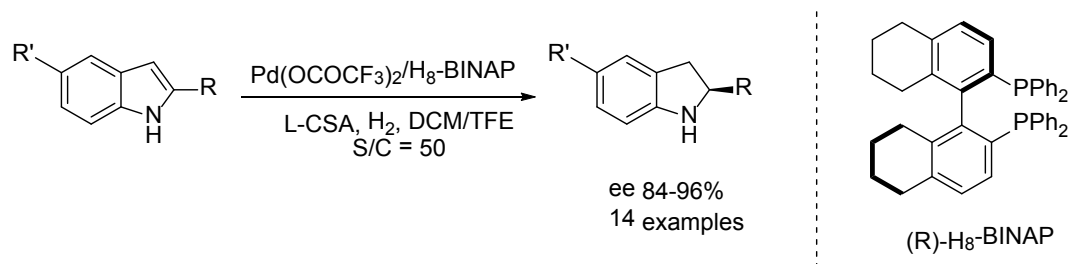


Scheme 1-19. Iridium-Catalyzed Asymmetric Hydrogenation of 2-Substituted Pyridinium Salts with a Directing Group.

1.2.5 Asymmetric Hydrogenation of other Heteroaromatics and Arenes

1.2.5.1 Asymmetric Hydrogenation of Indoles

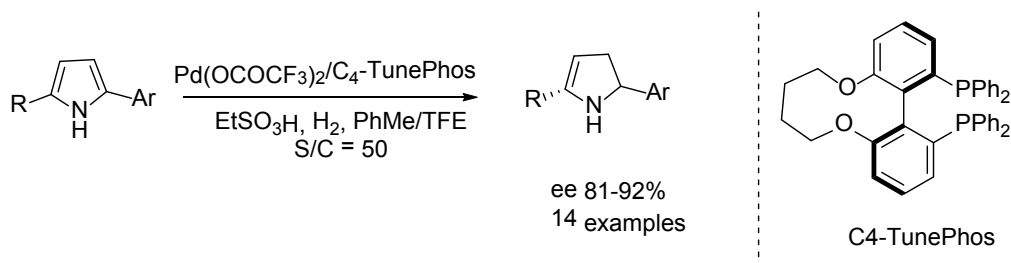
Chiral indolines are ubiquitous structural motifs in naturally occurring alkaloids and many biological active molecules.⁴⁵ Asymmetric hydrogenation of indoles is the most straight and powerful approach to make chiral indolines in terms of simplicity and atom efficiency. In 2000, Kuwano and Ito developed the first highly effective hydrogenation of a series of *N*-protected indoles using a Rh complex.⁴⁶ Since then some other catalytic systems such as ruthenium, iridium, and palladium were introduced.⁴⁷ In most these examples, the indole substrates have to bear an electron-withdrawing protecting group, such as Ac, Ts, or Boc on the nitrogen atom. In 2010, Zhou and co-workers reported the first example of highly enantioselective hydrogenation of *N*-unprotected simple indoles with a Brønsted acid as an activator to form the iminium intermediate *in situ*, which was hydrogenated using Pd(OCOCF₃)₂/(*R*)-H8-BINAP catalyst system. This method provides an efficient route to 2-substituted and 2,3-disubstituted indolines with up to 96% ee (Scheme 1-20).⁴⁸



Scheme 1-20. Pd-Catalyzed Asymmetric Hydrogenation of *N*-Unprotected Indoles.

1.2.5.2 Asymmetric Hydrogenation of Pyrroles

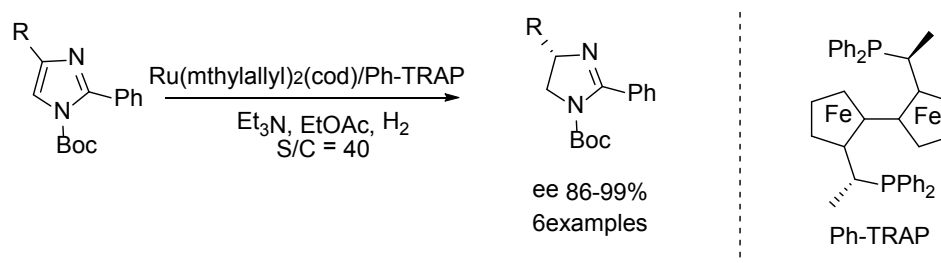
In 2008, Kuwano and co-workers reported their pioneering work for asymmetric hydrogenation of *N*-Boc-protected pyrroles using a chiral Ru catalyst.⁴⁹ Considering the similarity of indoles and pyrroles, both of which are electron-enriched arenes and can be protonated by Brønsted acid, the previous strategy for the hydrogenation of the former was employed by Zhou and co-workers. A highly enantioselective Pd-catalyzed partial hydrogenation of simple 2,5-disubstituted pyrroles with a Brønsted acid as an activator was successfully developed, providing chiral 2,5-disubstituted 1-pyrrolines with up to 92% ee (Scheme 1-21).⁵⁰



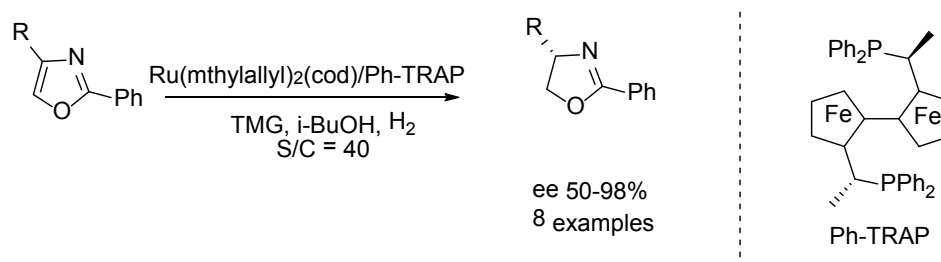
Scheme 1-21. Pd-Catalyzed Asymmetric Hydrogenation of Simple Pyrroles.

1.2.5.3 Asymmetric Hydrogenation of Imidazoles and Oxazoles

Both imidazoles and oxazoles are five-membered aromatic compounds containing two different heteroatoms, and both were hydrogenated by the same catalytic system developed by Kuwano group to afford the products with high to excellent ee values (Scheme 1-22 and Scheme 1-23).⁵¹



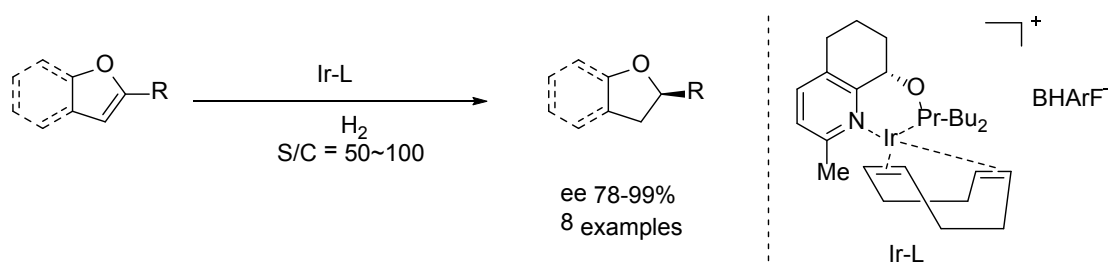
Scheme 1-22. Ru-Catalyzed Asymmetric Hydrogenation of Imidazoles.



Scheme 1-23. Ru-Catalyzed 4-Substituted 2-Phenyloxazoles.

1.2.5.4 Asymmetric Hydrogenation of Furans

Ruthenium and rhodium catalysts were tested for the asymmetric hydrogenation of furans.⁵² Meanwhile, diastereoselective and heterogeneous-catalyzed hydrogenation was also developed.^{39, 52} Chiral iridium complexes based on the P,N-ligands were often applied in the hydrogenation of unfunctionalized olefins. Therefore, Pfaltz and co-workers applied this pyridine-phosphinite-ligated iridium complexes effectively in the asymmetric hydrogenation of furans and benzofurans (Scheme 1-24).⁵³

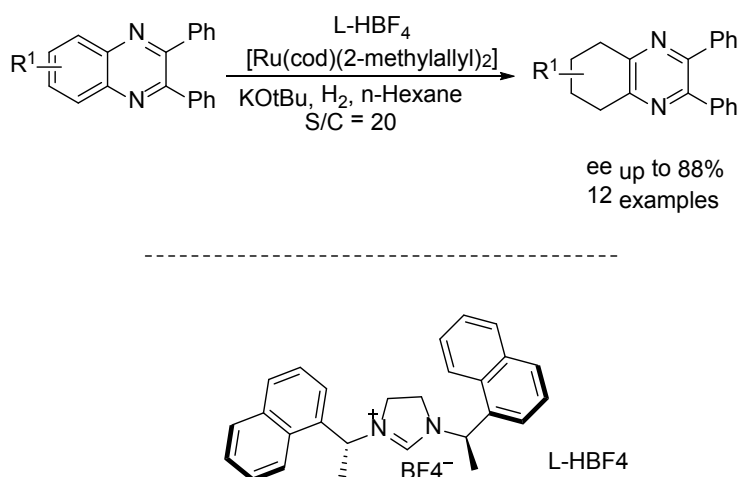


Scheme 1-24. Iridium-Catalyzed Asymmetric Hydrogenation of Furan Derivatives.

1.2.5.5 Asymmetric Hydrogenation of Arenes

Due to its strong aromaticity and low coordinating ability, asymmetric hydrogenation of arenes is the most challenging subject in asymmetric catalysis. At present, limited efforts have been tried, but very poor enantioselectivity was obtained.⁵⁴ In 2011, Glorius and co-workers found that a homogeneous chiral

ruthenium NHC (*N*-heterocyclic carbene) complex could selectively hydrogenation of the aromatic carbocyclic ring of substituted quinoxalines.⁵⁵ Notably, this is the first example of homogeneous catalytic asymmetric hydrogenation of carbocyclic ring of aromatic compounds (Scheme 1-25).



Scheme 1-25. Ru/NHC-Catalyzed Asymmetric Hydrogenation of Carbocyclic Ring of Quinoxalines

1.3 Strategies for Asymmetric Hydrogenation of Aromatic Compounds

As mentioned in the above overview, over the past decades, a number of effective catalytic systems have been developed for the asymmetric hydrogenation of heteroarenes and arenes. Several novel and efficient strategies were crucial for the development of successful asymmetric hydrogenation of aromatic compounds. First strategy is catalyst activation involving the addition of additives to form more active catalyst species and by fine tuning chiral ligands. Iodine is most common used

additive to activate the catalyst. Substrate activation is another important strategy, which introduces an activator to interact with the substrate and decrease the aromaticity partially. Sometimes a secondary coordination group is involved to assist coordination between substrate and catalyst. Chloroformates and Bronsted acid were commonly applied to activate the substrates. Relay catalysis is a step-wise strategy involving two hydrogenation catalysts for asymmetric hydrogenation of aromatic compounds: achiral catalyst hydrogenates the aromatic compounds to afford the partial hydrogenation intermediates, followed by enantioselective hydrogenation of the intermediates with chiral catalyst.

Despite the significant progresses achieved in asymmetric reduction of heteroarenes and arenes, this field is still far from being mature and full of unsettled problems. For instance, the asymmetric hydrogenation of easily accessible phenols, anilines, simple pyridines and arenes is among the most attractive targets. New and highly efficient chiral catalysts and activation strategies for such transformations are expected in the coming years.

References:

1. (a) Y. Izumi, A. Tai, *Stereo-Differentiating Reactions: The Nature of Asymmetric Reactions*; Academic Press: New York, **1977**. (b) B. Bosnich, Ed. In *Asymmetric Catalysis*; Martinus Nijhoff: New York, **1986**. (c) I. Ojima, Ed. In *Catalytic Asymmetric Synthesis*; VCH: New York, **1993**. (d) R. Noyori, *Asymmetric Catalysis in Organic Synthesis*; Wiley: New York, **1994**. (e) G. Jannes, Dubois, V., Eds. In *Chiral Reactions in Heterogeneous Catalysis*; Plenum: New York, **1995**. (f) B. Cornils, W. A. Herrmann, Eds. In *Applied Homogeneous Catalysis with Organometallic Compounds*; VCH: Weinheim, **1996**; Vols. 1 and 2. (g) I. Ojima, Ed. In *catalytic Asymmetric Synthesis*; Wiley-VCH; New York, 2010.
2. (a) R. Noyori, M. Kitamura, In *Modern Synthetic Methods*; R. Scheffold, Ed.; Springer: Berlin, **1989**; Vol. 5, p 115. (b) H. Takaya, T. Ohta, R. Noyori, In *Catalytic Asymmetric Synthesis*; Ojima, I., Ed.; VCH: New York, **1993**; p 1. (c) W. Tang, X. Zhang, *Chem. Rev.* **2003**, *103*, 3029.
3. For a review, see: *Asymmetric Catalysis on Industrial Scale: Challenges, Approaches and Solutions* Blaser, H.-U.; Schmidt E. Eds., Wiley-VCH, Weinheim, **2004**.
4. W. S. Knowles, M. J. Sabacky, *Chem. Commun.* **1968**, 1445.
5. (a) H. B. Kagan, T. P. Dang, *Chem. Commun.* **1971**, 481. (b) H. B. Kagan, T. P. Dang, *J. Am. Chem. Soc.* **1972**, *94*, 6429. (c) H. B. Kagan, N. Langlois, T. P. Dang, *J. Organomet. Chem.* **1975**, *90*, 353.
6. A. Miyashita, A. Yasuda, H. Takaya, K. Toriumi, T. Ito, T. Souchi, R. Noyori, *J. Am. Chem. Soc.* **1980**, *102*, 7932.
7. (a) M. J. Burk, *J. Am. Chem. Soc.* **1991**, *113*, 8518. (b) M. J. Burk, J. E. Feaster, W. A. Nugent, R. L. Harlow, *J. Am. Chem. Soc.* **1993**, *115*, 10125. (c) M. J. Burk, *Acc. Chem. Res.* **2000**, *33*, 363.
8. (a) A. Togni, C. Breutel, A. Schnyder, F. Spindler, H. Landert, A. Tijani, *J. Am. Chem. Soc.* **1994**, *116*, 4062. (b) H.-U. Blaser, W. Brieden, B. Pugin, F. Spindler, M. Studer, A. Togni, *Top. Catal.* **2002**, *19*, 3.
9. (a) G. Helmchen, A. Pfaltz, *Acc. Chem. Res.* **2000**, *33*, 336. (b) A. Pfaltz, W. J. Drury III, *Proc. Natl. Acad. Sci.* **2004**, *101*, 5723. (c) S. Bell, B. Wustenberg, S. Kaiser, F. Menges, T. Netscher, A. Pfaltz, *Science* **2006**, *311*, 642.
10. (a) C. Claver, E. Fernandez, A. Gillon, K. Heslop, D. J. Hyett, A. Martorell, A. G. Orpen, P. G. Pringle, *Chem. Commun.* **2000**, 961. (b) M. T. Reetz, G. Mehler, *Angew. Chem. Int. Ed.* **2000**, *39*, 3889. (c) M. Van den Berg, A. J. Minnaard, E. P. Schudde, J. van Esch, A. H. M. de Vries, J. G. de Vries, B. L. Feringa, *J. Am. Chem. Soc.* **2000**, *122*, 11539.
11. (a) M. J. Burk, *J. Am. Chem. Soc.* **1991**, *113*, 8518. (b) M. J. Burk, J. E. Feaster, W. A. Nugent, R. L. Harlow, *J. Am. Chem. Soc.*, **1993**, *115*, 10125. (c) M. J. Burk, *Acc. Chem. Res.* **2000**, *33*, 363.
12. (a) T. Imamoto, J. Watanabe, Y. Wada, H. Masuda, H. Tsuruta, S. Matsukawa, K. Yamaguchi, *J. Am. Chem. Soc.*, **1998**, *120*, 1635; (b) I. D. Gridnev, Y. Yamanoi, N. Higashi, H. Tsuruta, M. Yasutake, T. Imamoto, *Adv. Synth. Catal.*

- 2001**, 343, 118; (c) K. V. L. Crepy, T. Imamoto, *Adv. Synth. Catal.* **2003**, 345, 79.
13. (a) W. Tang, X. Zhang, *Angew. Chem. Int. Ed.* **2002**, 41, 1612; (b) W. Tang, X. Zhang, *Org. Lett.* **2002**, 4, 4159; (c) W. Tang, D. Liu, X. Zhang, *Org. Lett.* **2003**, 5, 205; (d) Q. Yang, G. Shang, W. Gao, J. Deng, X. Zhang, *Angew. Chem. Int. Ed.* **2006**, 45, 3832; (e) G. Shang, Q. Yang, X. Zhang, *Angew. Chem. Int. Ed.* **2006**, 45, 6360.
 14. (a) D. Liu, X. Zhang, *Eur. J. Org. Chem.* **2005**, 646; (b) X. Zhang, W. Tang, (The Penn State Research Foundation) US 2004/0229846 A1, 2004
 15. (a) W. Tang, X. Zhang, *Chem. Rev.* **2003**, 103, 3029. (b) J.-H. Xie, S.-F. Zhu, Q.-L. Zhou, *Chem. Soc. Rev.* **2012**, 41, 4126; (c) I. Ojima (Ed.), *Handbook of Homogeneous Hydrogenation*, Wiley-VCH, Hoboken, **2010**.
 16. C. Bird, W. *Tetrahedron* **1992**, 48, 335
 17. S. Murata, T. Sugimoto, S. Matsuura, *Heterocycles* **1987**, 26, 763
 18. T. Ohta, T. Miyake, N. Seido, H. Kumobayashi, H. Takaya, *J. Org. Chem.* **1995**, 60, 357
 19. US 5945534 Lonz G, **1997**
 20. C. Bianchini, P. Barbaro, G. Scapacci, E. Farnetti, M. Graziani, *Organometallics* **1998**, 17, 3308
 21. W.-B. Wang, S.-M. Lu, P.-Y. Yang, X.-W. Han, Y.-G. Zhou, *J. Am. Chem. Soc.* **2003**, 125, 10536.
 22. S.-M. Lu, W.-B. Wang, X.-W. Han, Y.-G. Zhou, *Angew. Chem. Int. Ed.* **2006**, 45, 2260
 23. D.-S. Wang, Y.-G. Zhou, *Tetrahedron Lett.* **2010**, 51, 3014
 24. D.-W. Wang, W. Zeng, Y.-G. Zhou, *Tetrahedron: Asymmetry* **2007**, 18, 1103
 25. D.-W. Wang, D.-S. Wang, Q.-A. Chen, Y.-G. Zhou, *Chem.-Eur. J.* **2010**, 16, 1133
 26. (a) D. Heller, A. H. M. de Vries, J. G. , de Vries, In *Handbook of Homogeneous Hydrogenation*; de Vries, J. G.; Elsevier, C. J., Eds.; Wiley-VCH Publishers: Weinheim, **2007**; (b) R. Crabtree, *Acc. Chem. Res.* **1979**, 12, 331
 27. (a) H.-F. Zhou, Z.-W. Li, Z.-J. Wang, T.-L. Wang, L.-J. Xu, Y.-M. He, Q.-H. Fan, J. Pan, L.-Q. Gu, A. S. C. Chan, *Angew. Chem., Int. Ed.* **2008**, 47, 8464; (b) T.-L. Wng, L.G. Zhuo, Z.-W. Li, F. Chen, Z.-Y. Ding, Y.-M. He, Q.-H. Fan, J.-F. Xiang, Z.-X. Yu, A.S.C.Chan, *J. Am. Chem. Soc.* **2011**, 133, 9878
 28. (a) M. Fantin, M. Marti, Yves P. Auberson, M. Morari, *Journal of Neurochemistry* **2007**, 103(6), 2200-2211; (b) TenBrink, R. E.; Im, W. B.; Sethy, V. H.; Tang, A. H.; Carter, D. B. *J. Med. Chem.* **1994**, 37, 758; (c) Li, S.; Tian, X.; Hartley, D. M.; Feig, L. A. *J. Neurosci.* **2006**, 26, 172
 29. W.-J. Tang; L.-J. Xu; Q.-H. Fan; J. Wang; B. M. Fan; Z. Y. Zhou; K.-H. Lam; A. S. C Chan; *Angew. Chem., Int. Ed.* **2009**, 48, 9135
 30. D. Cartigny; T. Nagano; T. Ayad; J.-P. Genêt; T. Ohshima; K. Mashima; V. Ratovelomanana-Vidal; *Adv. Synth. Catal.* **2010**, 352, 1886
 31. H. Tadaoka; Cartigny, D.; Nagano, T.; Gosavi, T.; Ayad, T.; Genet, J. P.; Ohshima, T.; Ratovelomanana-Vidal, V.; Mashima, K. *Chem.-Eur. J.* **2009**, 15, 9990

32. M. Rueping; F. Tato; F. R. Schoepke; *Chem.-Eur. J.* **2010**, 16, 2688
33. *Chiral Amine Synthesis*, T. C. Nugent, Ed.; Wiley-VCH, Weinheim, **2010**.
34. (a) L. Blomquist; K. Leander; B. Luning; J. Rosenblom; *Acta Chem. Scand.* **1972**, 26, 3203. (b) B. Tursch; D. Daloze; J. C. Braekman; C. Hootele; A. Caravador; D. Losman; R. Karlsson, *Tetrahedron Lett.* **1974**, 409. (c) J. Bosch; J. Bonjoch; In *Studies in Natural Products Chemistry*; Ed.; Elsevier: **1988**; Vol. 1, pp 31. (d) Y. Zhang; Y.-B. Liu; Y. Li; S.-G. Ma; L. Li; J. Qu; D. Zhang; X.-G. Chen; J.-D. Jiang; S.-S. Yu, *J. Nat. Prod.*, **2013**, 76, 1058. (e) M. R. Wood; S. D. Kuduk; M. G. Bock; R. K. Chang. *U.S. Patent* US2006/0128765 A1, **2006**. (f) S. V. Faraone; J. Biederman; C. P. Morley; T. J. Spencer; *J Am Acad Child Adolesc Psychiatry* **2008**, 47, 994. (f) C. Chen; R. B. Clark; Y. Deng; L. Plamondon; C. Sun; X.. Xiao; *International Patent* WO2012/021712 A1, **2012**.
35. a) M. Ye; G. Gao; A. J. F. Edmunds; P. A. Worthington; J. A. Morris; and Jin-Quan Yu. *J. Am. Chem. Soc.* **2011**, 133, 19090. (b) T. M. Nguyen and D. A. Nicewicz. *J. Am. Chem. Soc.* **2013**, 135, 9588. (c) K. D. Hesp; D. P. Fernando; W. Jiao; and A. T. Londregan. *Org. Lett.* **2014**, 16, 413. (d) Z. Peng; J. W. Wong; E. C. Hansen; A. L. A. Puchlopek-Dermenci; and H. J. Clarke. *Org. Lett.* **2014**, 16, 860. (e) H. Huang; T. C. Lacy; B. Bzachut; G. X. Ortiz Jr.; and Q. Wang. *Org. Lett.* **2013**, 15, 1818. (f) K. E. Henegar; R. Lira; H. Kim; and J. Gonzalez-Hernandez. *Org. Process Res. Dev.* **2013**, 17, 985. (g) D. J. Wallace; C. A. Baxter; K. J. M. Brands; N. Bremeyer; S. E. Brewer; R. Desmond; K. M. Emerson; J. Foley; P. Fernandez; W. Hu; S. P. Keen; P. Mullens; D. Muzzio; P. Sajonz; L. Tan; R. D. Wilson; G. Zhou; and G. Zhou. *Org. Process Res. Dev.* **2011**, 15, 831.
36. N. Douja; M. Besson; P. Gallezot; C. Pinel; *J. Mol. Catal. A: Chem.* **2002**, 186, 145.
37. N. Douja; R. Malacea; M. Banciu; M. Besson; C. Pinel; *Tetrahedron Lett.* **2003**, 44, 6991.
38. F. Glorius; N. Spielkamp; S. Holle; R. Goddard; C. W. Lehmann; *Angew. Chem. Int. Ed.* **2004**, 43, 2850.
39. M. Studer; C. Wedemeyer-Exl; F. Spindler; H. Blaser; *U. Monatsh. Chem.* **2000**, 131, 1335.
40. A. W. Lei; M. Che; M. S. He; X. Zhang; *Eur. J. Org. Chem.* **2006**, 4343.
41. C. Y. Legault, A. B. Charette, *J. Am. Chem. Soc.* **2005**, 127, 8966.
42. X.-B. Wang, W. Zeng, Y.-G. Zhou, *Tetrahedron Lett.* **2018**, 49, 4922.
43. M. Rueping; A.P. Antonchick; *Angew. Chem. Int. Ed.* **2007**, 46, 4562.
44. Z.-S. Ye, M.-W. Chen, Q.-A. Chen, L. Shi, Y. Duan, Y.-G. Zhou, *Angew Chem Int Ed.* **2012** 51, 10181.
45. (a) I. W. Southon; J. Buckingham; *Dictionary of Alkaloids*; Chapman and Hall: New York, **1989**; (b) N. Neuss; M. N. Neuss, In *The Alkaloids*; A. Brossi, M. Suffness, Eds.; Academic Press: San Diego, **1990**; p 229; (c) F. Gueritte; J. Fahy; In *Anticancer Agents from Natural Products*; G. M. Cragg, D. G. I. Kingston, D. J. Newman, Eds.; CRC Press: Boca Raton, FL, **2005**; p 123; (d) *Modern*

- Alkaloids*; E. Fattorusso, O. Taglialatela-Scafati, Eds.; Wiley-VCH: Weinheim, **2008**, and references therein.
46. R. Kuwano; K. Sato; T. Kurokawa; D. Karube; Y. Ito, *J. Am. Chem. Soc.* **2000**, 122, 7614
 47. (a) R. Kuwano; K. Kaneda; T. Ito; K. Sato; T. Kurokawa; Y. Ito, *Org. Lett.* **2004**, 6, 2213; (b) R. Kuwano; M. Kashiwabara; K. Sato; T. Ito; K. Kaneda; Y. Ito, *Tetrahedron: Asymmetry* **2006**, 17, 521; (c) A. M. Maj; I. Suisse; C. Méliet; F. Agbossou-Niedercorn, *Tetrahedron: Asymmetry* **2010**, 21, 2010; (d) N. Mršić; T. Jerphagnon; A. J. Minnaard; B. L. Feringa; J. G. de Vries, *Tetrahedron: Asymmetry* **2010**, 21, 7; (e) A. Baeza; A. Pfaltz, *Chem.-Eur. J.* **2010**, 16, 2036.
 48. D.-S. Wang; Q.-A. Chen.; W. Li; C.-B. Yu; Y.-G. Zhou; X. Zhang, *J. Am. Chem. Soc.* **2010**, 132, 8909.
 49. R. Kuwano; M. Kashiwabara; M. Ohsumi; H. Kusano, *J. Am. Chem. Soc.* **2008**, 130, 808.
 50. D.-S. Wang; Z.-S. Ye; Q.-A. Chen; Y.-G. Zhou; C.-B. Yu; H.-J. Fan; Y. Duan, *J. Am. Chem. Soc.* **2011**, 133, 8866.
 51. (a) B. Bao; Q. Sun; X. Yao; J. Hong; C.-O. Lee; H. Y. Cho; J. H. Jung, *J. Nat. Prod.* **2007**, 70, 2; (b) R. J. Capon; F. Rooney; L. M. Murray; E. Collins; A. T. R. Sim; J. A. P. Rostas; M. S. Butler; A. R. Carroll, *J. Nat. Prod.* **1998**, 61, 660; (c) R. Kuwano; N. Kameyama; I. Ryuhei, *J. Am. Chem. Soc.* **2011**, 133, 7312.
 52. (a) T. Ohta; T. Miyake; N. Seido; H. Kumobayashi; H. Takaya, *J. Org. Chem.* **1995**, 60, 357; (b) F. Polyak; T. Dorofeeva; G. Zelchan, *Synth. Commun.* **1995**, 2895; (c) M. Sebek; J. Holz; A. Börner; K. Jähnisch, *Synlett* **2009**, 461; (c) P. Feiertag; M. Albert; U. Nettekoven; F. Spindler, *Org. Lett.* **2006**, 8, 4133.
 53. S. Kaiser; S. R. Smidt; A. Pfaltz, *Angew. Chem., Int. Ed.* **2006**, 45, 5194.
 54. (a) S. Jansat; D. Picurelli; K. Pelzer; K. Philippot; M. Gomez; G. Muller; P. Lecante; B. Chauret, *New J. Chem.* **2006**, 30, 115; (b) A. Gual; M. R. Axet; K. Philippot; B. Chauret; A. Denicourt-Nowicki; A. Roucoux; S. Castillon; C. Claver, *Chem. Commun.* **2008**, 2759.
 55. S. Urban; N. Ortega; F. Glorius, *Angew. Chem., Int. Ed.* **2011**, 50, 3803.

Chapter 2

Iridium-Catalyzed Asymmetric Hydrogenation of Pyridine

2.1 Introduction

Chiral piperidine derivatives play particularly important roles in pharmaceutical and agrochemical industry. They are ubiquitous structural motifs in natural products as well as key pharmacophores in many active pharmaceutical ingredients.¹ Examples include but not limited to PARP-1/2 inhibitor (Abbott), NK1 receptor antagonist (Vofopitant HCl, Pfizer), Bradykinin B1 antagonists (Merck) and SMO inhibitor (Pfizer), ropivacaine,² dexamethylphenidate,³ paroxetine,⁴ and alogliptin⁵ (Figure 2-1). Unsurprisingly, efforts have been made to developing diverse methodologies to meet the great demands of both academic research as well as industrial production of pharmaceutical intermediates. Among all the different strategies, direct asymmetric hydrogenation of N-heteroaromatic compounds has been the most efficient and widely investigated approach.⁶

Although asymmetric hydrogenation of prochiral unsaturated compounds is a powerful method in making chiral pharmaceuticals, the past effort has mainly focused on asymmetric hydrogenation of ketones and alkenes. In sharp contrast, the asymmetric hydrogenation of arenes/heteroarenes is a much less explored area. In this chapter, the focus is to explore the challenging asymmetric hydrogenation of pyridine

derivatives.

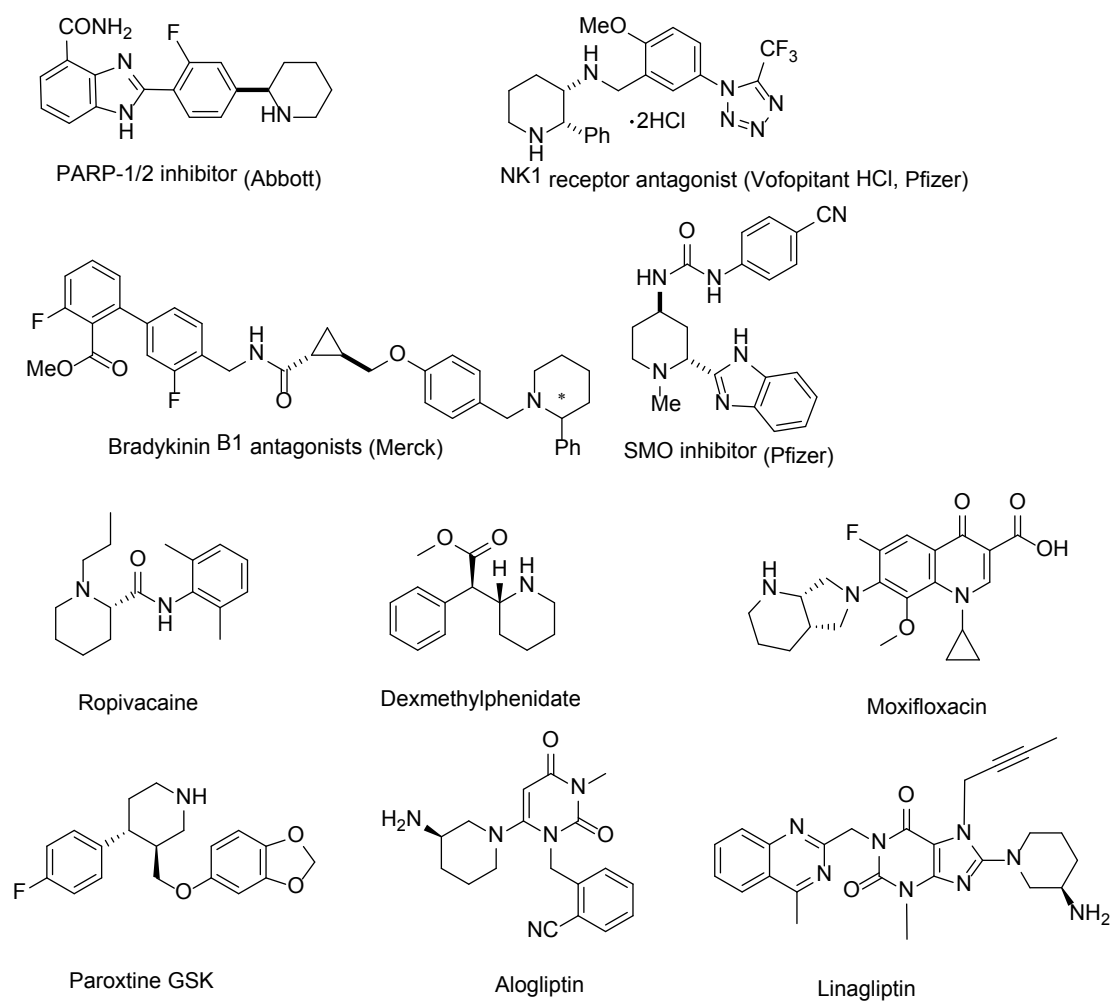


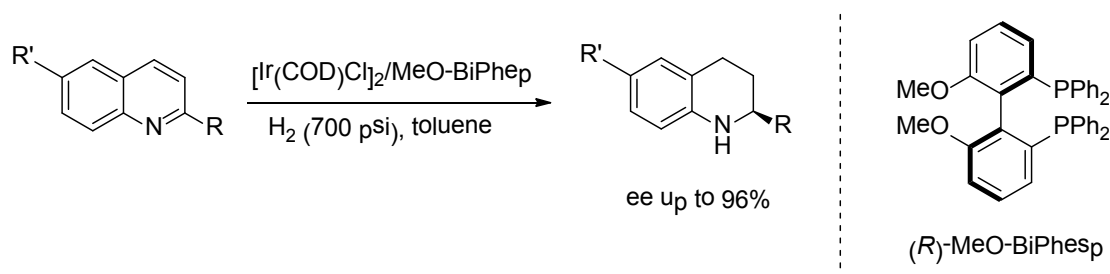
Figure 2-1. Selected Pharmaceutical Targets and Structures with Chiral Piperidine.

In contrast to the advances achieved in imine hydrogenation to access chiral piperidines, asymmetric hydrogenation of substituted pyridines represents a long standing problem. Those aromatic molecules are generally stable and resistant to hydrogenation under mild or even harsh conditions, which adversely affects the enantioselectivity;⁷ Low catalytic activities were usually observed due to the strong

coordination of the amine product to the transition metal catalyst, thus resulting in low turnover number and yields. In addition, the lack of secondary coordinating group in simple aromatic compounds may be responsible for the difficulty in achieving high activity and/or enantioselectivity. Nonetheless, bicyclic N-heteroaromatic compounds, such as quinolines and isoquinolines, are relatively easy to hydrogenate due to the relatively weak aromaticity. Therefore, some success has been achieved for the reduction of those bicyclic heteroaromatics.

The first example of homogeneous asymmetric hydrogenation of aromatic compounds was reported in 1987 by Murata and co-workers who hydrogenated 2-methylquinoxaline in ethanol using $\text{Rh}[(S,S)\text{-DIOP}]\text{H}$ as catalyst. A dismal 2% ee was obtained.⁸ In 1995 Takaya and co-workers reported a significant improvement (50% ee) in the hydrogenation of 2-methylfuran using a chiral Ru complex with (*R*)-BINAP ligand as catalyst.⁹ In 1998, Bianchini developed an orthometalated dihydride iridium complex for hydrogenation of 2-methylquinoxaline to 1,2,3,4-tetrahydro-2-methylquinoxaline with up to 90% ee,¹⁰ while conversion is not satisfactory. These pioneering works demonstrated the feasibility of highly enantioselective hydrogenation of aromatic compounds and have opened a new avenue to the synthesis of chiral heterocyclic compounds from readily available aromatic compounds. Considering the diversity of aromatic compounds and the great importance of the corresponding hydrogenated products, the discovery of new highly efficient catalytic systems will make a major impact in organic synthesis and industrial application.

In 2003 Zhou and coworkers reported the first highly enantioselective hydrogenation of quinolines example using iridium catalyst generated in situ from $[\text{Ir}(\text{COD})\text{Cl}]_2$ and MeO-BiPhep (Scheme 2-1) with good enantioselectivities. However, the system was not general for other classes of substituted pyridines.¹¹ Glorius and coworkers reported the use of a chiral auxiliary with a heterogeneous catalyst,¹² while Zhang and coworkers reported that step-wise reduction of the pyridine ring could lead to high enantioselectivities in certain cases.¹³ In 2006 Chan *et al.* developed the C_3 -TunePhos and applied in the asymmetric hydrogenation of quinoline using the same reaction conditions as Zhou's.¹⁴ Later on a phosphorus free Ru/Rh-diamine catalytic system was developed by Chan and Xiao, respectively, for the transfer-hydrogenation of quinolines.¹⁵



Scheme 2-1. First Highly Enantioselective Asymmetric Hydrogenation of Quinolines.

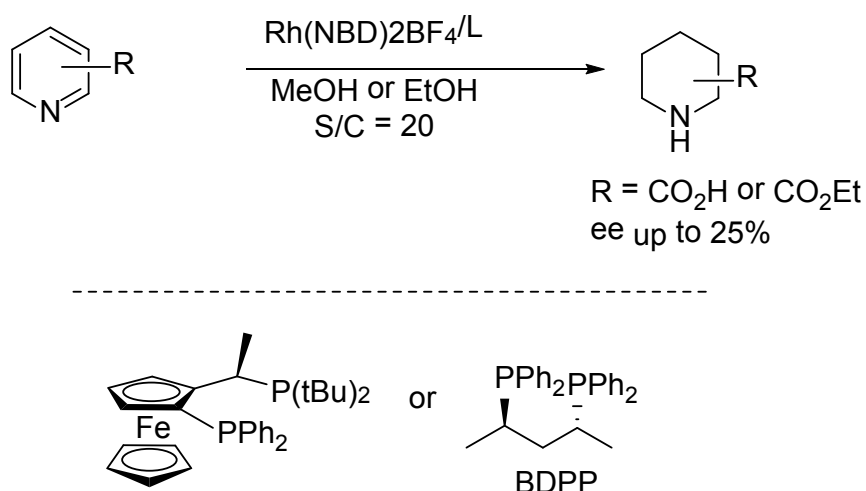
Compared with quinolines, isoquinolines are more difficult substrates. In 2006, Zhou's group reported the first iridium-catalyzed asymmetric hydrogenation of isoquinolines, which were activated by chloroformate, with moderate enantioselectivity and yield.¹⁶ A few years later they reported direct hydrogenation of 3,4-disubstituted

isoquinolines with $[\text{Ir}(\text{COD})\text{Cl}]_2/(\text{R})\text{-synphos}$ in the presence of 1-bromo-3-chloro-5,5-dimethyl-hydantoin (BCDMH) and obtained ee values up to 96%.¹⁷ Mashima and coworkers investigated asymmetric hydrogenation of 1- or/and 3-substituted isoquinolinium HCl salts and excellent enantioselectivities were achieved.¹⁸

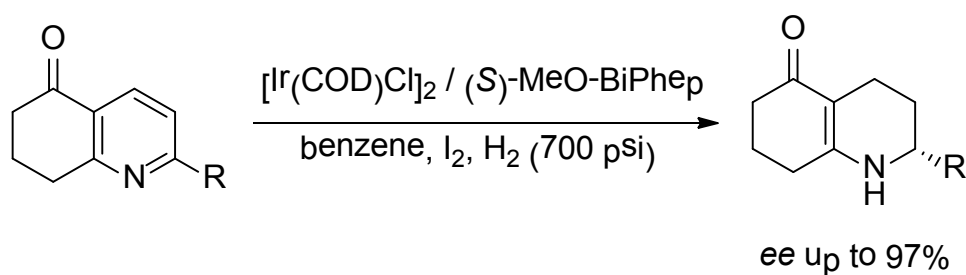
In contrast, the asymmetric hydrogenation of pyridines remains as a standing challenge. The examples for direct homogeneous transition-metal-catalyzed asymmetric hydrogenation of pyridines are very limited and the substrate scope was confined to only several compounds. The major challenge is to break the aromaticity of the pyridine ring. It is much harder to achieve compared with that of the fused *N*-aromatic rings like quinolines.

In 2000 Struder and coworkers reported the first example of pyridine reduction.¹⁹ Using $\text{Rh}(\text{NBD})_2\text{BF}_4$ / diphosphine as the catalyst, 2- and 3-pyridinecarboxylic acid ethyl esters were hydrogenated, although enantioselectivity was not satisfactory (only 25% *ee*) (Scheme 2-2). In 2008, Zhou and co-workers reported a $[\text{Ir}(\text{COD})\text{Cl}]_2$ / (S)-MeO-Biphep system partially reduced 7,8-dihydro-quinolin-5(6H)-ones with excellent enantioselectivities, but it was not efficient for other types of pyridines (Scheme 2-3).²⁰ Several indirect strategies for asymmetric hydrogenation of pyridines, were also developed to address this problem. Glorius introduced chiral auxiliary to the 2 position of pyridine to induce chirality, and then chopped off after hydrogenation (Scheme 2-4).²¹ Zhang's group utilized step-wise approach to reduce the pyridine ring (Scheme 2-5).²² In 2005 Charette *et al.* investigated the asymmetric hydrogenation of

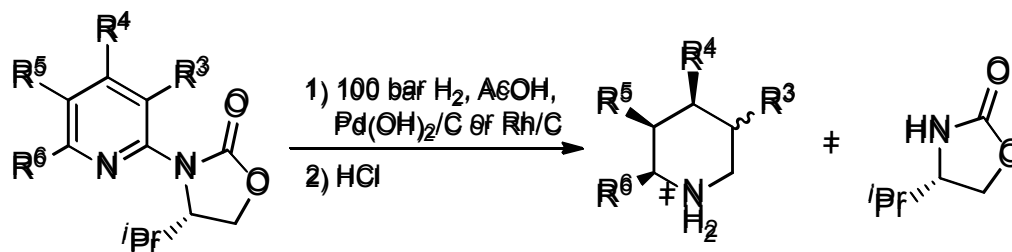
N-iminopyridinium ylides and excellent enantioselectivities were achieved (Scheme 2-6).^{23a}



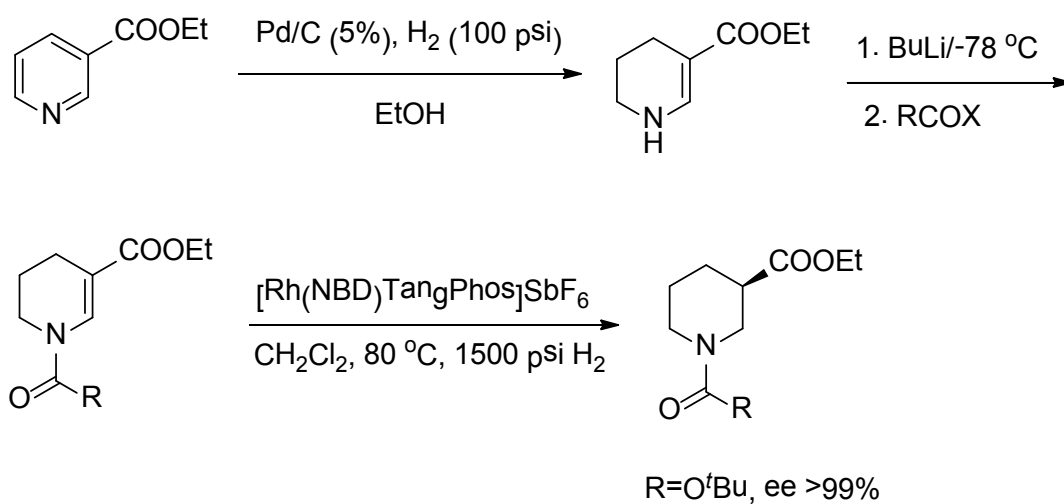
Scheme 2-2. The First Example for Asymmetric Hydrogenation of Pyridines.



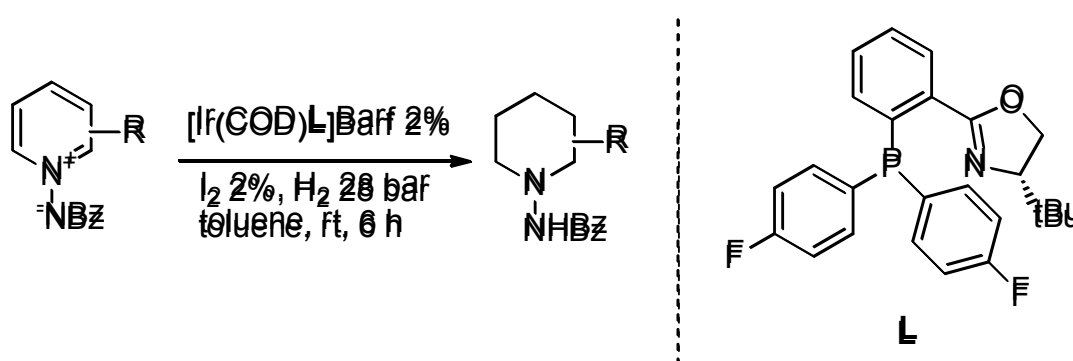
Scheme 2-3. Direct Asymmetric Hydrogenation of Pyridines.



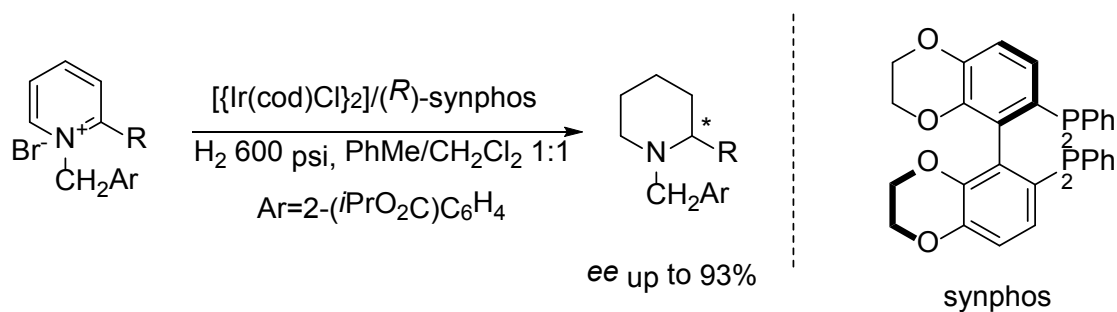
Scheme 2-4. Utility of Chiral Auxiliary on the 2-Position of Pyridine to Induce Chirality.

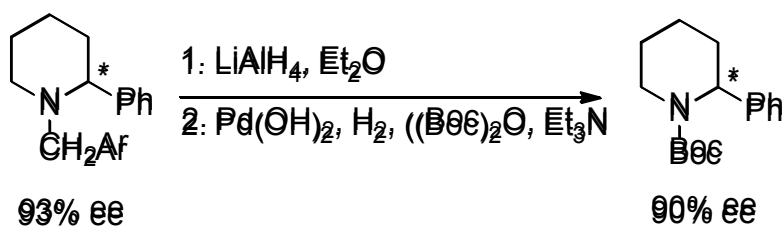


Scheme 2-5. Step-wise Hydrogenation of Pyridine.



Scheme 2-6. Asymmetric Hydrogenation of *N*-iminopyridinium Ylides.





Scheme 2-7. Asymmetric Hydrogenation of Pyridinium Salts.

Recently, Zhou and coworkers reported the successful asymmetric hydrogenation of *N*-(2-CO₂*i*Pr)benzylpyridinium salts in which the benzyl activating group bears an isopropyl ester moiety that acts as a directing group for the catalyst (Scheme 2-7).^{23b} But two steps were required for the products to remove the benzyl protecting group. Given that *N*-alkyl piperidines themselves are valuable synthons, an asymmetric hydrogenation method that utilized simple *N*-alkyl pyridinium salts without the need to build in a directing group on the *N*-alkyl substituent would increase the scope and utility of this approach.

2.2 Asymmetric Hydrogenation of Simple N-Bnzylpyridinium Salts

2.2.1 Initial Results and Reaction Optimization

A variety of strategies have been employed to prepare piperidine derivatives, including but not limited to, arylation of simple piperidines, construction of the piperidine ring from open chain precursors and hydrogenation of pyridines.²⁴

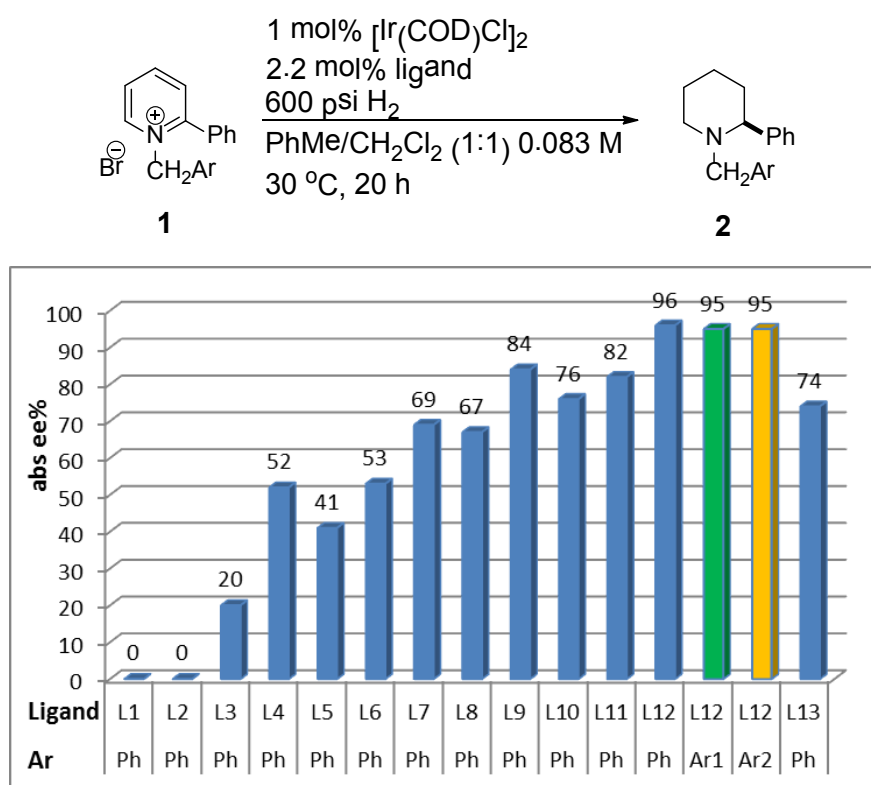
However, for the past decade the problem of synthesizing chiral piperidine in a state of art, in other words with complete control of chemo-regio- and stereoselectivities, have risen as the challenge for all synthetic chemists ever since.

In our group initial efforts were using bronsted acids (such as trifluoroacetic acid) to protonate the nitrogen of the pyridines and therefore dearomatize the pyridines in some degree. However, attempts to hydrogenate the trifluoroacetic acid salt of methyl nicotinate using 5 mol% of $[\text{Ir}(\text{COD})\text{Cl}]_2$ -f-Binaphane did not prove efficient. At best the reaction provided only 90% conversion and 23% *ee*.²⁵

After the fruitless attempts of screening Bronsted acid-assisted direct asymmetric hydrogenation, we decided to switch our efforts to a different approach. A simple *N*-benzyl group was chosen to activate 2-phenyl-pyridine **1** due to its ubiquity in protecting group chemistry.²⁶ Initial studies with this pyridinium salt offered not very satisfied enantioselectivity. While simple *N*-benzylpyridinium salts have been demonstrated to be very challenging substrates in asymmetric hydrogenation, we envisioned that an in-depth evaluation of ligand architecture with respect to reaction selectivity may result in the identification of an efficient catalyst.

A library of 240 chiral phosphine ligands were evaluated (Figure 2-2).²⁷ While the majority of the 240 chiral phosphine ligands screened gave <60% *ee*, several active ligands gave > 65% *ee*. Doubly-oxygenated atropisomeric C_2 -symmetric bisphosphine ligands, such as SynPhos, SEGPHOS and GarPhos (Figure 2-3), along with $[\text{Ir}(\text{COD})\text{Cl}]_2$ pre-catalyst showed good enantioselectivities in the asymmetric hydrogenation of **1** (Figure 2-2, **L7** to **L11**). The fine-tuning of the GarPhos and

SEGPPOS ligands structure also had notable impact on their enantioselectivities (Figure 2-2, **L8**, **L9** and **L10**, **L11**). Interestingly, high selectivities were only observed with the more electron-rich doubly-oxygenated ligand frameworks. When the phosphole-containing MP²-SEGPPOS (**L12**) was employed, chiral piperidine **2** (Ar = Ph) was obtained in 96% ee. High ee were also observed for two other structurally diverse *N*-benzylpyridinium bromides [Ar = 2-(CO₂Me)Ph and 4-(OMe)Ph], suggesting that a generalized protocol may be achievable. The size of the phosphole substituents was found to be critical (Figure 2-2, **L12** to **L13**), as evidenced by the decreased selectivity when more sterically encumbered phosphole was employed.



^aReactions were carried out using 0.01 mmol of substrate in 0.12 mL of mixed solvent. ^bAbsolute enantiomeric excesses were determined by chiral SFC. ^cAr1 = 2-(CO₂Me)Ph, Ar2 = 4-(OMe)Ph.

Figure 2-2. Selected Results of Ligand Screen for Asymmetric Hydrogenation of *N*-Alkyl-2-phenylpyridium Bromide Substrates Using Iridium Catalysts^{a,b,c}

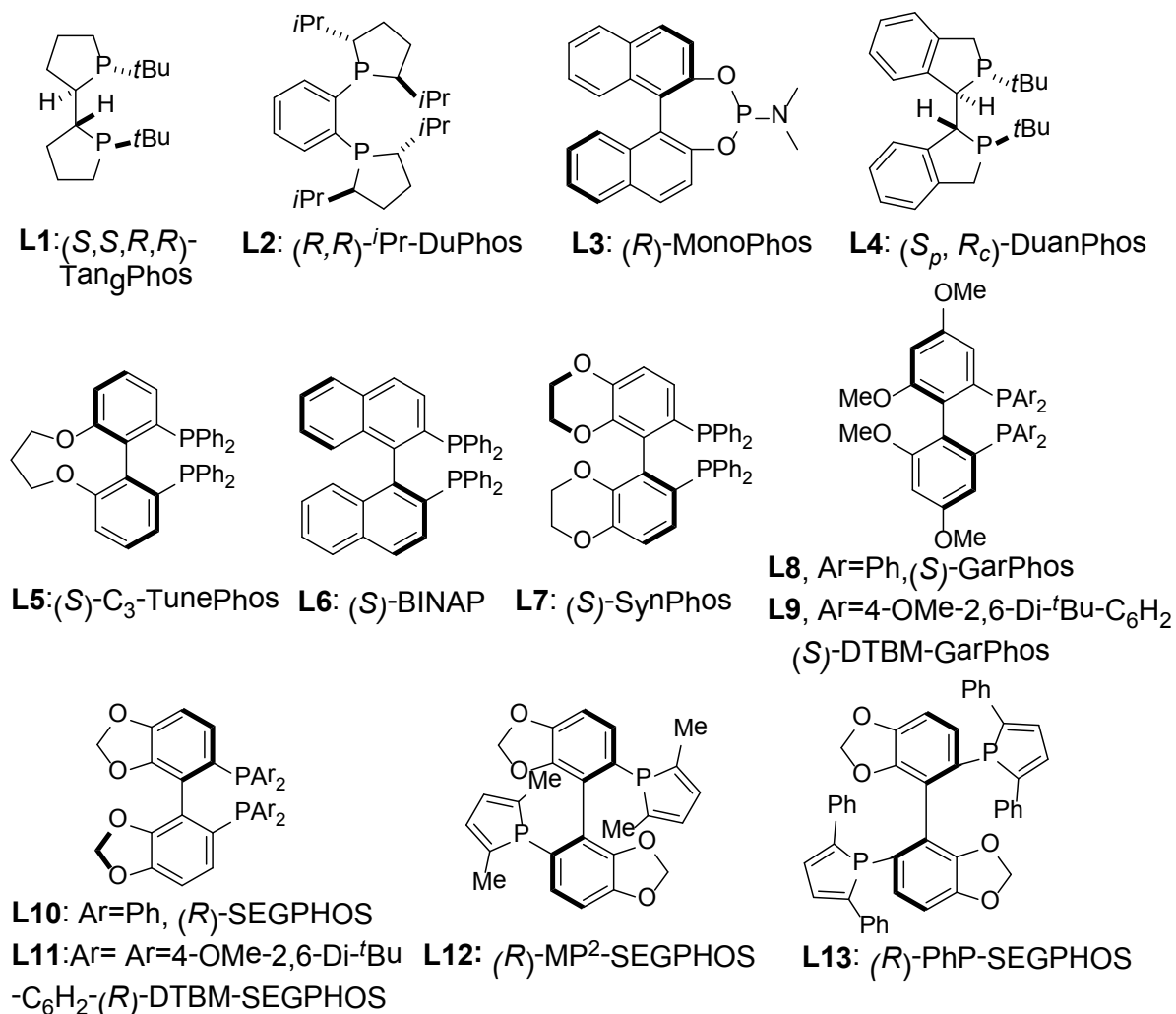
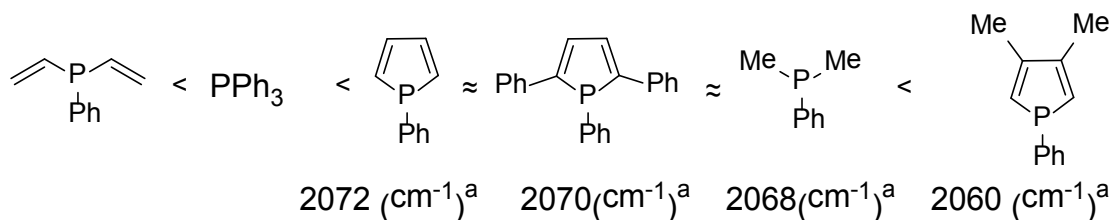


Figure 2-3. Chiral Ligands Structures.

The ligand MP²-SEGPHOS was reported by Takasago as early as in 2004 but found no application ever since.²⁸ It is worth noting that to the best of our knowledge the results obtained with **L12** represent the first examples of the use of this ligand in a highly efficient asymmetric reaction.²⁹ A number of unique features of phospholes may contribute to the observed high efficiency and enantioselectivity in the reactions employing MP²-SEGPHOS as a ligand. Firstly, the tangential relationship between the selectivity of the asymmetric hydrogenation and donor

capacity of the ligand would be further enhanced by the phosphole functionality of MP²-SEGP²HOS (Figure 2-4).³⁰ Secondly, the structure for MP²-SegPhos is unique. Unlike the original SegPhos, ‘two’ substituents on phosphorus of MP²-SegPhos are actually one piece. Its structural module is more like that of DuPhos. This diphosphine ligand is quite rigid and thus could define the steric environment around phosphorus very well. At the same time MP²-SegPhos is axial chiral thus gain some flexibility to accommodate various substrates with different size. The rigidity³¹ and planarity³² of the phosphole unit would be expected to provide a well-defined chiral pocket³³ around the reactive site that is substantially different from those seen with other C₂-symmetric bis(phosphine) ligands.



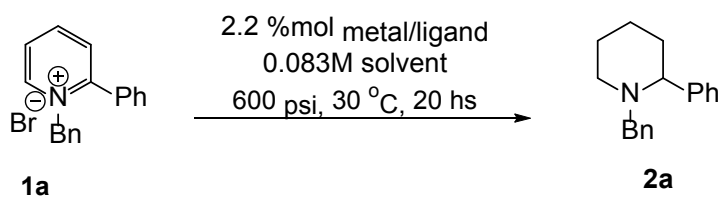
^aInfrared data for LMo(CO)₅ complexes.¹² Only the highest energy $\nu(\text{CO})$ is given.

Figure 2-4. Order of Electron Donating Ability of Phosphorus Ligands.

Having identified MP²-SEGP²HOS as the most selective ligand of those examined, we next screened the influence of different metals (Table 2-1). Iridium is a more effective metal than rhodium and ruthenium in this case. Counter ions such as Ir-BF₄,

Ir-BARF and Ir(COD)Cl dimer provide comparable results. We chose Ir(COD)Cl dimer for all the following the research conducted later.

Table 2-1. Screening of Metals for Asymmetric Hydrogenation of 2-Phenylpyridinium Salts. ^[a]



entry	Metal	solvent	conversion	ee[%] ^b
1	Ir-BARF	Acetone	94.9	94.5
2	Ir-BF ₄	Acetone	100	94.0
3	[Ir(COD)2Cl] ₂	Acetone	100	92.3
4	Rh(COD)Cl	Acetone	53.1	75.4
5	Ir-BARF	DCM	98.6	94.0
6	Ir-BF ₄	DCM	91.6	94.0
7	[Ir(COD)2Cl] ₂	DCM	100	92.6
8	Ir-BARF	DCE	93.6	94.0
9	Ir-BF ₄	DCE	93.6	94.4
10	[Ir(COD)2Cl] ₂	DCE	100	92.9
11	Ir-BF ₄	DCE/Tol	95.7	96.0
12	[Ir(COD)2Cl] ₂	DCE/Tol	100	95.4
13	Rh(nbd)BF ₄	DCE/Tol	11.8	82.7
14	Rh(COD)Cl	DCE/Tol	11.5	71

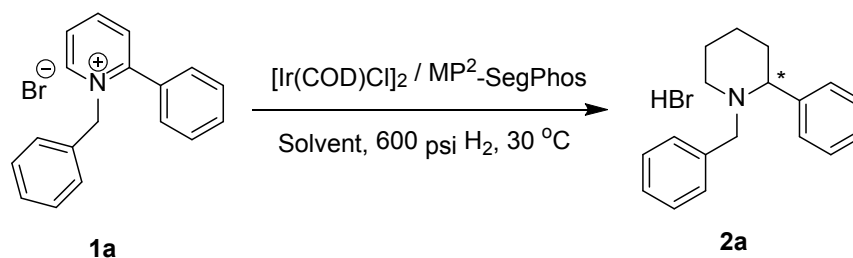
[a] 1 0.083M, metal (1 mol%), MP²-SegPhos (2.2 mol%), H₂ (600 psi), 20 h, 30 °C.

[b] Determined by SFC.

Next, we explored the influence of solvent (Table 2-2). Polar protic alcohol solvents did not yield good results. Excellent enantioselectivities were obtained from weakly

coordinated solvents such as dichloromethane, dioxane, toluene and acetone. While many single solvents led to excellent *ees* for substrate 1a, acceptable reactivity was only observed for THF, acetone and 1,2-dichloroethane (DCE). Even though many of the solvents yielded similar results, we chose the environmentally benign acetone to do further study. Several of the mixed solvents performed greatly in this reaction (Table 2-3). Various temperatures and hydrogen pressures were also screened (Table 2-4). Additionally, different loading of additive (I_2) was screened, which suggested additive is not necessary in our case (Table 2-5). Combination of acetone and DCE (1:1) under 600 psi hydrogen pressure and 30 °C proved optimal, allowing the Ir catalyst to be lowered to 0.5mol%. When the catalyst loading was reduced to 0.1 mol%, the *ee* was slightly lower with good conversion (Table 2-6). Other counter ions tested offered no advantage over bromide (Table 2-7).

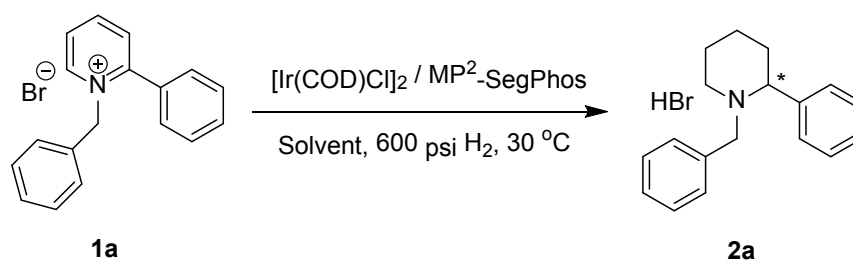
Table 2-2. Solvent Screening for Asymmetric Hydrogenation of *N*-Benzyl-2-Phenylpyridium Bromide.^[a]



Entry	Solvent	Conversion(%) ^[b]	Ee(%) ^[b]
1	CH ₂ ClCH ₂ Cl	99	94.1
2	EtOAc	57	93.6
3	CH ₂ Cl ₂	53	93.3
4	Acetone	100	93.1
5	Dioxane	62	92.8
6	Toluene	22	89.1
7	Anisole	81	89.5
8	DMF	100	89.4
9	MeOH	32	63.1
10	MeCN	95	57
11	CF ₃ CH ₂ OH	0	0

[a] Reaction conditions: [Ir(COD)Cl]₂ / MP2-Segphos 1 mol%, 600 psi of H₂, 30°C, 24 h. [b] Conversions of acetophenone and enantiomeric excesses were determined by chiral SFC on Waters 200 equipment.

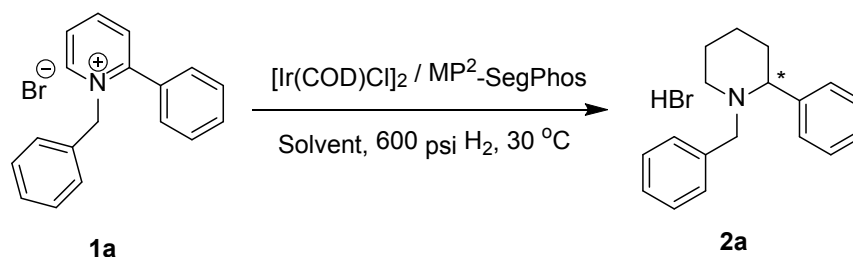
Table 2-3. Mixed Solvents Screening for Asymmetric Hydrogenation of *N*-Benzyl-2-phenylpyridium Bromide.^[a]



Entry	Solvent	Catalyst loading (mol%)	Conversion(%) ^[b]	Ee(%) ^[b]
1	CH ₂ Cl ₂ /Toluene 1:1	0.5	85	96.2
2	EtOAc/CH ₂ Cl ₂ 1:1	0.5	97	96.1
3	CH ₂ Cl ₂ /THF 1:1	0.5	98	96.0
4	CH ₂ Cl ₂ /Acetone 1:1	0.5	98	95.6
5	Acetone	0.5	100	94.6
4	Acetone/toluene 1:1	0.5	99	95.5
5	Acetone/THF 1:1	0.5	100	93.6
6	Acetone	0.25	92	96
7	Acetone	0.1	97	92

[a] Reaction conditions: [Ir(COD)Cl]₂ / MP2-Segphos 1 mol%, 600 psi of H₂, 30°C, 24 h. [b] Conversions of acetophenone and enantiomeric excesses were determined by chiral SFC on Waters 200 equipment.

Table 2-4. Temperature, Pressure and Catalyst loading Screening for Asymmetric Hydrogenation of *N*-Benzyl-2-phenylpyridium Bromide.^[a]



Pressure/temp.	cat. Loading%mol	concentration (M)	solvent	conversion	ee ^[b]
300psi/50c	0.5	0.1	Acetone	>99	94.3
600psi/50c	0.5	0.1	Acetone	>99	89.6
1200psi/50c	0.5	0.1	Acetone	>99	89.3
300psi/30c	0.5	0.1	Acetone	97	93.4
1200psi/30c	0.5	0.1	Acetone	96	90
300psi/50c	0.5	0.1	Acetone	>99	94.3
300psi/50c	0.1	0.1	Acetone	87	94.1
300psi/50c	0.5	0.25	Acetone	98	94.2
300psi/50c	0.1	0.25	Acetone	92	94.4
300psi/30c	0.5	0.1	Acetone	97	93.4
300psi/30c	0.1	0.1	Acetone	9	*
1200psi/30c	0.5	0.1	Acetone	96	90
1200psi/30c	0.1	0.1	Acetone	31	91.8
300psi/50c	0.5	0.1	Acetone	>99	94.3
300psi/30c	0.5	0.1	Acetone	97	93.4
1200psi/50c	0.5	0.1	Acetone	>99	89.3
1200psi/30c	0.5	0.1	Acetone	96	90
acetone/DCE					
600psi/30c	0.5	0.025	1:1	>99	96

[a] Reaction conditions: $[\text{Ir}(\text{COD})\text{Cl}]_2$ / MP2-Segphos 1 mol%, 600 psi of H_2 , 30°C, 24 h. [b] Conversions of acetophenone and enantiomeric excesses were determined by chiral SFC on Waters 200 equipment.

Table 2-5. Screening of Additive and Mix Solvents for Asymmetric Hydrogenation of 2-Phenylpyridinium Salts. ^[a]

0.5%mol $[\{\text{Ir}(\text{cod})\text{Cl}\}_2]/\text{ligand}$
solvent, additive
 H_2 600 psi, 30 °C, 20 hs

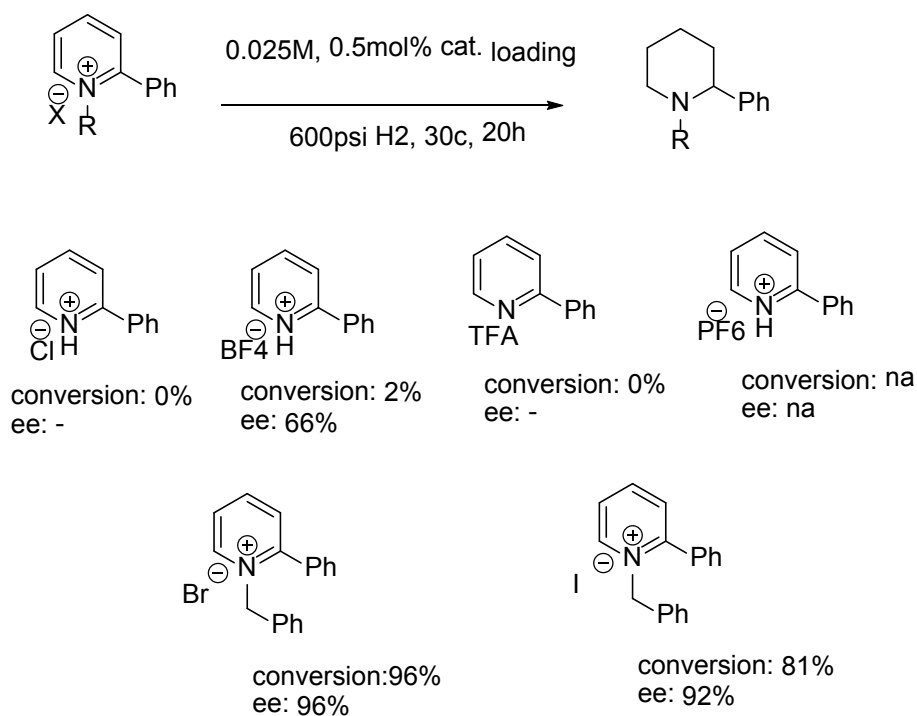
entry	Ar	solvent	additive	ee[%] ^b	Int/Prod (%)
1	2-ClC ₆ H ₄	acetone	5%mol	79.5	2.4
2	2-ClC ₆ H ₄	acetone/DCM (5:1)	5%mol	85.9	2.2
3	2-ClC ₆ H ₄	acetone/DCM (2:1)	5%mol	94.1	2.4
4	2-ClC ₆ H ₄	acetone/DCM (1:1)	5%mol	95.3	2.5
5	2-ClC ₆ H ₄	acetone/DCE (1:1)	0	95.7	2
6	Ph	acetone	0	94.7	4
7	Ph	acetone/DCM (5:1)	0	88.9	1.5
8	Ph	acetone/DCM (2:1)	0	92.8	3.5
9	Ph	acetone/DCM (1:1)	0	95.7	28
10	Ph	acetone/DCM (5:1)	5%mol	93.4	0
11	Ph	acetone/DCM (2:1)	5%mol	93.5	0
12	Ph	acetone/DCM (1:1)	5%mol	93.4	0.7
13	Ph	acetone/DCE (5:1)	0	90.8	0
14	Ph	acetone/DCE (1:1)	0	97.5	0
15	Ph	acetone/DCE (5:1)	2%mol	90.9	0
16	Ph	acetone/DCE (1:1)	2%mol	94.2	0

[a] 1 0.025M, $[\{\text{Ir}(\text{cod})\text{Cl}\}_2]$ (0.5 mol%), L (1.1 mol%), H_2 (600 psi), 2-Ph-pyridium, solvent, 20 h, 30 oC. [b] Determined by SFC.

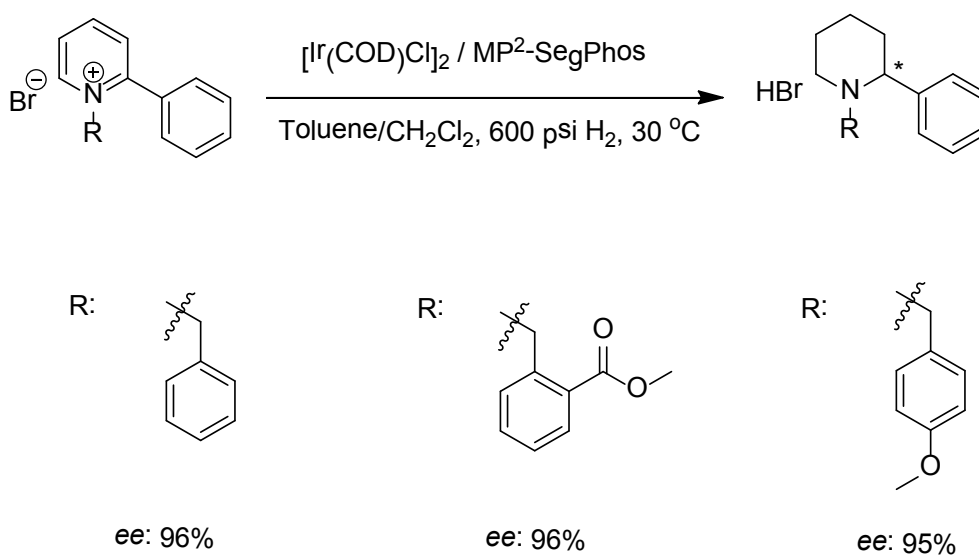
Table 2-6. Catalyst Loading and Concentration for Asymmetric Hydrogenation of 2-Phenylpyridinium Salts.^[a]

cat. loading	0.05%	0.1mol%	0.15mol%	0.25mol%	0.5mol%
concentration	<i>ee</i> (conv.)	<i>ee</i> (conv.)	<i>ee</i> (conv.)	<i>ee</i> (conv.)	<i>ee</i> (conv.)
0.025M	94.2 (4.2)	95.3 (17)	95.3 (34)	95.3 (100)	95.3 (100)
0.05M	95.4 (6.4)	95.1 (17.5)	95.6 (35.4)	95.5 (71)	95.3 (100)
0.1M	95.5 (13.1)	95.6 (20.5)	95.5 (25.1)	95.3 (55)	94.9 (100)
0.2M	95.5 (18.1)	95.4 (26.4)	95.3 (30.9)	95.1 (37.6)	-

Table 2-7. Counter ion Screening



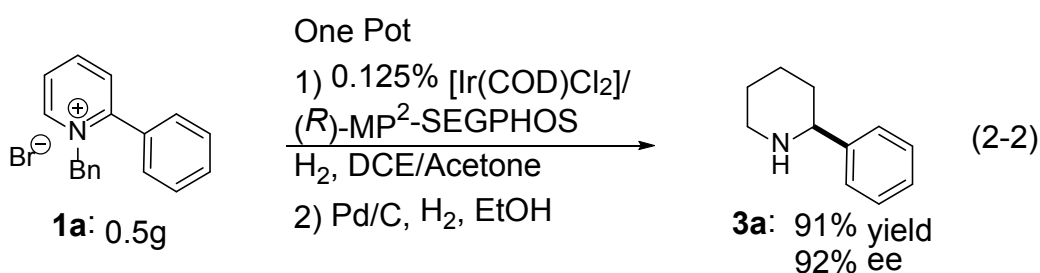
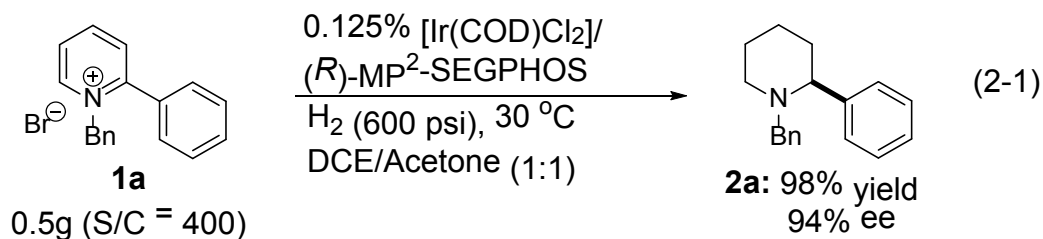
In comparison, different benzyl groups were tested (Scheme 2-8). All of them yielded excellent *ee*'s using $[\text{Ir}(\text{COD})\text{Cl}]_2$ -MP²-SegPhos catalytic system. The advantage for using *para*-methoxybenzyl group is that the conditions for the removal of this protecting group is very mild and no need of the commonly used Pd/C, which will add versatility and accommodation to different functional group to this method.



Scheme 2-8. Asymmetric Hydrogenation of Pyridinium Salts with Different Benzyl Substitutes.

To evaluate the practical utility of newly developed method, asymmetric hydrogenation of *N*-benzyl-2-phenylpyridium bromide **1a** was carried out on 0.5 gram scale. The desired product **2a** was obtained with 98% yield and 94% *ee* (Eq. 2-1) and the catalyst loading could be reduced to 0.25 mol% (S/C=400) at this scale. The facile removal of the *N*-benzyl group was demonstrated through a one-pot asymmetric

hydrogenation followed by deprotection, giving 2-phenylpiperidine in 91% overall yield and 92% ee (Eq. 2-2).

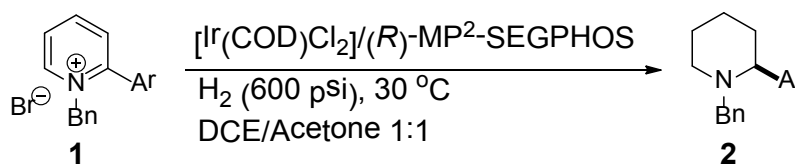


2.2.2 Substrate Scope

To explore the utility of newly developed Ir–MP²-SEGPHOS catalytic system, a range of *N*-benzyl-2-arylpyridinium bromide substrates were synthesized and studied under the optimized conditions. The results are summarized in Table 2-9. For all chosen substrates, chiral products **2** were obtained in excellent yields and enantioselectivities (*ees* ranged from 90% to 96%). To our delight, the catalytic system worked well for *ortho*-substituted sterically hindered substrates such as **1d**, **1k** and **1m** (Table 2-9, entries 4, 12 and 15), thus highlighting the enhanced reactivity of our system. The enantioselectivities in these cases were only slightly less than those

where the 2-aryl group bore substituents in the *meta* or *para* positions. Also, the electronic properties of the 2-aryl group did not exert any noticeable effect on the reaction. Both electron donating 4-MeO (**1f**) and electron withdrawing 4-Cl (**1i**), 3,5-F2 (**1l**) substrates provided similarly high enantioselectivities (Table 2-9, entries 6, 9 and 13). During our study, we observed that some substrates were quite sensitive to the solvent composition (*vide supra*), requiring adjustment of the ratio to achieve higher reactivity (Table 2-8; *cf.* entries 10, 11; 14,15).

Table 2-8. Substrate Scope for Asymmetric Hydrogenation of *N*-Benzylpyridinium Salts.

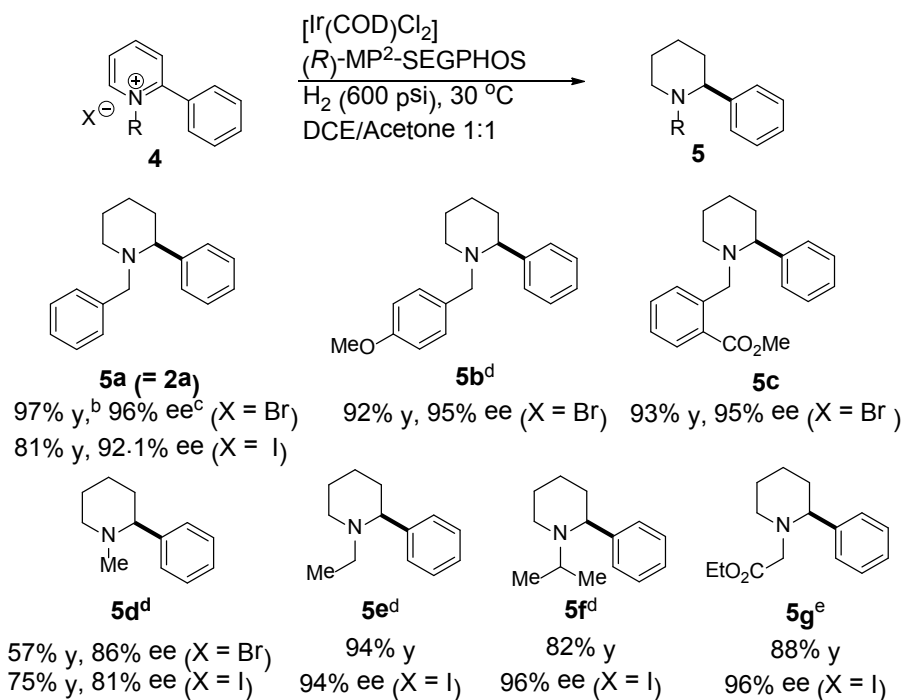


Entry	Ar	Product	Yield (%) ^b	ee (%) ^c
1	C ₆ H ₅ (1a)	2a	97	96
2	3-MeC ₆ H ₄ (1b)	2b	99	96
3	4-MeC ₆ H ₄ (1c)	2c	93	93
4	2-MeOC ₆ H ₄ (1d)	2d	90	90
5	3-MeOC ₆ H ₄ (1e)	2e	99	96
6	4-MeOC ₆ H ₄ (1f)	2f	95	94
7	4-Ac(H)NC ₆ H ₄ (1g)	2g	97	95
8	4- <i>t</i> BuC ₆ H ₄ (1h)	2h	96	93
9	4-ClC ₆ H ₄ (1i)	2i	96	95
10	4-PhC ₆ H ₄ (1j)	2j	86	90
11 ^d	4-PhC ₆ H ₄ (1j)	2j	96	95
12	2,4-Cl ₂ C ₆ H ₃ (1k)	2k	94	90

13	3,5-F ₂ C ₆ H ₃ (1l)	2l	95	96
14	2-naphthyl(1m)	2m	12	93
15 ^e	2-naphthyl(1m)	2m	88	94

[a] Reaction conditions: **1** 0.025 M, [Ir] / ligand / *N*-benzyl-2-arylpyridium bromide =0.5:0.55:100, 20 h. [b] Yields are isolated yields. [c] Enantiomeric excesses were determined by chiral SFC or chiral HPLC. [d] DCE/Acetone=5:1 as solvent. [e] Acetone as solvent.

Given the relative insensitivity of the reaction to steric effects of the 2-aryl substituent, the question arose as to whether the reaction would also tolerate *N*-alkyl substituents other than benzyl derivatives. As shown in **Scheme 2-9**, the Ir-phosphole catalyst still delivers remarkably high conversion and enantioselectivity with *N*-alkyl substituents as small as Et (**5e**), and even an *N*-Me pyridinium salt gave the resulting *N*-methylpiperidine product in good yield and 81% ee (**5d**). The (carboethoxy)methyl substituent (**5g**) was also tolerated, giving enantioselectivities comparable to those seen with benzyl substituents (**5a**); this substituent is particularly interesting due to its utility as a functional group for further elaboration. In all cases, the nature of the pyridinium counterion exerted a strong effect on both the activity and enantioselectivity of the reaction (e.g., *cf.* Scheme 1, **5a** and **5d**).¹⁶ In some cases, the bromide salts led to higher reactivity (**5a**), while in other cases the iodide salts proved superior(**5d**).



^a Reaction conditions: **4** 0.025 M, [Ir] / ligand / N-Alkyl-2-phenylpyridinium bromide = 0.5:0.55:100, 20 h. ^b Yields are isolated yields. ^c Enantiomeric excesses were determined by chiral SFC or chiral HPLC. ^d DCE as solvent. ^e DCE/Acetone=5:1 as solvent.

Scheme 2-9. Ir-Catalyzed Asymmetric Hydrogenation of 2-Phenylpyridinium Salts **4**.

2.2.3 Conclusion

In summary, we have developed a highly efficient enantioselective hydrogenation of simple *N*-alkyl-2-arylpyridinium salts. This protocol represents an advance over previous methods in that a directing group is not required. With this constraint removed, this new method tolerates a variety of *N*-benzyl as well as simple *N*-alkyl groups, which should greatly increase the scope and applicability of this approach to the synthesis of chiral piperidines. In addition, this method provides a rare example

of using a chiral phosphole-based ligand for highly efficient asymmetric catalysis. The demonstrated utility of the electron rich phosphole structural motif should inform future ligand design for asymmetric catalysis. Further applications of chiral phosphole-based complexes for the asymmetric hydrogenation of other heteroarenes will be discussed in the next chapter.

2.3 Asymmetric Hydrogenation of Di-substituted N-Benzylpyridinium Salts

Di-substituted chiral piperidines are present in numerous natural products and in pharmaceutical drugs and drug candidates (Figure 2-5). Enantiomerically pure piperidines can be prepared by racemic hydrogenation of pyridines followed by chiral separation or resolution. However, applications of these methods, especially on di-substituted substrates, are rather limited due to the inherent lengthy process, moderate overall yield and poor selectivity. Asymmetric hydrogenation is the most straightforward, atom-economic and powerful approach to directly access these useful piperidines bearing two stereo centers.

The success of our newly developed approach to asymmetric hydrogenation of the 2-aryl-pyridine encouraged us to explore the possible application of this methodology in di-substituted pyridines. A number of interesting substrates have been explored (Figure 2-6). For most substrates, however, there were no reactions under the standard condition for asymmetric hydrogenation of simple 2-phenyl N-benzylpyridinium salts **1a**. For example, substrates **7** was difficult to acylated with benzyl bromide probably

due to the steric hindrance. Substrates **10** also proved to be a difficult substrate obtaining only 16% ee with 34% conversion. Substrate **11** displayed better

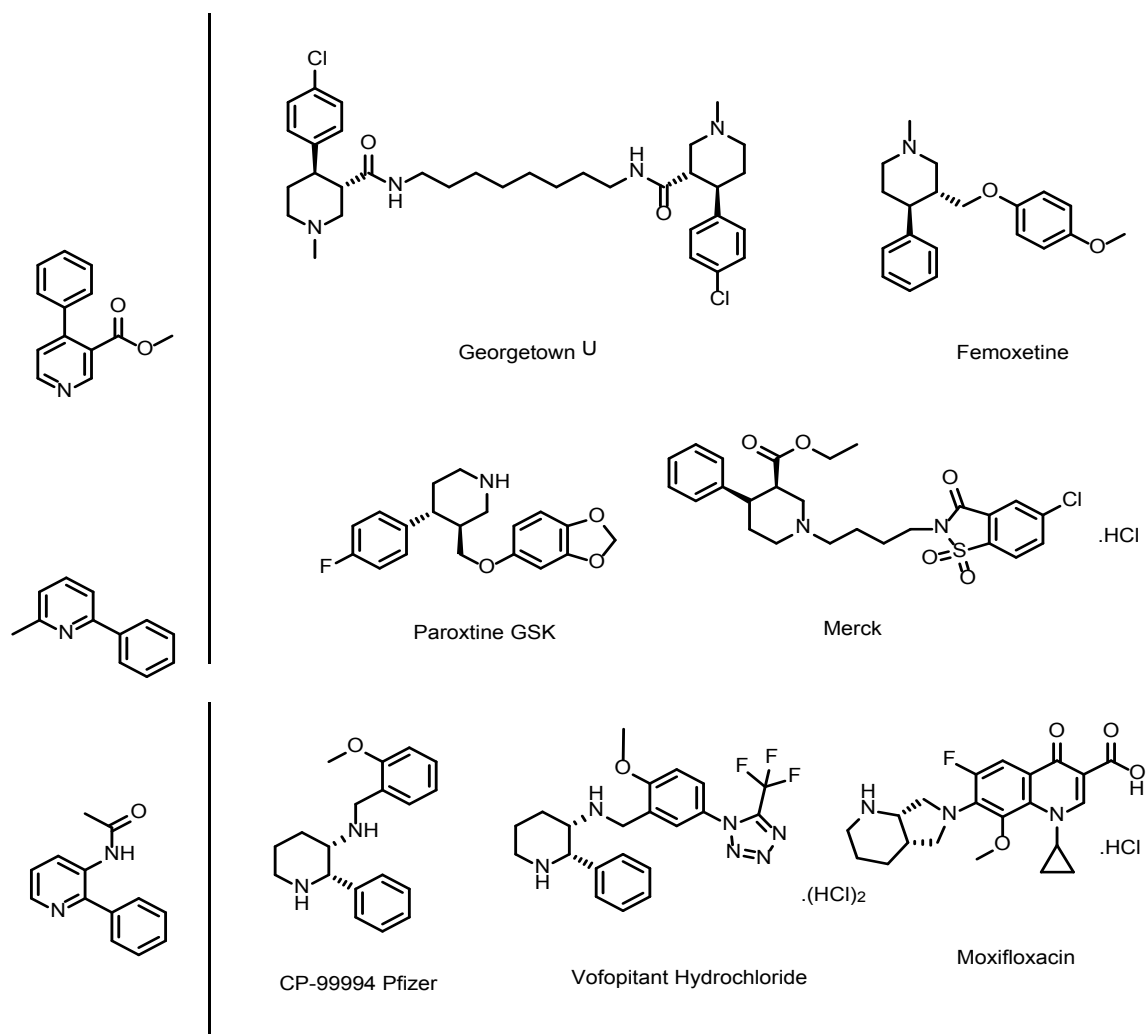


Figure 2-5. Di-substituted Chiral Piperidine in Pharmaceutical Drug Candidates

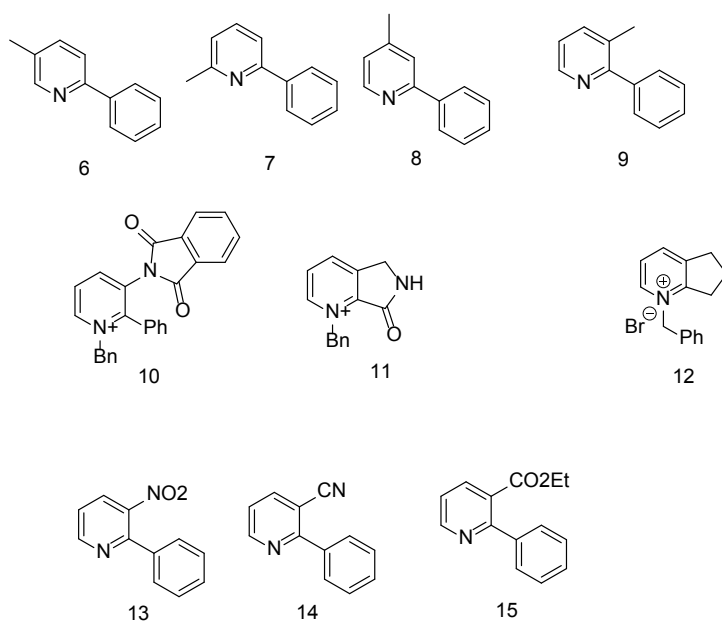


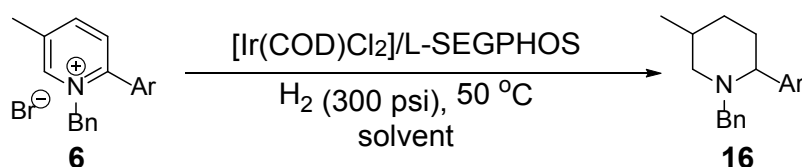
Figure 2-6. Interesting Di-substituted Substrates for Hydrogenation

conversion (85%) but the enantioselectivity was not satisfactory (34%). Substrates **13** to **15** are 2-aryl-pyridine with strong electron-withdrawing group at 3-position. All three substrates display low ee value although substrate **15** (ethyl ester at 3-position) show good conversion (78%) and NMR analysis indicated only cis products formed.

After the long searching, to our gratifying, we found 5-methyl-2-phenyl pyridine **6** reacted well. Under 300psi and 50°C, reaction was carried out using MP²-ligand or P3-MP²-SegPhos ligand, respectively. Three solvents were screened as well (Table 2-9). The preliminary results indicated MP²-SegPhos display superior performance than P3-MP². Very good enantioselectivity (93% and 84% ee) were achieved although the dr is at the low side (Table 2-10, entry 1). When we increased temperature to 60°C, lower dr was obtained (Table 2-10, entry 2). When we changed the acylating group to a more steric hindered bis-Ph group, higher dr was achieved yet the reaction suffered

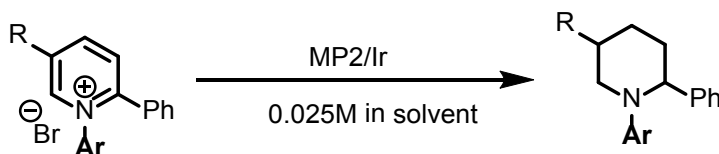
an erosion of ee value (Table 2-10, entry 3 and 4). When we used Iodine-bridged dimeric iridium complex $[\text{Ir}(\text{H})[\text{MP2-SegPhos } (\mu\text{-I})_3]^+\text{I}^-]$ as catalyst, unfortunately, both lower ee and dr were obtained, indicating the poor performance of this dimeric catalyst in the system (Table 2-10, entry 5).

Table 2-9 . Preliminary Screening Results for Hydrogenation of 2-Methyl-5-phenyl Pyridinium Salt^[a]



Entry	Ligand	solvent		dr	ee% ^[b] (A,B)	ee% ^[b] (C,D)
1	MP ²	Acetone/DCE	= 1:1	2.32	88%	84%
2	MP ²	Acetone	-	2.25	93%	84%
3	MP ²	DCE	-	2.43	93%	84%
4	P3-MP ²	Acetone/DCE	= 1:1	0.66	47%	75%
5	P3-MP ²	Acetone	-	0.67	52%	77%
6	P3-MP ²	DCE	-	0.46	32%	44%

[a] Reaction conditions: **1** 0.025 M, $[\text{Ir}]$ / ligand / *N*-benzyl-2-arylpyridium bromide = 0.5:0.55:100, 20 h. [b] Enantiomeric excesses were determined by chiral SFC or chiral HPLC.

Table 2-10. Asymmetric Hydrogenation of 2,5-Di-substituted Substrates

R						ee% ^[b]		ee% ^[b]
Entry	Ar	solvent	Temp.	Pressure	dr	(A,B)	(C,D)	
1 ^[a]	Me	Bn	DCE	50	300	2.43	93%	84%
2 ^[c]	Me	Bn	Acetone/DCE	60	300	1.1	72%	93%
3 ^[c]	Me	CH(Ph) ₂	Acetone/DCE	60	300	2.43	42%	19%
4 ^[c]	Me	CH(Ph) ₂	Acetone/DCE	30	600	4.7	50%	82%
5 ^{[c], [e]}	Me	Bn	Acetone/DCE	30	600	1.8	52%	77%
6 ^[d]	OMe	Bn	Acetone/DCE	50	300	1.67	88%	82%
7 ^[d]	Ph	Bn	Acetone/DCE	50	300	1.25	86%	72%

[a] Reaction conditions: **di-substituted substrate** 0.025 M, [Ir] / ligand / *N*-benzyl-2-arylpyridium bromide =0.5:0.55:100, 20 h. [b] Enantiomeric excesses were determined by chiral SFC or chiral HPLC. [c] [Ir] / ligand / *N*-benzyl-2-arylpyridium bromide =1:1.1:100. [d] [Ir] / ligand / *N*-benzyl-2-arylpyridium bromide =2:2.2:100. [e] Iodine-bridged dimeric iridium complex [Ir(H)[MP2-SegPhos (\square)₃]⁺I⁻ was used as catalyst.

Encouraged by this result, we explored a few other 2,5-di-substituted pyridine substrates (Table 2-10). We first took interests in 5-OH-pyridines. There is barely any report on asymmetric hydrogenation of aromatic compounds bearing a hydroxyl group to chiral ketones or alcohols. Taking pyridin-3-ol, for example, the high aromatic stability and strong coordination ability of the pyridine ring impede efficient

hydrogenation. Three types of unsaturated bonds ($C=C$, $C=N$, and $C=O$) may exist during the hydrogenation process, making the chemoselectivity and stereoselectivity problematic. Once the aromaticity of pyridin-3-ol is destroyed, fast enol/ketone isomerization often takes place. Thus, racemic product often generates for the *ortho*-substituted pyridin-3-ol. These issues render asymmetric hydrogenation of pyridin-3-ol highly challenging. Chiral piperidin-3-ol is a common motif widely embedded in natural products and pharmaceutical agents (Figure 2-7).³⁴ Its abundance and interesting biological activity have stimulated significant synthetic interests.

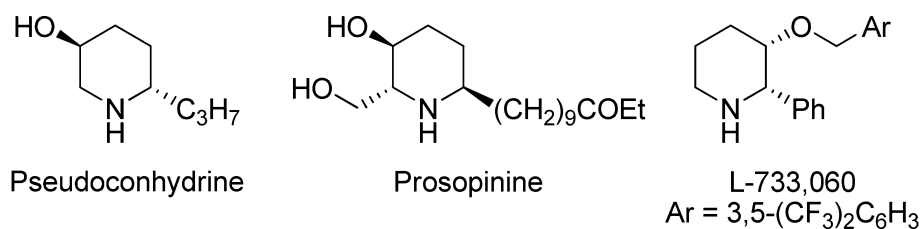


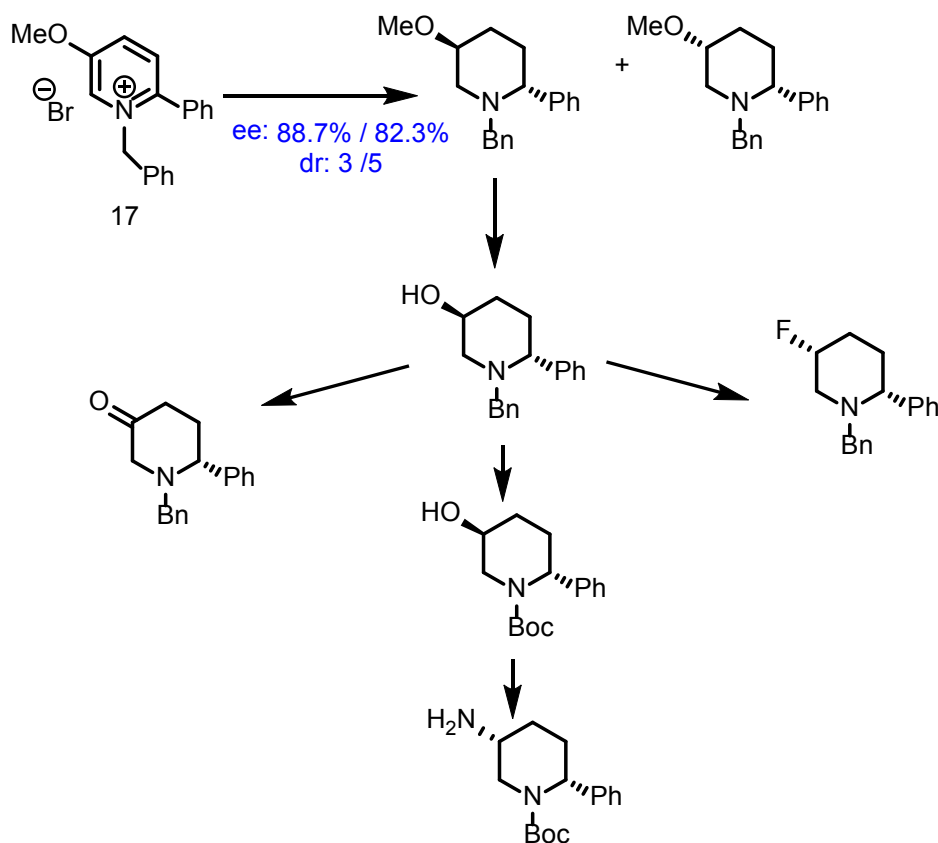
Figure 2-7. Natural Products and Pharmaceutical Agents Containing Chiral Piperidin-3-ol Motif.

Two common synthetic methodologies are intramolecular cyclization of acyclic amines with hydroxyl group at proper position,^{34a} and ring expansion of chiral prolinols.^{34b, 34c} Other useful methods include ring-closing metathesis of the unsaturated amines,^{35a} oxidative kinetic resolution of racemic piperidin-3-ols^{35b} and thermal reactions such as 1,3-dipolar cycloaddition or Diels–Alder.^{35c, 35d} Being widely used, but the existing methods suffer drawbacks such as chiral starting

materials, long synthetic steps, and low overall yields. Therefore, it is highly desirable to develop a direct and catalytic procedure to synthesize chiral piperidin-3-ols.

We started from direct acylation of the 5-OH-2-phenyl-pyridines. Conversely, we found hydroxyl group was quickly reacted with benzyl bromide first therefore led to a messy and complicated reaction. Alternatively, we chose 5-methoxy-pyridine as the model substrate. To our delight, methoxy at 5-position displayed similar results (88.7% and 82% ee, dr 1.67) as 5-methyl-2-phenyl-pyridine (Table 2-12, entry 6). We envision that with the removal of methyl group, enantiopure 5-hydroxy-2-aryl piperidines could then be obtained. Subsequent oxidation could offer the access to chiral piperidine-3-one. The chiral piperidin-3-one was a potentially useful intermediate for the diversified transformations of C=O. Chiral 5-hydroxy-2-aryl piperidines itself could be transformed through Mitsunobu reaction to azide then hydrogenation to chiral 5-amino-piperidines or fluorination to 5-fluoro-piperidine (Scheme 2-10). The success of these substrates indicated a broad application of this methodology.

Aside from 5-methoxy-2-phenyl-pyridine, 2,5-diphenyl pyridines were also hydrogenated giving good enantioselectivity (86% and 76% ee, respectively) (**Table 2-12, entry 7**). Once again, we anticipate that this approach to gain access to 2,5-di-aryl chiral piperidines will find an extremely broad application in pharmaceuticals and other chemical industries.

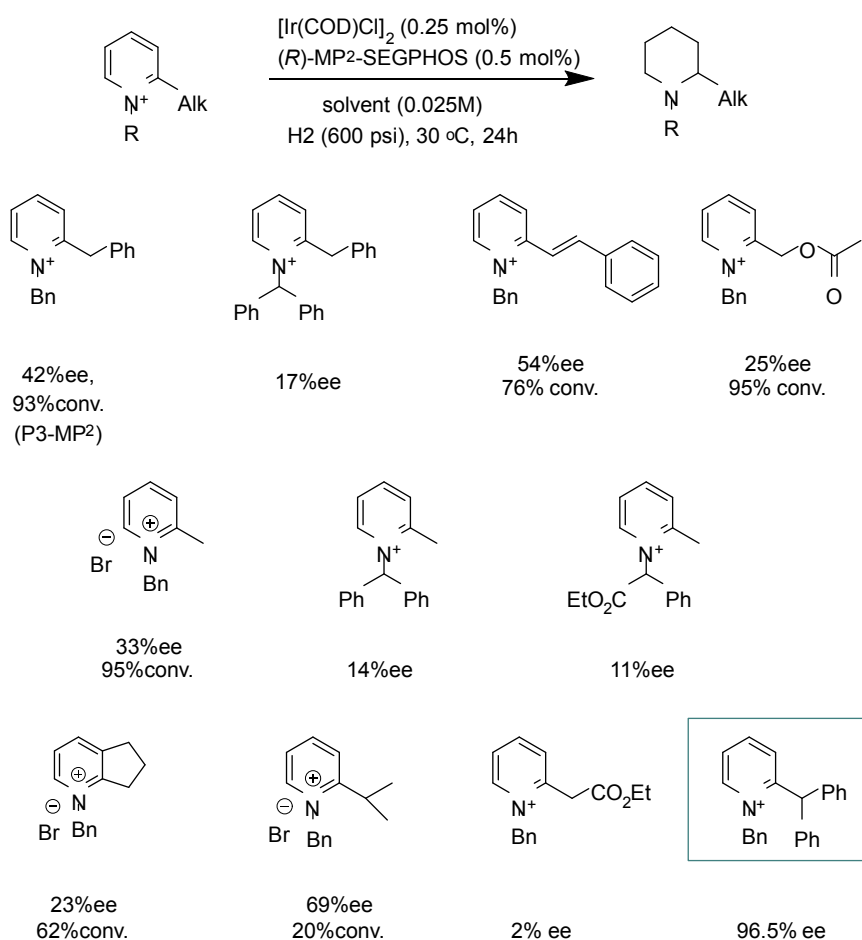


Scheme 2-10. Product Transformation from 5-Methoxy-2-aryl Piperidines **17**

2.4 Asymmetric Hydrogenation of 2-Alkyl N-Benzylpyridinium Salts

Compared to 2-aryl pyridines, 2-alkyl pyridines are more challenging substrates for asymmetric hydrogenation. The initial screening on 2-benzyl pyridinium salt only displayed a dismal 43% *ee* (Scheme 2-12). A number of 2-alkyl pyridinium salts have been investigated. For example, we investigated benzyl-styrylpyridine in an attempt to take advantage of the conjugate double to mimic the 2-aryl pyridine system. However, a mere 54% *ee* was obtained from this substrate. We also attempt to add carbonyl group in the substrate (Scheme 2-11, substrate 3) in a hope that the carbonyl group

might act as a secondary directing group. Different acylating agents other than benzyl bromide were also explored in attempts to fine-tune the electron or physical properties thus to improve the selectivities. Ultimately, none of the above approaches worked out well for the difficult 2-alkyl pyridine substrates.



Scheme 2-11. Asymmetric Hydrogenation of 2-Alkyl Pyridines.

Conversely, 2-bisphenyl-pyridinium salt was hydrogenated with an excellent enantioselectivity (96.5% ee). We rationalized that the efficiency of our catalytic system for this bis-phenyl substrate might be attributed to its structure resemble 2-aryl

pyridine closely (Scheme 2-11). We anticipate more discovery of new reaction manifolds from our system in the future.

In summary, we have explored a number of substrates in terms of structure diversity and broad application. We have demonstrated the broad application of our new approach to asymmetric hydrogenate pyridines, including some unprecedented or very challenging substrates, and its utility to easy removal of the benzyl protection group. On the other hand, the limited application of Ir/MP²-SegPhos system in di-substituted or 2-alkyl substituted pyridines proved that the performance of metal/ligand catalyst is strongly substrate-dependent; even within the same category of substrate, subtle changes in substrate structure may cause dramatic variation of the observed ee value and/or the reaction rate. Novel ligand development based upon rational design combined with an appropriate structural variation might be the future focus. Meanwhile the discovery of this newly developed catalytic system using the unusual MP²-SegPhos ligand also prompted us to study its mechanism, which we will discuss in Chapter Four.

2.5 Experimental Section

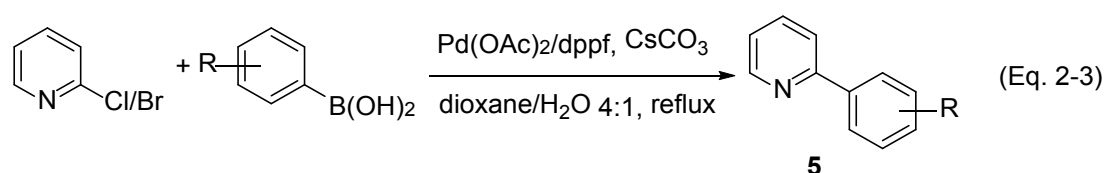
2.5.1 General Remarks

All reactions were performed in the nitrogen-filled glovebox or under nitrogen using standard Schlenk techniques unless otherwise noted. Column chromatography was performed using Sorbent silica gel 60 (230 – 450 mesh). ^1H NMR, and ^{13}C NMR spectral data were obtained from Bruker 400 MHz spectrometers or Varian 500 MHz spectrometers. Chemical shifts are reported in ppm. Enantiomeric excess values were determined by chiral HPLC on an Acquity H-class (Waters Corp., milford, MA) or chiral SFC on an Acquity UPC² (Waters Corp., milford, MA). All new products were further characterized by HRMS. A positive ion mass spectrum of sample was acquired on a Micromass 70-VSE mass spectrometer with an electron ionization source. Scale-up reaction was conducted in OptiMax 1001 (Serial #: B425732840 / Firmware: 5.2.2.0).

2.5.2 General Procedure for Synthesis of *N*-Benzylpyridinium Salts.

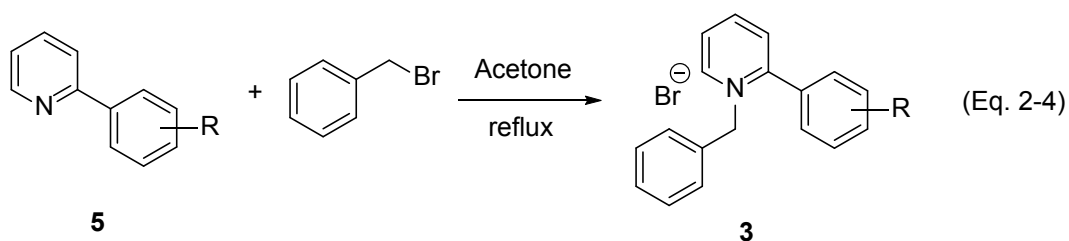
Most substrates were synthesized in two steps according to literature.

Step 1:



In glove box in a 40 ml vial was added 2-chloropyridine (or 2-bromopyridine) (5mmol) and dppf (0.5mmol), Pd (II) acetate (0.5 mmol), arylboronic acid (5 mmol), Cs₂CO₃ (10 mmol) in 5ml H₂O (degassed for 15min) and 20ml 1,4-dioxane. The suspension was stirred and heated to 70 °C for 20 hours. After cooled, removed from the glove box and then diluted with EtOAc, filtered through celite. Solvent was removed. The resulting residue was purified by chromatography (0-100% Hexane/EtOAc) to obtain colorless oil. NMR confirmed as desired product.

Step 2:



The solution of 2-arylpyridine (4 mmol) and benzyl bromide (4.4 mmol) in acetone was refluxed overnight. In most cases product will precipitate out. Then product was collected from filtration and further purified by recrystallization. In case there was no precipitate, the reaction mixture was purified by column chromatography on silica gel using CH₂Cl₂/MeOH (20:1) to give the desired products (47-87%).

N-benzyl-2-phenylpyridinium bromide (3a): White solid. ¹H NMR (400 MHz, CDCl₃) δ 9.80 (d, 1H), 8.54 (m, 1H), 8.20 (m, 1H), 7.86 (m, 1H), 7.50-7.78 (m, 5H), 7.30 (m, 4H), 7.10 (m, 2H), 6.20 (s, 2H).

2.5.3 General Procedure for Asymmetric Hydrogenation of *N*-Benzylpyridinium Salts.

In a nitrogen-filled glove box, ligands and metal sources were placed into 96 hydrogenation vials. 0.05 ml CH₂Cl₂ was added to each vials and stirring for 30 min. Then *N*-benzyl-2-phenylpyridium bromide dissolved in CH₂Cl₂ was added to each vial. Solvent was removed under reduced pressure in glove box. Then desired solvent or solvent pairs were added. The vials were placed in a parallel hydrogenation block and following three hydrogen purges, pressurized to 600 psi at 30 °C for 20 h. Selectivities and conversions were determined by direct sampling of the reaction mixture on SFC.

Scope of Asymmetric Pyridinium Salt Reductions

In a nitrogen-filled glove box, MP²-SEGPHOS (4.58 mg, 0.0099 mmol) and [Ir(COD)Cl]₂ (3.07 mg, 0.00457 mmol) were placed into a vial and stirring for 30 min in acetone (7.2 ml). Pyridinium salts (0.05 mmol) were placed into 4 ml hydrogenation vials. 0.2 ml catalyst solution and remaining solvent were added. The vials were placed in a parallel hydrogenation block and following three hydrogen purges, pressurized to 600 psi at 30 °C for 20 h. After carefully releasing the hydrogen, selectivities were determined by direct sampling of the reaction mixture on SFC or HPLC. Then saturated sodium carbonate was added and the mixture was stirred for

15-30 min. The organic layer was separated and extracted with CH₂Cl₂ twice, and the combined organic extracts were dried over Na₂SO₄ and concentrated in vacuum. Purification was performed by a silica gel column, eluted with hexane/EtOAc to give desired product.

Remove the Derivative Benzyl Protecting Group

After asymmetric hydrogenation of pyridinium salt (1.38 mmol), hydrogen gas was released from hydrogenation block. Solvent was evaporated under reduced pressure. 5 wt% Pd/C (20 wt%) and EtOH (20 ml) was charged. Then block was charged with 200 psi of H₂ without hydrogen purge. The hydrogenation was performed at 40 °C for 20 h and the hydrogen was released carefully. The solvent was then removed and the residue was purified by column chromatograph to give the corresponding product, which reacted with trifluoroacetic anhydride to yield the corresponding trifluoroacetamide, and then analyzed by chiral HPLC.

1-benzyl-2-phenylpiperidine (2a): 97% yield, 96% ee, white solid. The compound data were in good accordance with the literature.³ $[\alpha]_D^{20}$ -27.8 (c = 1.18 in CH₂Cl₂); ¹H-NMR (400 MHz, CDCl₃): δ 1.30-1.43 (m, 1H), 1.52-1.67 (m, 3H), 1.70-1.83 (m, 2H), 1.87-1.98 (dt, $J_1=3.4$ Hz, $J_2=11.5$ Hz, 1H), 2.80 (d, $J=13.2$ Hz, 1H), 2.92-3.00 (m, 1H), 3.10 (dt, $J_1=2.6$ Hz, $J_2=11.2$ Hz, 1H), 3.76 (d, $J=13.8$ Hz, 1H), 7.16-7.28 (m, 6H), 7.32 (t, $J=7.7$ Hz, 2H), 7.45 (d, $J=7.5$ Hz, 2H). ¹³C-NMR (400 MHz, CDCl₃): δ 25.3,

26.0, 37.0, 53.4, 59.8, 69.2, 126.5, 126.9, 127.5, 128.0, 128.5, 128.7, 139.9, 145.7.

Enantiomeric excess was determined by SFC: OJ-3 column (150*4.6 mm), 200 Bar, 40 °C, CO₂/MeOH with 25 mM IBA=95:5 (0-4 min), 60:40 (4-6.4 min), 35:65 (6.4-6.5 min), 3 ml/min. HRMS calcd for C₁₈H₂₂N⁺: 252.1747, found: 252.1751.

1-benzyl-2-(m-tolyl)piperidine (2b): 99% yield, 96% ee, yellow oil, unknown compound. ¹H-NMR (400 MHz, CDCl₃): δ 1.31-1.40 (m, 1H), 1.56-1.66 (m, 3H), 1.75-1.79 (m, 2H), 1.89-1.95 (dt, *J*₁=3.6 Hz, *J*₂=14.4 Hz, 1H), 2.35 (s, 3H), 2.79 (d, *J*=13.5 Hz, 1H), 2.96 (d, *J*=11.3, 1H), 3.06 (dd, *J*₁=2.3 Hz, *J*₂=10.9 Hz, 1H), 3.77 (d, *J*=13.5 Hz, 1H), 7.03 (d, *J*=7.2 Hz, 1H), 7.17-7.26 (m, 8H). ¹³C-NMR (400 MHz, CDCl₃): δ 21.5, 25.3, 26.0, 36.9, 53.4, 59.8, 69.3, 124.6, 126.5, 127.6, 128.0, 128.8, 137.9, 139.9, 145.7. Enantiomeric excess was determined by HPLC: Chiralpak AD-RH column (150*4.6 mm), MPA: 5 mM Na₂B₄O₇ pH=9.2, MPB: Acetonitrile, 80 % MPB isocratic at flow rate=1.0 ml/min. HRMS calcd for C₁₉H₂₄N⁺: 266.1903, found: 266.1905.

1-benzyl-2-(p-tolyl)piperidine (2c): 93% yield, 97% ee, yellow solid, unknown compound. ¹H-NMR (500 MHz, CD₃CN): δ 1.35-1.42 (m, 1H), 1.49-1.61 (m, 3H), 1.69-1.76 (m, 2H), 1.89-1.95 (m, 1H), 2.32 (s, 3H), 2.78 (d, *J*=13.5 Hz, 1H), 2.87 (d, *J*=11.47, 1H), 3.10 (d, *J*=10.33 Hz, 1H), 3.67 (d, *J*=13.59 Hz, 1H), 7.15-7.36 (m, 9H). ¹³C-NMR (400 MHz, CDCl₃): δ 21.1, 25.3, 26.1, 29.7, 37.0, 53.4, 59.7, 68.9, 126.5, 127.4, 128.0, 128.7, 129.2, 136.4, 139.9, 142.7. Enantiomeric excess was determined

by SFC: OJ-3 column (150*4.6 mm), 200 Bar, 40 °C, CO₂/MeOH with 25 mM IBA=95:5 (0-4 min), 60:40 (4-6.4 min), 35:65 (6.4-6.5 min), 3 ml/min. HRMS calcd for C₁₉H₂₄N⁺: 266.1903, found: 266.1908.

1-benzyl-2-(2-methoxyphenyl)piperidine (2d): 90% yield, 95% ee, yellow solid, unknown compound. ¹H-NMR (500 MHz, CD₃CN): δ 1.37-1.40 (m, 1H), 1.45-1.51 (m, 2H), 1.60-1.62 (m, 1H), 1.70-1.76 (m, 2H), 1.95-1.98 (m, 1H), 2.81 (d, *J*=13.33 Hz, 1H), 2.90 (d, *J*=11.11 Hz, 1H), 3.69 (d, *J*=13.35 Hz, 2H), 3.81 (s, 3H), 6.98 (dd, *J*₁=7.88 Hz, *J*₂=12.54 Hz, 2H), 7.19-7.26 (m, 6H), 7.68 (d, *J*=7.34 Hz, 1H). ¹³C-NMR (400 MHz, CDCl₃): δ 25.3, 26.2, 35.5, 53.7, 55.5, 59.6, 59.9, 110.6, 121.1, 126.4, 127.2, 127.8, 128.0, 133.6, 140.0, 156.8. Enantiomeric excess was determined by SFC: OD-3 column (150*4.6 mm), 200 Bar, 40 °C, CO₂/IPA with 25 mM IBA=88:12 (0-3 min), 3 ml/min. HRMS calcd for C₁₉H₂₄NO⁺: 282.1852, found: 282.1859.

1-benzyl-2-(3-methoxyphenyl)piperidine (2e): 99% yield, 98% ee, yellow oil, unknown compound. ¹H-NMR (400 MHz, CDCl₃): δ 1.31-1.38 (m, 1H), 1.55-1.60 (m, 3H), 1.76-1.79 (m, 2H), 1.89-1.96 (ddd, *J*₁=4.1 Hz, *J*₂=5.6 Hz, *J*₃=11.4 Hz, 1H), 2.81 (d, *J*=13.6 Hz, 1H), 2.96 (d, *J*=11.6 Hz, 1H), 3.08 (dd, *J*₁=2.4 Hz, *J*₂=11.0 Hz, 1H), 3.76 (d, *J*=4.9 Hz, 1H), 3.81 (s, 3H), 6.76 (ddd, *J*₁=0.9 Hz, *J*₂=2.6 Hz, *J*₃=8.2 Hz, 1H), 7.02-7.05 (m, 2H), 7.16-7.31 (m 6H). ¹³C-NMR (400 MHz, CDCl₃): δ 25.2, 26.0, 29.7, 36.9, 53.4, 55.2, 59.8, 69.2, 112.4, 112.7, 119.9, 125.5, 128.0, 128.7, 129.4, 139.9, 147.5, 159.9. Enantiomeric excess was determined by SFC: OJ-3 column (150*4.6

mm), 200 Bar, 40 °C, CO₂/MeOH with 25 mM IBA=95:5 (0-4 min), 60:40 (4-6.4 min), 35:65 (6.4-6.5 min), 3 ml/min. HRMS calcd for C₁₉H₂₄NO⁺: 282.1852, found: 282.1860.

1-benzyl-2-(4-methoxyphenyl)piperidine (2f): 95% yield, 97% ee, white solid, unknown compound. ¹H-NMR (400 MHz, CDCl₃): δ 1.28-1.41 (m, 1H), 1.54-1.61 (m, 3H), 1.73-1.79 (m, 2H), 1.89-1.95 (dt, *J*₁=3.9 Hz, *J*₂=11.4 Hz, 1H), 2.78 (d, *J*=13.5 Hz, 1H), 2.95 (d, *J*=11.4 Hz, 1H), 3.05 (dd, *J*₁=2.8 Hz, *J*₂=11.0 Hz, 1H), 3.74 (d, *J*=5.3 Hz, 1H), 3.79 (s, 3H), 6.87 (d, *J*=8.8 Hz, 2H), 7.16-7.28 (m, 5H), 7.36 (d, *J*=8.4 Hz, 2H). ¹³C-NMR (400 MHz, CDCl₃): δ 25.3, 26.1, 37.0, 53.4, 55.2, 59.6, 68.5, 113.9, 126.5, 127.9, 128.4, 128.7, 137.8, 140.0, 158.5. Enantiomeric excess was determined by SFC: OJ-3 column (150*4.6 mm), 200 Bar, 40 °C, CO₂/MeOH with 25 mM IBA=95:5 (0-4 min), 60:40 (4-6.4 min), 35:65 (6.4-6.5 min), 3 ml/min. HRMS calcd for C₁₉H₂₄NO⁺: 282.1852, found: 282.1858.

N-(4-(1-benzylpiperidin-2-yl)phenyl)acetamide (2g): 97% yield, 95% ee, yellow solid, unknown compound. ¹H-NMR (400 MHz, CDCl₃): δ 1.32-1.41 (m, 1H), 1.53-1.62 (m, 3H), 1.71-1.78 (m, 2H), 1.89-1.96 (dt, *J*₁=4.0 Hz, *J*₂=17.8 Hz, 1H), 2.13 (m, 3H), 2.79 (d, *J*=13.5 Hz, 1H), 2.95 (d, *J*=11.4 Hz, 1H), 3.07 (dd, *J*₁=2.0 Hz, *J*₂=10.8 Hz, 1H), 3.74 (d, *J*=13.5 Hz, 1H), 7.18-7.54 (m, 10H). ¹³C-NMR (400 MHz, CDCl₃): δ 14.1, 22.7, 24.5, 25.2, 25.9, 29.4, 31.9, 36.9, 53.3, 59.7, 68.6, 120.2, 126.6, 127.9, 128.0, 128.7, 136.7, 139.6, 141.7, 168.4. Enantiomeric excess was determined

by HPLC: Chiralcel OJ-RH column (150*4.6 mm), MPA: 5 mM Na₂B₄O₇ pH=9.2, MPB: Acetonitrile, 37 % MPB isocratic at flow rate=1.0 ml/min. HRMS calcd for C₂₀H₂₅N₂O⁺: 309.1961, found: 309.1968.

1-benzyl-2-(4-(tert-butyl)phenyl)piperidine (2h): 96% yield, 96% ee, white solid, unknown compound. ¹H-NMR (400 MHz, CDCl₃): δ 1.25-1.40 (m, 10H), 1.58-1.63 (m, 3H), 1.75-1.78 (m, 2H), 1.91 (ddd, *J*₁=4.7 Hz, *J*₂=7.6 Hz, *J*₃=11.4 Hz, 1H), 2.78 (d, *J*=13.6 Hz, 1H), 2.95 (d, *J*=11.3 Hz, 1H), 3.07 (dd, *J*₁=2.6 Hz, *J*₂=11.0 Hz, 1H), 3.78 (d, *J*=13.6 Hz, 1H), 7.18-7.37 (m, 9H). ¹³C-NMR (400 MHz, CDCl₃): δ 25.3, 26.1, 31.5, 34.4, 37.0, 53.5, 59.8, 68.9, 125.3, 126.5, 127.0, 128.0, 128.7, 140.1, 142.5, 149.6. Enantiomeric excess was determined by SFC: OZ-3 column (150*4.6 mm), 200 Bar, 40 °C, CO₂/MeOH with 25 mM IBA=97:3 (0-2 min), 3:40-60:40 (2-4 min), 60:40 (4-10 min), 3 ml/min. HRMS calcd for C₂₂H₃₀N⁺: 308.2373, found: 308.2375.

1-benzyl-2-(4-chlorophenyl)piperidine (2i): 96% yield, 98% ee, yellow solid, unknown compound. ¹H-NMR (400 MHz, CDCl₃): δ 1.26-1.41 (m, 1H), 1.50-1.59 (m, 3H), 1.72-1.79 (m, 2H), (dt, *J*₁=3.6 Hz, *J*₂=11.4 Hz, 1H), 2.8 (d, *J*=13.6 Hz, 1H), 2.96 (d, *J*=11.5 Hz, 1H), 3.09 (dd, *J*₁=2.5 Hz, *J*₂=11.0 Hz, 1H), 3.71 (d, *J*=13.5 Hz, 1H), 7.17-7.40 (m, 9H). ¹³C-NMR (400 MHz, CDCl₃): δ 25.1, 25.9, 37.0, 53.3, 59.8, 68.4, 126.6, 128.0, 128.6, 128.7, 128.8, 132.3, 139.5, 144.3. Enantiomeric excess was determined by SFC: OJ-3 column (150*4.6 mm), 200 Bar, 40 °C, CO₂/MeOH with 25

mM IBA=95:5 (0-4 min), 60:40 (4-6.4 min), 35:65 (6.4-6.5 min), 3 ml/min. HRMS calcd for C₁₈H₂₁NCl⁺: 286.1357, found: 286.1361.

2-([1,1'-biphenyl]-4-yl)-1-benzylpiperidine (2j): 96% yield, 94% ee, white solid, unknown compound. ¹H-NMR (400 MHz, CDCl₃): δ 1.37-1.43 (m, 1H), 1.62 (m, 3H), 1.80-1.82 (m, 2H), 1.96 (m, 1H), 2.85 (d, *J*=11.8 Hz, 1H), 3.00 (d, *J*=8.7 Hz, 1H), 3.16 (d, *J*=8.2 Hz, 1H), 3.83 (d, *J*=10.0 Hz, 1H), 7.21-7.59 (m, 14H). ¹³C-NMR (400 MHz, CDCl₃): δ 25.2, 26.0, 29.7, 37.0, 53.4, 59.9, 68.9, 126.6, 127.1, 127.3, 127.9, 128.1, 128.7, 139.8, 141.1. Enantiomeric excess was determined by SFC: AD-3 column (150*4.6 mm), 200 Bar, 40 °C, CO₂/IPA with 25 mM IBA=78:22 (0-4 min), 3 ml/min. HRMS calcd for C₂₄H₂₆N⁺: 328.2060, found: 328.2066.

1-benzyl-2-(2,4-dichlorophenyl)piperidine (2k): 94% yield, 93% ee, yellow solid, unknown compound. ¹H-NMR (400 MHz, CDCl₃): δ 1.36-1.42 (m, 2H), 1.55-1.63 (m, 2H), 1.78-1.83 (m, 2H), 2.00 (dt, *J*₁=2.9 Hz, *J*₂=11.6 Hz, 1H), 2.89 (d, *J*=13.7 Hz, 1H), 2.99 (d, *J*=11.4 Hz, 1H), 3.67 (m, 2H), 7.2-7.39 (m, 7H), 7.55 (d, *J*=8.4 Hz, 1H). ¹³C-NMR (400 MHz, CDCl₃): δ 24.9, 25.8, 35.1, 53.3, 59.6, 63.4, 126.7, 127.7, 128.1, 128.6, 129.1, 129.7, 132.5, 133.7, 139.1, 141.3. Enantiomeric excess was determined by SFC: OJ-3 column (150*4.6 mm), 200 Bar, 40 °C, CO₂/MeOH with 25 mM IBA=95:5 (0-4 min), 60:40 (4-6.4 min), 35:65 (6.4-6.5 min), 3 ml/min. HRMS calcd for C₁₈H₂₀NC₂⁺: 320.0967, found: 320.0974.

1-benzyl-2-(3,5-difluorophenyl)piperidine (2l): 95% yield, 98% ee, white solid, unknown compound. $^1\text{H-NMR}$ (400 MHz, CDCl_3): δ 1.28-1.39 (m, 1H), 1.48-1.61 (m, 3H), 1.73-1.78 (m, 2H), 1.92 (dt, $J_1=3.3$ Hz, $J_2=11.6$ Hz, 1H), 2.83 (d, $J=13.5$ Hz, 1H), 2.95 (d, $J=13.4$ Hz, 1H), 3.10 (dd, $J_1=2.6$ Hz, $J_2=11.0$ Hz, 1H), 3.73 (d, $J=13.5$ Hz, 1H), 6.65 (tt, $J_1=2.4$ Hz, $J_2=8.9$ Hz, 1H), 7.00 (dd, $J_1=2.1$ Hz, $J_2=8.5$ Hz, 2H), 7.19-7.30 (m, 5H). $^{13}\text{C-NMR}$ (400 MHz, CDCl_3): δ 24.9, 25.8, 36.8, 53.1, 60.0, 68.6, 101.9, 102.2, 102.5, 109.9, 110.2, 126.8, 128.1, 128.6, 139.2, 150.2, 161.9, 164.5. Enantiomeric excess was determined by HPLC: Chiralpak OJ-RH column (150*4.6 mm), MPA: 5 mM $\text{Na}_2\text{B}_4\text{O}_7$ pH=9.2, MPB: Acetonitrile, 60% (0-10 min), 70% (10-13 min) MPB isocratic at flow rate=1.0 ml/min. HRMS calcd for $\text{C}_{18}\text{H}_{20}\text{NF}_2$: 288.1558, found: 288.1565.

1-benzyl-2-(naphthalen-2-yl)piperidine (2m): 88% yield, 94% ee, yellow solid, unknown compound. $^1\text{H-NMR}$ (400 MHz, CDCl_3): δ 1.35-1.43 (m, 1H), 1.59-1.61 (m, 3H), 1.76-1.82 (m, 2H), 1.93-2.01 (m, 1H), 2.85 (d, $J=13.5$ Hz, 1H), 3.01 (d, $J=13.5$ Hz, 1H), 3.29 (dd, $J_1=2.6$ Hz, $J_2=10.8$ Hz, 1H), 3.79 (d, $J=13.5$ Hz, 1H), 7.15-7.26 (m, 5H), 7.39-7.64 (m, 2H), 7.68-7.87 (m, 5H). $^{13}\text{C-NMR}$ (400 MHz, CDCl_3): δ 25.3, 26.1, 29.5, 36.9, 53.4, 59.9, 69.3, 125.4, 125.7, 125.9, 126.2, 126.6, 127.7, 128.0, 128.3, 128.8, 132.9, 133.6, 139.7, 143.3. Enantiomeric excess was determined by SFC: OJ-3 column (150*4.6 mm), 200 Bar, 40 °C, CO_2/MeOH with 25 mM IBA=95:5 (0-4 min), 60:40 (4-6.4 min), 35:65 (6.4-6.5 min), 3 ml/min. HRMS calcd for $\text{C}_{22}\text{H}_{24}\text{N}$: 302.1903, found: 302.1909.

1-benzyl-2-methylpiperidine (2n): 81% yield, 33% ee, colorless solid. The compound data were in good accordance with the literature.⁴ ¹H-NMR (400 MHz, CDCl₃): δ 1.21 (d, J = 6.4 Hz, 3H), 1.27-1.54 (m, 4H), 1.64-1.70 (m, 2H), 1.97 (td, J = 11.6, 3.6 Hz, 1H), 2.29-2.35 (m, 1H), 2.76 (dt, $J_1=3.9$ Hz, $J_2=11.4$ Hz, 1H), 3.19 (d, J = 13.4 Hz, 1H), 4.00 (d, J = 13.4 Hz, 1H), 7.23-7.36 (m, 5H). ¹³C-NMR (400 MHz, CDCl₃) δ 19.9, 24.3, 26.3, 34.9, 52.4, 56.6, 58.7, 126.9, 128.3, 129.4, 139.6. Enantiomeric excess was determined by SFC: OZ-3 column (150*4.6 mm), 200 Bar, 40 °C, CO₂/MeOH with 25 mM IBA=99:1 to 60:40 (0-5 min), 60:40 (5-8 min), 3 ml/min. HRMS calcd for C₁₃H₂₀N⁺: 190.1596, found: 190.1598.

1-benzyl-2-isopropylpiperidine (2o): 24% yield, 69% ee, colorless solid. The compound data were in good accordance with the literature.⁵ ¹H-NMR (400 MHz, CDCl₃): δ 0.91-0.94 (m, 6H), 1.21-1.31 (m, 2H), 1.37-1.44 (m, 2H), 1.58-1.62 (m, 1H), 1.72-1.75 (m, 1H), 1.91-1.97 (m, 1H), 1.99-2.02 (m, 1H), 2.21-2.29 (m, 1H), 2.81 (dtd, $J_1=1.5$ Hz, $J_2=3.6$ Hz, $J_3=3.8$ Hz, $J_4=11.9$ Hz, 1H), 3.09 (d, J=13.4 Hz, 1H), 4.10 (d, J=13.4 Hz, 1H), 7.19-7.34 (m, 5H). ¹³C-NMR (400 MHz, CDCl₃): δ 16.0, 20.2, 23.5, 27.6, 52.7, 56.6, 66.5, 126.5, 128.1, 128.8, 140.4. Enantiomeric excess was determined by SFC: OZ-3 column (150*4.6 mm), 200 Bar, 40 °C, CO₂/MeOH with 25 mM IBA=99:1 to 60:40 (0-5 min), 60:40 (5-8 min), 3 ml/min. HRMS calcd for C₁₅H₂₄N⁺: 218.1909, found: 218.1905.

1,2-dibenzylpiperidine (2p): 99% yield, 42% ee, colorless solid. The compound data were in good accordance with the literature.⁶ ¹H-NMR (400 MHz, CDCl₃): δ 1.22-1.36 (m, 2H), 1.48-1.56 (m, 3H), 1.58-1.66 (m, 1H), 2.22 (m, 1H), 2.60 (m, 2H), 2.64-2.69 (m, 1H), 2.77 (m, 1H), 3.17 (d, J = 9.8 Hz, 1H), 3.49 (d, J = 13.6 Hz, 1H), 4.05 (d, J = 13.6 Hz, 1H), 7.16-7.38 (m, 10H). ¹³C-NMR (400 MHz, CDCl₃): δ 22.5, 25.4, 29.4, 50.9, 58.6, 61.8, 125.8, 126.7, 128.2, 128.3, 128.9, 129.4, 139.8, 140.5. Enantiomeric excess was determined by SFC: OJ-3 column (150*4.6 mm), 200 Bar, 40 °C, CO₂/MeOH with 25 mM IBA=95:5 (0-4 min), 60:40 (4-6.4 min), 35:65 (6.4-6.5 min), 3 ml/min. HRMS calcd for C₁₉H₂₄N⁺: 266.1909, found: 266.1917.

2-phenylpiperidine (3a): 91% yield, 92% ee, yellow oil. The compound data were in good accordance with the literature.⁷ ¹H-NMR (400 MHz, CDCl₃): δ 1.48-1.90 (m, 6H), 2.79 (m, 1H), 3.19 (d, J =11.0 Hz, 1H), 3.58 (d, J =11.2 Hz, 1H), 7.20-7.38 (m, 5H). ¹³C-NMR (400 MHz, CDCl₃): δ 25.4, 25.9, 35.0, 47.8, 62.4, 126.6, 127.0, 128.4, 145.6. Enantiomeric excess was determined by GC: Beta-390 column, 140 °C, 1 ml/min, 45 min.

1-(4-methoxybenzyl)-2-phenylpiperidine (5b): 96% yield, 95% ee, yellow solid. The compound data were in good accordance with the literature.⁸ ¹H-NMR (500 MHz, CD₃CN): δ 1.39-1.44 (m, 1H), 1.48-1.65 (m, 3H), 1.74-1.77 (m, 2H), 1.93-1.95 (m, 1H), 2.76 (d, J =13.3 Hz, 1H), 2.90-2.92 (d, J =11.65 Hz, 1H), 3.13-3.16 (dd, J_1 =2.53 Hz, J_2 =11.04 Hz, 1H), 3.61-3.63 (d, J =13.25 Hz, 1H), 3.78 (m, 3H), 6.85-6.88 (t,

$J=5.74$ Hz, 2H), 7.18 (d, $J=8.4$ Hz, 2H), 7.27 (t, $J=7.35$ Hz, 1H), 7.38 (t, $J=7.72$ Hz, 2H), 7.50 (d, $J=7.29$ Hz, 2H). ^{13}C -NMR (400 MHz, CDCl_3): δ 25.3, 26.0, 37.0, 53.2, 55.2, 59.1, 69.1, 113.4, 126.8, 127.5, 128.5, 129.8, 131.7, 145.8, 158.4. Enantiomeric excess was determined by SFC: OJ-3 column (150*4.6 mm), 200 Bar, 40 °C, CO_2/MeOH with 25 mM IBA=95:5 (0-4 min), 60:40 (4-6.4 min), 35:65 (6.4-6.5 min), 3 ml/min. HRMS calcd for $\text{C}_{19}\text{H}_{24}\text{NO}^+$: 282.1852, found: 282.1863.

Methyl 2-((2-phenylpiperidin-1-yl)methyl)benzoate (5c): 93% yield, 94.4% ee, white solid, unknown compound. ^1H -NMR (500 MHz, CD_3CN): δ 1.43-1.49 (m, 1H), 1.61-1.65 (m, 3H), 1.80-1.83 (m, 2H), 2.03 (dd, $J_1=11.27$ Hz, $J_2=15.2$ Hz, 1H), 2.87 (d, $J=11.5$ Hz, 1H), 3.28 (d, $J=11.4$ Hz, 1H), 3.40 (d, $J=15.8$ Hz, 1H), 3.78-3.81 (m, 4H), 7.23 (t, $J=7.30$ Hz, 1H), 7.31 (t, $J=7.45$ Hz, 3H), 7.45 (d, $J=7.58$ Hz, 2H), 7.53 (t, $J=7.57$ Hz, 1H), 7.70 (d, $J=7.72$ Hz, 1H), 7.85 (d, $J=7.80$ Hz, 1H). ^{13}C -NMR (400 MHz, CDCl_3): δ 25.3, 26.1, 37.1, 51.8, 54.0, 56.9, 69.4, 125.9, 126.8, 127.4, 128.4, 129.1, 129.7, 130.0, 131.7, 142.0, 145.5, 168.3. Enantiomeric excess was determined by SFC: OJ-3 column (150*4.6 mm), 200 Bar, 40 °C, CO_2/MeOH with 25 mM IBA=95:5 (0-4 min), 60:40 (4-6.4 min), 35:65 (6.4-6.5 min), 3 ml/min. HRMS calcd for $\text{C}_{20}\text{H}_{24}\text{NO}_2^+$: 310.1802, found: 310.1812.

1-methyl-2-phenylpiperidine (5d): 75% yield, 81% ee, white oil. The compound data were in good accordance with the literature.⁹ ^1H -NMR (400 MHz, CDCl_3): δ 1.35 (m, 1H), 1.6 (m, 4H), 1.7 (m, 3H), 1.8 (m, 1H), 1.99 (s, 3H), 2.1 (m, 1H), 2.75

(m, 1H), 3.10 (d, $J=8.4$ Hz, 1H), 7.2-7.4 (m, 5H). ^{13}C -NMR (400 MHz, CDCl_3): δ 25.0, 26.2, 35.9, 44.5, 57.6, 71.1, 126.9, 127.4, 128.7, 144.8. Enantiomeric excess was determined by HPLC: OJ-3R column (150*4.6 mm), MeCN/5mM $\text{Na}_2\text{B}_4\text{O}_7$ (PH~9.2, aq)=80:20, 1mL/min. HRMS calcd for $\text{C}_{12}\text{H}_{18}\text{N}^+$: 176.1434, found: 176.1436.

1-ethyl-2-phenylpiperidine (5e): 94% yield, 94% ee, white solid, unknown compound. ^1H -NMR (400 MHz, CDCl_3): δ 1.19-1.31 (m, 4H), 1.50 (m, 1H), 1.56-1.65 (m, 4H), 1.89-2.00 (m, 2H), 2.46 (dd, $J_1=7.1$ Hz, $J_2=12.7$ Hz, 1H), 2.95 (d, $J=10.8$ Hz, 1H), 3.10 (d, $J=10.4$ Hz, 1H), 7.16-7.25 (m, 5H). ^{13}C -NMR (400 MHz, CDCl_3): δ 11.0, 25.2, 26.1, 29.7, 36.6, 49.1, 52.6, 68.8, 126.7, 127.5, 128.3. Enantiomeric excess was determined by HPLC: OJ-3R column (150*4.6 mm), MeCN/5mM $\text{Na}_2\text{B}_4\text{O}_7$ (PH~9.2, aq)=80:20, 1mL/min. HRMS calcd for $\text{C}_{13}\text{H}_{20}\text{N}^+$: 190.1590, found: 190.1599.

1-isopropyl-2-phenylpiperidine (5f): 82% yield, 96% ee, white solid. The compound data were in good accordance with the literature.¹⁰ ^1H -NMR (400 MHz, CDCl_3): δ 0.70 (t, $J=7.4$ Hz, 3H), 1.33-1.39 (m, 3H), 1.53-1.70 (m, 5H), 1.84 (m, 1H), 2.03 (dt, $J_1=3.4$ Hz, $J_2=11.5$ Hz, 1H), 2.36 (ddd, $J_1=7.1$ Hz, $J_2=9.6$ Hz, $J_3=12.6$ Hz, 1H), 2.98 (dd, $J_1=2.7$ Hz, $J_2=11.0$ Hz, 1H), 3.17 (d, $J=11.2$ Hz, 1H), 7.21-7.33 (m, 5H). ^{13}C -NMR (400 MHz, CDCl_3): δ 11.8, 19.2, 25.2, 26.2, 36.8, 53.3, 57.3, 69.2, 126.6, 127.5, 128.3, 145.6. Enantiomeric excess was determined by SFC: Column Lux 4 Cellulose (150*4.6 mm), 200 Bar, 40 °C, CO_2/MeOH with 25 mM IBA=70:30, 3

ml/min. HRMS calcd for C₁₄H₂₂N⁺: 204.1747, found: 204.1755.

Ethyl 2-(2-phenylpiperidin-1-yl)acetate (5g): 82% yield, 96% ee, yellow solid, unknown compound. ¹H-NMR (400 MHz, CDCl₃): δ 1.18-1.26 (m, 3H), 1.37-1.44 (m, 1H), 1.60-1.79 (m, 5H), 2.49 (dt, *J*₁=4.1 Hz, *J*₂=11.1 Hz, 1H), 2.89 (d, *J*=16.7 Hz, 1H), 3.09 (d, *J*=11.4 Hz, 1H), 3.22 (d, *J*=16.7 Hz, 1H), 3.43 (dd, *J*₁=2.6 Hz, *J*₂=11.0 Hz, 1H), 4.08 (m, 2H), 7.23-7.35 (m, 5H). ¹³C-NMR (400 MHz, CDCl₃): δ 14.2, 25.0, 26.1, 36.2, 53.9, 56.5, 60.0, 66.9, 127.2, 127.7, 128.5, 144.1, 171.2. Enantiomeric excess was determined by HPLC: OJ-3R column (150*4.6 mm), MeCN/5mM Na₂B₄O₇ (PH~9.2, aq)=80:20, 1mL/min. HRMS calcd for C₁₄H₂₀NO₂⁺: 234.1489, found: 234.1495.

Reference:

1. (a) S. Källström, R. Leino, *Bioorg. Med. Chem.* **2008**, *16*, 601. (b) P. A. Petukhov, J. Zhang, C. Z. Wang, Y. P. Ye, K. M. Johnson and A. P. Kozikowski, *J. Med. Chem.* **2004**, *47*, 3009. (c) P. D. Bailey, P. A. Millwood and P. D. Smith, *Chem. Commun.* **1998**, 633.
2. Hansen TG. *Expert Rev Neurother.* **2004**, *4*, 781.
3. A. Gutman, I. Zaltsman, A. Shalimov, M. Sotrihin, G. Nisnevich, L. Yudovich, I. Fedotev, *U.S. Pat. Appl. Publ.* US 20040180928 A1 20040916, **2004**.
4. J. Buus Lassen, *Psychopharmacology* **1989**, *98*, 257.
5. J. Feng, Z. Zhang, M. B. Wallace, J. A. Stafford, S. W. Kaldor, D. B. Kassel, M. Navre, L. Shi, R. J. Skene, T. Asakawa, *et al*, *J. Med. Chem.* **2007**, *50*, 2297.
6. For selected reviews, see: a) P. D. Bailey, P. A. Millwood, P. D. Smith, *Chem. Commun.* **1998**, 633; b) F. Glorius, *Org. Biomol. Chem.* **2005**, *3*, 4171; c) D.-S. Wang, Q.-A. Chen, S.-M. Lu, Y.-G. Zhou, *Chem. Rev.* **2012**, *112*, 2557.
7. Bird, C. W. *Tetrahedron* **1992**, *48*, 335
8. Murata, S.; Sugimoto, T.; Matsuura, S. *Heterocycles* **1987**, *26*, 763
9. Ohta, T.; Miyake, T.; Seido, N.; Kumobayashi, H.; Takaya, H. *J. Org. Chem.* **1995**, *60*, 357
10. Bianchini, C.; Barbaro, P.; Scapacci, G.; Farnetti, E.; Graziani, M. *Organometallics* **1998**, *17*, 3308
11. W.-B. Wang, S.-M. Lu, P.-Y. Yang, X.-W. Han, Y.-G. Zhou, *J. Am. Chem. Soc.* **2003**, *125*, 10536.
12. F. Glorius, N. Spielkamp, S. Holle, R. Goddard, C.W. Lehmann, *Angew. Chem.* **2004**, *116*, 2910; *Angew. Chem.Int. Ed.* **2004**, *43*, 2850.
13. A. Lei, M. Chen, M. He, X. Zhang, *Eur. J. Org. Chem.* **2006**, 4343.
14. L. Q. Qiu, F. Y. Kwong, J. Wu, W. H. Lam, S. Chan, W.-Y. Yu, Y.-M. Li, R. W. Guo, Z. Zhou, A. S. C. Chan, *J. Am. Chem. Soc.* **2006**, *128*, 5955.
15. (a) H.-F. Zhou, Z.-W. Li, Z.-J. Wang, T.-L. Wang, L.-J. Xu, Y.-M. He, Q.-H. Fan, J. Pan, L.-Q. Gu, A. S. C. Chan, *Angew. Chem., Int. Ed.* **2008**, *47*, 8464. (b) T.-L. Wang, L. G. Zhuo, Z.-W. Li, F. Chen, Z.-Y. Ding, Y.-M. He, Q.-H. Fan, J.-F. Xiang, Z.-X. Yu, A. S. C. Chan, *J. Am. Chem. Soc.* **2011**, *133*, 9878. (c) C. Wang, C. Q. Li, X. F. Wu, A. Pettman, J. L. Xiao, *Angew. Chem., Int. Ed.* **2009**, *48*, 6524.
16. S.-M. Lu, Y.-Q. Wang, X.-W. Han, Y.-G. Zhou, *Angew. Chem. Int. Ed.* **2006**, *45*, 2260.
17. (a) L. Shi, Z.-S. Ye, L.-L. Cao, R.-N. Guo, Y. Hu, Y.-G. Zhou, *Angew. Chem. Int. Ed.* **2012**, *51*, 8286. (b) Z.-S. Ye, R.-N. Guo, X.-F. Cai, M.-W. Chen, L. Shi, Y.-G. Zhou, *Angew. Chem. Int. Ed.* **2013**, *52*, 3685.
18. A. Iimuro, K. Yamaji, S. Kandula, T. Nagano, Y. Kita, K. Mashima, *Angew. Chem. Int. Ed.* **2013**, *52*, 2046.
19. M. Studer, C. Wedemeyer-Exl, F. Spindler, H. U. Blaser, *Monatsh. Chem.* **2000**, *131*, 1335.
20. X.-B. Wang, W. Zeng, Y.-G. Zhou, *Tetrahedron Lett.* **2008**, *49*, 4922.
21. F. Glorius, N. Spielkamp, S. Holle, R. Goddard, C. W. Lehmann, *Angew. Chem.*

- Int. Ed.* **2004**, *43*, 2850.
22. A. W. Lei, M. Chen, M. S. He, X. Zhang, *Eur. J. Org. Chem.* **2006**, 4343.
 23. (a) C. Y. Legault, A. B. Charette, *J. Am. Chem. Soc.* **2005**, *127*, 8966. (b) Z.-S. Ye, M.-W. Chen, Q.-A. Chen, L. S., Y. Duan, Y.-G. Zhou, *Angew. Chem. Int. Ed.* **2012**, *51*, 10181.
 24. (a) M. Ye; G. Gao; A. J. F. Edmunds; P. A. Worthington; J. A. Morris; and Jin-Quan Yu. *J. Am. Chem. Soc.* **2011**, *133*, 19090. (b) T. M. Nguyen and D. A. Nicewicz. *J. Am. Chem. Soc.* **2013**, *135*, 9588. (c) K. D. Hesp; D. P. Fernando; W. Jiao; and A. T. Londregan. *Org. Lett.* **2014**, *16*, 413. (d) Z. Peng; J. W. Wong; E. C. Hansen; A. L. A. Puchlopek-Dermenci; and H. J. Clarke. *Org. Lett.* **2014**, *16*, 860. (e) H. Huang; T. C. Lacy; B. Bzachut; G. X. Ortiz Jr.; and Q. Wang. *Org. Lett.* **2013**, *15*, 1818. (f) K. E. Henegar; R. Lira; H. Kim; and J. Gonzalez-Hernandez. *Org. Process Res. Dev.* **2013**, *17*, 985.
 25. This initial work on Bronsted acid salt of pyridine hydrogenation was conducted by M. Chang in Zhang's group.
 26. T. W. Greene, P. G. M. Wuts, *Protective Groups in Organic Synthesis*, Wiley-Interscience, New York, **1999**.
 27. This work was collaborated with Dr. Y. Chen (Merck), M.Chang and S.Liu of Zhang's group and was published in *Angew. Chem.Int. Ed.* **2014**, *53*, 12761.
 28. H. Shimizu, T. Saito, I. Nagasaki, *U.S. Pat. Appl. Publ.* US 20040092388 A1 20040513, **2004**.
 29. The only reported use of MP²-SEGPPOS was for asymmetric hydrogenation of *N*-acetamidocinnamic acid, which gave the product in 60% *ee*, see: H. Shimizu, T. Saito, I. Nagasaki, EP 1419815 A1, **2004**.
 30. (a) W. Schafer, A. Schweig, G. Markl, H. Hauptmann, F. Mathey, *Angew. Chem. Int. Ed.* **1973**, *12*, 145; *Angew. Chem.* **1973**, *85*, 140; b) Schafer, W.; Schweig, A.; Mathey, F.; *J. Am. Chem. Soc.* **1976**, *98*, 407.
 31. The value of the intracyclic CPC angle of phosphole (90.7° for phenylphosphole) is much smaller than normal CPC angles (100°) which indicates that the system is very strained and rigid; see: P. Coggon, A. T. McPhail, *J. Chem. Soc., Dalton Trans.* **1973**, 1888.
 32. W. Egan, R. Tang, G. Zon, K. Mislow, *J. Am. Chem. Soc.* **1971**, *93*, 6205.
 33. For a recent example, see: G. Liu, X. Liu, Z. Cai, G. Jiao, G. Xu, W. Tang, *Angew. Chem. Int. Ed.* **2013**, *52*, 4235; *Angew. Chem.* **2013**, *125*, 4329.
 34. (a) M. A. Wijdeven; J. Willemsen; F. P. J. T. Rutjes, *Eur. J. Org. Chem.* 2010, **2010**, 2831–2844; (b) D. Gomez Pardo; J. Cossy, *Chem. - Eur. J.* **2014**, *20*, 4516– 4525; (c) J. Cossy, *Chem. Rec.* **2005**, *5*, 70–80.
 35. (a) A. Niethe; D. Fischer; S. Blechert, *J. Org. Chem.* 2008, *73*, 3088–3093; (b) K. Murakami; Y. Sasano; M. Tomizawa; M. Shibuya; E. Kwon; Y. Iwabuchi, *J. Am. Chem. Soc.* 2014, *136*, 17591– 17600; (c) C. Herdeis; P. Kupper; S. Ple, *Org. Biomol. Chem.* 2006, *4*, 524-529; (d) T. Sato; S. Aoyagi; C. Kibayashi, *Org. Lett.* 2003, **5**, 3839–3842.

Chapter 3

Iridium-Catalyzed Enantioselective Hydrogenation of Isoquinolines and Quinolines

3.1 Introduction and Background

Tetrahydroquinolines (THQs) and tetrahydroisoquinolines (THIQs) are an important family of biologically active molecules.¹ They are present in numerous natural alkaloids and important pharmaceutical products such as (+)-cryptostyline II,² (+)-cryptostyline III,² and solifenacin³ (Figure 3-1). The 1-arylTHIQ compound Solifenacin, for example, is a competitive antagonist that prevents binding of acetylcholine to the human muscarinic acetylcholine receptor and reduces contractions of the bladder muscles.

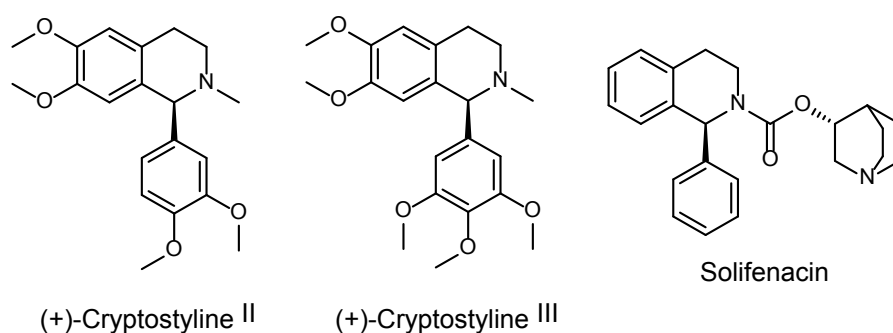
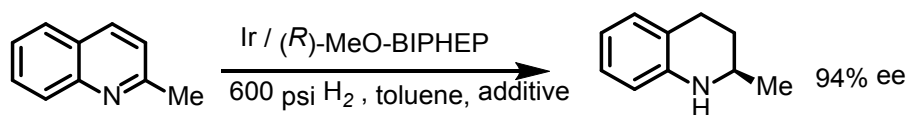


Figure 3-1. Structures of Selected Chiral THIQ.

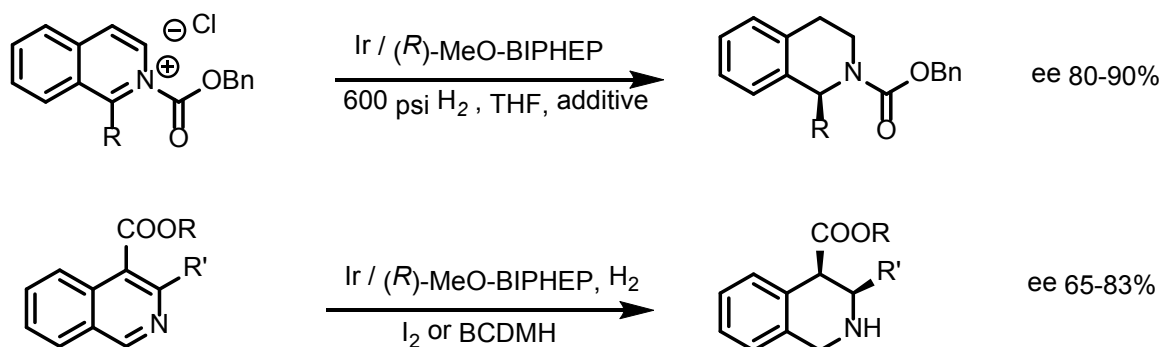
Three main strategies have been developed for the enantioselective syntheses of THIQs. The most common approach involves a Bischler–Napieralski cyclization followed by reduction of the resulting imine with a chiral hydride reducing agent or catalytic hydrogenation in the presence of a chiral catalyst.^{8a} A second strategy employs asymmetric Pictet–Spengler condensations.^{4h} Finally, chiral THIQs have been prepared by the introduction of nucleophiles or electrophiles to the 1-position of isoquinoline derivatives.⁴ⁱ Among various synthetic approaches to afford enantiomerically pure THQs and THIQs, asymmetric hydrogenation, with a high atom economy, relatively simple procedure and easy work-up, shows the most promising and efficient method.^{1,4,5} To the best of our knowledge, however, asymmetric hydrogenation of N-heteroaromatics, especially isoquinolines, remains a challenging task.⁶ Only a few examples with moderate enantioselectivity have been described so far. These examples also tend to rely on unique catalyst systems and suffer from a limited scope of suitable substrates.

In 2003, Zhou and co-workers developed the first asymmetric hydrogenation of quinolines using $[\{\text{IrCl}(\text{COD})\}_2]/\text{MeO-biphep}/\text{I}_2$ as the catalyst system. (Scheme 3-1).⁷ It was found that the substrate scope was limited to quinoline alkyl derivatives and that the hydrogenation reaction cannot proceed for isoquinolines under standard conditions. Zhou's group then achieved to obtain high enantioselectivity in both THQ and THIQ by activating quinolines or

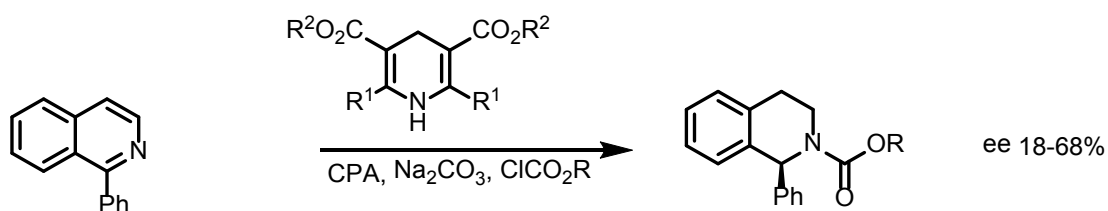
isoquinolines with chloroformate or the addition of BCDMH.⁸ (Scheme 3-2). By introducing chiral phosphoric acid, transfer hydrogenation of isoquinoline was achieved by Zhou in 2014 and N-protected 1,2-dihydroisoquinolines were synthesized with moderate enantioselectivities (Scheme 3-3).⁹ In 2013, Mashima's group synthesized chiral THIQ using a dinuclear iridium(III)–bisphosphine complex, but the substrate scope is still limited to aromatic or bulky substituents (Scheme 3-4).¹⁰ Most recently, Zhang group reported a Rhodium catalyzed asymmetric hydrogenation for both isoquinolines and quinolines (Scheme 3-5).¹¹ By introducing strong Bronsted acid HCl, anion binding between the substrate and the ligand (a ferrocene-based thiourea chiral phosphine system) was established to achieve high reactivity and high enantioselectivity (up to 99% conversion and 99% ee). However, the substrates scope for this approach is limited to simple alkyl groups. As discussed above, although the recent development of an asymmetric hydrogenation of aromatic and heteroaromatic compounds was remarkable, the development of more general and straightforward synthetic methods toward 1- and 3-substituted THIQs is still in high demand.



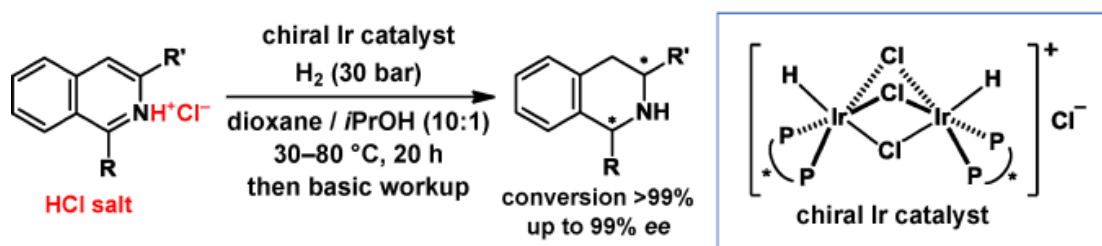
Scheme 3-1. First Asymmetric Hydrogenation of 2-Methyl-quinoline.



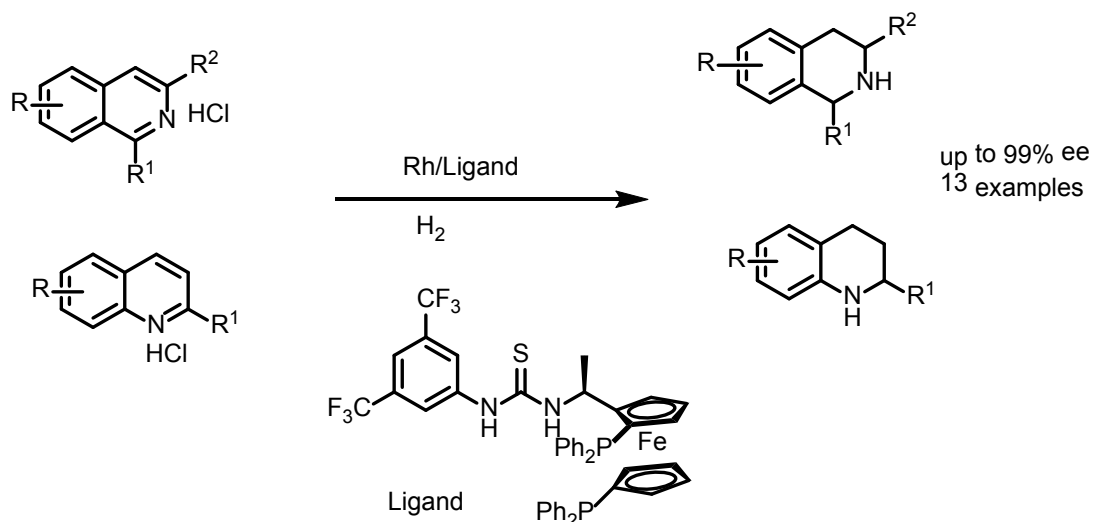
Scheme 3-2. Asymmetric Hydrogenation Requiring Activating Reagents.



Scheme 3-3. Ir-Asymmetric Transfer Hydrogenation.



Scheme 3-4. Dinuclear Iridium Complexes Catalyzed Asymmetric Hydrogenation.



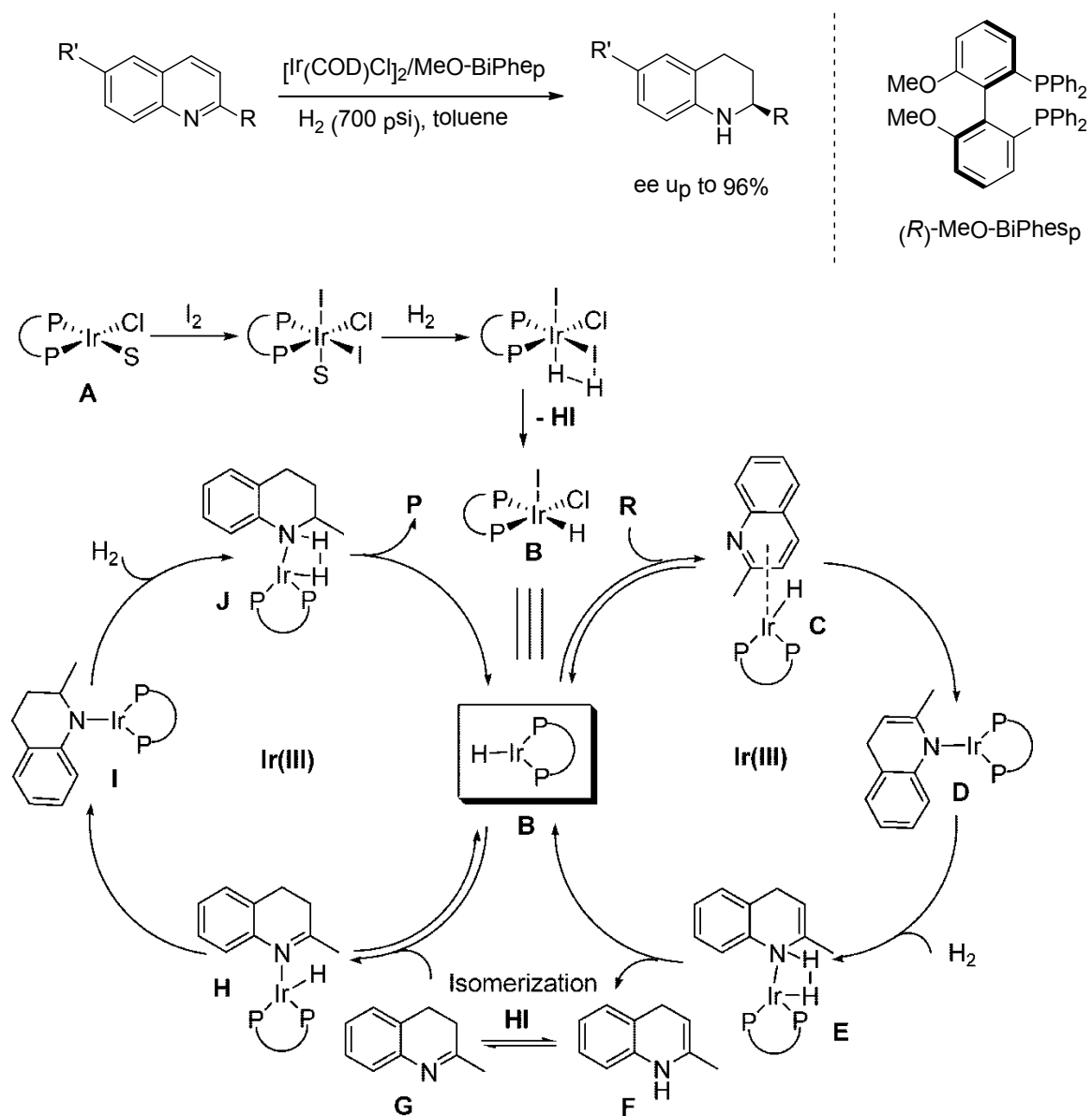
Scheme 3-5. Strong Bronsted Acid Promoted Asymmetric Hydrogenation of Isoquinolines and Quinolines by Rh-thiourea Chiral Phosphine Complex via Anion Binding

3.2 Iridium-catalyzed Asymmetric Hydrogenation of Quinolines/Isoquinolines

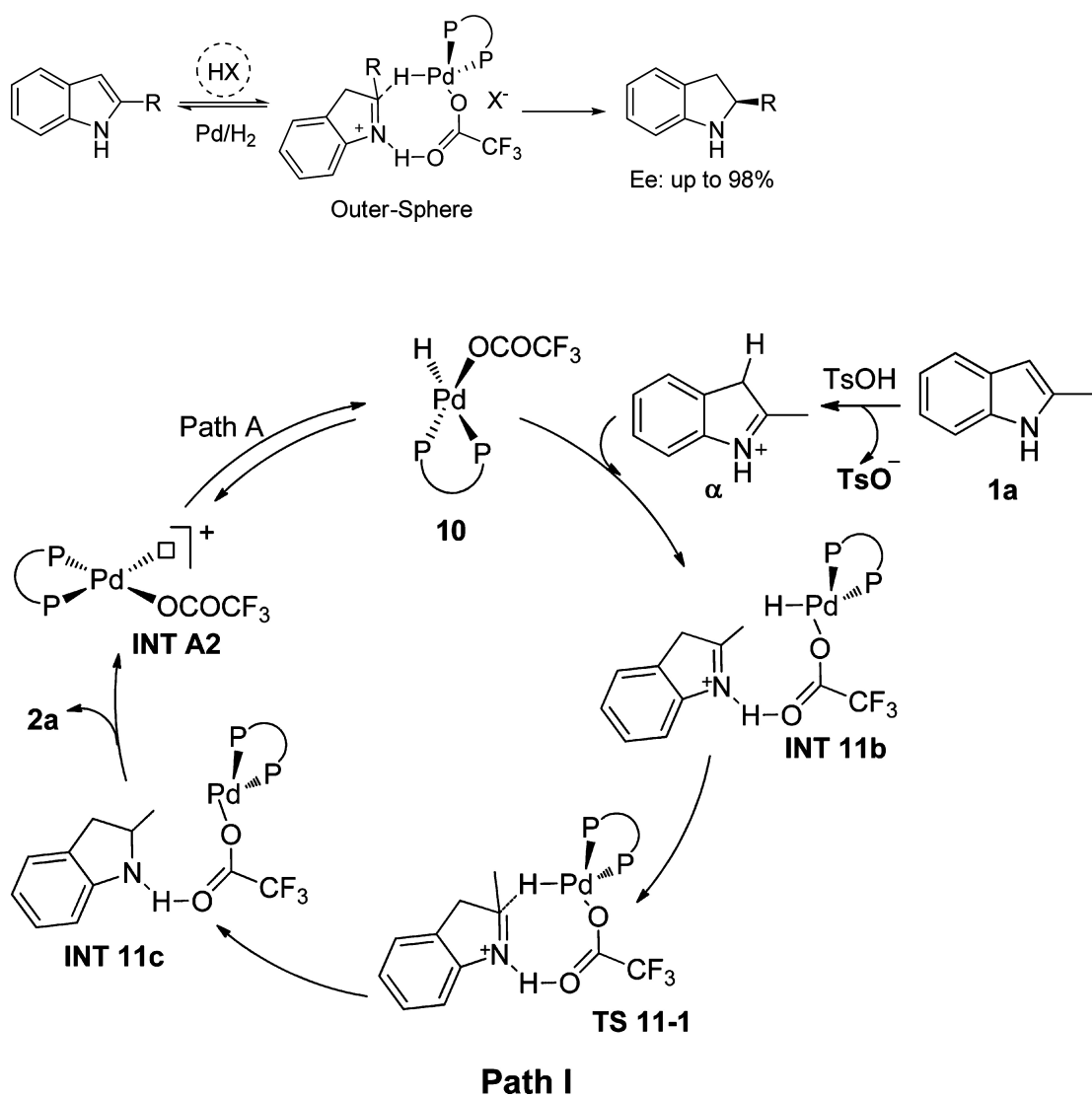
Mechanism

Over the past decade, mechanisms for iridium-catalyzed quinoline/isoquinoline reduction were proposed.¹² Recent reports revealed an outer-sphere mechanism for bisphosphine–transition metal catalyzed hydrogenation. In 2003 Zhou and coworkers reported the first highly enantioselective hydrogenation of quinolines example utilizing iridium catalyst generated in situ from $[\text{Ir}(\text{COD})\text{Cl}]_2$ and axially chiral bisphosphine ligand MeO-BiPhep with iodine as additive.⁷ A plausible mechanism was proposed later (Scheme 3-6).¹³ In 2014, Zhou reported detailed studies on palladium catalyzed asymmetric hydrogenation of protonated indoles and proposed a mechanism involving hydride transfer from a Pd–H complex to an iminium

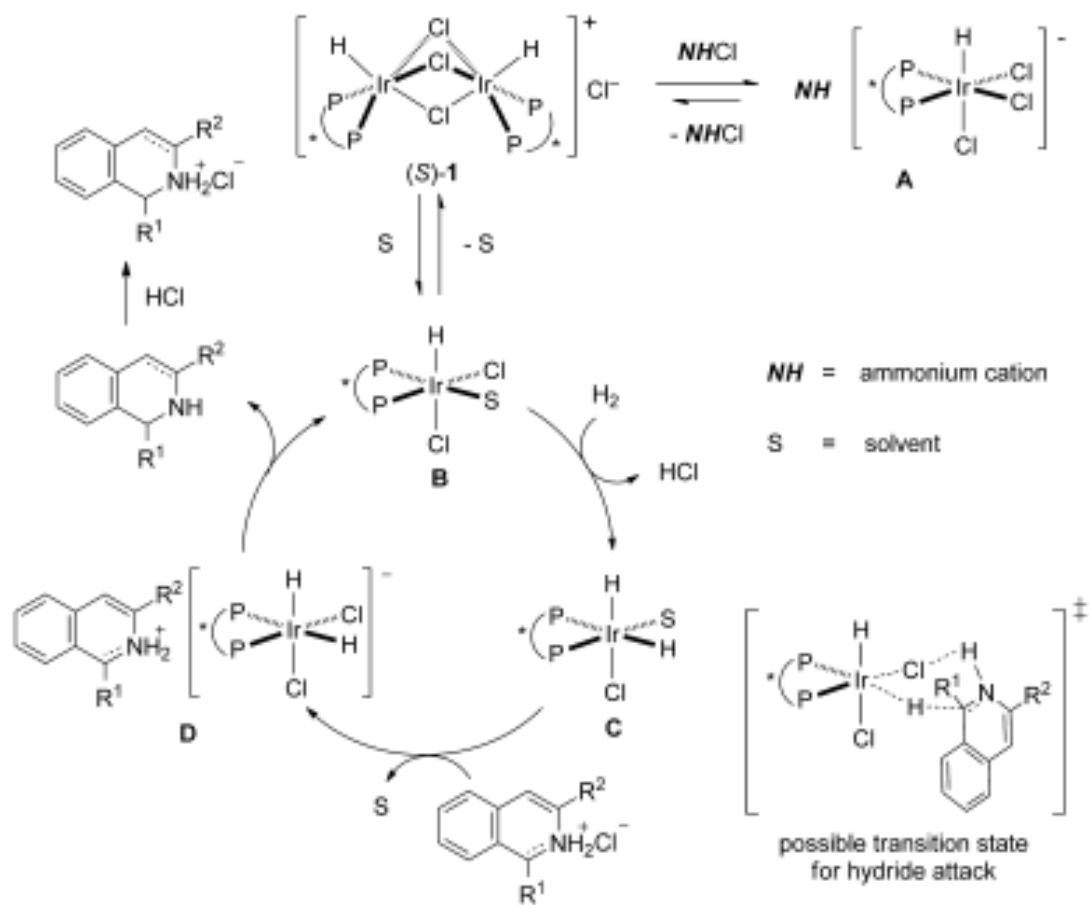
intermediate (Scheme 3-7).¹⁴ In 2015, Mashima's group proposed an outer-sphere mechanism for iridium-catalyzed asymmetric hydrogenation of isoquinoline hydrogen halide salts, in which the chloride anion of the substrates coordinated to an iridium dihydride species along with a hydrogen bond between the chloride ligand and the N-H proton of the substrate salt. (Scheme 3-8).¹⁵ Similarly, from our lab's recent work of rhodium catalyzed asymmetric hydrogenation of both isoquinolines and quinolines,¹¹ we suggested that the unsaturated bonds of the protonated (iso)quinolines seemed not directly coordinate to the metal rhodium complex. Instead, a hydride transfer mechanism was more likely in this catalytic case. Based on previous reports and deuterium labeling experiments, a catalytic cycle was proposed to explain a plausible outer-sphere mechanism (Scheme 3-9), in which an NMR study suggested an anion binding between the catalyst and the substrate. Deuterium labeling experiments revealed an enamine–iminium tautomerization equilibrium after the first hydride transfer step. The iminium then would undergo the insertion of hydride from a rhodium dihydride complex. The chirality of the product originated in this step. Another molecule of hydrogen will react and form the active rhodium dihydride species, finishing the catalytic cycle.



Scheme 3-6. Proposed Mechanism for Asymmetric Hydrogenation of Quinolines.

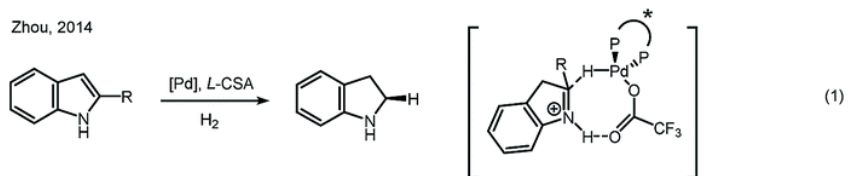


Scheme 3-7. Proposed Mechanism for the Asymmetric Hydrogenation of Indoles.

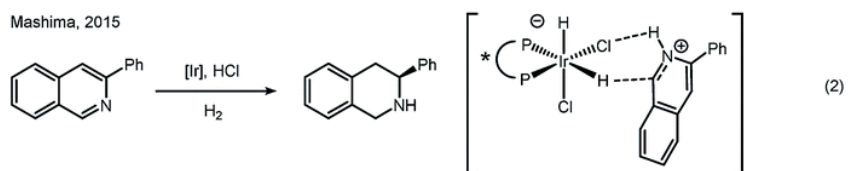


Scheme 3-8. Enhancing Effects of Salt Formation on Catalytic Activity and Enantioselectivity for Asymmetric Hydrogenation of Isoquinolinium Salts by Dinuclear Halide-Bridged Iridium Complexes Bearing Chiral Diphosphine Ligands

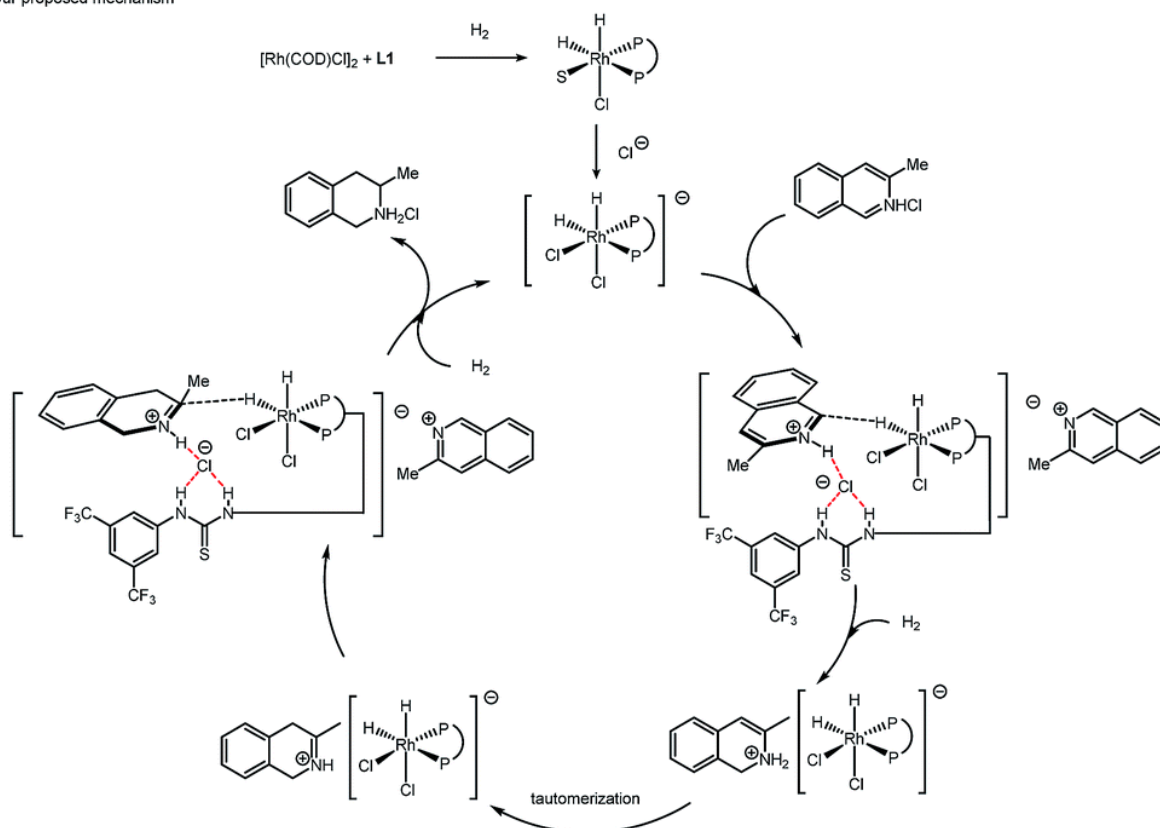
Zhou, 2014



Mashima, 2015



Our proposed mechanism



Scheme 3-9. Iridium-Catalyzed Isoquinoline Reduction Mechanism.

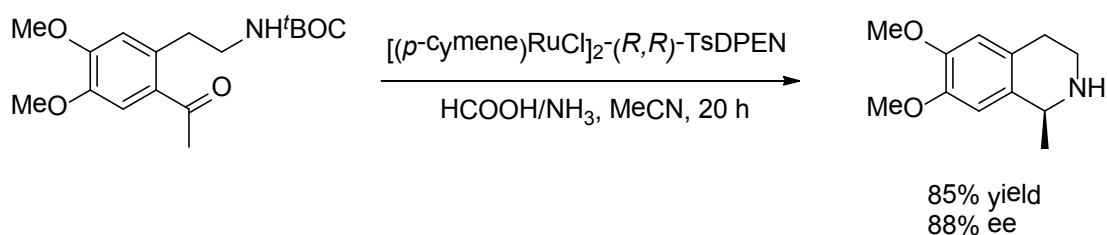
3.3 Asymmetric Hydrogenation of Isoquinoline

3.3.1 Background

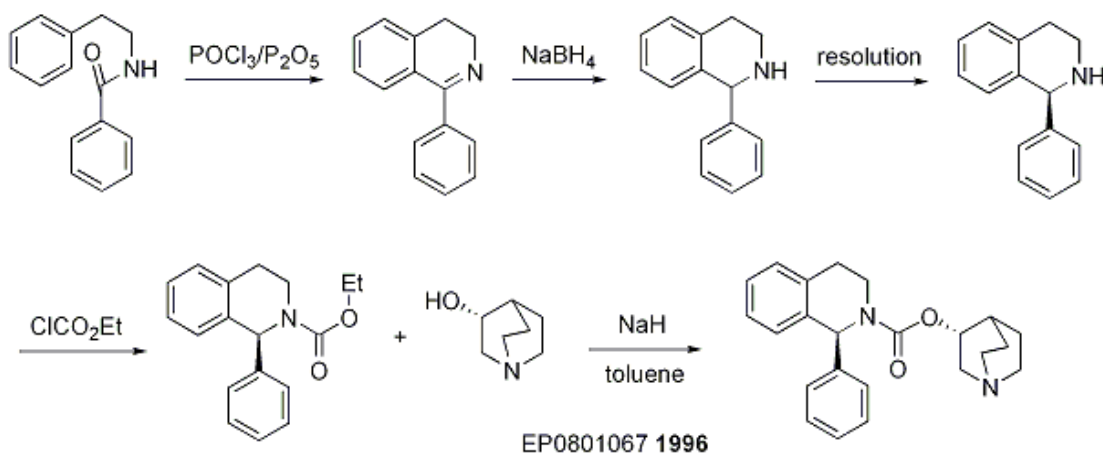
During the past two decades, efforts have been focus on the development of catalytic systems for asymmetric hydrogenation¹⁶ and asymmetric transfer hydrogenation¹⁷ of imines to obtain THIQ. For example, Wills and co-worker synthesized chiral amine 1-methyl-1,2,3,4-tetrahydro-6,7-dimethoxyisoquinoline via intramolecular reductive amination (Scheme 3-10).¹⁸ In 1994, Buchwald *et al.*, developed the hydrogenation of 1-methyl-3,4-dihydro-6,7-dimethoxyisoquinoline with the chiral titanocene at 98% *ee*.^{16a} In 1996, Noyori and co-workers developed the transfer hydrogenation of 3,4-dihydroisoquinolines by Ru(II)-TsDPEN complex with high enantioselectivity.^{17a} Since then, intense research has been focused on this system and modifications have taken place on all components of this catalytic complex, the diamine ligand, the transition metal center, the coordinating-arene, and the counterion.^{16h,17b-17i} Although these titanocene and Ru/Rh-DPEN systems addressed the reduction of 1-alkyl-3,4-dihydroisoquinolines effectively, the asymmetric hydrogenation leading to enantiomerically pure 1-aryl-tetrahydro-isoquinolines remains a challenge, probably due to the relatively rigid and space demanding spatial features of these class of substrates. In 2011, Zhang group reported a highly effective iodine-bridged dimeric $[\{\text{Ir}(\text{H})[(S,S)\text{-}(\text{f})\text{-Binaphane}]\}_2(\mu\text{-I})_3]^+\text{I}^-$ complex on the asymmetric hydrogenation of

a wide range of 3,4-dihydro-isoquinolines with excellent enantioselectivities and high turnover numbers (up to 10,000).¹⁹

Currently asymmetric hydrogenation of 1-phenyl-3,4-dihydroisoquinoline leads to a pharmaceutical drug, solifenacin (Figure 3-1), and the industrial production of this particular tetrahydroisoquinoline depends on optical resolution of the racemic mixture using tartaric acid (Scheme 3-11).²⁰ Apparently direct asymmetric hydrogenation of isoquinolines will be more desirable because it will offer a more efficient and direct access to the enantiomeric pure THIQ. As discussed earlier in this chapter there were some reports on the asymmetric hydrogenation of the corresponding isoquinolines.⁸⁻¹¹ But more efficient enantioselective catalytic catalysts are still in demand for this transformation. As continuous research efforts, we decided to focus on Ir catalyst systems based on our studies of asymmetric hydrogenation of pyridinium salts using Ir–MP²SegPhos catalyst.



Scheme 3-10. Intramolecular Reductive Amination.



Scheme 3-11. Industrial Production of Solifenacin.

3.3.2 Results and Discussion

Inspired by the success of benzyl bromide as alkylating reagent to facilitate the hydrogenation of pyridines, we decided to apply this methodology in the hydrogenation of isoquinolines. With 1-phenyl-isoquinoline benzyl salt **1a** as the standard substrate, several chiral ligands (Figure 3-2) were initially explored as hydrogenation ligands. Results are summarized in Table 3-1. DuanPhos and JosiPhos were tested and yielded poor conversions and enantioselectivities (Table 3-1, entries 8 and 12). Interestingly BINAP did not offer good ee but its analog ligands such as SynPhos (Table 3-1, entry 10), DifluorPhos (Table 3-1, entry 11) and MeO-BiPhep (Table 3-1, entry 13) showed good efficiency. Ir catalyst prepared *in situ* from $[\text{Ir}(\text{COD})\text{Cl}]_2$ precursor and MP²-SegPhos, gave 92% ee with very good conversion (Table 3-1, entry 1).

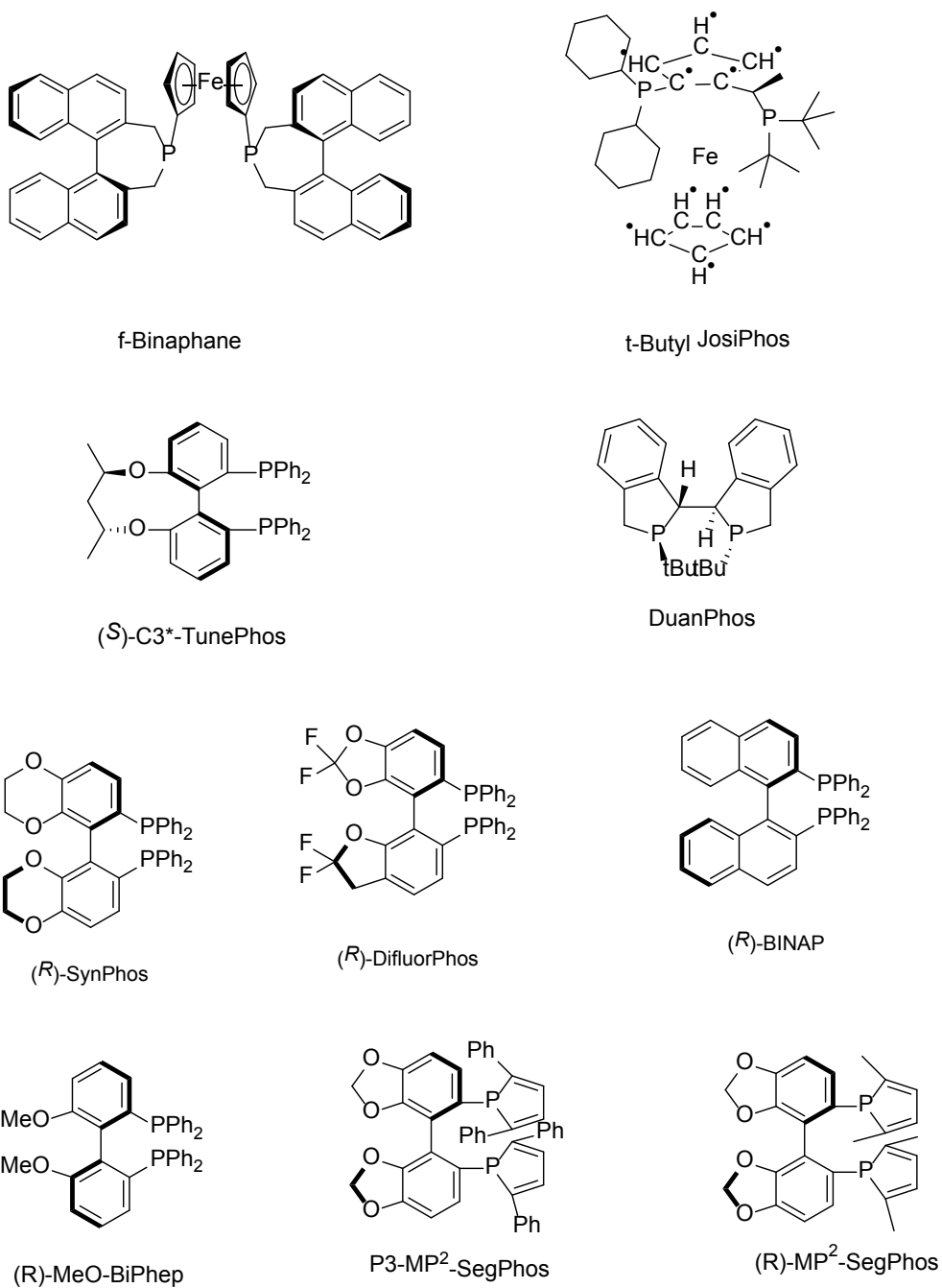


Figure 3-2. Structures of Chiral Ligands for Initial Screening.

MP2-SegPhos with other metal precursors were also investigated (Table 3-1). None of the other metal precursors offered higher enantioselectivity or conversion compared with $[\text{Ir}(\text{COD})\text{Cl}]_2$.

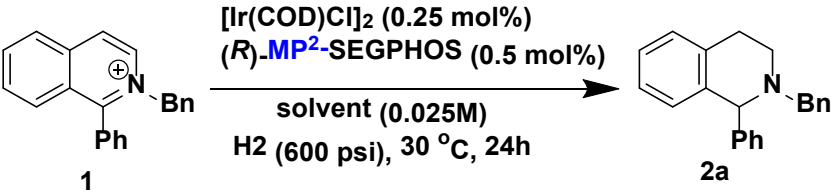
Table 3-1. Asymmetric Hydrogenation of 1-Phenyl-isoquinoline with Chiral Ligands.^[a]

Entry	Metal Precursor	Ligand	Conv. [%] ^[b,c]	ee [%] (Config.) ^[b]
1	$[\text{Ir}(\text{COD})\text{Cl}]_2$	MP ² -SegPhos	95	92
2	$[\text{Ir}(\text{COD})_2]\text{BARF}$	MP ² -SegPhos	14	92
3	$\text{Rh}(\text{COD})_2\text{Cl}$	MP ² -SegPhos	11	9
4	$\text{Rh}(\text{COD})\text{BF}_4$	MP ² -SegPhos	3	57
5	$[\text{Ir}(\text{COD})_2]\text{BARF}$	f-Binaphane	4	67
6	$[\text{Ir}(\text{COD})\text{Cl}]_2$	C3*-TunePhos	95	98
7	$[\text{Ir}(\text{COD})\text{Cl}]_2$	P3-MP2-SegPhos	25	82
8	$[\text{Ir}(\text{COD})\text{Cl}]_2$	DuanPhos	4	31
9	$[\text{Ir}(\text{COD})\text{Cl}]_2$	BINAP	97	47
10 ^[c]	$[\text{Ir}(\text{COD})\text{Cl}]_2$	SynPhos	98	89
11 ^[c]	$[\text{Ir}(\text{COD})\text{Cl}]_2$	DifluoroPhos	14	87
12 ^[d]	$[\text{Ir}(\text{COD})\text{Cl}]_2$	JosiPhos	5	15
13 ^[d]	$[\text{Ir}(\text{COD})\text{Cl}]_2$	MeO-BiPhep	89	87

- [a] The reactions were carried out with 0.2 mmol of substrate in 2.4 mL of solvent in the presence of 1 mol% of *in situ* prepared Ir catalyst under an initial hydrogen pressure of 50 atm for 25 h.
- [b] Conversions and enantiomeric excesses were determined by chiral GC after the amine products were converted to the corresponding trifluoroacetamides.
- [c] 2mol% catalyst loading
- [d] 4mol% catalyst loading

Subsequently the effect of solvents was investigated (Table 3-2). The highest enantioselectivity was achieved from DCE (Table 3-2, entry 4). Acetone appears to provide the higher conversion. We chose the combination of Acetone and DCE (1:1) as solvent to run most of the rest reactions later on. We also noted that no reaction occurred when isoquinoline was only simply made to salt with strong Bronsted acid, such as HCl (Table 3-2, entry 2). When reaction temperature was increased to 60 °C and the pressure was decreased to 300 psi, similarly *ee* (91%) and conversion (98%) were achieved compared to standard condition (Table 3-2, entry 13).

Table 3-2. Solvent Effects on Asymmetric Hydrogenation of 1-Phenyl-isoquinoline.^[a]

			
Entry	Solvent	Conv. [%] ^[b,c]	<i>ee</i> [%] ^[b,c]
1	Acetone/DCE	98	90.3
2 ^[d,f]	Acetone/DCE	n.r.	n.d.
3	Acetone	97	87
4	DCE	95	92

5	Toluene/DCM	85	90
6	DCM	94	91
7	THF	88	88
8	IPA	>99	75
9	TFE	messy	nd
10	TBME	98	81
11	Dioxane	82	85
12	EtOAc	95	88
13 ^[e]	Acetone/DCE	98	91

^[a] The reactions were carried out with 0.05 mmol of substrate in 2 mL of solvent in the presence of 0.5 mol% of *in situ* prepared Ir/MP2 catalyst under an initial hydrogen pressure of 600 psi for 24 h.

^[b] Conversions and enantiomeric excesses were determined by SFC

^[c] Reaction temperature was 30 °C.

^[d] Isoquinoline is a HCl salt.

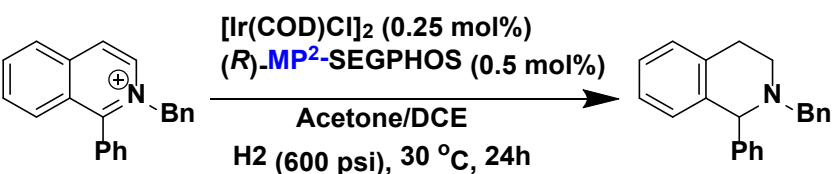
^[e] Reaction temperature was 60 °C. Hydrogen pressure of 300 psi.

^[f] n.r.= no reaction. n.d.= not determined.

The additive effect was also studied (Table 3-3). The reaction appeared to be very messy in the presence of 0.2 equivalent of acids, such as Trichloroisocyanuric acid (TCCA, Table 3-3, entry 6), or DCDMH, DBDMH and L-CSA. Surprisingly, catalytic amount of I₂ also caused a messy reaction. While basic additives, such as Na₂CO₃ (Table 3-3, entry 1), normally provided cleaner reactions, the enantioselectivity and reactivity offered no superior results than the original condition. Inspired by Genet and co-workers' work,^{16c} we prepared the iodine-bridged dimeric iridium complex [Ir(H)[MP2-SegPhos (μ-I)₃]⁺I⁻. To our disappointment, this complex

appeared not as reactive as expected. Although comparable *ee* (91%) was achieved albeit with relatively low conversion (43%) (Table 3-3, entry 7).

Table 3-3. Additive Effects on Asymmetric Hydrogenation of 1-Phenyl-isoquinoline.^[a]

			
Entry	Additive	Conv. [%] ^[b]	<i>ee</i> [%] ^[b]
1	Na ₂ CO ₃	95	88
2	Cs ₂ CO ₃	98	85
3	K ₃ PO ₄	98	85
4	piperidine	80	60
5	I ₂	messy	nd
6	TCCA	messy	nd
7	HI ^[c]	43	91

^[a] The reactions were carried out with 0.05 mmol of substrate in 2 mL of solvent in the presence of 0.5 mol% of *in situ* prepared Ir/MP2 catalyst under an initial hydrogen pressure of 600 psi for 24 h.

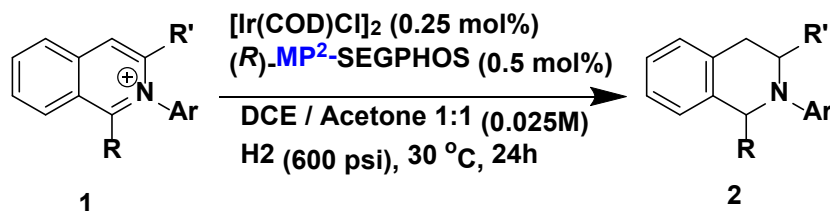
^[b] Conversions and enantiomeric excesses were determined by SFC.

^[c] Iodine-bridged dimeric iridium complex [Ir(H)[MP2-SegPhos (Δ)]₃⁺I⁻ was used as catalyst.

To explore the applicability of this Ir-MP²SegPhos catalytic system, a range of substituted aryl isoquinolines and alkyl isoquinolines were prepared and hydrogenated under the optimal conditions. The results are summarized in Table 3-4. It is evident that the electronic properties of the substituents at para position of phenyl ring have

no obvious effects on conversion and enantioselectivity (Table 3-4, entries 4–6). However, when the substituents go to meta and ortho position, the conversion varies dramatically (Table 3-4, entries 2–4). When it was acylated with other acylating reagent other than benzyl bromide, both enantioselectivity and conversion dropped (Table 3-4, entry 10 and entry 11). This catalytic system does not work well for alkyl substituted isoquinolines and only 9% *ee* was achieved (Table 3-4, entry 12). Substituted at 3-position (3-phenyl-isoquinoline), to our delight, was also hydrogenated with a very good 85% enantioselectivity (Table 3-4, entry 13).

Table 3-4. Asymmetric Hydrogenation of Isoquinoline by Ir–MP²-SegPhos.^[a]



Entry	Substrate	R/R'	Ar	Conv. [%] ^[b]	<i>ee</i> [%] ^[b]
1	1a	C ₆ H ₅ /H	Bn	>99	92.3
2	1b ^[c]	2-Me-C ₆ H ₄ /H	Bn	n.r.	n.d.
3	1c	3-Me-C ₆ H ₄ /H	Bn	>99	91
4	1d	4-Me-C ₆ H ₄ /H	Bn	>99	91
5	1e	4-OMe-C ₆ H ₄ /H	Bn	>99	91

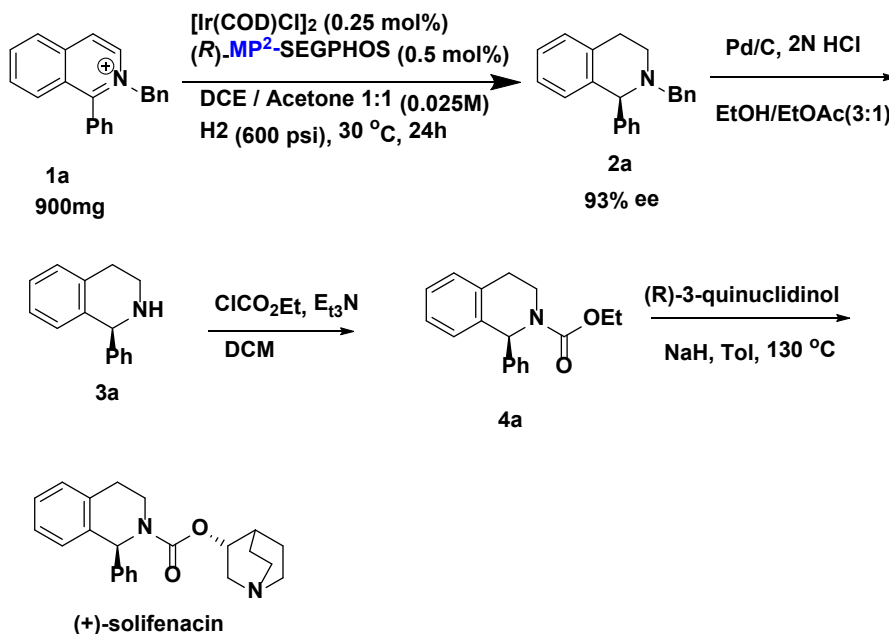
6	1f	4-Br-C ₆ H ₄ /H	Bn	>99	91
7	1g	4-CF ₃ -C ₆ H ₄ /H	Bn	50	83
8	1h	4-F-C ₆ H ₄ /H	Bn	72	91
9	1i	4-nap-C ₆ H ₄ /H	Bn	96	92
10	1j	C ₆ H ₅ /H	Me	36	47
11	1k	C ₆ H ₅ /H	CO ₂ Et	26	88
12	1l	Me/H	Bn	>95	9
13	1m	H/C ₆ H ₅	Bn	>95	85

^[a] The reactions were carried out with 0.05 mmol of substrate in 2 mL of solvent in the presence of 0.5 mol% of *in situ* prepared Ir catalyst under an initial hydrogen pressure of 600 psi for 24 h at 30 °C.

^[b] Conversions and enantiomeric excesses were determined by chiral SFC.

^[c] n.r.= no reaction. n.d.= not determined.

To highlight the practical utility of our approach, a gram-scale asymmetric hydrogenation of **1a** was performed. Excellent conversion and enantioselectivity maintained with 0.5 mol% catalyst loading. We anticipate that hydrogenolysis of the hydrogenation product **2a** would afford the product **3a** in the presence of a Pd/C catalyst without loss of enantioselectivity. Subsequent acylation and transesterification with (R)-3-quinuclidinol would furnish the (+)-Solifenacin.



Scheme 3-12. Product Scale-up toward the Synthesis of Chiral Drug (+)-Solifenacin.

3.3.3 Conclusion

In conclusion, an Ir–MP²-SegPhos catalyst has been applied in asymmetric hydrogenation of a series of Aryl substituted isoquinoline N-benzyl salts. Very good enantioselectivity were achieved for various 2-substituted aryl isoquinolines. This catalytic system proved to be suitable for the reduction of isoquinolines, therefore, provides us an efficient approach for the synthesis of chiral THIQ.

3.4 Asymmetric Hydrogenation of 2-Alkyl/Aryl-Quinolines

3.4.1 Background

Tetrahydroquinolines (THQs) are an important family of biologically active molecules,¹ including natural alkaloids and important pharmaceutical products (Figure 3-3). As discussed in the earlier chapters, several efficient catalytic systems have been successfully developed for the asymmetric hydrogenation of quinolines. These methodologies provide multiple choices for the synthesis of the corresponding chiral tetrahydroquinolines with high enantioselectivities. Noticeably, a wide range of chiral ligands have been evaluated for the iridium-catalyzed asymmetric hydrogenation of 2-substituted quinolines. Among various synthetic methods developed in recent decades to afford enantiomerically pure tetrahydroquinolines,^{1,4} catalytic asymmetric hydrogenation of corresponding quinolines shows most promising as a highly efficient and straightforward approach.⁵ Encouraged by the success of our MP²-SegPhos system in the asymmetric hydrogenation of isoquinolines, we explored the application of this system for the hydrogenation of quinolines.

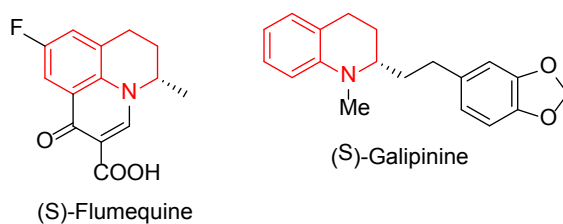


Figure 3-3. Pharmaceutical Products Containing THQ.

3.4.2 Results and Discussion

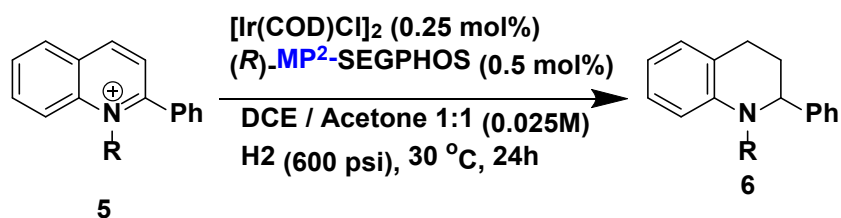
We chose 2-phenyl-isoquinoline as the model substrate for asymmetric hydrogenation with the MP²-SegPhos system (Table 3-5). Initially we tried to alkylated 2-phenyl-quinoline with benzyl bromide to form the activated salt form. However, we found no salt formation was achieved probably due to the steric hinder from the phenyl group. Thus we explored other alkylating reagents, such as trifluoroacetic anhydride. The resulting TFA salt was hydrogenated under 600 psi hydrogen pressure and 50 °C, and very good conversion (92%) was obtained albeit poor enantioselectivity (50% ee). Methyl Iodide was also used to alkylating reagent. The resulted salt was hydrogenated under the standard condition with good conversion (>90%) and dismal ee (14%).

3.4.3 Conclusion

In summary, Ir-MP2-SegPhos complex has been applied in asymmetric hydrogenation of a 2-phenyl-3,4-dihydro-quinolines. Different *N*-alkyl groups were tested but in all cases proved unfruitful. The efficiency of our catalytic system for isoquinoline substrates was not extended to the quinoline substrates, which demonstrated a substrate-control manner. Further investigation of this complex on asymmetric hydrogenation of 2-aryl-quinolines are in progress. Preliminary mechanism study on the asymmetric hydrogenation of isoquinoline benzyl salt will be

present in the Chapter Four.

Table 3-5. Asymmetric Hydrogenation of 2-Phenyl-quinoline by MP²-SegPhos.^[a]



Entry	Ir precursor	Ligand	R	Temperature	Conv. [%] ^[b]	ee [%] ^[b]
1	[Ir(COD)Cl] ₂	MP ² -SegPhos	Bn	-	-	-
2	[Ir(COD)Cl] ₂	MP ² -SegPhos	CF ₃ CO	50 °C	92	50
3	[Ir(COD)Cl] ₂	MP ² -SegPhos	Me	30 °C	90	14

[a] Reaction conditions: [Ir] / ligand / substrate=1:1:100, ligand / metal 1:1, 600 psi of H₂, 24 h.

[b] Conversions and enantiomeric excesses were determined by chiral SFC

3.5 Experimental Section

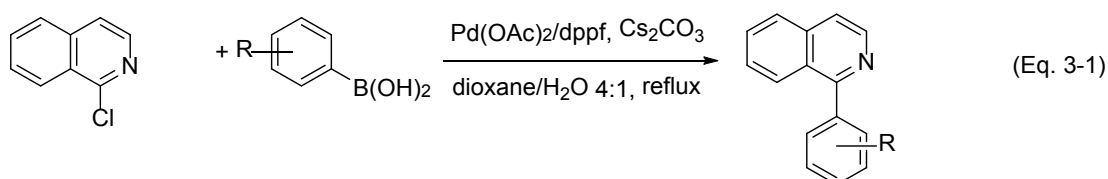
3.5.1 General Remarks.

All reactions were performed in the nitrogen-filled glove box or under nitrogen using standard Schlenk techniques unless otherwise noted. Column chromatography was performed using Sorbent silica gel 60 (230 – 450 mesh). ^1H NMR, and ^{13}C NMR spectral data were obtained from Bruker 400 MHz spectrometers or Varian 500 MHz spectrometers. Chemical shifts are reported in ppm. Enantiomeric excess values were determined by chiral HPLC on an Acquity H-class (Waters Corp., milford, MA) or chiral SFC on an Acquity UPC² (Waters Corp., milford, MA). All new products were further characterized by HRMS. A positive ion mass spectrum of sample was acquired on a Micromass 70-VSE mass spectrometer with an electron ionization source.

3.5.2 General Procedure for Synthesis of Isoquinoline 1.

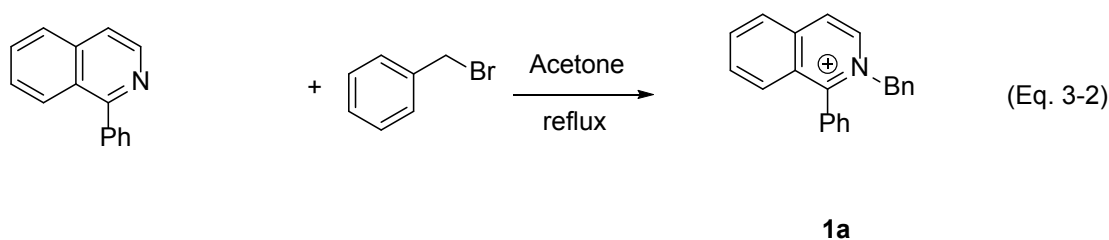
Most substrates were synthesized in two steps according to literature.

Step 1:



In glove box in a 40 ml vial was added 2-chloroisoquinoline (5mmol) and dppf (0.5mmol), Pd (II) acetate (0.5 mmol), arylboronic acid (5 mmol) ,Cs₂CO₃ (10 mmol) in 5ml H₂O (degassed for 15min) and 20ml 1,4-dioxane. The suspension was stirred and heated to 70 °C for 20 hours. After cooled, removed from the glove box and then diluted with EtOAc, filtered through celite. Solvent was removed. The resulting residue was purified by chromatography (0-100% Hexane/EtOAc) to obtain colorless oil. NMR confirmed as desired product.

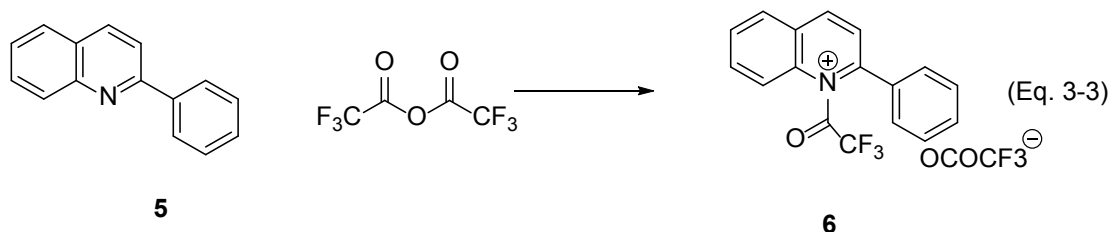
Step 2:



The solution of 2-arylisquinoline (4 mmol) and benzyl bromide (4.4 mmol) in acetone was refluxed overnight. In most cases product will precipitate out. Then product was collected from filtration and further purified by recrystallization. In case there was no precipitate, the reaction mixture was purified by column chromatography on silica gel using CH₂Cl₂/MeOH (20:1) to give the desired products (47-87%).

N-benzyl-2-phenylpyridinium bromide (**1a**): White solid. ¹H NMR (400 MHz, CDCl₃) δ 9.80 (d, 1H), 8.54 (m, 1H), 8.20 (m, 1H), 7.86 (m, 1H), 7.50-7.78 (m, 5H), 7.30 (m,

4H), 7.10 (m, 2H), 6.20 (s, 2H).



N-trifluoroacetamide quinoline was synthesized according to the literature.²¹

To a stirred solution of the 3-phenylisoquinoline in 1,2-Dichloroethane (10 ml) (10 mL) was added Reactant 5 (710 mg, 5.00 mmol) BF₃ ether and 2,2,2-trifluoroacetic anhydride (2100 mg, 10.00 mmol) at room temperature. The reaction mixture was stirred at room temperature for overnight. EtOAc was added and washed with water. The organic layer was washed with brine, separated and concentrated. The resulting residue was purified by ISCO 0-30% MeOH/CH₂Cl₂ to give corresponding salt as a white solid Product 6 (706 mg, 1.700 mmol, 68.0 % yield).

¹H NMR (400 MHz, CD₃OD) δ 8.96 (d, 1H), 8.28 (m, 3H), 8.15 (m, 3H), 7.97 (m, 1H), 7.54 (m, 3H).

3.5.3 General Procedure for Asymmetric Hydrogenation of *N*-Benzylisoquinoline Salts.

In a nitrogen-filled glove box, ligands and metal sources were placed into 96 hydrogenation vials. 0.05 ml CH₂Cl₂ was added to each vials and stirring for 30 min.

Then *N*-benzyl-2-phenylisoquinoline bromide dissolved in CH_2Cl_2 was added to each vial. Solvent was removed under reduced pressure in glove box. Then desired solvent or solvent pairs were added. The vials were placed in a parallel hydrogenation block and following three hydrogen purges, pressurized to 600 psi at 30 °C for 24 h. Selectivities and conversions were determined by direct sampling of the reaction mixture on SFC.

Scope of Asymmetric Pyridinium Salt Reductions

In a nitrogen-filled glove box, $\text{MP}^2\text{-SEGP}^{\text{HOS}}$ (4.58 mg, 0.0099 mmol) and $[\text{Ir}(\text{COD})\text{Cl}]_2$ (3.07 mg, 0.00457 mmol) were placed into a vial and stirring for 30 min in acetone (7.2 ml). Isoquinoline salts (0.05 mmol) were placed into 4 ml hydrogenation vials. 0.2 ml catalyst solution and remaining solvent were added. The vials were placed in a parallel hydrogenation block and following three hydrogen purges, pressurized to 600 psi at 30 °C for 20 h. After carefully releasing the hydrogen, selectivities were determined by direct sampling of the reaction mixture on SFC or HPLC. Then saturated sodium carbonate was added and the mixture was stirred for 15-30 min. The organic layer was separated and extracted with CH_2Cl_2 twice, and the combined organic extracts were dried over Na_2SO_4 and concentrated in vacuum. Purification was performed by a silica gel column, eluted with hexane/EtOAc to give desired product.

$[\text{Ir}(\text{H})[(S,S)\text{-f-Binaphane}]\text{I}(\mu\text{-I})_3]^+\text{I}^-$ was prepared according to literature report.²² To a mixture of $[\text{Ir}(\text{cod})_2\text{Cl}]_2$ (20.2 mg, 30 μmol) and $(S,S)\text{-f-Binaphane}$ (53.3 mg, 66.0 μmol) in toluene (5 mL) was added aqueous HI (45%, 33 μL) via a syringe at room temperature. Then the reaction mixture was stirred overnight. Solvent was removed under reduced pressure. The residue was dissolved in dichloromethane. Upon addition of hexane, product precipitated as an air stable pale yellow powder (53.6 mg, 75% yield), ^{31}P NMR (162 MHz, CDCl_3) δ -0.42 (d, $J=8.1$ Hz), -2.88 (d, $J=8.1$ Hz). HRMALDI: Calculated for $\text{C}_{108}\text{H}_{82}\text{Fe}_2\text{I}_4\text{Ir}_2\text{P}_4$ (M^+): 2507.9509, found 2507.9484.

N-benzyl-1-phenyl-1,2,3,4-tetrahydroisoquinoline (2a):²³ white solid. The compound data were in good accordance with the literature.³ ^1H NMR (400 MHz, CDCl_3) δ 7.48-7.27 (m, 10H), 7.20—7.15 (m, 2H), 7.10-7.06 (m, 1H), 6.18 (d, $J=7.8$ Hz, 1H), 4.69 (s, 1H), 3.90 (d, $J=13.6$ Hz, 1H), 3.32 (t, $J=13.6$ Hz, 1H), 3.21-3.11 (m, 2H), 2.88-2.81 (m, 1H), 2.63-2.56 (m, 1H). ^{13}C NMR (400 MHz, CDCl_3) δ 142.2, 136.0, 134.4, 129.3, 129.0, 128.6, 128.2, 128.1, 128.0, 126.9, 126.1, 60.7, 40.7, 28.3. Enantiomeric excess was determined by SFC: OD-3 column (150*4.6 mm), 200 Bar, 40 °C, CO_2/MeOH with 25 mM IBA= 99:1 to 60:40 (0-5 min), 3 ml/min.

N-Benzyl-1-(3'-methylphenyl)-1,2,3,4-dihydroisoquinoline (2c):²⁴ white solid. ^1H NMR (500 MHz, CDCl_3) δ 7.37 – 7.19 (m, 8H), 7.17 – 7.08 (m, 3H), 7.04 (t, $J=6.3$ Hz, 1H), 6.78 (d, $J=7.8$ Hz, 1H), 4.60 (s, 1H), 3.86 (d, $J=13.6$ Hz, 1H), 3.27 (d, $J=13.6$ Hz, 1H), 3.17 – 3.07 (m, 2H), 2.86 – 2.77 (m, 1H), 2.58 – 2.49 (m, 1H), 2.38 (s,

3H). ^{13}C NMR (126 MHz, CDCl_3) δ 144.29, 139.65, 138.71, 137.81, 134.79, 130.32, 128.88, 128.75, 128.44, 128.14, 128.00, 126.86, 126.78, 125.83, 125.61, 68.97, 58.92, 47.43, 29.31, 21.53. Enantiomeric excess was determined by SFC: OD-3 column (150*4.6 mm), 200 Bar, 40 °C, CO_2/MeOH with 25 mM IBA= 99:1 to 60:40 (0-5 min), 3 ml/min.

N-Benzyl-1-(4'-Methylphenyl)-1,2,3,4-tetrahydroisoquinoline (2d):²⁵ white solid. ^1H NMR (500 MHz, , Acetonitrile- d_3) δ 7.33 – 7.28 (m, 6H), 7.25 (dt, J = 8.4, 4.2 Hz, 1H), 7.19 (d, J = 7.8 Hz, 2H), 7.17 – 7.09 (m, 2H), 7.02 (t, J = 7.1 Hz, 1H), 6.73 (d, J = 7.8 Hz, 1H), 4.63 (s, 1H), 3.75 (d, J = 13.7 Hz, 1H), 3.29 (d, J = 13.7 Hz, 1H), 3.08 – 2.99 (m, 2H), 2.82 – 2.75 (m, 1H), 2.53 – 2.45 (m, 1H), 2.34 (s, 3H). ^{13}C NMR (126 MHz, , Acetonitrile- d_3) δ 141.78, 139.67, 138.84, 136.88, 134.92, 129.44, 128.88, 128.61, 128.50, 128.16, 126.80, 125.81, 125.49, 68.18, 58.31, 46.97, 29.00, 20.14. Enantiomeric excess was determined by SFC: OD-3 column (150*4.6 mm), 200 Bar, 40 °C, CO_2/MeOH with 25 mM IBA= 99:1 to 60:40 (0-5 min), 3 ml/min.

N-Benzyl-1-(4'-methoxyphenyl)-1,2,3,4-dihydroisoquinoline (2e):²⁵ white solid. ^1H NMR (500 MHz, Acetonitrile- d_3) δ 7.35 – 7.29 (m, 6H), 7.26 (h, J = 4.1 Hz, 1H), 7.13 (dt, J = 15.2, 7.9 Hz, 2H), 7.03 (t, J = 7.8 Hz, 1H), 6.92 (d, J = 8.8 Hz, 2H), 6.74 (d, J = 7.8 Hz, 1H), 4.62 (s, 1H), 3.79 (s, 3H), 3.76 (d, J = 13.7 Hz, 1H), 3.29 (d, J = 13.7 Hz, 1H), 3.07 – 2.98 (m, 2H), 2.82 – 2.74 (m, 1H), 2.53 – 2.46 (m, 1H). ^{13}C

NMR (126 MHz, CD₃CN) δ 158.93, 139.71, 138.97, 136.68, 134.93, 130.52, 128.64, 128.53, 128.49, 128.16, 126.80, 125.80, 125.49, 113.54, 67.76, 58.25, 54.87, 46.93, 28.94. Enantiomeric excess was determined by SFC: OD-3 column (150*4.6 mm), 200 Bar, 40 °C, CO₂/MeOH with 25 mM IBA= 99:1 to 60:40 (0-5 min), 3 ml/min.

N-Benzyl-1-(4'-bromophenyl)-1,2,3,4-dihydroisoquinoline (2f):²⁵ white solid. ¹H NMR (500 MHz, Acetonitrile-*d*₃) δ 7.53 (d, *J* = 8.5 Hz, 2H), 7.38 – 7.23 (m, 7H), 7.15 (dt, *J* = 14.6, 7.2 Hz, 2H), 7.04 (t, *J* = 7.4 Hz, 1H), 6.73 (d, *J* = 7.8 Hz, 1H), 4.68 (s, 1H), 3.74 (d, *J* = 13.7 Hz, 1H), 3.33 (d, *J* = 13.7 Hz, 1H), 3.08 – 2.98 (m, 2H), 2.83 – 2.75 (m, 1H), 2.55 – 2.47 (m, 1H). ¹³C NMR (126 MHz, CD₃CN) δ 144.34, 139.38, 137.94, 134.98, 131.44, 131.26, 128.64, 128.57, 128.20, 126.90, 126.08, 125.66, 120.43, 67.66, 58.35, 46.80, 28.80. Enantiomeric excess was determined by SFC: OD-3 column (150*4.6 mm), 200 Bar, 40 °C, CO₂/MeOH with 25 mM IBA= 99:1 to 60:40 (0-5 min), 3 ml/min.

N-Benzyl-1-(4'-trifluoromethylphenyl)-1,2,3,4-dihydroisoquinoline (2g):²⁵ white solid. ¹H NMR (500 MHz, Acetonitrile-*d*₃) δ 7.71 – 7.59 (m, 4H), 7.32 (d, *J* = 4.0 Hz, 4H), 7.29 – 7.23 (m, 1H), 7.19 (d, *J* = 7.5 Hz, 1H), 7.14 (d, *J* = 8.4 Hz, 1H), 7.05 (t, *J* = 7.5 Hz, 1H), 6.73 (d, *J* = 7.6 Hz, 1H), 4.79 (s, 1H), 3.72 (d, *J* = 13.7 Hz, 1H), 3.36 (d, *J* = 13.7 Hz, 1H), 3.09 – 3.01 (m, 2H), 2.85 – 2.78 (m, 1H), 2.58 – 2.51 (m, 1H). ¹³C NMR (126 MHz, CD₃CN) δ 149.65, 139.25, 137.57, 135.05, 130.07, 128.83, 128.74, 128.56, 128.54, 128.22, 126.95, 126.20, 125.73, 125.20, 125.17, 125.14,

125.11, 67.82, 58.44, 46.78. Enantiomeric excess was determined by SFC: OJ-3 column (150*4.6 mm), 120 Bar, 40 °C, CO₂/MeOH with 0.1% DIPA= 90:10 (0-6 min), 3 ml/min.

N-Benzyl-1-(4'-fluorophenyl)-1,2,3,4-dihydroisoquinoline (2h): white solid. ¹H NMR (500 MHz, Acetonitrile-*d*₃) δ 7.43 (dd, *J* = 8.7, 5.6 Hz, 2H), 7.32 (d, *J* = 4.7 Hz, 4H), 7.29 – 7.23 (m, 1H), 7.16 (t, *J* = 6.8 Hz, 1H), 7.13 – 7.07 (m, 3H), 7.04 (t, *J* = 7.5 Hz, 1H), 6.73 (d, *J* = 7.8 Hz, 1H), 4.69 (s, 1H), 3.74 (d, *J* = 13.7 Hz, 1H), 3.31 (d, *J* = 13.7 Hz, 1H), 3.08 – 2.98 (m, 2H), 2.79 (dt, *J* = 15.9, 4.1 Hz, 1H), 2.51 (ddd, *J* = 12.8, 10.3, 3.9 Hz, 1H). ¹³C NMR (126 MHz, CD₃CN) δ 162.92, 160.99, 140.84, 139.42, 138.31, 134.95, 131.23, 128.61, 128.22, 126.92, 126.04, 125.65, 114.96, 114.79, 67.58, 58.30, 46.87, 28.82. Enantiomeric excess was determined by SFC: AD-3 column (150*4.6 mm), 120 Bar, 40 °C, CO₂/MeOH with 0.1% DIPA= 90:10 (0-6 min), 3 ml/min.

N-Benzyl-1-(Naphthalen-2-yl)-1,2,3,4-dihydroisoquinoline (2i): ¹H NMR (500 MHz, Chloroform-*d*) δ 7.93 – 7.82 (m, 4H), 7.60 – 7.47 (m, 3H), 7.39 – 7.30 (m, 4H), 7.27 (dd, *J* = 11.8, 4.7 Hz, 1H), 7.23 – 7.13 (m, 2H), 7.03 (t, *J* = 7.4 Hz, 1H), 6.82 (d, *J* = 7.8 Hz, 1H), 4.85 (s, 1H), 3.95 (d, *J* = 13.5 Hz, 1H), 3.35 (d, *J* = 11.6 Hz, 1H), 3.28 – 3.14 (m, 2H), 2.86 (d, *J* = 16.8 Hz, 1H), 2.65 (d, *J* = 10.7 Hz, 1H). ¹³C NMR (126 MHz, CDCl₃/DMSO) δ 133.12, 133.05, 129.06, 128.84, 128.57, 128.49, 128.21, 127.83, 127.75, 127.34, 126.93, 126.06, 125.82, 125.74, 69.13, 58.86, 47.48, 29.31.

Enantiomeric excess was determined by SFC: AD-3 column (150*4.6 mm), 120 Bar, 40 °C, CO₂/MeOH with 0.1% DIPA= 90:10 (0-6 min), 3 ml/min.

N-Ethyl acetate-1-phenyl-1,2,3,4-dihydroisoquinoline (2k): yellow solid. ¹H NMR (500 MHz, Chloroform-*d*) δ 7.36 – 7.25 (m, 6H), 7.14 (dt, *J* = 14.6, 7.6 Hz, 2H), 7.02 (t, *J* = 7.4 Hz, 1H), 6.71 (d, *J* = 7.8 Hz, 1H), 5.01 (s, 1H), 4.22 – 4.12 (m, 2H), 3.38 (d, *J* = 17.2 Hz, 1H), 3.29 – 3.19 (m, 3H), 3.14 – 3.06 (m, 1H), 2.88 (d, *J* = 14.3 Hz, 1H), 1.36 – 1.20 (m, 4H). ¹³C NMR (126 MHz, CDCl₃) δ 171.00, 143.24, 138.06, 134.34, 129.74, 128.77, 128.50, 128.37, 127.52, 125.98, 125.68, 66.61, 60.31, 55.57, 48.48, 29.28, 14.29. SFC: AD-3 column (150*4.6 mm), 120 Bar, 40 °C, CO₂/IPA with 0.1% DIPA= 85:15 (0-6 min), 3 ml/min.

N-Benzyl-1-methyl-1,2,3,4-dihydroisoquinoline (2l): ²⁵ white solid. ¹H NMR (500 MHz, CDCl₃) δ 7.47-7.30 (m, 5H), 7.22-7.11 (m, 4H), 3.96 (q, *J* = 6.7 Hz, 1H), 3.89 (d, *J* = 13.6 Hz, 1H), 3.77 (d, *J* = 13.6 Hz, 1H), 3.14-3.10 (m, 1H), 2.97-2.93 (m, 1H), 2.80-2.76 (m, 2H), 1.46 (d, *J* = 6.7 Hz, 3H). ¹³C NMR (100 MHz, CDCl₃) δ 142.2, 136.0, 134.4, 129.3, 129.0, 128.6, 128.2, 128.1, 128.0, 126.9, 126.1, 60.7, 40.7, 28.3. Enantiomeric excess was determined by SFC: OD-3 column (150*4.6 mm), 200 Bar, 40 °C, CO₂/MeOH with 25 mM IBA= 99:1 to 60:40 (0-5 min), 3 ml/min.

N-Benzyl-3-phenyl-1,2,3,4-dihydroisoquinoline (2m): ²⁵ white solid.

Enantiomeric excess was determined by SFC: OD-3 column (150*4.6 mm), 200 Bar,

40 °C, CO₂/MeOH with 25 mM IBA= 99:1 to 60:40 (0-5 min), 3 ml/min.

Reference:

1. (a) R. Paul, J. A. Coppola, E. Cohen, *J. Med. Chem.* **1972**, *15*, 720. (b) J. D. Phillipson, M. F. Roberts, M. H. Zenk (Eds.), *The Chemistry and Biology of Isoquinoline Alkaloids*, Springer, Berlin, **1985**. (c) D. Jack, R. Williams, *Chem. Rev.* **2002**, *102*, 1669. (d) P. M. Dewick, *Medicinal Natural Products: A Biosynthetic Approach*, Wiley, Chichester, **2002**, pp. 315. (e) K. W. Bentley, *Nat. Prod. Rep.* **2006**, *23*, 444. (f) M. Chrzanowska, M. D. Rozwadowska, *Chem. Rev.* **2004**, *104*, 3341.
2. 6. A. Brossi, S. Teitel, *Helv. Chim. Acta* **1971**, *54*, 1564.
3. 7. H. M. Kothari, M. G. Dave, B. Pandey, Patent WO 2011048607, **2011**.
4. (a) D. Taniyama, M. Hasegawa, K. Tomioka, *Tetrahedron: Asymmetry* **1999**, *10*, 221. (b) K. T. Wanner, H. Beerb, G. Hofnera, M. Ludwig, *Eur. J. Org. Chem.* **1998**, 2019. (c) K. Kurihara, Y. Yamamoto, N. Miyauraa, *Adv. Synth. Catal.* **2009**, *351*, 260. (d) K. Umetsu, N. Asao, *Tetrahedron Lett.* **2008**, *49*, 2722. (e) S. Wang, M. B. Onaran, C. T. Seto, *Org. Lett.* **2010**, *12*, 2690. (f) F. Louafi, J.-P. Hurvois, A. Chibani, T. Roisnel, *J. Org. Chem.* **2010**, *75*, 5721. (g) M. Amat, V. Elias, N. Llor, F. Subrizi, E. Molins, J. Bosch, *Eur. J. Org. Chem.* **2010**, 4017. (h) M. Taylor, E. Jacobsen, *J. Am. Chem. Soc.* **2004**, *126*, 10558. (i) M. Taylor, N. Tokunaga, E. Jacobsen, *Angew. Chem. Int. Ed.* **2005**, *44*, 6700.
5. T. Ohkuma, M. Kitamura, R. Noyori, in *Catalytic Asymmetric Synthesis*, 2nd edn., (Ed.: I. Ojima), Wiley, New York, **2000**, pp. 1.
6. (a) Y. Zhou, *Acc. Chem. Res.*, **2007**, *40*, 1357. (b) D. Wang, Q. Chen, S. Lu and Y. Zhou, *Chem. Rev.*, 2012, **112**, 2557.
7. W. Wang, S. Lu, P. Yang, X. Han, Y. Zhou, *J. Am. Chem. Soc.* **2003**, *125*, 10536.
8. (a) S. M. Lu, Y. Q. Wang, X. W. Han and Y. G. Zhou, *Angew. Chem., Int. Ed.*, **2006**, *45*, 2260. (b) L. Shi, Z. Ye, L. Cao, R. Guo, Y. Hu and Y. Zhou, *Angew. Chem., Int. Ed.*, **2012**, *51*, 8286.
9. L. Shi, Y. Ji, W. Huang and Y. Zhou, *Acta Chim. Sin.*, **2014**, *72*, 820–824.
10. A. Iimuro, K. Yamaji, S. Kandula, T. Nagano, Y. Kita and K. Mashima, *Angew. Chem., Int. Ed.*, **2013**, *52*, 2046.
11. J. Wen, R. Tan, S. Liu, Q. Zhao, X. Zhang, *Chemical Science*, **2016**, ahead of print.
12. (a) K. H. Hopmann, A. Bayer, *Organometallics* **2011**, *30*, 2483. (b) V. Herrera, B. Munoz, V. Landaeta, N. Canduas, *J. Mol. Catal. A: Chem.* **2001**, *174*, 141. (c) D. Balcells, A. Noca, E. Clot, D. Gnanamgari, R. H. Crabtree, O. Eisenstein, *Organometallics* **2008**, *27*, 2529. (d) A. Fabrello, A. Bacheliera, M. Urrutigoitya, P. Kalcka, *Coord. Chem. Rev.* **2010**, *254*, 273. (e) M. Martín, E. Sola, S. Tejero, J.-L. Andres, L. A. Oro, *Chem.—Eur. J.* **2006**, *12*, 4043. (f) M. Martín, E. Sola, S. Tejero, J. A. Lopez, L. A. Oro, *Chem.—Eur. J.* **2006**, *12*, 4057.
13. D. Wang, X. Wang, D.-S. Wang, S. Lu, Y. Zhou, Y. Li, *J. Org. Chem.*, **2009**,

- 2780.
14. Y. Duan, L. Li, M. Chen, C. Yu, H. Fan and Y. Zhou, *J. Am. Chem. Soc.*, **2014**, 136, 7688
 15. Y. Kita, K. Yamaji, K. Higashida, K. Sathaiah, A. Iimuro and K. Mashima, *Chem.–Eur. J.*, **2015**, 21, 1915
 16. (a) C. A. Willoughby, S. L. Buchwald, *J. Am. Chem. Soc.* **1994**, 116, 8952. (b) T. Morimoto, K. Achiwa, *Tetrahedron: Asymmetry* **1995**, 6, 2661. (c) T. Morimoto, N. Suzuki, K. Achiwa, *Heterocycles* **1996**, 43, 2557. (d) G. Zhu, X. Zhang, *Tetrahedron: Asymmetry* **1998**, 9, 2415. (e) C. J. Cobley, J. P. Henschke, *Adv. Synth. Catal.* **2003**, 345, 195. (f) E. Guiu, C. Claver, J. Benet-Buchholz, S. Castillon, *Tetrahedron: Asymmetry* **2004**, 15, 3365. (g) M. Jackson, I. C. Lennon, *Tetrahedron Lett.* **2007**, 48, 1831. (h) C. Li, J. Xiao, *J. Am. Chem. Soc.* **2008**, 130, 13208.
 17. (a) N. Uematsu, A. Fujii, S. Hashiguchi, T. Ikariya, R. Noyori, *J. Am. Chem. Soc.* **1996**, 118, 4916. (b) J. Mao, D. C. Baker, *Org. Lett.* **1999**, 1, 841. (c) P. Roszkowski, K. Wojtasiewicz, A. Leniewski, J. K. Maurin, T. Lis, Z. Czarnocki, *J. Mol. Catal. A: Chem.* **2005**, 232, 143. (d) J. Wu, F. Wang, Y. Ma, X. Cui, L. Cun, J. Zhu, J. Deng, B. Yu, *Chem. Commun.* **2006**, 1766. (e) J. Canivet, G. Suss-Fink, *Green Chem.* **2007**, 9, 391. (f) D. S. Matharu, J. E. D. Martins, M. Wills, *Chem. Asian J.* **2008**, 3, 1374. (g) J. E. D. Martins, G. J. Clarkson, M. Wills, *Org. Lett.* **2009**, 11, 847. (h) L. Evanno, J. Ormala, P. M. Pihko, *Chem. Eur. J.* **2009**, 15, 12963. (i) J. E. D. Martins, M. A. C. Redondo, M. Wills, *Tetrahedron: Asymmetry* **2010**, 21, 2258.
 18. G. D. Williams, R. A. Pike, C. E. Wade, M. Wills, *Org. Lett.* **2003**, 5, 4227.
 19. M. Chang, W. Li, X. Zhang, *Angew. Chem. Int. Ed.*, **2011**, 50, 10679.
 20. Y. Ishii, K. Takaoka, M. Inakoshi, S. Nakagawa, K. Nagata, N. Yorimoto, M. Takeuchi, Y. Yonetoku, Patent WO 2005075474 A1, **2005**.
 21. A. Anderson, E. Davidson, E. Daus, G. Kao, R. Lindquist, K. Quenemoen, *J. Am. Chem. Soc.* **1985**, 1896
 22. T. Yamagata, H. Tadaoka, M. Nagata, T. Hirao, Y. Kataoka, V. Ratovelomanana-Vidal, J. P. Genet, K. Mashima, *Organometallics* **2006**, 25, 2505.
 23. M. Movassaghi, M. D. Hill, *Org. Lett.* **2008**, 10, 3485.
 24. M. Ludwig, C. E. Hoesl, G. Hoefner, K. T. Wanner, *Eur. J. Med. Chem.* **2006**, 41, 1003.
 25. R. Paul, J. A. Coppola, E. Cohen, *J. Med. Chem.* **1972**, 15, 720.

Chapter 4

Mechanism Studies on Iridium-Catalyzed Asymmetric Hydrogenation of Pyridinium Salts

4.1 Introduction and Background

Piperidine core is present in numerous natural products and synthetic bioactive compounds and has attracted a tremendous amount of attention in the chemical and pharmaceutical industries.¹ For instance, the piperidine derivatives Risperdal used for treatment of schizophrenia,² Concerta for ADHD,³ Aricept for Alzheimer's disease,⁴ Paroxetine as an antidepressant⁵ and Fentanyl as a pain reliever⁶ are well-known prescription drugs (Figure 4-1). Given their immense pharmaceutical utilities, the synthesis of piperidines has been extensively studied.^{1c,e-i} Hydrogenation of readily accessible pyridines provides probably the most economic and efficient route for accessing piperidines.⁷ Successful examples of pyridine reduction using heterogeneous catalysts, homogeneous metal complexes and organocatalysts have been reported time to time.⁸ Despite the progress made in asymmetric hydrogenation of pyridines, efforts on the mechanism studies remain limited.

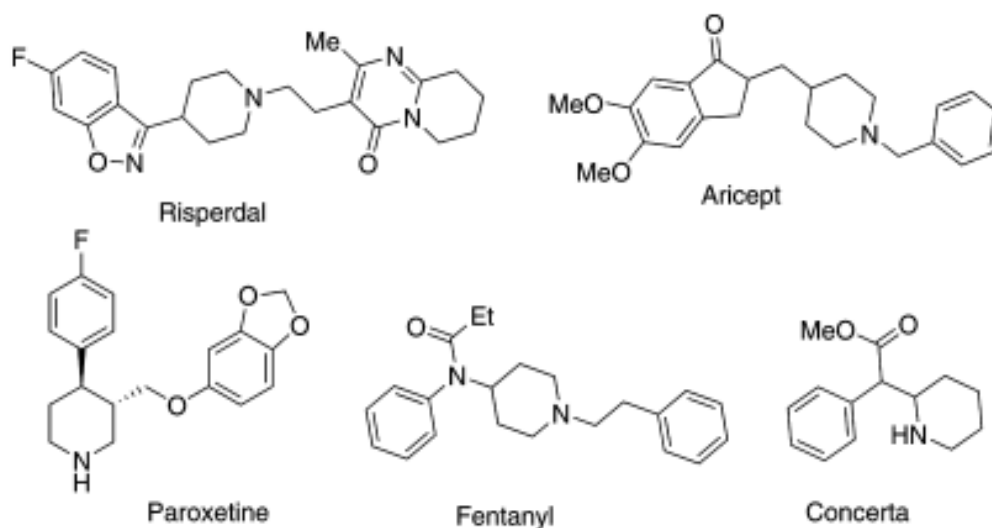
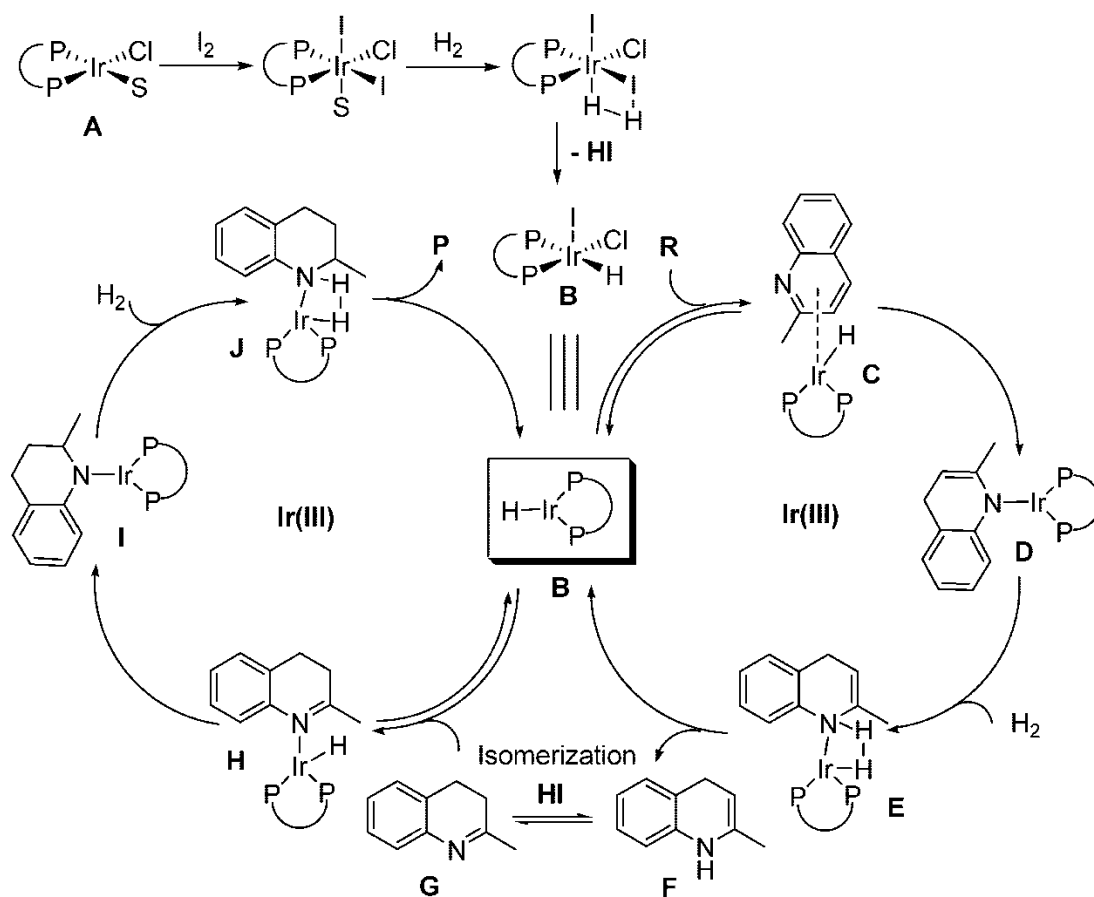
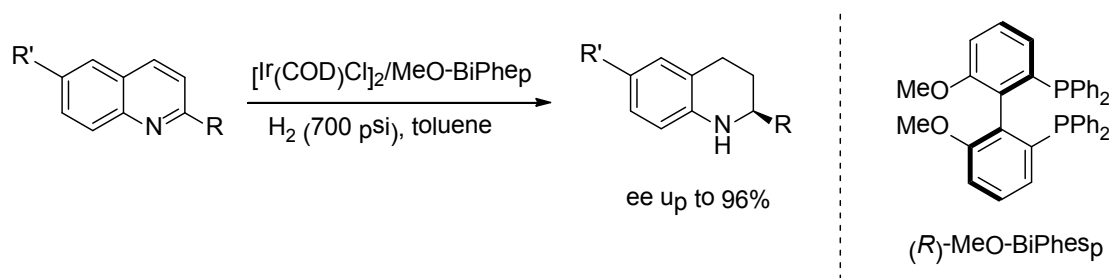


Figure 4-1. Piperidine Derivatives as Prescription Drugs.

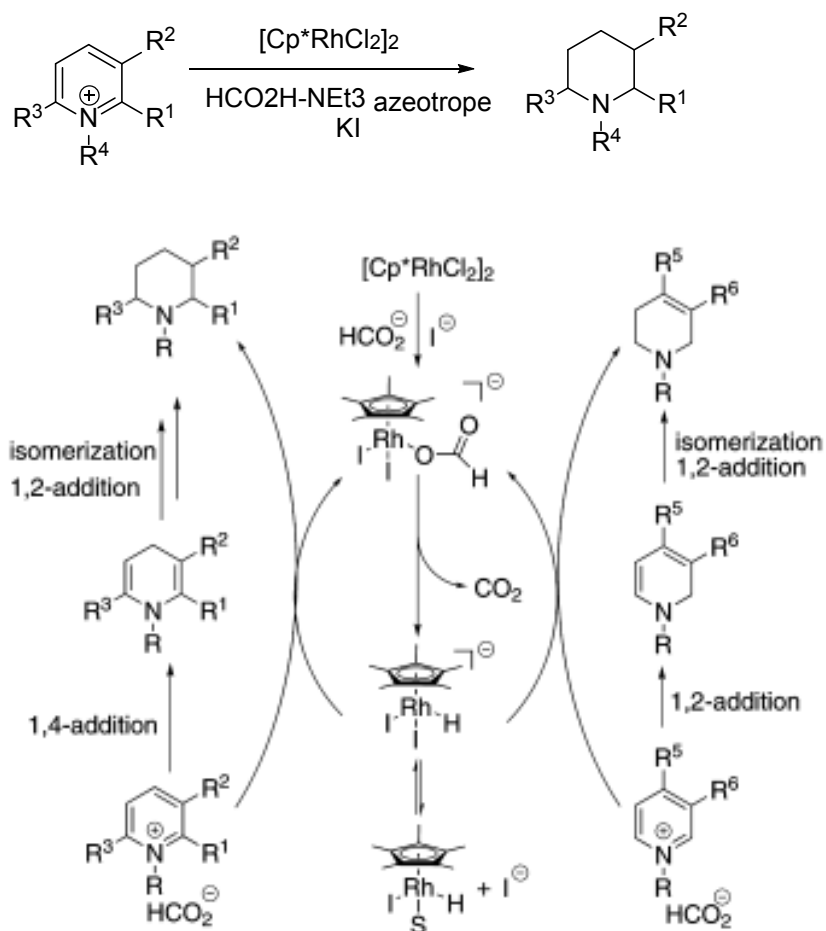
Over the past decades, there were only a few reports on the mechanism of enantioselective hydrogenation of heteroaromatic compounds. In 2009 Zhou and coworkers reported the first highly enantioselective hydrogenation of quinolines example utilizing iridium catalyst generated in situ from $[\text{Ir}(\text{COD})\text{Cl}]_2$ and axially chiral bisphosphine ligand MeO-BiPhep with iodine as additive.⁹ A plausible mechanism was proposed (Scheme 4-1).¹⁰ Their mechanistic studies revealed the hydrogenation mechanism of quinolines involves a 1,4-hydride addition, isomerization, and 1,2-hydride addition, and the catalytic active species may be an Ir(III) complex with chloride and iodide.

In 2012, Xiao and co-workers reported a rhodium complex dimer, $[\text{Cp}^*\text{RhCl}_2]_2$, promoted by iodide anion, catalyzes efficiently the transfer hydrogenation of various quaternary pyridinium salts under mild conditions, affording not only piperidines but

also 1,2,3,6-tetrahydropyridines in a highly chemoselective fashion.¹¹ A plausible mechanism explaining the role of iodide and the observed chemoselectivity is shown in Scheme 4-2. As suggested before,¹² the substrate is likely to be reduced with an anionic diiodo Rh—H hydride species. Both the iodide and anionic charge would render the hydride more hydridic. In the absence of a 4-substituent, the hydride adds preferentially at the 4 position (i.e., 1,4-addition); the resulting enamine isomerizes to an iminium species and is then reduced *via* a 1,2-hydride addition. When the 4-position is substituted, 1,2-addition takes place to give 1,2-dihydropyridine; isomerization of the resulting enamine followed by another 1,2-addition affords the *N*-substituted 1,2,3,6-tetrahydropyridines.



Scheme 4-1. Proposed Mechanism for Asymmetric Hydrogenation of Quinolines.



Scheme 4-2. Plausible Mechanism for the Chemoselective Transfer Hydrogenation.

We recently reported the development of Ir-catalyzed asymmetric hydrogenation of simple *N*-benzylpyridinium salts using a unique phosphole (**Figure 4-2**) as catalyst with high enantioselectivity (Chapter 2). Although the hydrogenation is synthetically useful, the mechanism of Ir-catalyzed asymmetric hydrogenation remains unclear. The three double bonds present in the pyridine ring add more complexities in the mechanistic evaluation.

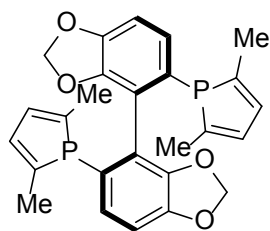


Figure 4-2. Structure of MP²-SegPhos

4.2 Results and Discussion

4.2.1 NMR Studies On Catalyst Complex

We first conducted NMR studies on the catalyst complex itself. We mixed [Ir(COD)Cl]₂ and MP₂-SegPhos under nitrogen and the ¹H-NMR under 1 bar nitrogen indicated that COD has asymmetric chemical shifts. In addition, ³¹P-NMR also showed two major ³¹P signals, consistent with the feature of structural asymmetry. Then we mixed [Ir(COD)Cl]₂ and MP₂-SegPhos under nitrogen in a J Young tube following with the charge of 1 bar Hydrogen for 5 minutes. This sample under low hydrogen pressure was not stable. However we did observe multiple hydride signals spanning a wide region. ¹H-³¹P HMBC showed hydride-³¹P coupling across Ir(III). NOE also provided evidence that there was a slow exchanging dihydride species and fast exchanging Hydride species. Next we mixed [Ir(COD)Cl]₂, MP₂-SegPhos and substrate (N-benzyl 2-ph-pyridium bromide salt). To our delight, the bromide anion seemed somehow to stabilize the complex. The spectrum looked cleaner and similar

^1H - ^{31}P HMBC pattern and NOE data were observed.

To obtain a more stable sample for NMR studies, we next ran complex samples under high hydrogen pressure (600 psi) for a long period of time (16 hours). We also tried to add three different counter anions (NH_4Br , NH_4BF_4 , NH_4PF_6) in hope to stabilize the activated catalyst species. In fact, bromide anion seemed superior in stabilizing the complex than the other two anions by providing cleaner spectrum. Indeed, Multiple hydride signals were observed. Two new triplets at -24 & -25 ppm were clearly observed with 600psi H_2 activation. ^1H - ^{31}P coupling reveals both a dihydride species and a monohydride species. Even though we tried to cool down the sample to -15°C , the sample still decayed significantly within a day. Based on the initial NMR studies, we proposed the structure of catalyst structures in Figure 4-3.

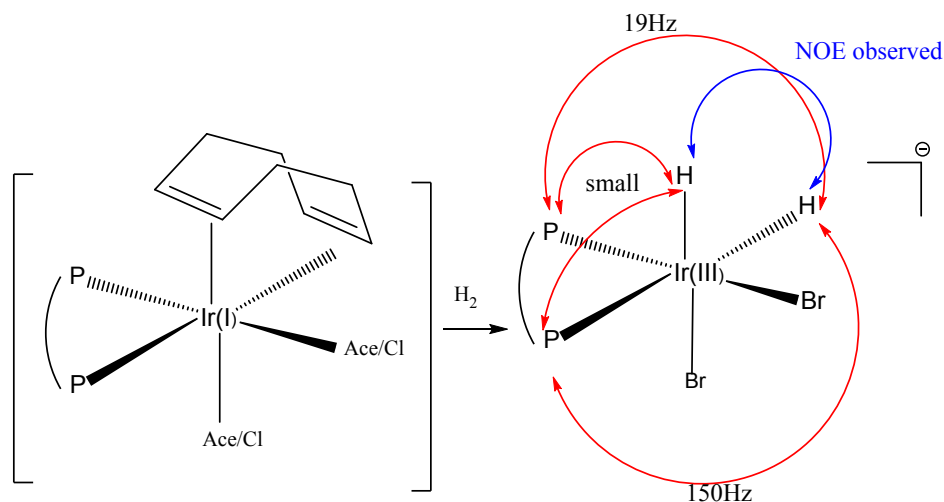
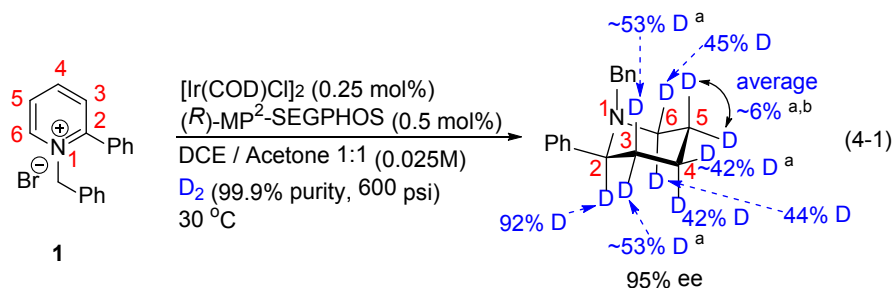
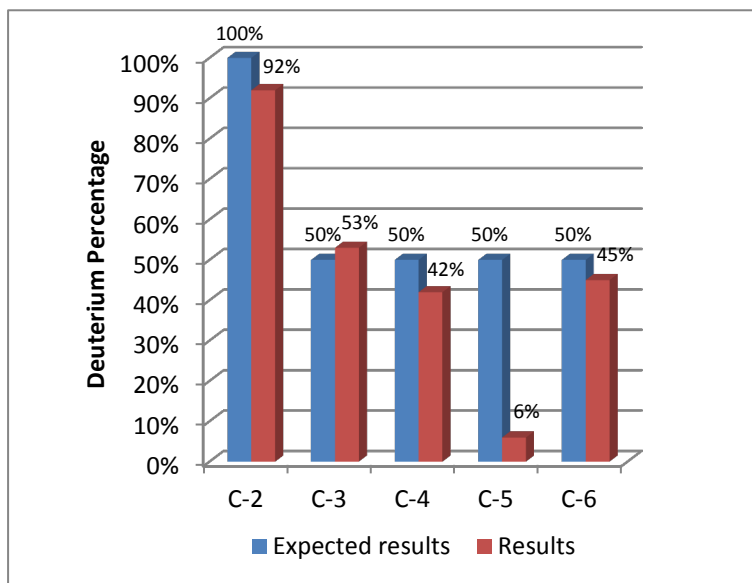


Figure 4-3 Proposed catalyst complex structure

4.2.2 Isomerization

Initially we conducted isotopic labeling experiments using deuterium gas (Eq. 4-1).¹³ When *N*-benzyl-2-phenylpyridinium bromide **1** was subjected to hydrogenation with D₂, NMR analysis indicated that only 6% deuterium content at the C5-position (Equation 4-1) which suggested a fast, reversible process of protonation and deprotonation from other proton source other than D₂. Deuterium distribution at the C2-, C3-, C4-, and C6-position were determined to be close to expected values (Figure 4-3). Furthermore, control experiment using deuterated solvents under H₂ reveals no deuterium content in the product. From this, we realized that the residual H₂O in solvents could serve proton source at C-5 since in previous experiments we used commercial available anhydrous solvents without further processing.

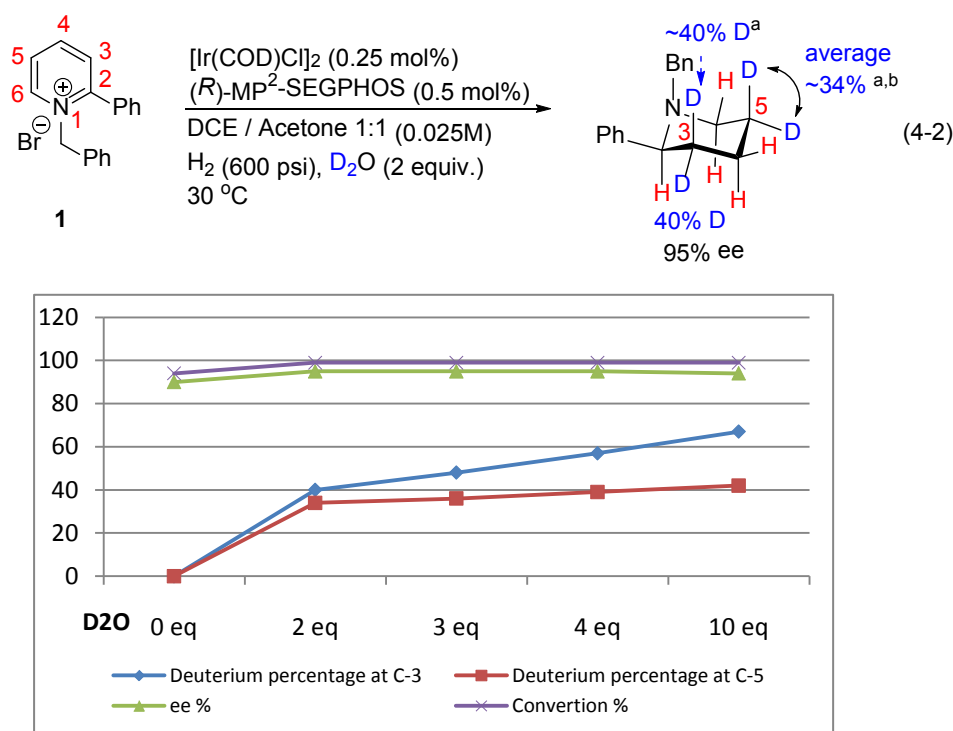




[a] Estimated value; see supporting information for further details. [b] Axial and equatorial proton chemical shifts are overlapped.

Figure 4-4 Isotopic Labeling Experiment Using Deuterium Gas.

With this in mind, we performed the reaction of **1** under strictly anhydrous condition. Commercial anhydrous solvents were further dried over molecular sieves prior use. In a separate experiment we introduced D₂O (2 equivalent) as additive (Equation 4-2) for a parallel comparison. As expected, the deuterium atoms were detected but only at C3- and C5-position (40% and 34%, respectively). This finding demonstrates that water is one of the proton sources for reductions at these two carbons. To gain more insights on the role water plays, we evaluated the effect of different equivalents of D₂O as additive in the reaction. Interestingly, with the increasing amount of D₂O additive, deuterium distribution percentage at both C3- and C5-position increases and the increasing rate at C3 is faster than that at C5-position, which indicates a more active protonation and deprotonation activity at C3-position (Figure 4-4).



[a] Estimated value; see supporting information for further details. [b] Axial and equatorial proton chemical shifts are overlapped.

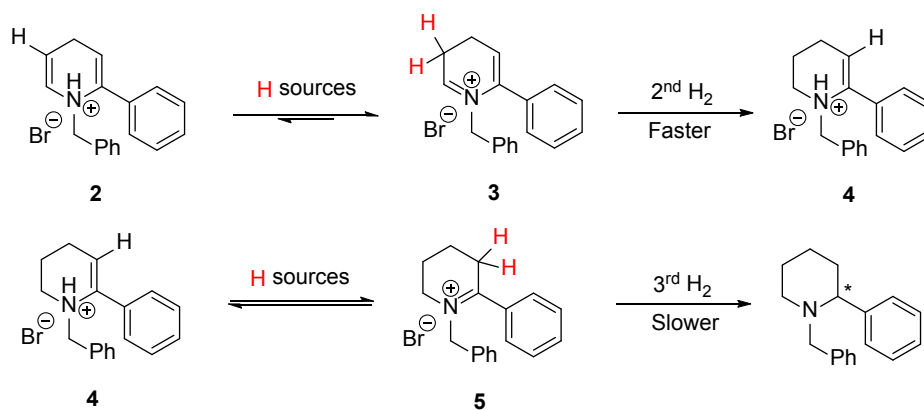
Figure 4-5 Isotopic Labeling Experiment Using Deuterium Water as Additive.

The above experiments posed an important question: While more deuterium was incorporated at C-3 in the D_2O addition experiment (Equation 4-2), why in the asymmetric deuteration of **1** with D_2 experiment (Equation 4-1), deuterium content at C-3 is so close to “expected” value?

There are 4 types of proton sources in the reaction: 1) proton from hydrogen gas; 2) proton from water residue in the commercial solvents; 3) proton from HBr which is part of the product; and 4) proton from proton exchanged water (this proton could either be proton from hydrogen gas or proton from starting material). At the inception

of deuterization of *N*-benzyl-2-phenylpyridium bromide with D₂ (Equation 4-1), the only proton source for proton exchange is type-two proton. Consequently, deuterium distribution at C-5 is only 6% as deuterium at this position has exchanged with H⁺ from residue water in the solvents. After the initial proton exchange, partially reduced intermediate was generated and deuterium exists at much higher concentration in the reaction system competing for the proton exchange process. Therefore, when proton exchange undergoes at C3-position, deuterium was exchanged with larger possibility. This also rationalizes that deuterium at C3-position is more than that at C5 and is close to “expected” value.

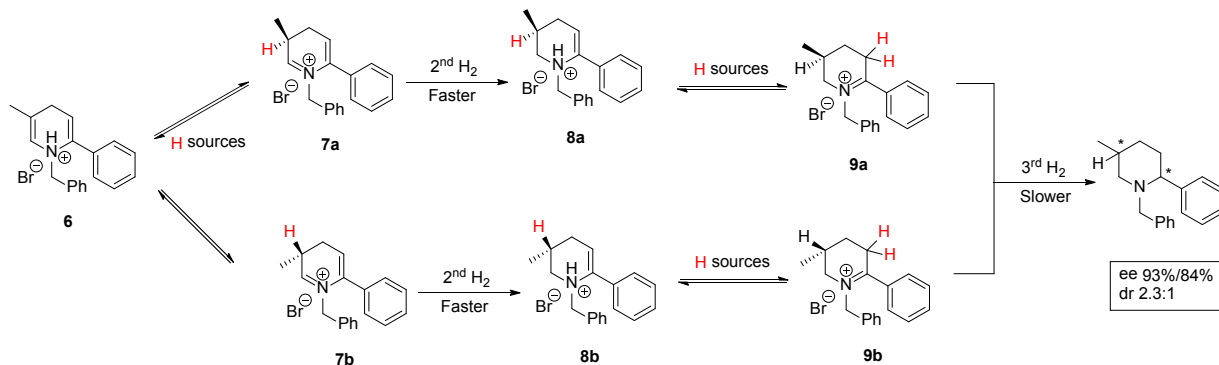
Based on the above deuterium labeling experimental evidences, we propose that tautomerizations between the partly-reduced enaminium and iminium intermediates are involved in this reaction (Scheme 4-3). Enamine **2**, generated via 1,4-hydrogen addition, rapidly captures one proton to tautomerize to iminium **3**. After second hydrogen addition, the corresponding enamine **4** was generated. The second tautomerization of **4** results in an iminium **5**. Subsequent chiral reduction of **5** affords the final chiral piperidine. Generally, reduction rate of tetra-substituted iminium **5** is slower compared to the tautomerization rate of enamine **4**. Therefore, the second tautomerization has longer time to undergo a reversible process of protonation and deprotonation, which explains the aforementioned higher deuterium content at C-3 with D₂O as additive in the hydrogenation of **1** (Equation 4-2).



Scheme 4-3 Proposed Tautomerization Process.

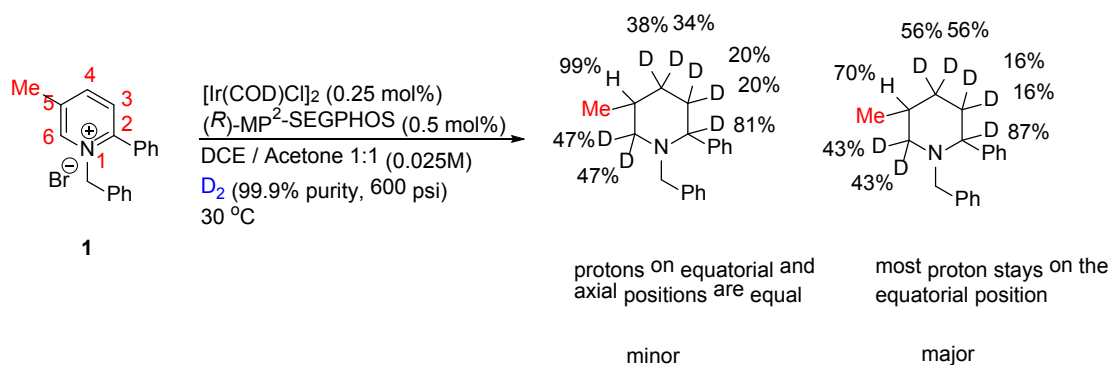
To further demonstrate the above proposed mechanism involving tautomerizations, we investigated the asymmetric hydrogenation of disubstituted pyridinium salt, which would generate two stereogenic centers and represent an advantageous feature of our asymmetric hydrogenation protocol for heteroaromatics. We chose 2-Me-5-phenyl-pyridinium salt **6** to run the model study under the previously reported optimal condition. To our delight, we obtained the corresponding hydrogenated products with 93% ee and 83% ee (dr=2.3). As shown in Scheme 4-4 stereochemistry observed in the asymmetric hydrogenation of 2-Me-5-phenyl-pyridinium salt **6** can be rationalized. The rapid tautomerization between the enamine **6** and imine **7** provided a mixture of syn and anti isomers of the imines and this reduction determined the ratio of the syn and anti isomers of the 4,5-dihydropyridinium salts. The difference between the two transition states was considered small, resulting low diastereoselectivity. The final reduction determines the chirality at the C2-position with high enantioselectivity, as described in our

previous report. The result of this experiments offers another proof to our previous proposed mechanism.



Scheme 4-4. Hydrogenation of Di-substituted Pyridinium Salt.

Isotopic labeling experiments using deuterium gas on this 5-methyl-2-phenyl di-substituted pyridine also provided similar result as on mono-substituted pyridine. The D₂ ratio is pretty much as expected: low on positions meta to nitrogen but higher otherwise. But there is one very interesting difference. For the major diastereomer, D₂ are added to only one side of the ring, unlike the minor diastereomer and the unsubstituted version where D₂ was equally added to both sides (Figure 4-5).



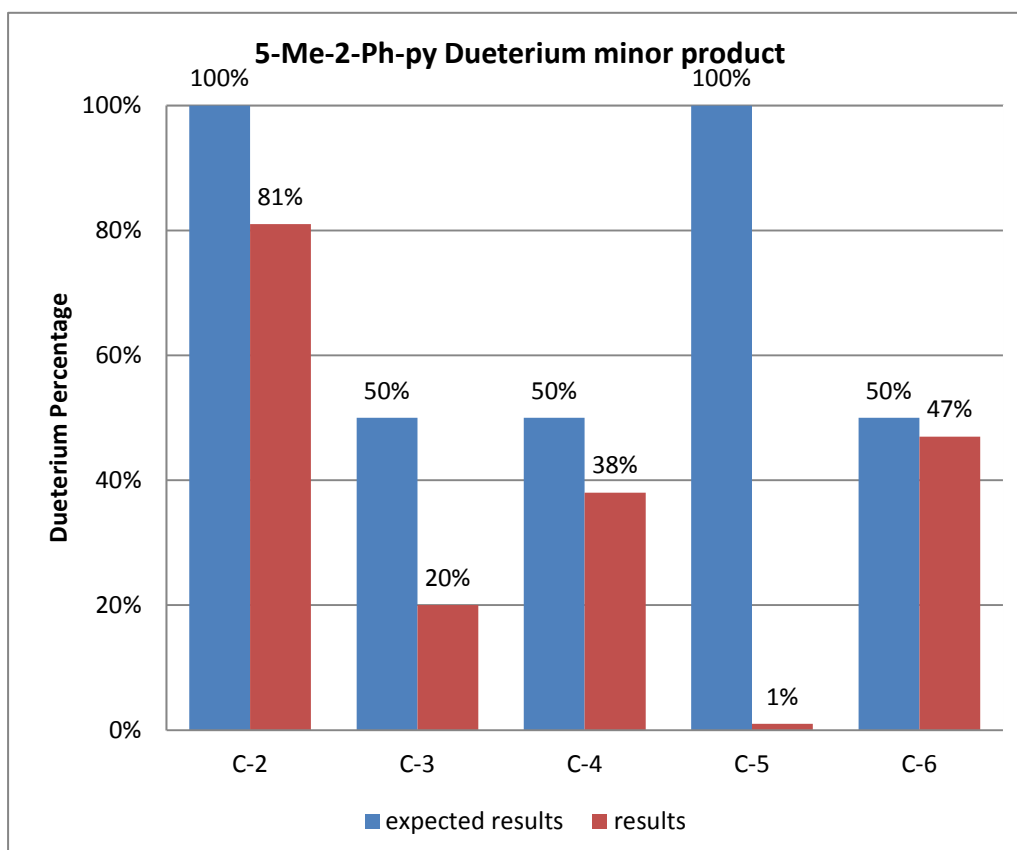
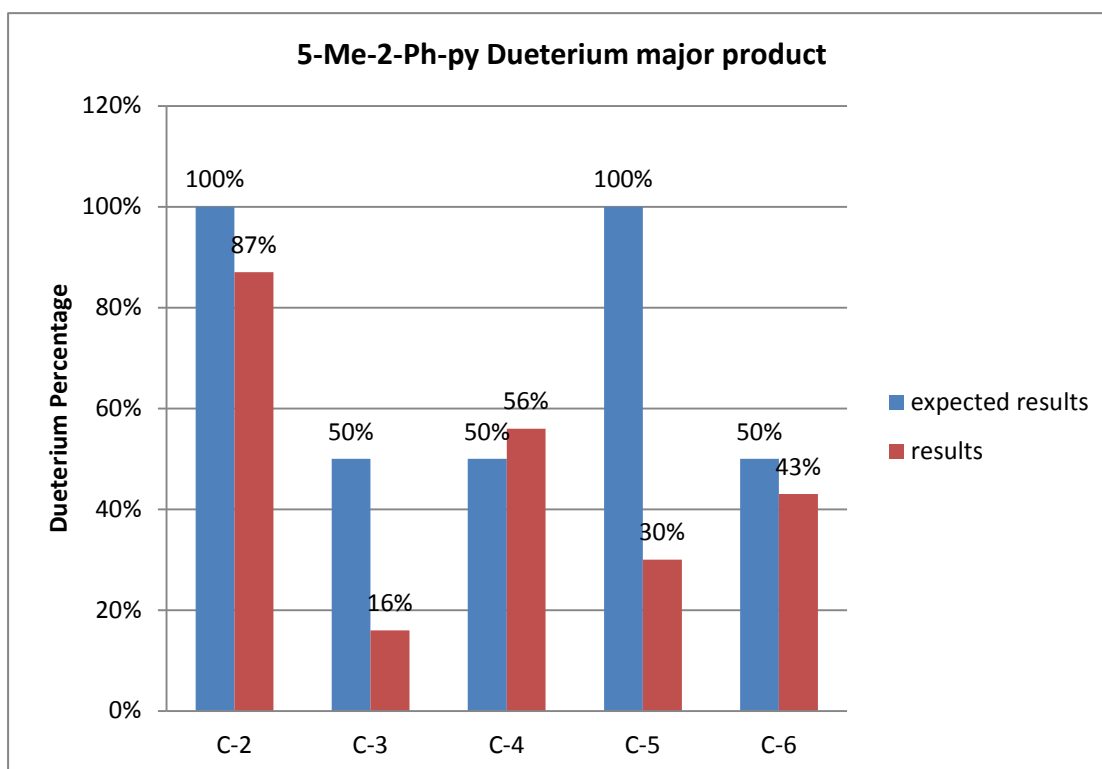


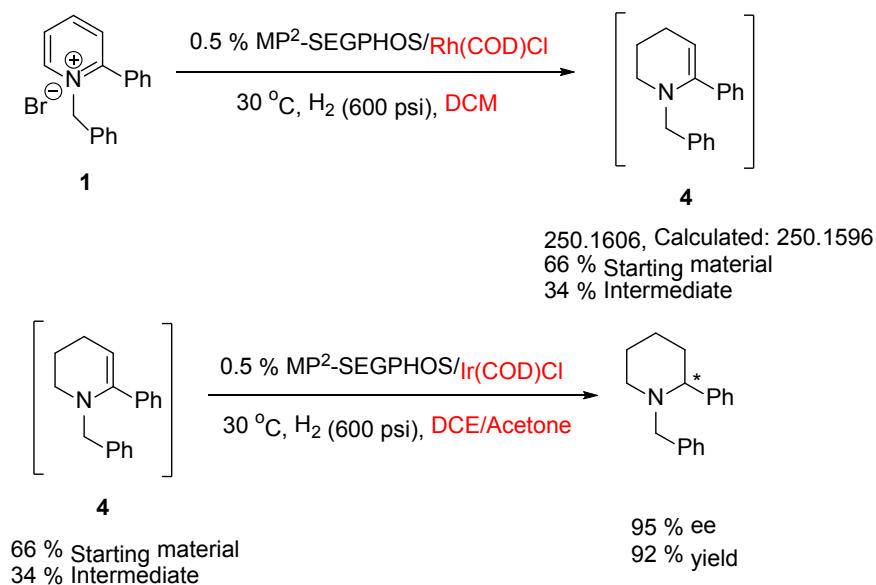
Figure 4-6. Isotopic Labeling Experiment on Di-substituted Pyridine.

4.2.3 Identification of Intermediates

Recent reports have revealed an outer-sphere mechanism for bisphosphine-transition metal catalyzed hydrogenation. We envisioned that hydrogenation of pyridine might go through a similar step-wise outer-sphere pathway. We therefore interrogated this reaction in some details and sought to capture the presence of the intermediates generated over the process of the hydrogenation reaction, which could provide direct proof to support the mechanism. Initially we carried out the reaction with **1** as model substrate over shorter reaction time and observed small new peak corresponding tetrahydropyridine (M+4) by HPLC. However, this intermediate is somewhat not stable and decomposed upon chromatography separation.

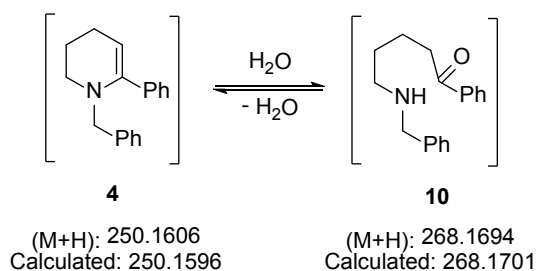
Through metal and solvent screenings, we found that hydrogenation with Rh metal in dichloromethane provides significant amount of tetrahydropyridine intermediate **4**: 34% intermediate was detected by HPLC (Scheme 4-5). It seems Rh catalyst could not effectively catalyze the last reduction transformation. Subsequent electrospray ionization mass spectroscopic analysis of the mixture solution showed peak at m/z^+ 250.1606, which agreed with the enamine intermediate **4**. The NMR spectrum of the mixture solution also confirms the presence of the enamine intermediate **4**. The solvent of this mixture solution was then removed in glove box, and Ir(COD)Cl/MP²-SEGPHOS and DCE/acetone were added as described in previous hydrogenation condition (Scheme 4-5). As expected, the reaction proceeded

smoothly to the desired piperidine product with 95% ee and 92 % isolated yield, which confirms that this enamine **4** is one of the relatively stable intermediates generated over the hydrogenation process.



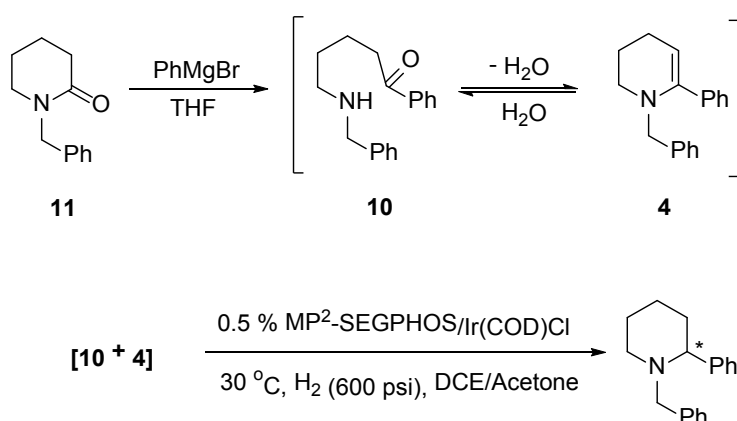
Scheme 4-5 Hydrogenation of Enamine **4** to Piperidine

Noteworthy, when the reaction carried out with commercial anhydrous solvent acetone and DCE, a new intermediate was detected, HRMS showed peak at m/z + 268.1694 (calculated m/z =250.1596), which implied an addition of water. From C^{13} -NMR, we found this peak belongs to carbonyl group around 200. Due to instability, clean proton NMR is unable to achieve. But all evidences supported ketone compound **10** as an intermediate (Scheme 4-6).



Scheme 4-6. By-product Ketone Formed with Water Present.

We are intrigued by this rare finding and sought to confirm the ketone **10** is a viable intermediate generated in the hydrogenation process. Thus we synthesized this ketone by conveniently reacting amide **11** with phenylmagnesium bromide. UPLC, HRMS and crude NMR all support this reaction product is the same as the ketone intermediate found in hydrogenation reaction. After removing solvent in glove box, the crude material was subjected under the original hydrogenation condition and corresponding product was indeed detected by UPLC (Scheme 4-7). Therefore, we confirm that ketone **10** exists as one of the intermediates in the hydrogenation of **1**, especially when water exists.



Scheme 4-7. Synthesize Ketone **10**

4.2.4 Kinetic Studies

Kinetic analysis was investigated employing 2-ph-pyridinium benzyl bromide salt **1** as model substrate. Such studies are undoubtedly challenging: special technical facilities are needed to monitor the reaction under high hydrogen pressure. Initially we relied on NMR analysis. At desired time points hydrogen pressure was carefully and slowly lowered to 50 psi for removal of aliquots for NMR analysis then hydrogen pressure was resumed to continue the reaction course. However this practice basically interrupted the reaction and was time-consuming and proved to be unpracticable.

In an attempt to solve this issue, we installed a remote IR sensor to monitor the intensity of the characteristic peak of **1**, at 1640 cm^{-1} . However, the solubility of *N*-benzyl-2-phenylpyridium bromide **1** was particularly low in organic solvents. At 50 °C, the maximum concentration achieved was 0.04 mmol/ml (acetone/DCE=1:1), which is inadequate for IR detection. Considering only small amount of intermediates exist during the reaction course, it presents an even bigger challenge for monitoring the reaction. Bearing these challenges in mind, we first conducted the validation of the IR-sensor monitor method, carrying out the hydrogenation of **1** at 50 °C under 300 psi of hydrogen gas with 0.5% mol iridium catalyst in a mixture of dichloroethane and acetone. The concentration of **1** monitored by IR was recorded against NMR samples taken over the reaction course under the same condition in a control experiment (Figure 4-6). To our delight, the two profile are in good agreement.

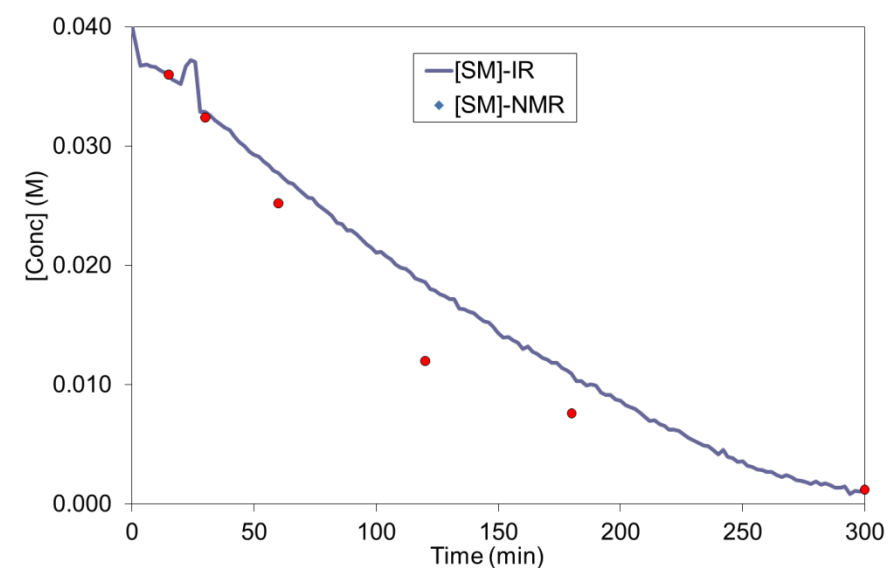


Figure 4-7. Validation of IR-Sensor Monitor Method Against NMR Analysis.

Next, half concentration of starting material against time course was sketched over the first 3-4 hours' reaction in comparison to the full standard concentration reaction (Figure 4-7). The time adjusted profile overlays quite well with the standard reaction. The results of this experiment indicates no appreciable catalyst deactivation. In other words, the catalyst remains stable over the reaction course.

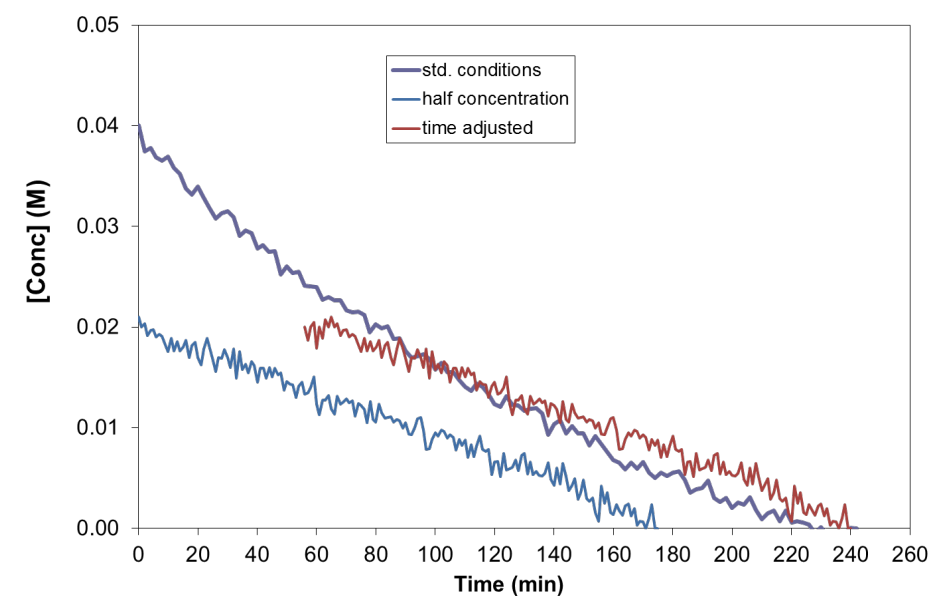


Figure 4-8. Half concentration of (**1**) versus Standard Concentration Time-Adjusted Profile.

Confident that the IR could serve the purpose of monitoring the reaction, we proceeded to study the kinetic orders of starting material and catalyst. The results revealed that the hydrogenation is zero order to the concentration of starting material and first order to the concentration of iridium catalyst (Figure 4-8).

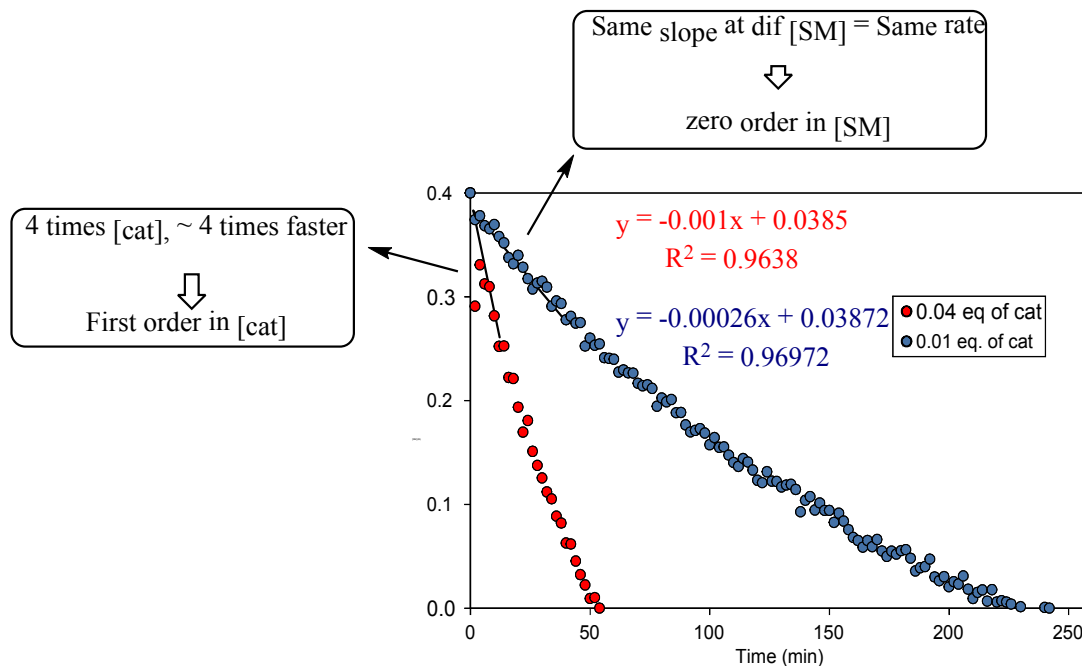


Figure 4-9. Kinetic Analysis of the Reaction of (1) to (2)

4.2.5 Outer-sphere Mechanism Proposal

It was commonly believed that one challenging in asymmetric hydrogenation of pyridines is that this kind of substrates possess strong coordination ability, which presumably cause the deactivation of catalysts. With this generally so-call inner sphere pathway involving direct coordination of unsaturated bonds to the metal, one might suggest that lone electron pair of pyridine will occupy coordination site of catalyst as a δ donor that will leave no space for substrate to bind with catalyst as a π donor. Despite this assumption, pyridine, 2,6-lutidine, *t*Bu-lutidine were added as additives in the hydrogenation of pyridine reaction (Figure 4-9) and, strikingly, all

reactions proceed smoothly to the product with no significant drop in either conversion or enantioselectivity. Even when one equivalent of pyridine was added (additive : catalyst = 400:1), chiral piperidine was obtained in excellent conversion and selectivity (97% and 93% ee). The evidence suggested a hydride transfer mechanism is more possible in this catalytic case. Base on previous reports and our deuterium labeling experiments, we propose a mechanism hypothesis involving an outer-sphere pathway.

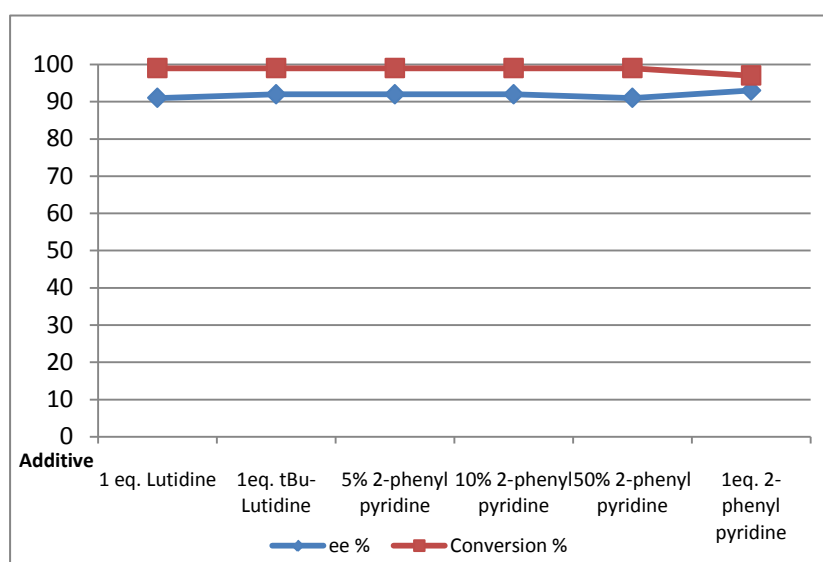


Figure 4-10. Additive Effects

Based on the combination of isotopic experimental evidences, kinetic, spectroscopic and structural data together we propose the catalytic reaction mechanism illustrated in Scheme 4-8. In the present hydrogenation dihydrogen is first coordinated to the bromide-displaced ligand complex 1a. Subsequent heterolytic cleavage of H₂ forms the active ionic complex 1b. The pyridinium salt 1 then

coordinates with mono hydride complex 1b, and then a 1,4-hydride transfer generates enamine 2 and regenerates the ligand complex 1a. Enamine 2 rapidly isomerizes to iminium 3. Through outer-sphere pathway the active ligand complex 1b delivers hydride to iminium 3 to afford enamine 4. In a similar manner, enamine 4 isomerizes to iminium 5 which exists in its ketone form when encountering water. Hydride delivery and chiral reduction of 5 takes place through another outer-sphere pathway to release the final chiral piperidine to complete the catalytic cycle. The high enantioselectivity can then be ascribed to the formation of the anionic complex 1b that dominantly selected the enantioface of the pyridium salt. The transition state for hydride attack is proposed to be a five-membered ring, involving the bromide-nitrogen bond of the substrate salt.

4.3 Conclusion

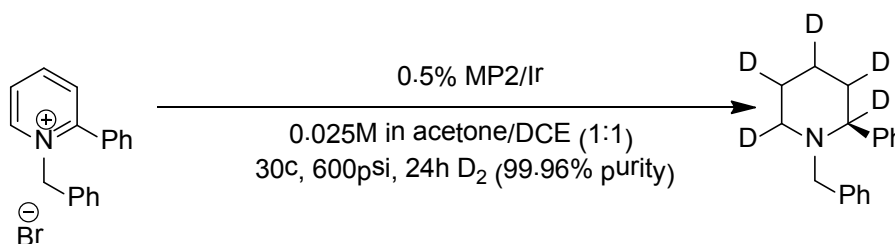
In summary, we proposed a mechanism for the hydrogenation of *N*-benzyl-2-phenylpyridium bromide salt by using an unusual MP2-SegPhos iridium catalyst. A combination of experimental and kinetic studies have suggested this iridium hydrogenation undergoes outer-sphere pathway involving sequential proton and hydride transfer. Two tautomerizations were proposed based on the evidences of deprotonation and protonation process at C-3 and C-5 positions. Two intermediates in this proposed mechanism have been isolated or spectroscopically characterized, while stoichiometric and catalytic experiments with the isolated intermediates provide



4.4 Experimental Section

All reactions were performed in the nitrogen-filled glovebox or under nitrogen using standard Schlenk techniques unless otherwise noted. Column chromatography was performed using Sorbent silica gel 60 (230 – 450 mesh). ^1H NMR, and ^{13}C NMR spectral data were obtained from Bruker 400 MHz spectrometers or Varian 500 MHz spectrometers. Chemical shifts are reported in ppm. Enantiomeric excess values were determined by chiral HPLC on an Acquity H-class (Waters Corp., milford, MA) or chiral SFC on an Acquity UPC² (Waters Corp., milford, MA). All new products were further characterized by HRMS. A positive ion mass spectrum of sample was acquired on a Micromass 70-VSE mass spectrometer with an electron ionization source. Scale-up reaction was conducted in OptiMax 1001 (Serial #: B425732840 / Firmware: 5.2.2.0).

4.4.1 Typical Procedure of Deuterium Hydrogenation of Pyridinium Salts

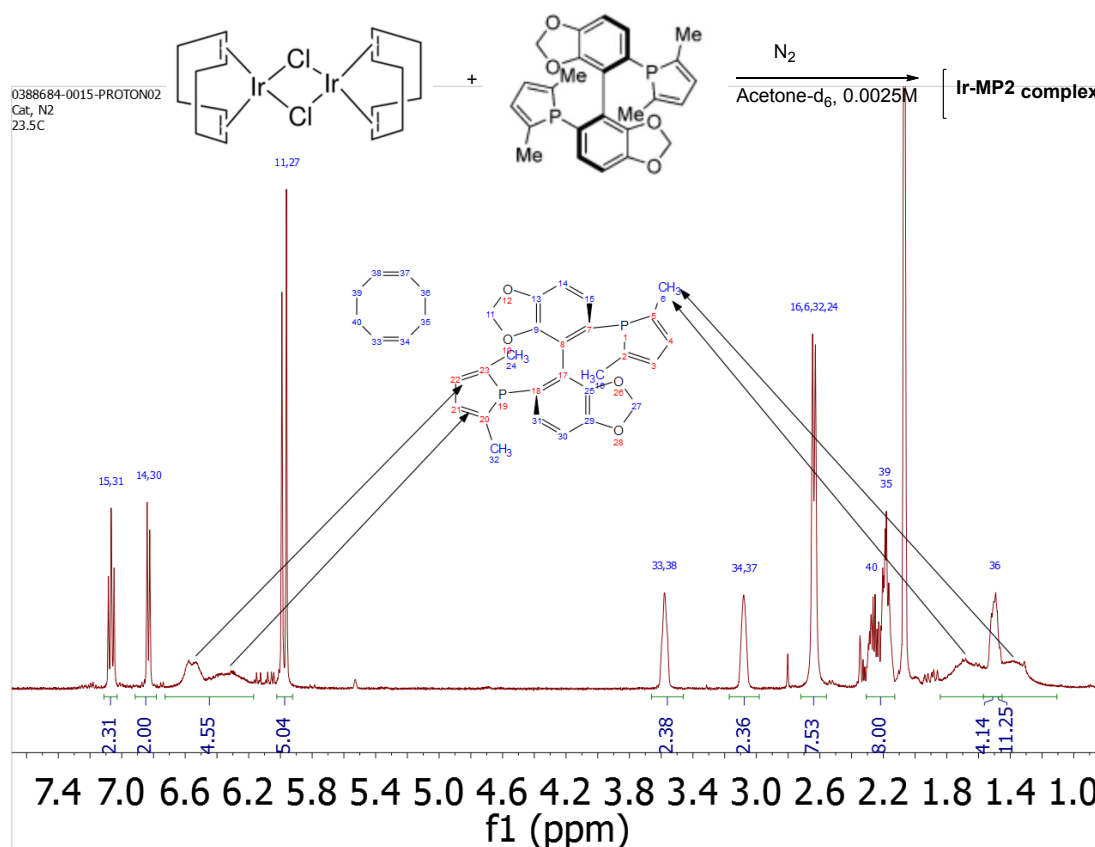


In a nitrogen-filled glove box, MP²-SEGPPOS (4.58 mg, 0.0099 mmol) and [Ir(COD)Cl]₂ (3.07 mg, 0.00457 mmol) were placed into a vial and stirring for 30 min in acetone (7.2 ml). Pyridinium salt (0.05 mmol) were placed into 4 ml hydrogenation

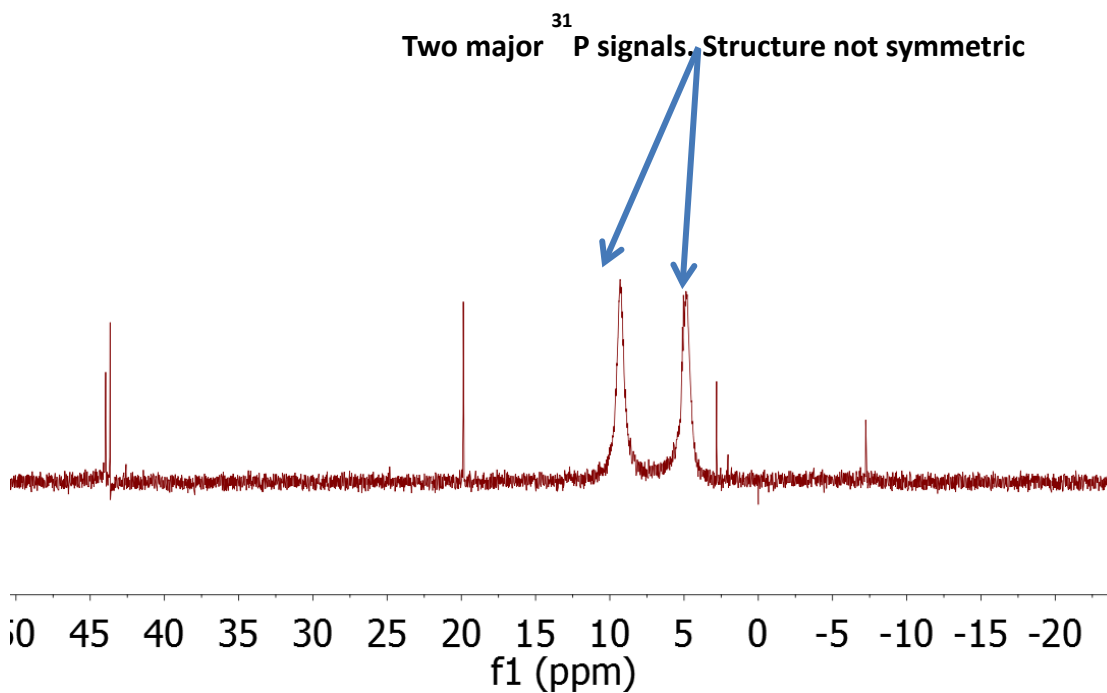
vials. 0.2 ml catalyst solution and remaining solvent were added. The vials were placed in a parallel hydrogenation block and following three D₂ purges, pressurized to 600 psi at 30 °C for 20 h. After carefully releasing the hydrogen, selectivities were determined by direct sampling of the reaction mixture on SFC or HPLC. Then saturated sodium carbonate was added and the mixture was stirred for 15-30 min. The organic layer was separated and extracted with CH₂Cl₂ twice, and the combined organic extracts were dried over Na₂SO₄ and concentrated in vacuo. Purification was performed by a silica gel column, eluted with hexane/EtOAc to give desired product.

4.4.2 NMR studies on catalyst complex

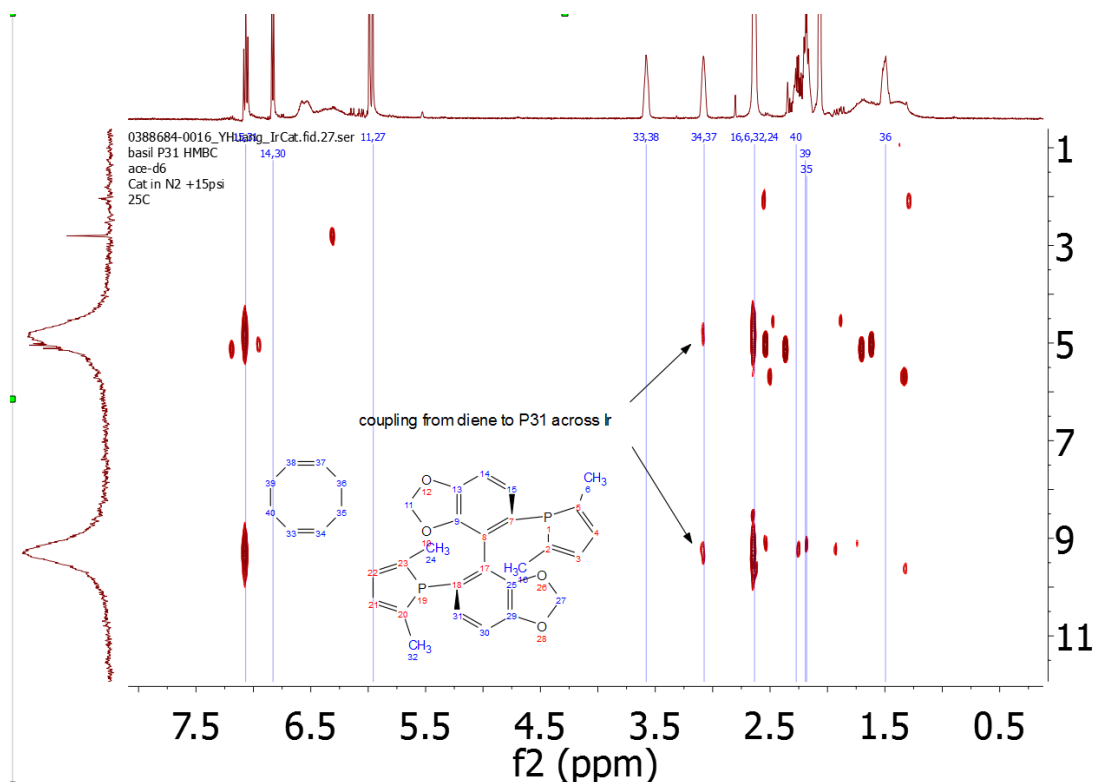
¹H NMR under N₂.



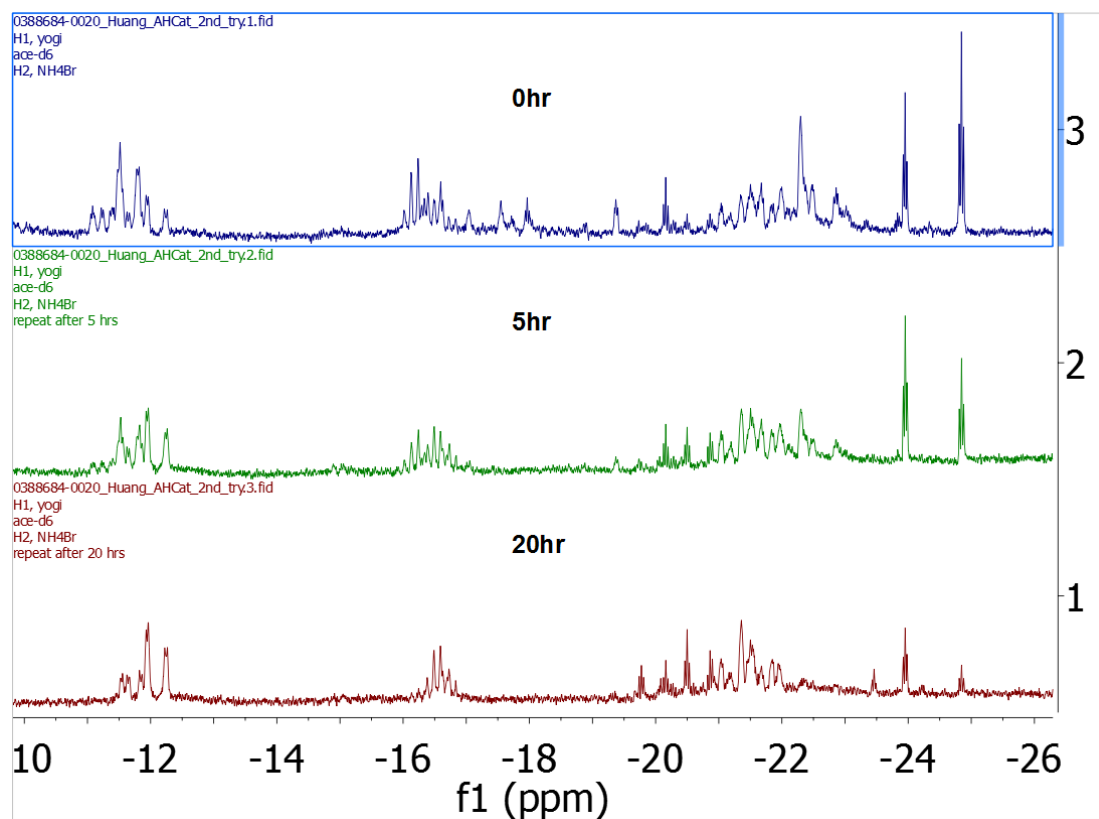
0388684-0016_YHuang_IrCat.fid.26.fid
 basil P31
 ace-d6
 Cat in N2 +15psi
 25C



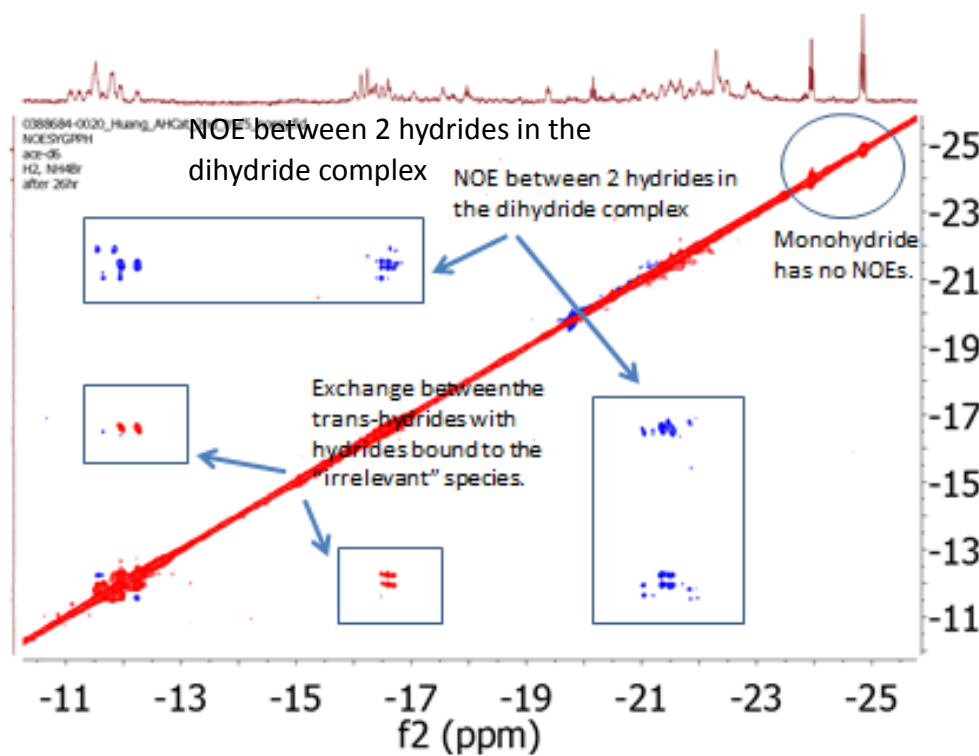
^1H - ^{31}P HMBC, showing COD coupling to ^{31}P across Ir



Stability of $+NH_4Br$ sample, showing the hydride region

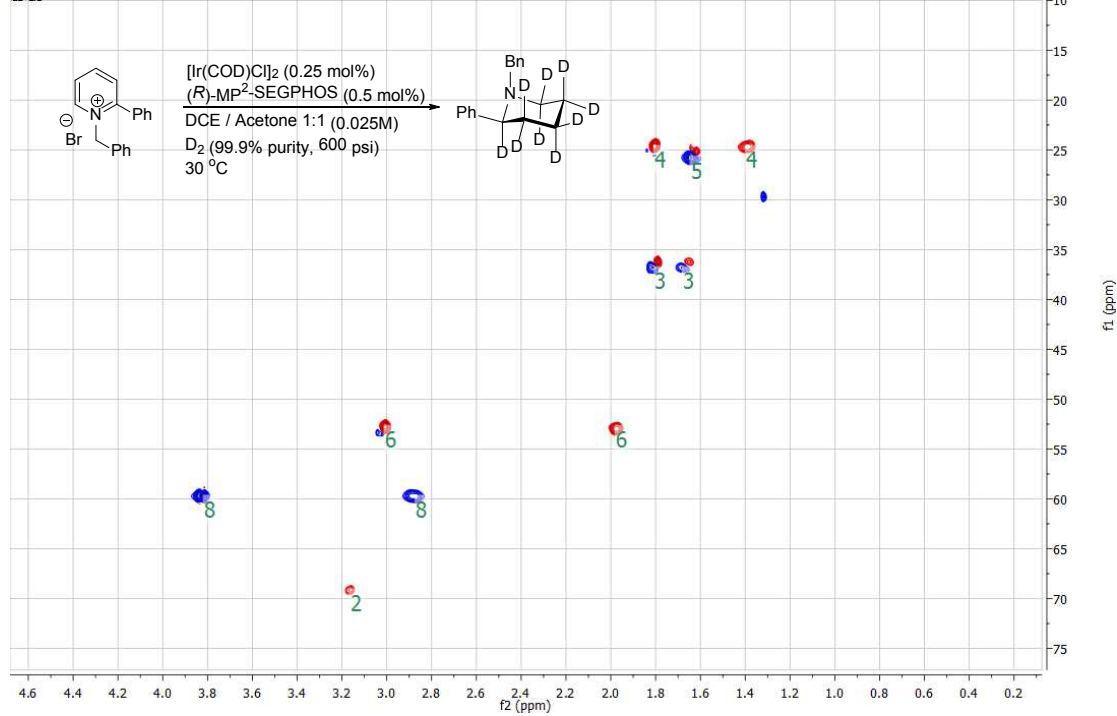
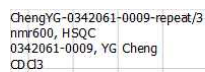


Evidence from NOE

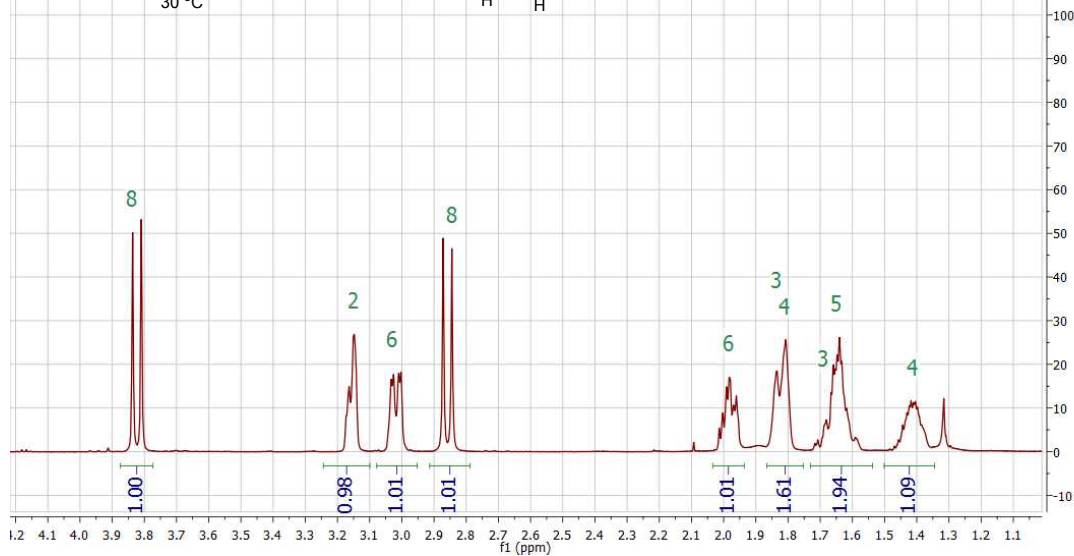
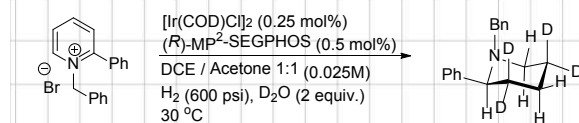


4.4.3 Deuterium Content Quantification by NMR

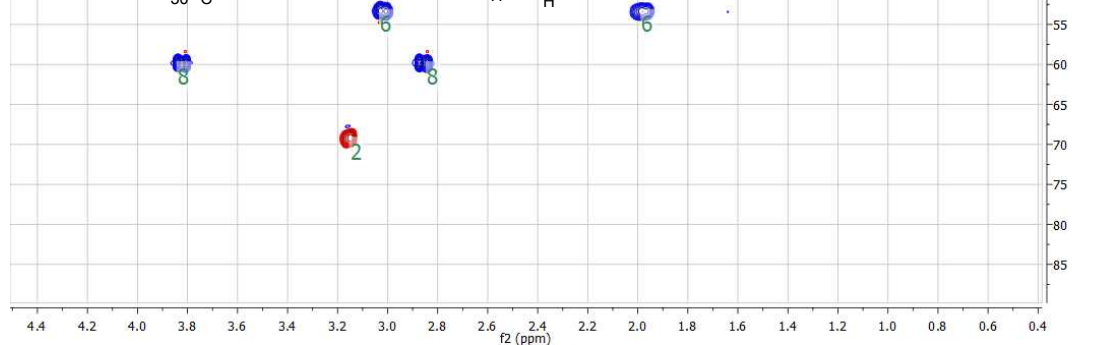
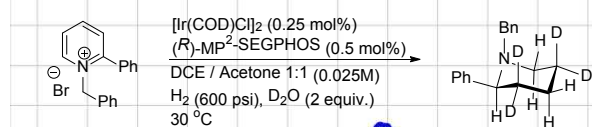
Deuterium incorporation during hydrogenation was quantified by 1D ^1H spectrum and qualitatively verified by 2D multiplicity-edited HSQC spectrum. Integration was calibrated with the methylene protons (8) from the benzyl group. The two protons of position 5 are degenerate and their chemical shifts also overlap with that of proton 3 axial; Equatorial protons of positions 3 and 4 also coincide. For these overlapping signals, quantification was made based on the assumption that the deuterium ratio is similar for both protons on the same methylene group. This assumption is valid according to multiplicity-edited HSQC. In FigS#, the blue contours represent signals from methylene CH_2 while the red contours represent signals from methylene CHD or methine CH. For positions 4 and 6, CHD is clearly predominant for both axial and equatorial protons, while on positions 3 and 5, CH_2 is the major form as manifested by blue contours immediately to the downfield of the red CHD signals due to a small isotopic shift. The intensity ratio of red vs blue contours approximates of the D/H ratio of the corresponding germinal position.

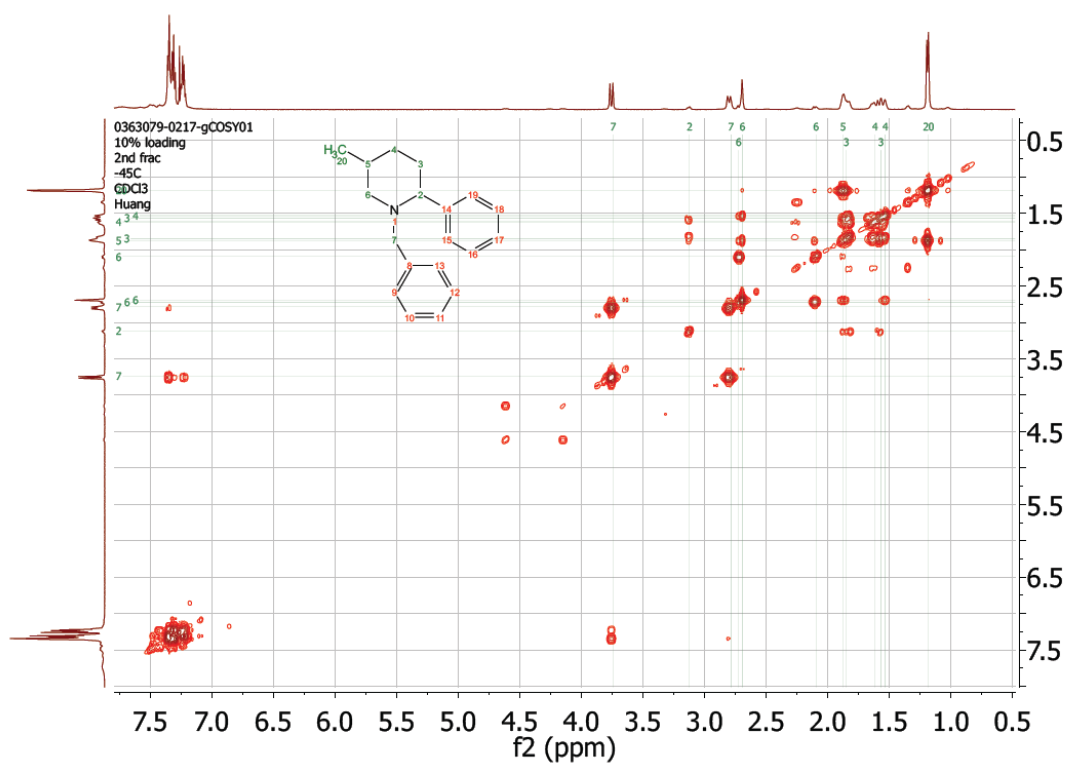
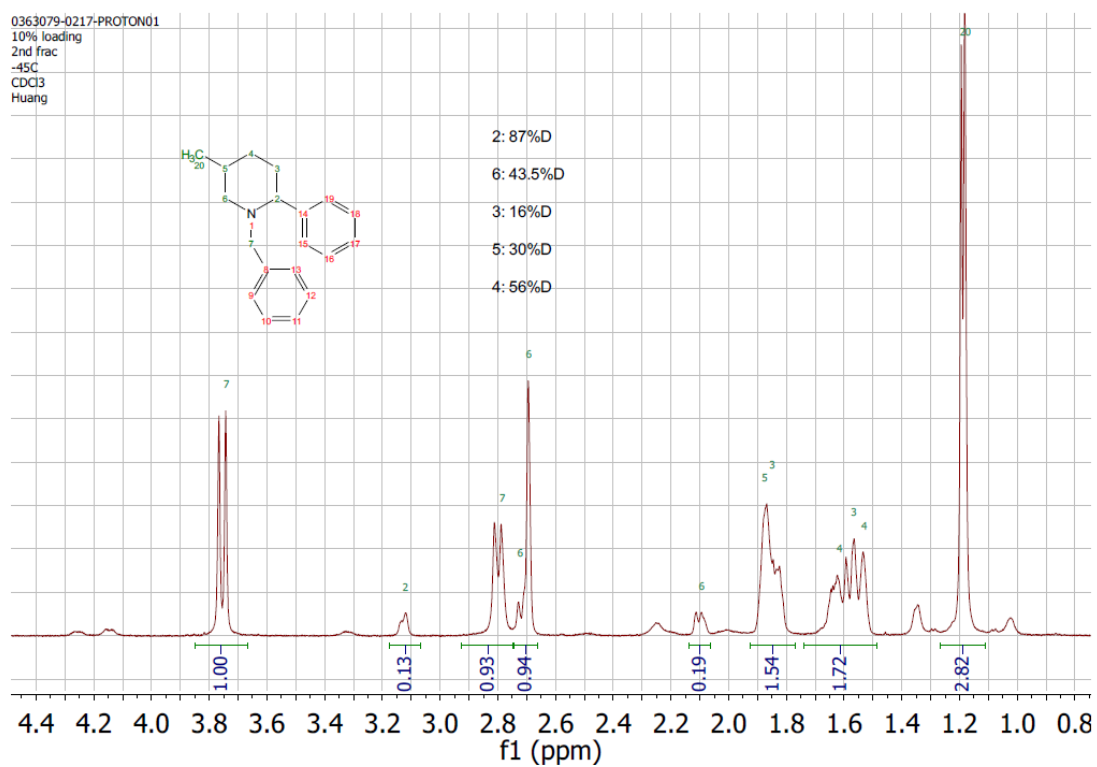


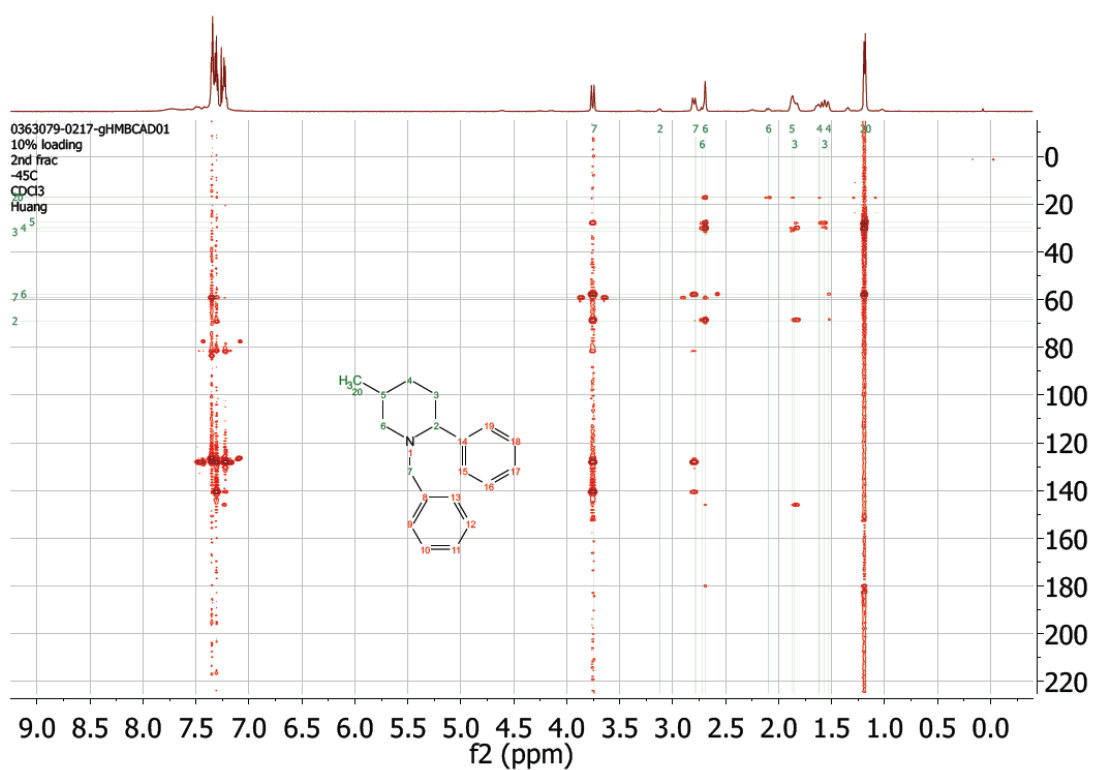
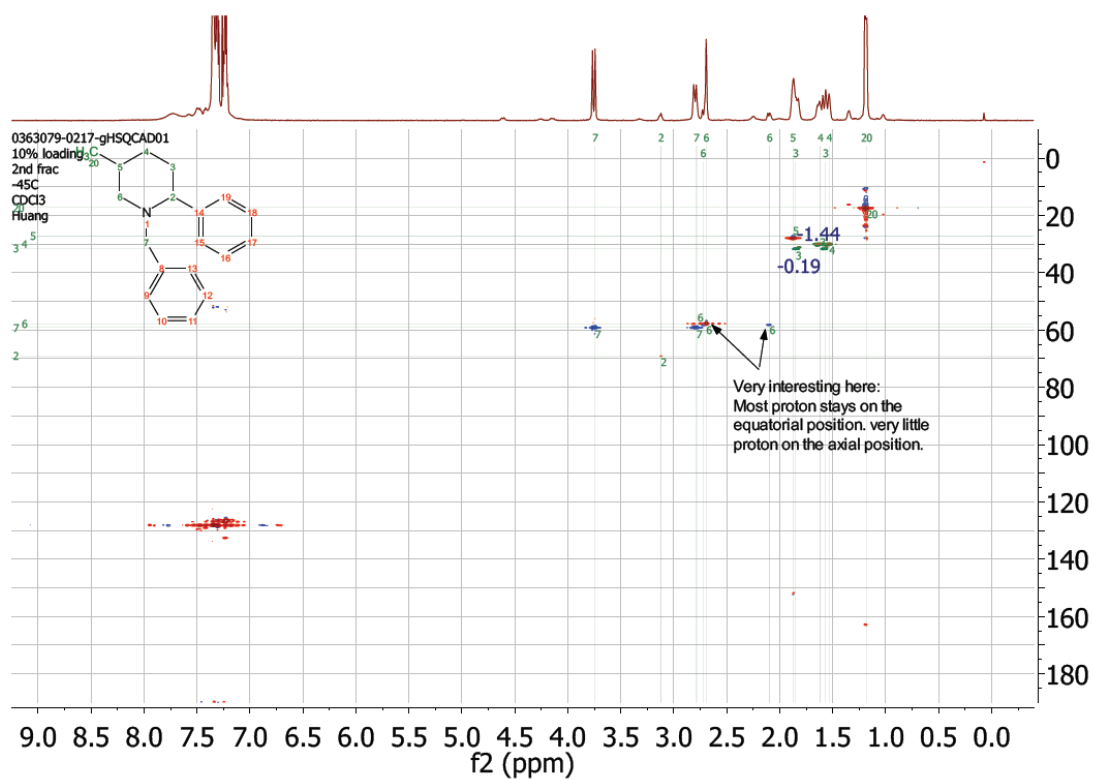
Chen-0363079-0026/21
nmr500b H-1
340897-144, sample #2: 2eq D2O
CDCl₃



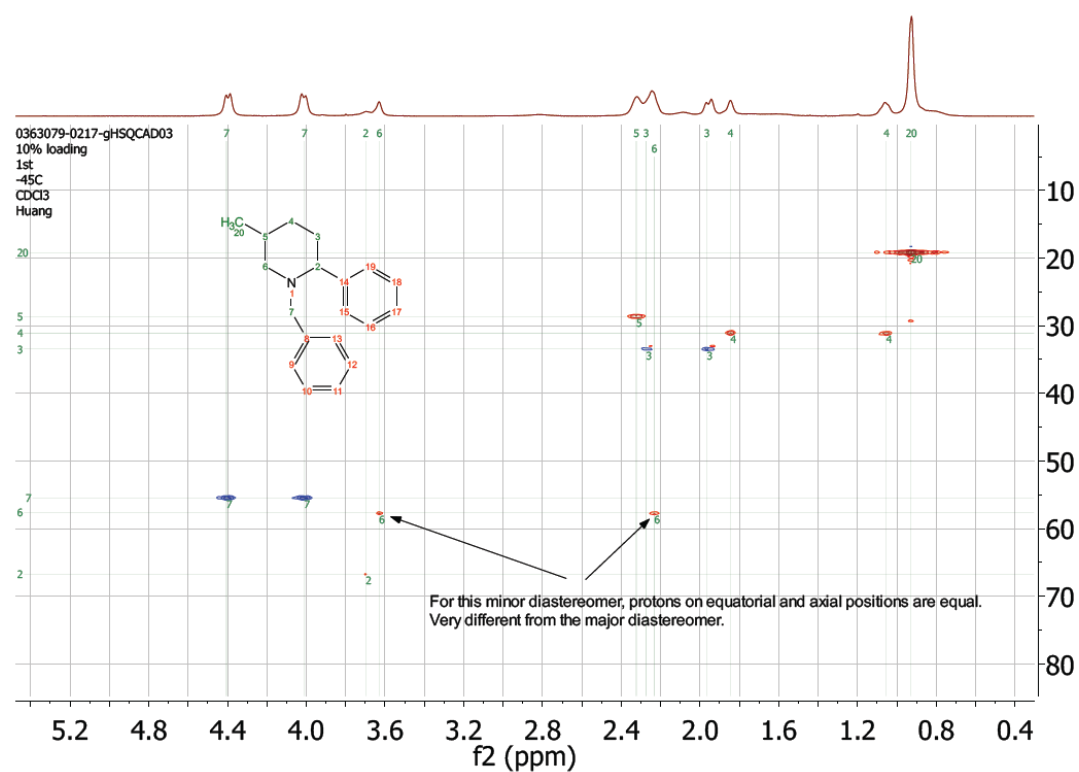
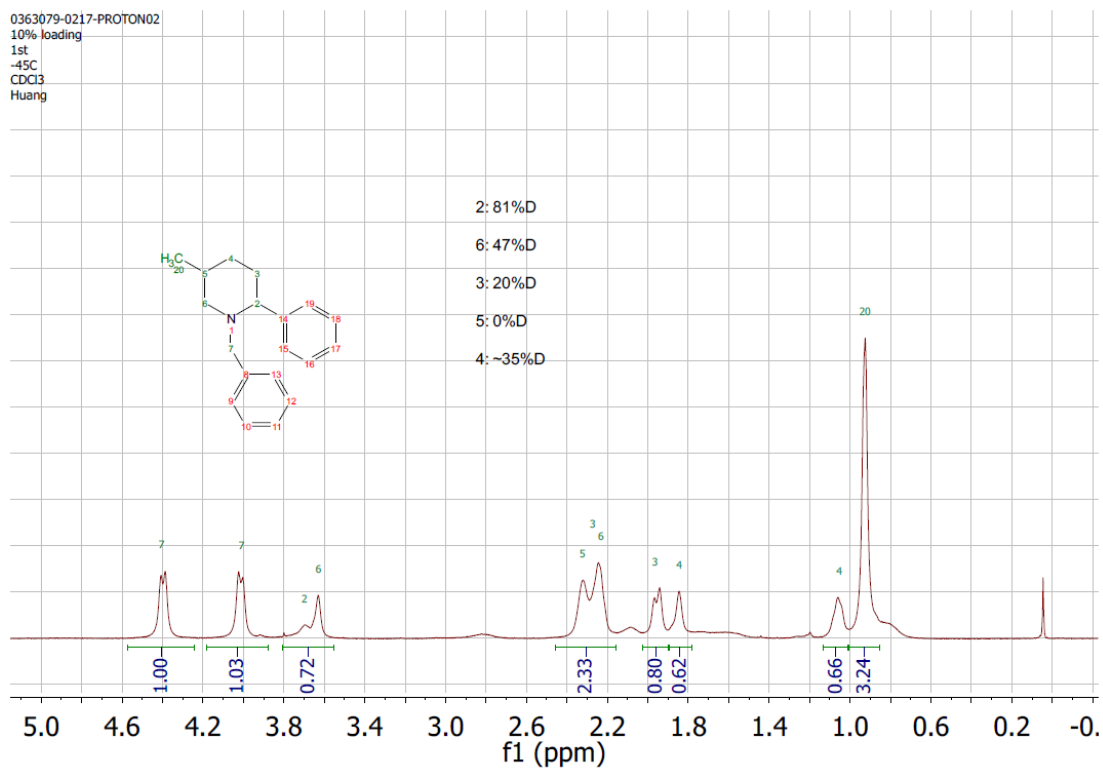
Chen-0363079-0026/22
HSQCEDETGPSISP2.3
340897-144, sample #2: 2eq D2O
CDCl₃



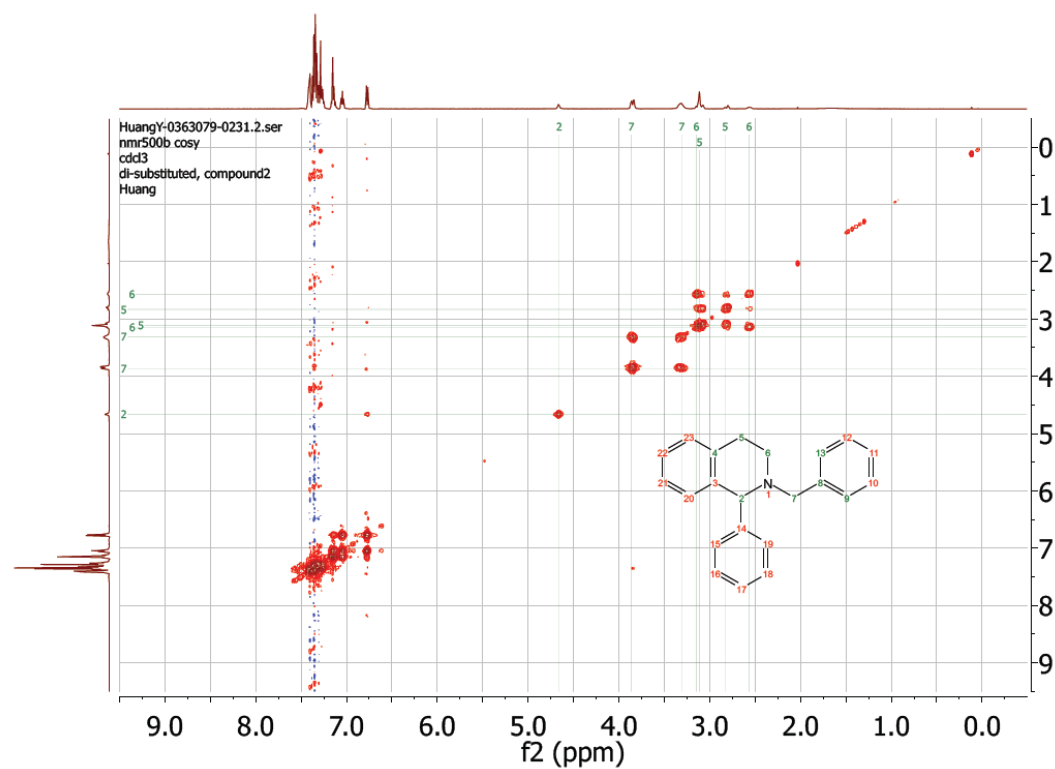
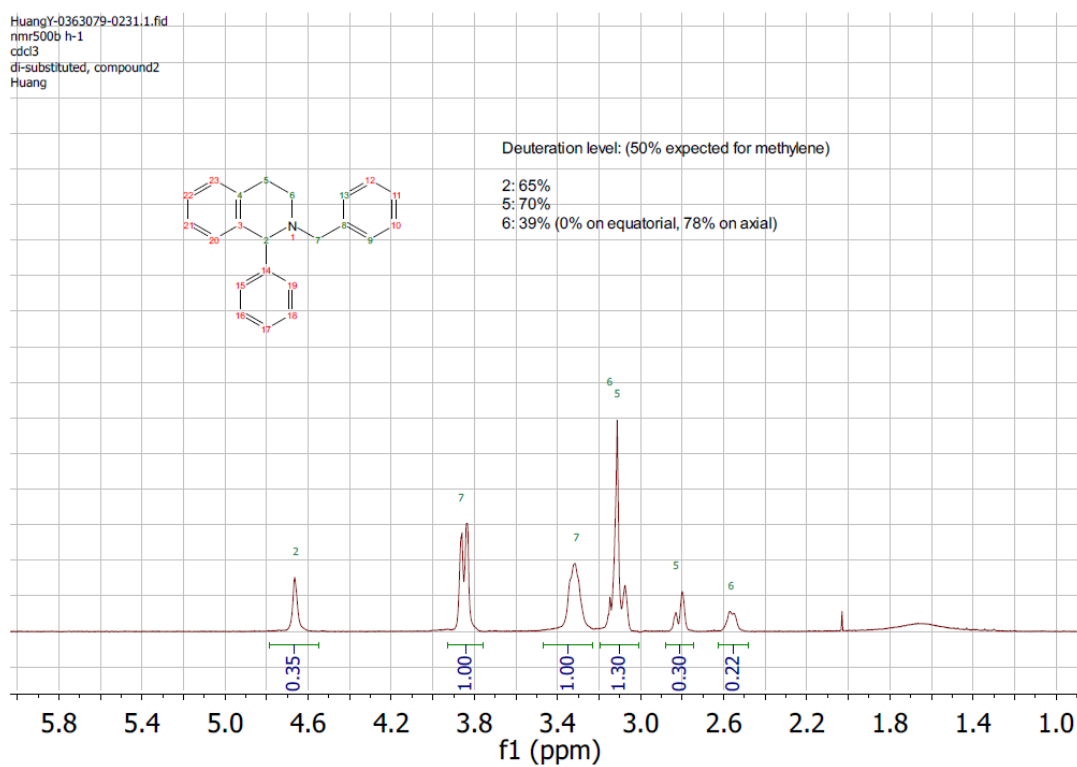
Duterium content in Major diastereomer:

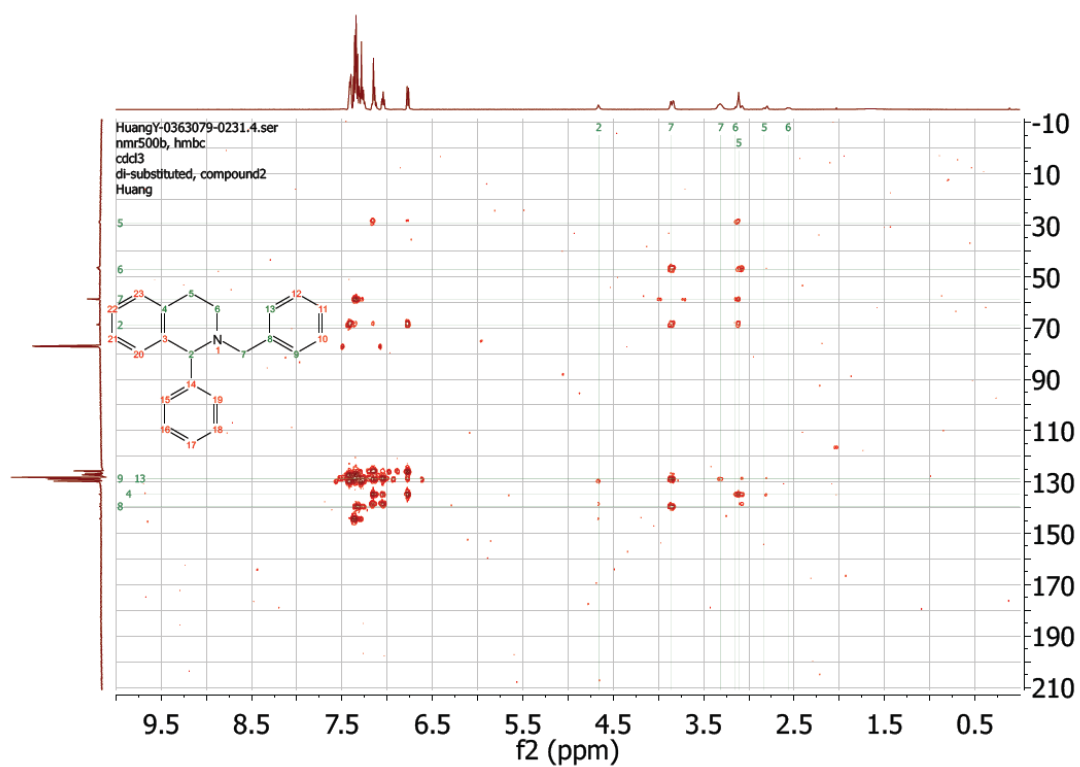
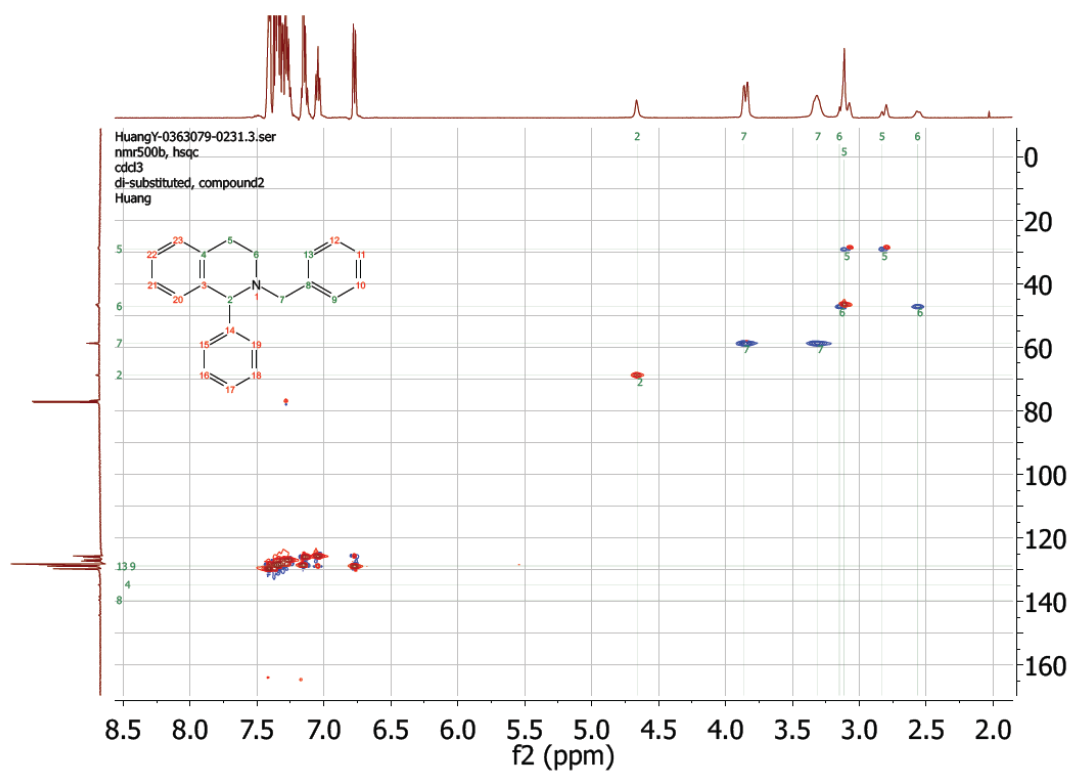


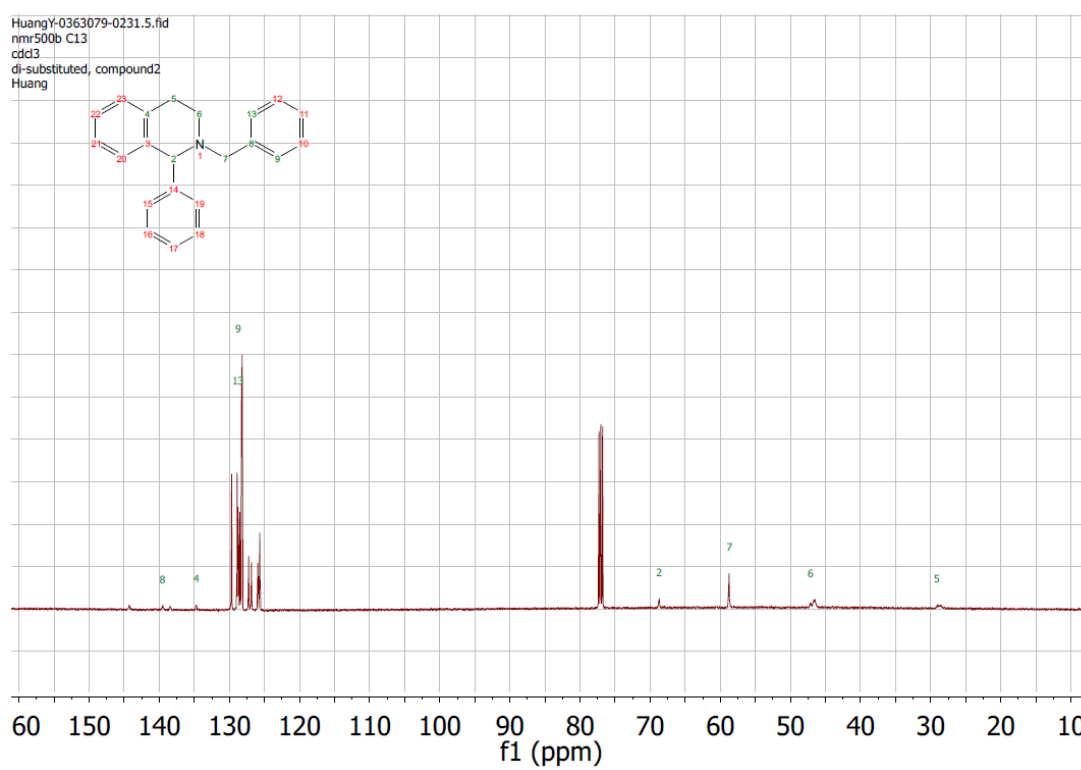
Duterium content in Minor diastereomer:

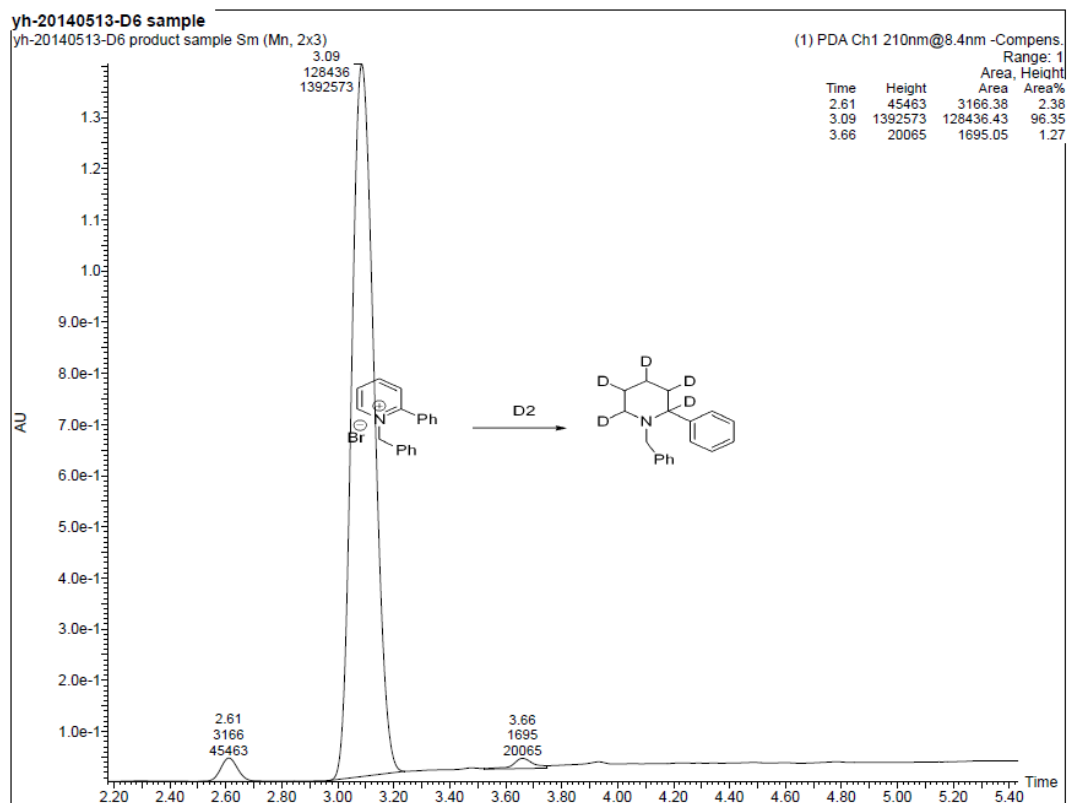


HuangY-0363079-0231.1.fid
nmr500b h-1
cdcl3
di-substituted, compound2
Huang

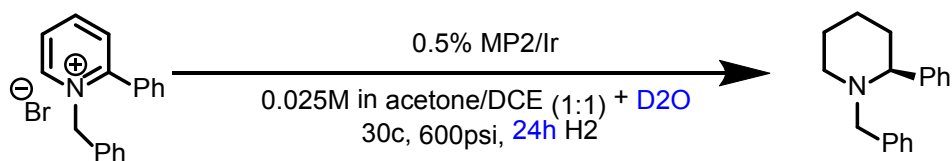




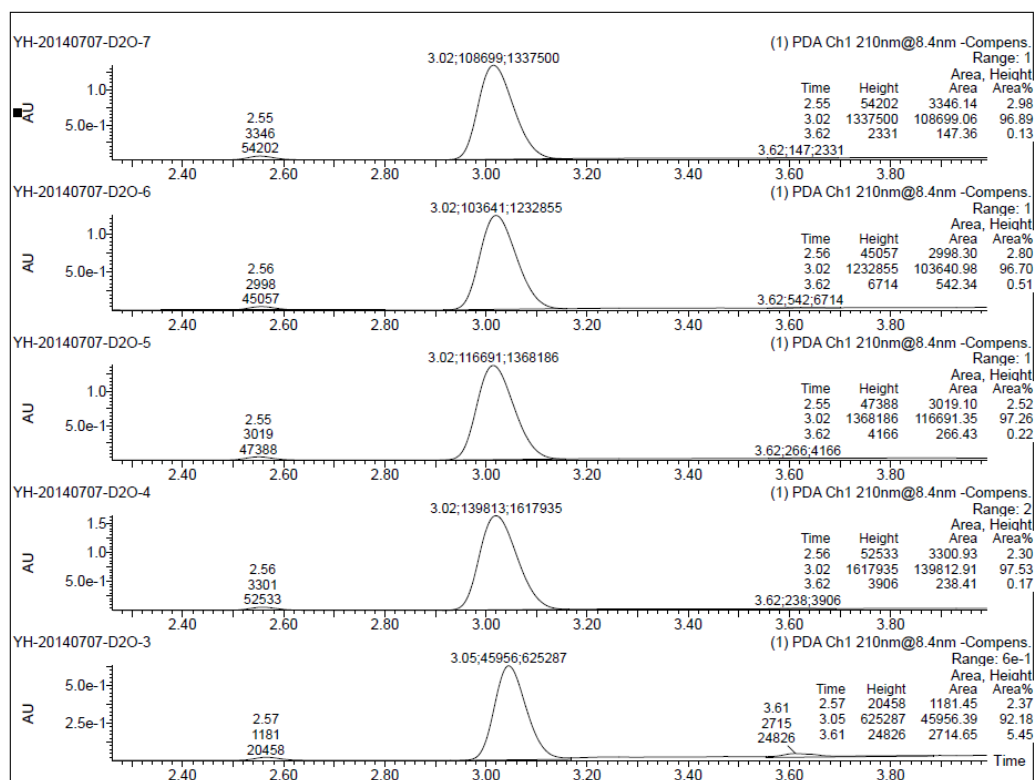


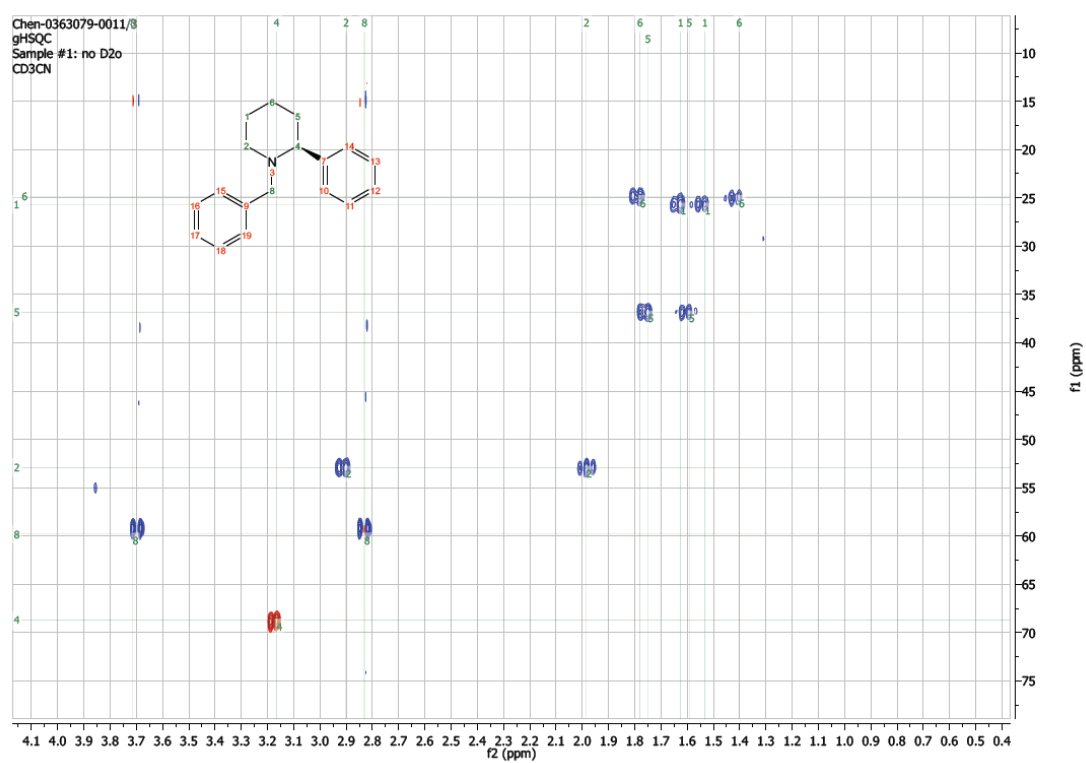


Deuterium Water as Additive

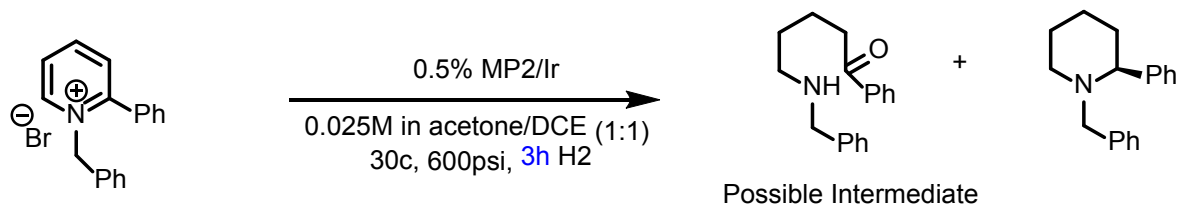


	0eq D2O	2eq D2O	3eq D2O	4eq D2O	10eq D2O
D2 ratio at 3		40%	48%	57%	67%
D2 ratio at 5		34%	36%	39%	42%
ee%	90	95	95	95	94
conversion	94	>99	>99	>98	>99

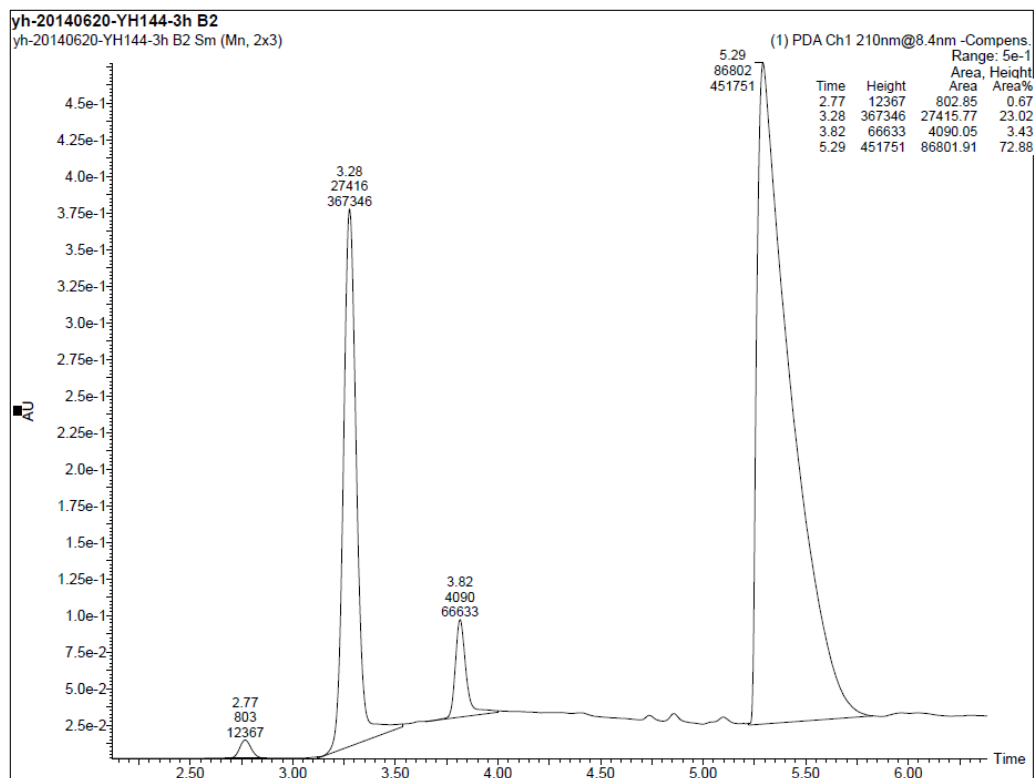


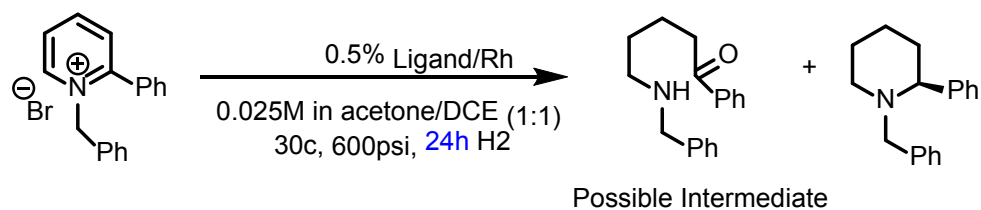


4.4.4 Enamine and Ketone Identification

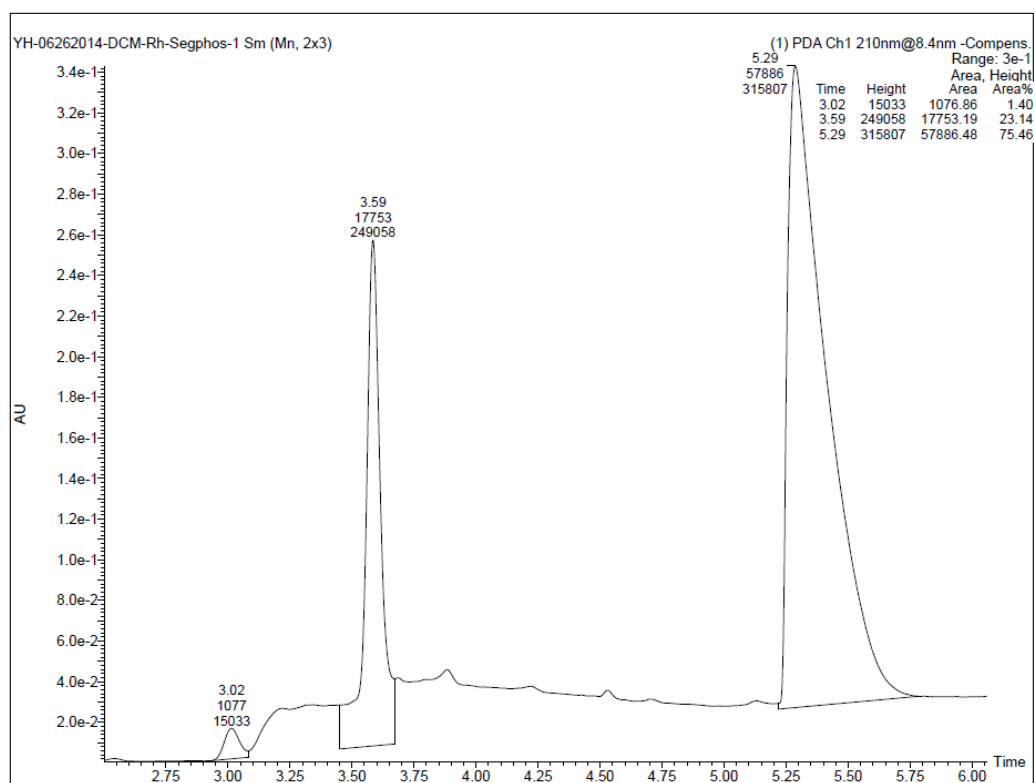


			ee%	prodt%	Inter%	SM
B1: 0.025M, cat. 0.5%mol	Acetone-D6:DCE-D4=1:1		94.8	7.8	3.9	88.2
B2: 0.05M, cat. 0.5%mol	Acetone-D6:DCE-D4=1:1		94.9	23.6	3.4	72.9
B3: 0.025M, cat. 1%mol		Acetone-D6	95.1	49.6	0	50.3
B4: 0.05M, cat. 1%mol		Acetone-D6	95.3	68.3	0	31.6





	Inter%	prod%	SM%
B5: Rh(COD)Cl/DBTM GarPhos/DCE	9.9	0	87
B6: Rh(COD)Cl/DBTM GarPhos/DCE	10	0	85
A5: Rh(COD)Cl/MP2 /DCM	23	0	75
A6: Rh(COD)Cl/MP2 /DCM	24	0	64

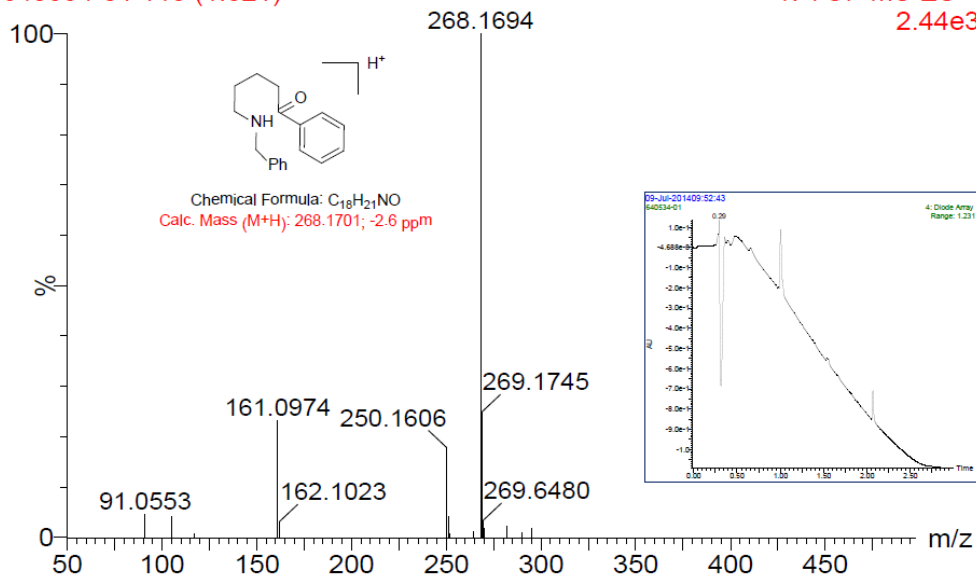


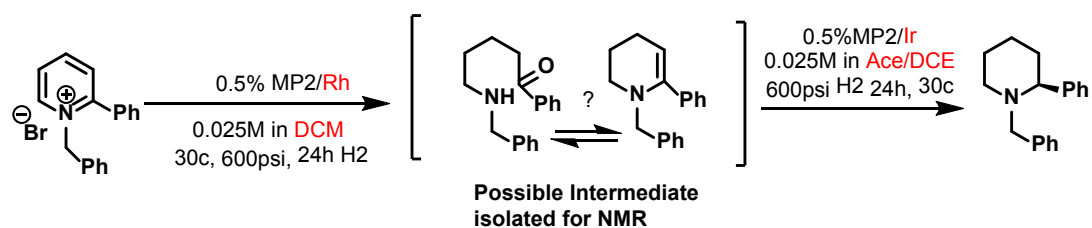
AMM analysis of 0342911-0063, MW 267
SWMS 32-78-6115; ELN 0355728-0027

22222
10

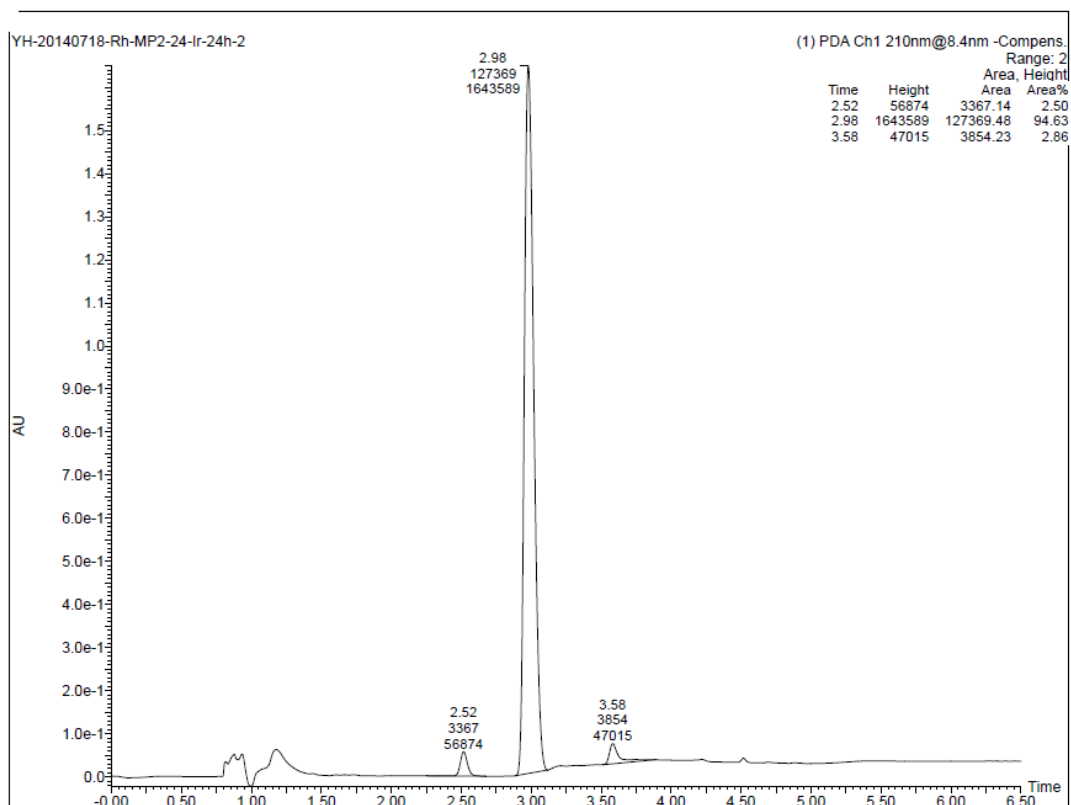
640534-01 113 (1.021)

1: TOF MS ES+
2.44e3





change Rh to Ir after 24h				
Data File	Location	ee%	Conversio	Inter%
YH-20140718-Rh-MP2-24-Ir-24h-1.Raw	1:E:1	94.5%	96.4%	3.6%
YH-20140718-Rh-MP2-24-Ir-24h-2.Raw	1:E:2	94.9%	97.4%	2.6%



Identification of enamine (4) and ketone (10) intermediates by NMR

Structures of the enamine and ketone intermediates are determined by ^1H and ^{13}C chemical shifts, ^1H - ^1H J -correlations from COSY, and ^1H - ^{13}C J -correlations from HMBC. The multiplicity-edited HSQC for enamine is shown in Figure S5. The olefin is clearly identified. The multiplicity-edited HSQC and HMBC for a mixture of enamine and ketone are shown in Figure S6 and S7 respectively. A carbon chemical shift @202ppm (Fig S7) strongly supports the ketone form.

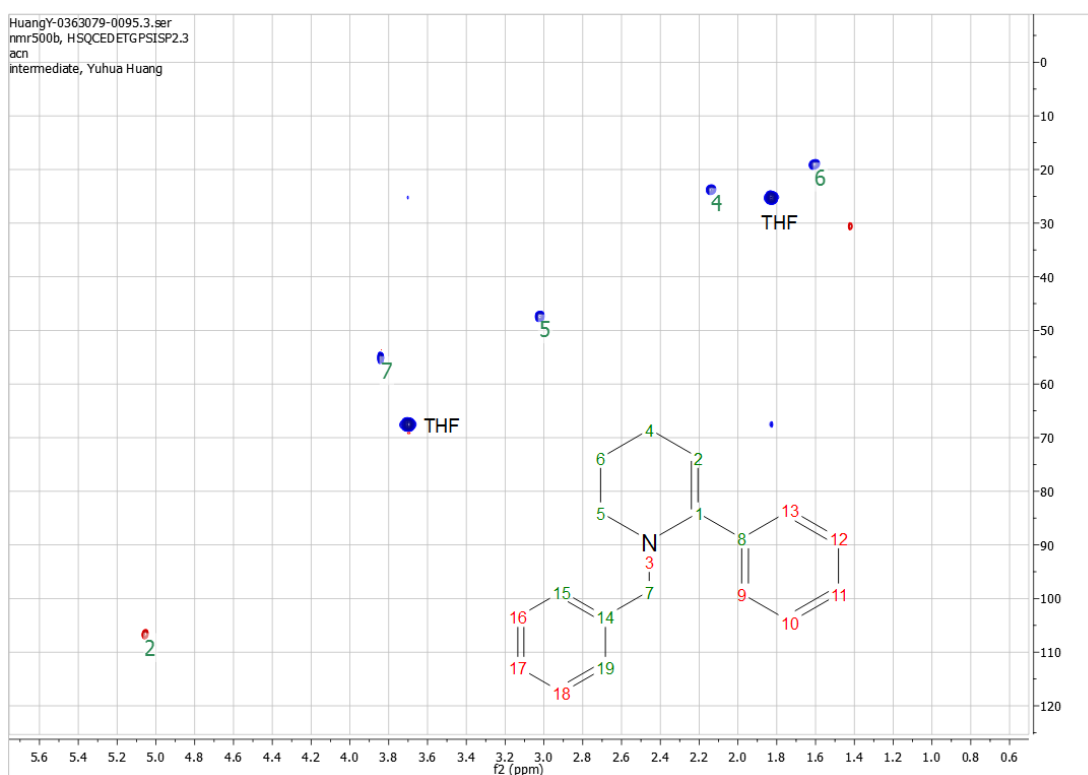


Figure 4-11. Multiplicity-edited HSQC of the enamine intermediate (4).

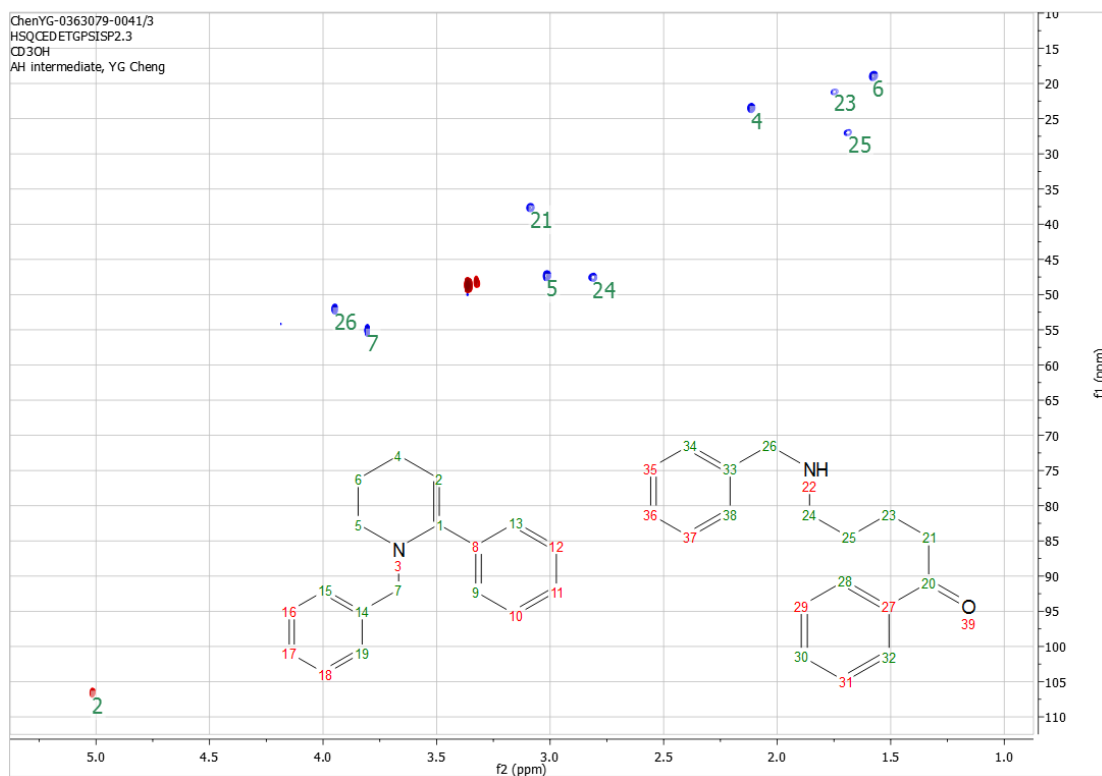


Figure 4-12. Multiplicity-edited HSQC of the mixture of enamine (4) and ketone (10) intermediates.

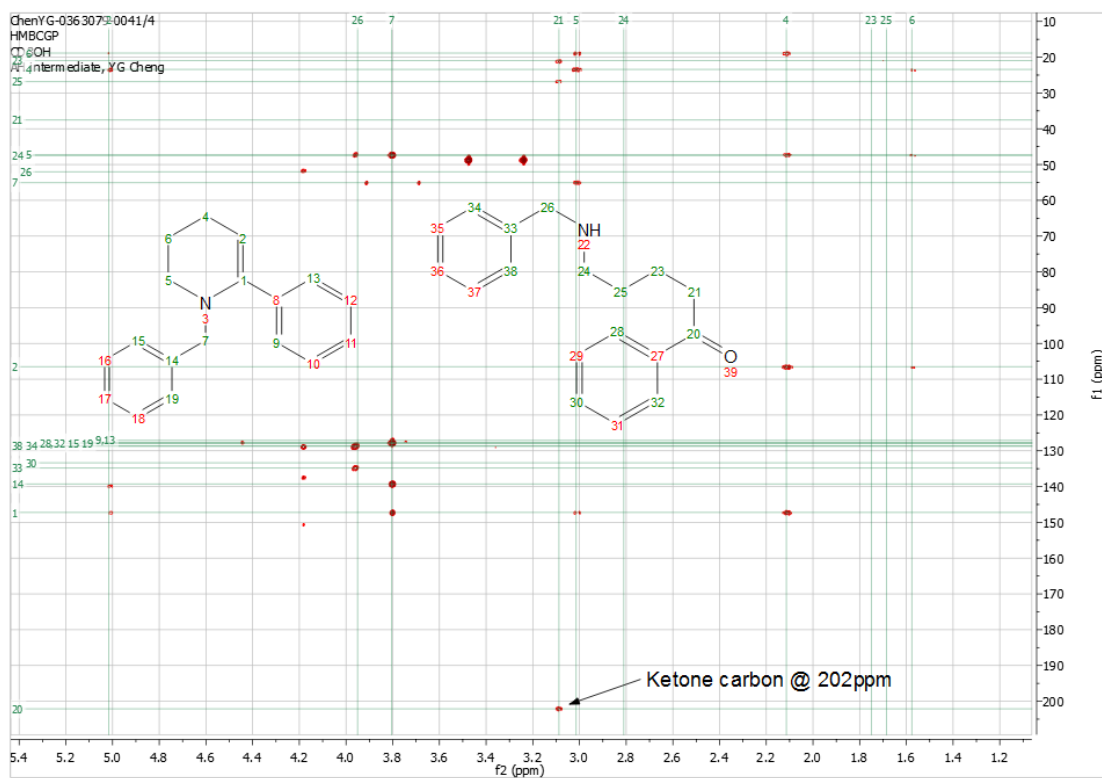
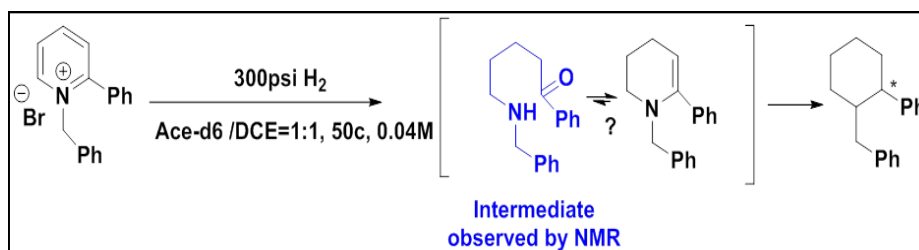


Figure 4-13. ^1H - ^{13}C HMBC spectrum of the mixture of enamine (4) and ketone (10) intermediates.

intermediates. The characteristic ketone carbon @202ppm is indicated.

4.4.5 Kinetics time course data



sample	time (min)	P1(rt=1.697)%	P2 (rt=1.99)%	IM (rt=2.52)%	SM(rt=4.836)%	ee%
1	15					
2	30	0	5	4	91	
3	60	0	14	6.4	79	
4	120	1.6	44	6	48	93
5	180	2	72	4	21	94.4
7	300	2.5	96.3	0	1	94.9
8(control)	300	2.7	97	0	0	94.5

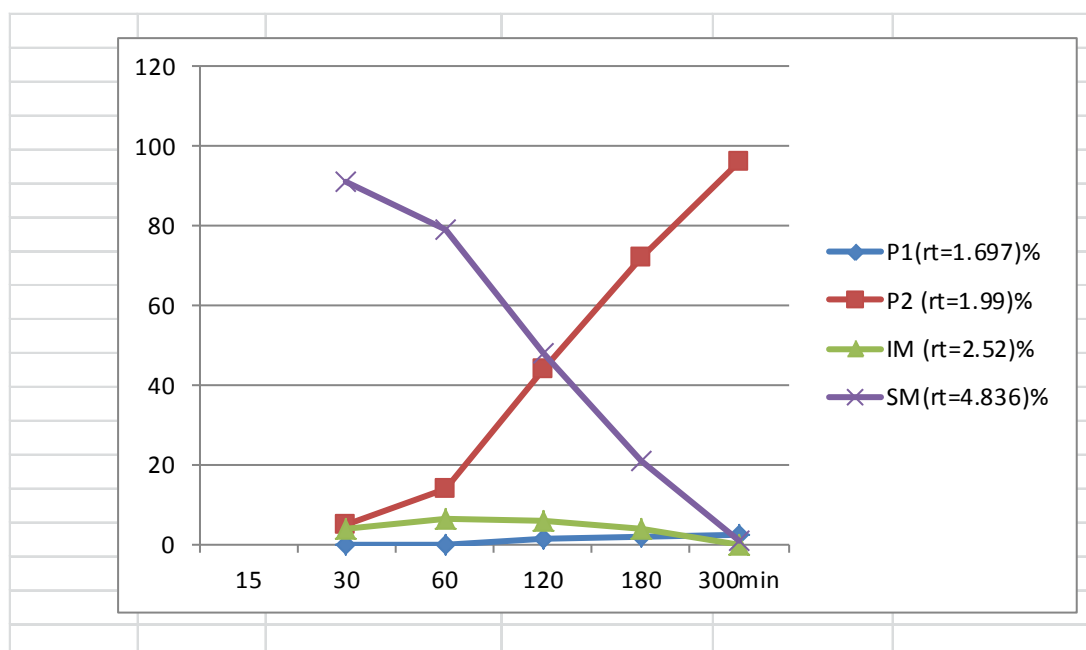
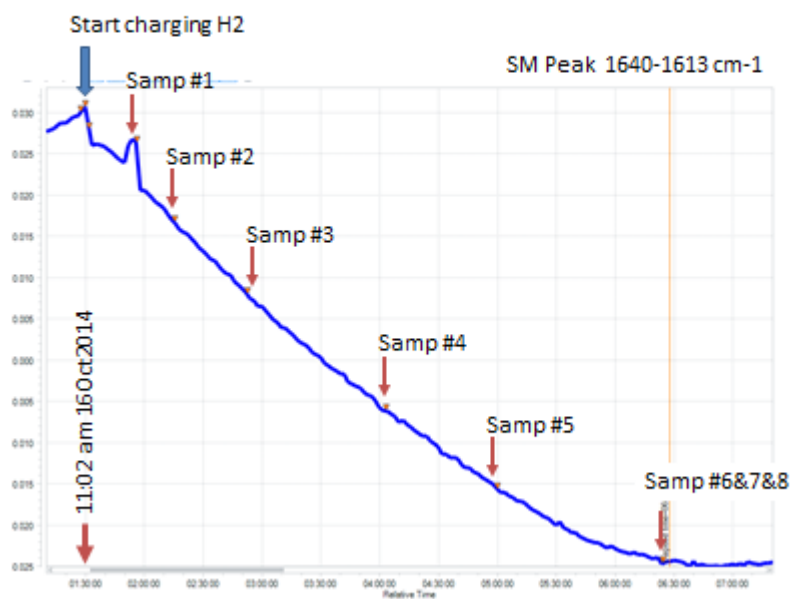


Figure 4-14. NMR data collected at 6 time point and the end point.

Kinetic data (IR)

IR spectrum data collected every minute for the first 8 hours and then every 5 minutes after that.

Starting material profile (YH175)



SM by concirt	PeakArea1640_1480/SM	Annotations
0.0632841	0.031172	
0.0650468	0.0316795	
0.0665616	0.0317026	
0.067005	0.0323411	Charged Hydrogen
0.0678831	0.0328962	
0.0385752	0.0280617	One full scan after charging H2
0.0358139	0.0282785	started stirring, time=0
0.0349191	0.0280479	
0.034234	0.0279206	
0.0337182	0.027574	
0.0327824	0.0273037	
0.0320988	0.0269642	
0.0318849	0.0263985	
0.0314669	0.0261204	
0.0308961	0.0258559	
0.03046	0.0280291	
0.0299693	0.0288154	
0.0313334	0.0285707	
0.0293547	0.0223835	First Sample Taken
0.0274975	0.02239	
0.026649	0.0219165	
0.026381	0.0214334	
0.0268157	0.0208962	
0.0259873	0.0204879	
0.0260707	0.0201837	
0.0262354	0.019351	
0.0259206	0.0186789	
0.0259852	0.0182479	Sample 2 collected
0.0280449	0.0174955	
0.0277788	0.017086	
0.0281641	0.0168767	
0.0280078	0.0162849	
0.0274633	0.0158348	
0.0257989	0.0151393	
0.0249302	0.0148404	
0.0250733	0.0142562	
0.0256315	0.0137059	
0.0261025	0.0135349	
0.0252317	0.0129038	
0.0256656	0.0123407	
0.0233238	0.0118278	
0.0224195	0.0117282	
0.0215919	0.0109337	

0.0229292	0.010477	
0.024428	0.0100326	
0.0222034	0.00955307	
0.0242538	0.00868137	Sample 3 Taken
0.0220235	0.008535	
0.0214127	0.00777758	
0.0206495	0.00779431	
0.0207275	0.00729732	
0.0200226	0.00666389	
0.0196999	0.00606804	
0.0197207	0.00569931	
0.0195465	0.0050566	
0.0193304	0.00510717	
0.0189787	0.00459167	
0.0180588	0.00416915	
0.0179854	0.0035852	
0.0175473	0.00318365	
0.0176196	0.00300259	
0.016754	0.00255424	
0.0167631	0.00189715	
0.0166265	0.0016696	
0.0167256	0.00139696	
0.0161033	0.000566228	
0.0154675	0.000352145	
0.0154459	-0.000104413	
0.0150817	-0.000333628	
0.0143201	-0.000717391	
0.0150975	-0.00072256	
0.015047	-0.00183025	
0.0141591	-0.00194595	
0.0138707	-0.00223662	
0.0138091	-0.00243105	
0.0137389	-0.00299431	
0.0131432	-0.00343512	
0.0134906	-0.0035432	
0.0128832	-0.00409042	
0.0129557	-0.00494013	
0.0114998	-0.00541543	
0.0151946	-0.00540065	Sample 4 taken
0.0121518	-0.00577154	
0.0122574	-0.00608704	
0.0120031	-0.00687126	
0.0124179	-0.00652734	
0.0120115	-0.00715948	

0.0121282	-0.00744615
0.0119644	-0.00791257
0.0118186	-0.00819593
0.0115667	-0.00855437
0.0115687	-0.0085983
0.0113053	-0.00921588
0.0113285	-0.00951171
0.0113628	-0.00988377
0.0107739	-0.0108122
0.0117125	-0.0108078
0.0114471	-0.0113385
0.0111229	-0.0112426
0.010864	-0.0113817
0.0107135	-0.0121993
0.00999146	-0.0125337
0.010828	-0.0125555
0.0100169	-0.0130949
0.00999025	-0.0132101
0.00998843	-0.0137458
0.00951893	-0.0140092
0.0100393	-0.0142415
0.00878068	-0.014706
0.0105446	-0.0152825
0.0118251	-0.0157563
0.00997373	-0.0156441
0.00946838	-0.016099
0.00965415	-0.0163185
0.00997902	-0.0167815
0.00932351	-0.0167747
0.00965518	-0.016981
0.00988475	-0.0174264
0.00889916	-0.0178058
0.00941138	-0.018102
0.00869101	-0.0184119
0.00896903	-0.0187698
0.00876801	-0.0188281
0.00898831	-0.0193337
0.00853741	-0.0198264
0.0087631	-0.0193053
0.00676408	-0.0201594
0.00661508	-0.0203278
0.0074645	-0.0207731
0.00781864	-0.0206882
0.00778165	-0.0212086

Sample 5 taken

0.00691987	-0.0214096
0.00707477	-0.0216954
0.00764147	-0.0217972
0.00679545	-0.0220329
0.006426	-0.0220139
0.00658298	-0.0224088
0.00650058	-0.0226776
0.00626131	-0.0223778
0.00587595	-0.0226511
0.00554639	-0.0230047
0.00548451	-0.0231208
0.00470178	-0.0232567
0.0049527	-0.0234775
0.0064963	-0.0231927
0.00650925	-0.0235536
0.0060785	-0.0234421
0.00585815	-0.0236344
0.00162012	-0.0239435
0.000948509	-0.0239806
0.00403901	-0.0238428
0.0143078	-0.024719
0.00287696	-0.0243523
0.00100788	-0.0244348
0.000129115	-0.0242108
-0.00152046	-0.0242876
-0.00164036	-0.0244147
-0.00253459	-0.0245878
-0.0042175	-0.0250368
-0.00318295	-0.0243174
-0.00339077	-0.0249317
-0.00338412	-0.024707
-0.00313364	-0.0248947
-0.0024951	-0.0249817
-0.00261827	-0.0249468
-0.00306355	-0.0249135
-0.0020798	-0.0250632

Sample 7 taken Sample 8 (control) taken

Reference

1. (a) U. Eisner, J. Kuthan, *Chem. Rev.* **1972**, 72, 1 ; (b) Y. Kasé, T. Miyata, *Adv. Biochem. Psychopharmacol.* **1976**, 15, 5; (c) V. Baliah, R. Jeyaraman, L. Chandrasekaran, *Chem. Rev.* **1983**, 83, 379; (d) D. O'Hagan, *Nat. Prod. Rep.* **2000**, 17, 435; (e) S. Laschat, T. Dickner, *Synthesis* **2000**, 1781; (f) P. M. Weintraub, J. S. Sabol, J. M. Kane, D. R. Borcharding, *Tetrahedron* **2003**, 59, 2953; (g) M. G. P. Buffat, *Tetrahedron* **2004**, 60, 1701; (h) S. Källström, R. Leino, *Bioorg. Med. Chem.* **2008**, 16, 601; (i) P. Merino, T. Tejero, G. Greco, E. Marca, I. Delso, A. Gomez-SanJuan, R. Matute, *Heterocycles* **2012**, 84, 75; (j) B. T. Green, S. T. Lee, K. E. Panter, D. R. Brown, *Food Chem. Toxicol.* **2012**, 50, 2049.
2. (a) A. A. H. P. Megens, F. H. L. Awouters, A. Schotte, T. F. Meert, C. Dugovic, C. J. E. Niemegeers, J. E. Leysen, *Psychopharmacology* **1994**, 114, 9; (b) P. Tyrer, P. C. Oliver-Africano, Z. Ahmed, N. Bouras, S. Cooray, S. Deb, D. Murphy, M. Hare, M. Meade, B. Reece, K. Kramo, S. Bhaumik, D. Harley, A. Regan, D. Thomas, B. Rao, B. North, J. Eliahoo, S. Karatela, A. Soni, M. Crawford, *Lancet* **2008**, 371, 57.
3. W. E. Pelham, E. M. Gnagy, L. Burrows-Maclean, A. Williams, G. A. Fabiano, S. M. Morrissey, A. M. Chronis, G. L. Forehand, C. A. Nguyen, M. T. Hoffman, T. M. Lock, K. Fielbelkorn, E. K. Coles, C. J. Panahon, R. L. Steiner, D. L. Meichenbaum, A. N. Onyango, G. D. Morse, *Pediatrics* **2001**, 107, 105.
4. A. Burns, M. Rossor, J. Hecker, S. Gauthier, H. Petit, H. J. Möller, S. L. Rogers, L. T. Friedhoff, *Dementia Geriatr. Cognit. Disord.* **1999**, 10, 237.
5. (a) K. L. Dechant, S. P. Clissold, *Drugs* **1991**, 41, 225; (b) M. Bourin, P. Chue, Y. Guillon, *CNS Drug Rev.* **2001**, 7, 25.
6. W. Jeal, P. Benfield, *Drugs* **1997**, 53, 109.
7. (a) P. N. Rylander, *Catalytic Hydrogenation in Organic Synthesis*, Academic Press, New York, **1979**; (b) R. L. Augustine, *Heterogeneous Catalysis for the Synthetic Chemist*, Marcel Dekker, New York, **1995**; (c) M. Freifelder, *Adv. Catal.* **1963**, 14, 203.
8. Reviews on asymmetric hydrogenation of heteroaromatics: (a) F. Glorious, *Org. Biomol. Chem.* **2005**, 3, 4171; (b) D. S. Wang, Q.A. Chen, S.M. Lu, Y.G. Zhou, *Chem. Rev.* **2012**, 112, 2557; (c) Z. Yu, W. Jin, Q. Jiang, *Angew. Chem.* **2012**, 124, 6164; *Angew. Chem. Int. Ed.* **2012**, 51, 6060.
9. W. Wang, S. Lu, P. Yang, X. Han, Y. Zhou, *J. Am. Chem. Soc.* **2003**, 125, 10536.
10. (a) S. M. Lu, Y. Q. Wang, X. W. Han and Y. G. Zhou, *Angew. Chem., Int. Ed.*, 2006, **45**, 2260. (b) L. Shi, Z. Ye, L. Cao, R. Guo, Y. Hu and Y. Zhou, *Angew. Chem., Int. Ed.*, 2012, **51**, 8286.
11. J. Wu, W. Tang, A. Pettman, J. Xiao, *Adv. Synth. Catal.* **2013**, 355, 35-40
12. J. Wu, C. Wang, W. Tang, A. Pettman, J. Xiao, *Chem. Eur. J.* **2012**, 18, 9525.

13. Isotopic labeling experiment on 2-ph-pyridinium salt in section 4.2.2 and work illustrated in scheme 4-5 were collaborated work with S. Liu of Zhang's group. The work is to be published as co-author.